Agnieszka Kozieł

Aerobic metabolism of human endothelial cells under physiological and pathophysiological conditions

Adam Mickiewicz University
Faculty of Biology
Department of Bioenergetics
Institute of Molecular Biology and Biotechnology
Poznań, Poland

SUPERVISOR: Prof. dr hab. Wiesława Jarmuszkiewicz

Poznań, 2016

First of all, I would like to express my sincere gratitude to my PhD supervisor, Prof. Wiesława Jarmuszkiewicz. I am most grateful for extending your confidence and accepting me as PhD student. I would like to thank for guidance and constant, substantive support, advices and critical remarks at all stages of the preparation for this thesis.

I am thankful to Wioletta Nobik, Dr Anna Kicińska and Dr Małgorzata Budzińska for technical, substantive and personal support throughout my PhD studies. I dare to say, thank you for being my friends.

I am thankful to Dr Andrzej Woyda-Płoszczca for helping me during Q10 extraction and HPLC measurements and MSc Izabela Broniarek for supporting me with digitally quantification protein bands.

I would like to thank all members of the Department of Bioenergetics of Adam Mickiewicz University, with whom I had opportunity to work during my PhD studies, for creating a unique work environment. You made this time unforgettable.

Składam najserdeczniejsze podziękowania moim Najbliższym;

Najwspanialszym Rodzicom, Piotrowi oraz Rodzeństwu.

Dziękuję Wam za bezwarunkową miłość i przyjaźń,

za wsparcie w dążeniu do celu, niezachwianą wiarę we mnie i siłe,

za nieprzerwaną troskę, ogromną cierpliwość i wyrozumiałoć.

Founding

- European Union from the resources of the European Regional Developmental Found under the Innovative Economy Programme (POIG.01.01.02-00-069/09)
- Grand from the National Science Centre, Poland (Preludium, 2012/07/N/NZ3/00495)
- Fellowship from Jagiellonian Medical Research Centre (JMRC) Foundation
- Fellowship for PhD students from KNOW Poznan RNA Centre (01/KNOW2/2014)

Abstract

Endothelium is a single layer of cells lining each blood vessel that accomplishes a vast variety of specialised functions, which disturbances are implicated in the development of many cardiovascular diseases. In endothelial cells, the ATP synthesis occurs in a major part via a glycolytic pathway. The relatively slight dependence of endothelial cells on mitochondrial oxidative phosphorylation could suggest that mitochondria play no significant role. Several recent observations clearly indicate that endothelial mitochondria not only can contribute to ATP generation but also are involved in maintaining the fine regulatory balance among mitochondrial calcium concentration, reactive oxygen species (ROS) production and nitric oxide (NO) production. The endothelial mitochondria may function as sensors of alternations in the local environment, contributing to survival of endothelial cells under oxidative stress. Endothelial mitochondria may play a central role in many cardiovascular diseases. The general goal of the doctoral thesis was to study the aerobic metabolism of endothelial cells under physiological and pathophysiological conditions. Mitochondrial oxidative metabolism, the main subject in these studies, was elucidated at the cellular and isolated mitochondria levels.

The realisation of the project required elaboration of efficient procedures of a large-scale culture of human umbilical vein endothelial cells (EA.hy926 line) and isolation of a big amount of bioenergetically active well-coupled endothelial mitochondria. The presented results demonstrate that primarily glycolytic endothelial cells possess highly active, well-coupled mitochondria.

The first goal of this study was to assess the influence of chronic high-glucose exposure on mitochondrial oxidative metabolism in human endothelial EA.hy926 cells. Endothelial cells were grown in medium containing either 5.5 mM or 25 mM glucose, representing normal-glucose and high-glucose conditions, respectively. The respiratory response to elevated glucose was observed in cells grown in 25 mM glucose for at least 6 days or longer. In endothelial cells, growth in high-glucose concentrations induced considerably lower mitochondrial respiration with glycolytic fuels, less pronounced with glutamine, and higher respiration with palmitate. The Crabtree effect was observed in both types of cells. High-glucose conditions produced elevated levels of cellular coenzyme Q10, increased ROS generation, increased hexokinase I (HKI), lactate dehydrogenase (LDH), acyl-CoA dehydrogenase (ACADS), uncoupling protein 2 (UCP2), and superoxide dismutase 2 (SOD2) expression, and decreased E3-binding protein of pyruvate dehydrogenase expression (E3BP).

In isolated mitochondria, high-glucose levels induced an increase in the oxidation of palmitoylcarnitine and glycerol-3-phosphate (lipid-derived fuels) and a decrease in the oxidation of pyruvate (a mitochondrial fuel). The results demonstrate that high-glucose exposure induces a shift of the endothelial aerobic metabolism towards the oxidation of lipids and amino acids.

Uncoupling proteins (UCPs), members of the mitochondrial anion carrier protein family, are present in the inner mitochondrial membrane and mediate free fatty acid-activated, purine nucleotide-inhibited proton conductance. UCPs are involved in the control of cellular energy balance and prevent mitochondrial reactive oxygen species (mROS) production. This study describes a functional characteristics and an antioxidative role for UCP2 in endothelial cells and isolated mitochondria and how this function is altered by long-term growth in high concentrations of glucose. Human endothelial EA.hy926 cells were grown in media with either high (25 mM) or normal (5.5 mM) glucose concentrations. Under non-phosphorylating and phosphorylating conditions, UCP activity was significantly higher in mitochondria isolated from high-glucose-treated cells. A more pronounced control of the respiratory rate, membrane potential and mROS by UCP2 was observed in these mitochondria. A greater UCP2-mediated decrease in ROS generation indicates an improved antioxidative role for UCP2 under high-glucose conditions. Mitochondrial and non-mitochondrial ROS generation was significantly higher in high-glucose cells independent of UCP2 expression. UCP2 gene silencing led to elevated mROS formation and intracellular adhesion molecule 1 (ICAM1) expression, especially in high-glucose-cultured cells. UCP2 influenced endothelial cell viability and resistance to oxidative stress. Endothelial cells exposed to high-glucose concentrations were significantly more resistant to hydrogen peroxide. In these cells, the increased activity of UCP2 led to improved stress resistance and protection against acute oxidative stress. These results indicate that endothelial UCP2 may function as a sensor and negative regulator of mROS production in response to high-glucose levels.

The next goal of this study was to assess the influence of chronic exposure to hypoxia on mitochondrial oxidative metabolism in human endothelial EA.hy926 cells cultured for 6 days at 1% O_2 tension. The hypoxia-induced effects were elucidated at the cellular and isolated mitochondria levels. Hypoxia elevated fermentation but did not change mitochondrial biogenesis or aerobic respiratory capacity of endothelial cells. In endothelial cells, hypoxia caused a general decrease in mitochondrial respiration during carbohydrate, fatty acid or amino acid oxidation except for increased exclusively ketogenic amino acid oxidation. Hypoxia induced an elevation of intracellular and mitochondrial ROS formation, although cell

viability and antioxidant systems (superoxide dismutases SOD1 and SOD2, and uncoupling proteins UCPs) were not increased. In mitochondria from hypoxic cells, the opposite changes at the level of respiratory chain, i.e., a considerably elevated expression and activity of complex II, and a decreased expression and activity of complex I were observed. The elevated activity of complex II resulted in an increase in succinate-sustained mROS formation mainly through the increased reverse electron transport. The hypoxia-induced decrease in UCP2 expression and activity was also observed. The results indicate that the exposure to chronic hypoxia induces a shift in endothelial catabolic metabolism from aerobic toward anaerobic. The hypoxia-induced non-excessive increase in intracellular and mitochondrial ROS formation may be involved in endothelial signalling of hypoxic responses. These results indicate an important role of succinate, complex II, and reverse electron transport in hypoxia-induced adjustments of endothelial cells and highlight the role of endothelial mitochondria in response to metabolic adaptations related to hypoxia.

The existence of a large-conductance Ca^{2+}-activated potassium channel (BK_{Ca}) in the mitochondria of human endothelial EA.hy926 cells was also described. Immunological analysis with antibodies raised against proteins of the plasma membrane BK_{Ca} channel identified a pore-forming α-subunit and an auxiliary β2-subunit of the channel in the endothelial mitochondrial inner membrane. The substances known to modulate BK_{Ca} channel activity influenced the bioenergetics of isolated endothelial mitochondria. Activators 100 μM Ca^{2+}, 10 μM NS1619, and 0.5 μM NS11021 depolarized the mitochondrial membrane potential and stimulated non-phosphorylating respiration. These effects were blocked by iberiotoxin and paxilline in a potassium-dependent manner. Under phosphorylating conditions, NS1619-induced iberiotoxin-sensitive uncoupling diverted energy from ATP synthesis during the phosphorylating respiration of the endothelial mitochondria. In conclusion, these results show for the first time that the inner mitochondrial membrane in human endothelial EA.hy926 cells contains a large-conductance calcium-dependent potassium channel with properties similar to those of the surface membrane BK_{Ca}.

Contents

List of abbreviations

$[Ca^{2+}]$c – cytosolic Ca^{2+} concentration

$[Ca^{2+}]$m **–** mitochondrial matrix Ca^{2+} concentration

ACADS – acyl-coenzyme A dehydrogenase

Acyl-CoA – acyl-coenzyme A

ADP – adenosine diphosphate

ADP/O ratio – amount of ATP produced from the movement of two electrons through electron transport chain, donated by reduction of an oxygen atom

AMPK(α) – AMP protein kinase (α subunit)

ASK1 – apoptosis signal-regulating kinase 1

ATP – adenosine triphosphate

BAEC – adherent bovine aortic endothelial cells

Bax – Bcl-2 associated X protein

BAT – brown adipose tissue

Bcl-2 – B-cell lymphoma 2

Bid – BH3 domain-containing proapoptotic Bcl2 family member

BK_{Ca} – plasma membrane large-conductance Ca^{2+}-activated potassium channel

BREC – bovine retinal endothelial cells

BSA - bovine serum albumin

COX – cytochrome *c* oxidase, complex IV

CS – citrate synthase

DMEM – Dulbecco's modified Eagle's medium

DMEJ – modified DMEM

DPI – diphenyleneiodonium, an inhibitor of NADPH oxidase

DTNB – 5,5'-di-thiobis-(2-nitrobenzoic acid)

EA.hy926 – human umbilical vein endothelial cell line

E3BP – E3-binding protein of the pyruvate dehydrogenase complex

EDTA - ethylenediaminetetraacetic acid

EGTA – ethylene glycol-bis(β-aminoethyl ether)-N,N,N',N'-tetraacetic acid

eNOS – endothelial nitric oxide synthase

ER – endoplasmic reticulum

FA – fatty acid

FAD, $FADH_2$ – flavin adenine dinucleotide, oxidised and reduced forms, respectively

FBS – fetal bovine serum

FCCP – proton ionophore (uncoupler), carbonyl cyanide 4-(trifluoromethoxy) phenylhydrazone

FMN – flavin mononucleotide

GAPDH – glyceraldehyde 3-phosphate dehydrogenase

GSH – glutathione

GSSH – glutathione disulphide

GTP - guanosine triphosphate

H_2O_2 – hydrogen peroxide

HEPES - 4-(2-hydroxyethyl)-1-piperazineethanesulfonic acid

HIF – hypoxia-inducible factor

HIF1(α,β) – hypoxia-inducible factor 1 (α-, β-subunit)

HKI – hexokinase I

HMEC – human microvascular endothelial cells

HRE – hypoxia-responsive elements

HUVEC – human umbilical vein endothelial cells

ICAM – intercellular adhesion molecule 1

IMM – inner mitochondrial membrane

JNK – c-Jun N-terminal protein kinase

K_{Ca} – Ca^{2+}-regulated K^+ channel

kDa – kilodaltons

LDH – lactate dehydrogenase

LOX – lipoxygenase

MAM – mitochondria-associated ER-membrane

mitoBK$_{Ca}$ – mitochondrial large-conductance Ca^{2+}-activated potassium channel

mitoK$_{ATP}$ – mitochondrial ATP-sensitive potassium channel

MitoSox – specific fluorescent mitochondrial superoxide indicator

mROS – mitochondrial reactive oxygen species

mtDNA – mitochondrial DNA

NAD, NADH – nicotinamide adenine dinucleotide, oxidised and reduced forms, respectively

NBT – nitroblue tetrazolium

NF-KB - nuclear factor kappa-light-chain-enhancer of activated B cells

NO – nitric oxide

NOS – nitric oxide synthase

Nox (1-5) – NADPH oxidase (1-5 isoforms)

NS11021 – 1-(3,5-bis-trifluoromethyl-phenyl)-3-[4-bromo-2-(1H-tetrazol-5-yl)-phenyl]-thiourea

NS1619 – 1,3-dihydro-1-[2-hydroxy-5-(trifluoromethyl)phenyl]-5-(trifluoromethyl)-2H-benzimidazole-2-one

$O_2^{-\bullet}$ - superoxide anion

OCR – oxygen consumption rate

OH• - hydroxyl radical

ox-LDL – oxidised low density lipoprotein

OXPHOS – oxidative phosphorylation

PaO_2 – partial pressure of oxygen

PBS – phosphate-buffered saline

PDH – pyruvate dehydrogenase

PDK1 – pyruvate dehydrogenase kinase 1

PGC1α – peroxisome proliferator-activated receptor gamma coactivator 1 alpha

PHD – prolyl hydroxylase

PTP – permeability transition pore

pVHL – von Hippel Lindau protein

p66Shc – a member of the ShcA (Src homologous- collagen homologue) adaptor protein family

pS – picosiemens

Q – ubiquinone (coenzyme Q)

QH_2 – reduced Q (ubiquinol)

QH_2/Qtot – reduction level of Q

Qtot – total pool of endogenous Q in the inner mitochondrial membrane

RCR – respiratory control ratio (state 3 respiratory rate/state 4 respiratory rate)

RNS – reactive nitrogen species

ROS – reactive oxygen species

SDS-PAGE – sodium dodecyl sulphate polyacrylamide gel electrophoresis

siRNA – small interfering RNA

SOD – superoxide dismutase

SOD1 (**CuZn-SOD**) – copper-zinc SOD

SOD2 (**Mg-SOD**) – manganese SOD

SOD3 (**EC-SOD**)– extracellular SOD

state 3 – phosphorylating respiration (in the presence of ADP)

state 4 – resting non-phosprylating respiration (in the absence of added ADP)

TCA cycle – tricarboxylic acid cycle

TMPD – N,N,N′N′-tetramethyl-p-phenylenediamine

TNFα – tumour necrosis factor

TNFR1 – tumour necrosis factor receptor 1

TPP^+ – tetraphenylphosphonium

Txnip – thioredoxin-interacting protein

UCP – uncoupling protein

VDAC – voltage-dependent mitochondrial anion channel

$\Delta\mu H^+$ – proton electrochemical gradient

ΔpH – mitochondrial proton gradient

$\Delta\Psi$ – mitochondrial membrane (electrical) potential

1. Introduction

1.1 Endothelial cell physiology

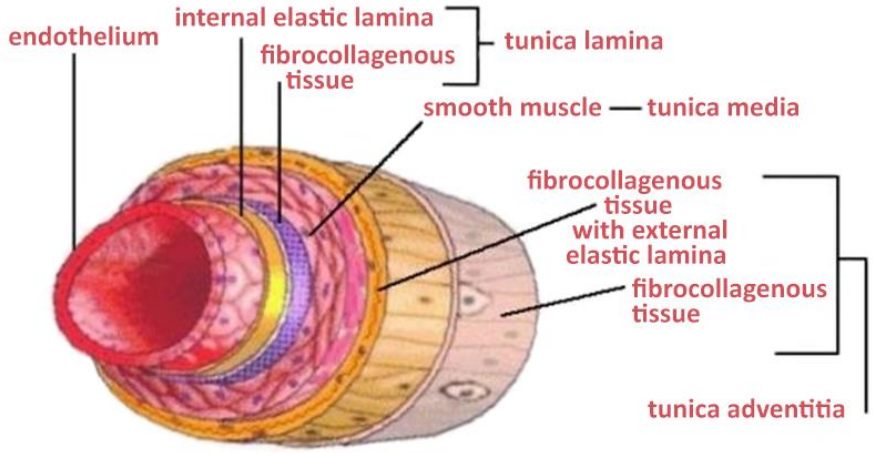

Figure 1.1 A schematic cross-section of an artery composed of three layers: the tunica intima, the tunica media, and the adventitia. Tunica intima has flat endothelial cells lined by elastic membrane. Tunica media is a thick coat of unstriped muscles. Tunica adventitia has a thick coat made up of loosely arranged elastic and collagen fibres and it has a narrow lumen (Guyton and Hall, 2015).

The artery contains three layers (Libby et al., 2011) (Figure 1.1). The inner layer, the tunica intima, is lined by a monolayer of endothelial cells that is in contact with blood. The middle layer, or tunica media, contains smooth muscle cells embedded in a complex extracellular matrix. The adventitia, the outer layer of artery, contains mast cells, nerve endings, and microvessels. The direct contact of endothelial cells with the blood flow means that they are partially vulnerable to damage molecules in the blood on one hand, and that they have ideally "guard" roles on the other hand (Davidson and Duchen, 2007).

The major function of the endothelium may be categorized as: trophic, tonic, and trafficking (Davidson, 2010). A trophic role is performed by controlling access of overlying cells to glucose, fatty acids (FAs) and other metabolites, while also exerting a negative influence on smooth muscle proliferation. A tonic role of the endothelium controls vascular tone by acting as the primary source of nitric oxide (NO), vascular derived hyperpolarising factor, and other secreted hormones and molecules that control vascular smooth muscle contraction and, consequently, the extent of vasodilation or vasoconstriction. A trafficking role of the endothelium controls traffic of macrophages and leucocytes that require passage through the endothelial layer to perform they functions in the interstitium in addition to externing antiplatelet, anticoagulant, and fibrinolytic actions on the luminal side of the vessel.

As the blood vessel's innermost layer, the vascular endothelium fulfils a great multiple of regulatory and sensory functions (Cines et al., 1998). Impairment of any of these functions leads to distinct entities of cardiovascular diseases that collectively represent one of the major causes of overall morbidity and mortality in developed countries (Murray and Lopez, 1997).

1.2 Mitochondria – an overview

Mitochondria are highly active, dynamic, pleomorphic organelles that are found in most eukaryotic cells. Mitochondria are a membrane bound cellular structures, which very often are described as "the powerhouse of the cell" because they generate most of the cell's supply of adenosine triphosphate (ATP), used as a source of chemical energy. The mitochondria are also involved in other cellular activities such as signalling, cellular differentiation, and cell senescence (Groschner et al., 2012). They control of cell cycle and cell growth. Mitochondria affect human health, like mitochondrial disorder and cardiac dysfunction, and they also play an important role in the aging process.

Peter D. Mitchell proposed the chemiosmotic theory in 1961 (Mitchell, 1961). The theory suggests essentially that most ATP synthesis in respiring cells comes from the electrochemical gradient across the inner membrane of mitochondria by using the energy of NADH and $FADH_2$ formed from the breaking down of energy-rich molecules.

1.2.1 Mitochondrial structure

Mitochondria comprise at least six compartments: outer membrane, inner boundary membrane of significantly larger surface area, intermembrane space (space between the outer and inner membranes), cristal membranes, incristal space (formed by infoldings of the inner membrane), and protein-rich matrix (space within the inner membrane) (Figure 1.2).

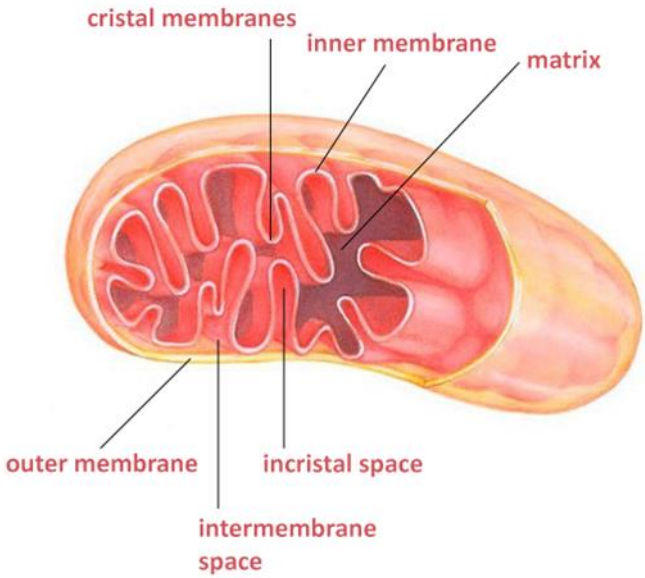

Figure 1.2 A schematic drawing of typical mitochondrion components (www.nhp-hinz.de – modified).

The outer membrane is freely permeable to nutrient molecules, ions, energy molecules like the ATP and ADP molecules. The outer membrane also contains enzymes involved in such diverse activities as the elongation of fatty acids (FAs), oxidation of epinephrine, and the degradation of tryptophan. These enzymes include monoamine oxidase, rotenone-insensitive NADH-cytochrome *c*-reductase, kynurenine hydroxylase, and fatty acid CoA ligase. Disruption of the outer membrane permits proteins in the intermembrane space to leak into the cytosol, leading to certain cell death (Chipuk et al., 2006). The mitochondrial outer membrane can associate with the endoplasmic reticulum (ER) membrane, in a structure called MAM (mitochondria-associated ER-membrane) (Wieckowski et al., 2009). This is important in the ER-mitochondria calcium signalling and is involved in the transfer of lipids between the ER and mitochondria (Hayashi et al., 2009).

The inner membrane of mitochondria (IMM) is more complex in structure and is folded into a number of folds many times and is known as the cristae (Kuhlbrandt, 2015). The inner mitochondrial membrane contains proteins with five types of functions: (i) proteins that perform the redox reactions of oxidative phosphorylation OXPHOS, (ii) ATP synthase, which generates ATP in the matrix, (iii) specific transport proteins that regulate metabolite passage into and out of the matrix, (iv) protein import machinery, and (v) mitochondrial fusion and fission protein. The inner membrane contains more than 151 different polypeptides, and has a very high protein-to-phospholipid ratio (more than 3:1 by weight, which is approximately 1 protein for 15 phospholipids). The inner membrane is home to around 1/5 of the total protein in a mitochondrion. In addition, IMM is rich in an unusual phospholipid, cardiolipin. Cardiolipin contains four FAs rather than two, and may help to make the inner membrane

impermeable. Unlike the outer membrane, IMM does not contain porins, and is highly impermeable to all molecules. The inner membrane is permeable only to oxygen, ATP and also helps in regulating transfer of metabolites across the membrane. Almost all ions and molecules require special membrane transporters to enter or exit the matrix. In addition, there is a membrane potential ($\Delta\Psi$) across the inner membrane, formed by the action of the enzymes of the electron transport chain. The cristae proteins of IMM aid in the production of ATP molecules. Various chemical reactions take place in IMM. Intermembrane space is the space between the outer and inner membrane of the mitochondria, it has the same composition as that of the cell's cytoplasm. There is a difference in the protein content in the intermembrane space compared to the matrix. The matrix is the space enclosed by IMM. It contains about 2/3 of the total protein in a mitochondrion. The matrix is important in the production of ATP with the aid of the ATP synthase located in IMM. The matrix contains a highly concentrated mixture of hundreds of enzymes, special mitochondrial ribosomes, tRNA, and several copies of mitochondrial DNA (mtDNA). The major functions of enzymes of the matrix include oxidation of pyruvate and FAs, and the tricarboxylic acid cycle (the TCA cycle).

1.2.2 Mitochondrial genome

The human mitochondrial genome is a circular DNA molecule of about 16 kilobases (Chan, 2006). It encodes 37 genes: 13 for subunits of respiratory complexes I, III, IV and ATP synthase, 22 for mitochondrial tRNA (for the 20 standard amino acids, plus an extra gene for leucine and serine), and 2 for rRNA. One mitochondrion can contain 2 to 10 copies of its DNA. Although mitochondria contain their own small mtDNA and some RNA components of mitochondrial translation apparatus, the vast majority of the mitochondrial proteins are encoded by nuclear DNA, synthesized in the cytosol, and then imported post-transcriptionally into the mitochondria (Logan, 2006).

1.2.3 Mitochondrial function

Mitochondria are involved in the crucial metabolic processes including the TCA cycle, pyruvate decarboxylation, oxidative decarboxylation of FAs (β-oxidation), and degradation of branched amino acids. Mitochondria also substantially contribute to biosynthesis processes taking place in the cytosol by providing key intermediates to urea cycle, FAs and heme synthesis. However, the major role of mitochondria is synthesis more than 95% of ATP for cellular utilisation. Mitochondria are also deeply involved in the production of reactive

oxygen species (ROS) through electron carriers in the respiratory chain. Oxidative stress can induce apoptotic death and mitochondria have a central role in this process by cytochrome *c* release into the cytoplasm and opening of permeability transition pore (PTP) (Lenaz, 1998). Mitochondria are crucial for maintenance of normal physiological function of tissue cells and mitochondrial dysfunction may cause pathological changes in the human body. Moreover, eukaryotic cells have the ability to initiate adaptive responses to different environmental stimuli (cell growth, death and differentiation, or modification of energy demands) by altering the number, morphology, or remodelling of mitochondria (Pauw et al., 2009).

To encapsulate: mitochondria are mostly known for their role in meeting the cells' energy requirements in the form of ATP through OXPHOS. However, mitochondria also have functions in several other physiological processes: (i) buffering cytoplasmic calcium, (ii) controlling cellular redox status, (iii) generating and releasing ROS, (iv) releasing metabolites that regulate critical processes and pathways such a succinate and α-ketoglutarate, (v) regulating apoptosis, (vi) adapting cells to changes in substrate availability through different signalling pathways, and (vii) remodelling their structure and dynamics as sensor of their quality control.

1.2.3.1 Mitochondrial respiratory chain and oxidative phosphorylation

Oxidative phosphorylation, the aerobic production of ATP by mitochondria, requires a stepwise oxidation of electron donors reduced through catabolism of fuels comprising lipids, amino acids, and carbohydrates. This process depends on the orchestrated action of huge multiheterometric protein complexes anchored to IMM and encoded by both nuclear and mtDNA, commonly referred to as the mitochondrial respiratory chain.

Mitochondrial respiratory chain consists of four main protein complexes (I-IV) embedded in IMM (Nicholls and Ferguson, 2002). Cytochrome *c* is not membrane-bound. The spatial orientation of mitochondrial respiratory chain is shown in Figure 1.3. Mitochondrial respiratory complexes are responsible for the oxidation of the reducing equivalents, in the form of NADH or $FADH_2$, originating from different metabolic pathways (glycolysis, FA oxidation or the TCA cycle). Oxidation of NADH and $FADH_2$ is coupled to the pumping of protons into the intermembrane space, and the resulting proton gradient is used by ATP synthase to generate utilisable energy in the form of ATP. Complex I and complex II provide two electrons to ubiquinone (coenzyme Q, Q) resulting ubiquinol (QH_2, reduced ubiquinone). Ubiquinol transfer its electrons to complex III (bc_1 complex), which donates its electrons to cytochrome *c*. Reduced cytochrome *c* can transfer its electrons to

complex IV (cytochrome *c* oxidase). Subsequently, complex IV transfers the electrons to molecular oxygen. The movement of electrons through the electron transport chain is coupled to proton translocation from the mitochondrial matrix to the inner membrane space **(**Figure 1.3**)**. The pumping of protons across IMM generates an electrochemical gradient of protons ($\Delta\mu H^+$) consisting of pH gradient (ΔpH) and $\Delta\Psi$. These protons return down their gradient trough a proton leak or the ATP synthase. The ATP synthase couples the proton transport across the membrane to the synthesis of ATP from ADP to phosphate (Pi). The phosphate for phosphorylation is transported into the mitochondria by the phosphate carrier, and the ATP is exported to the cytosol in exchange for ADP by the adenine nucleotide carrier located in IMM.

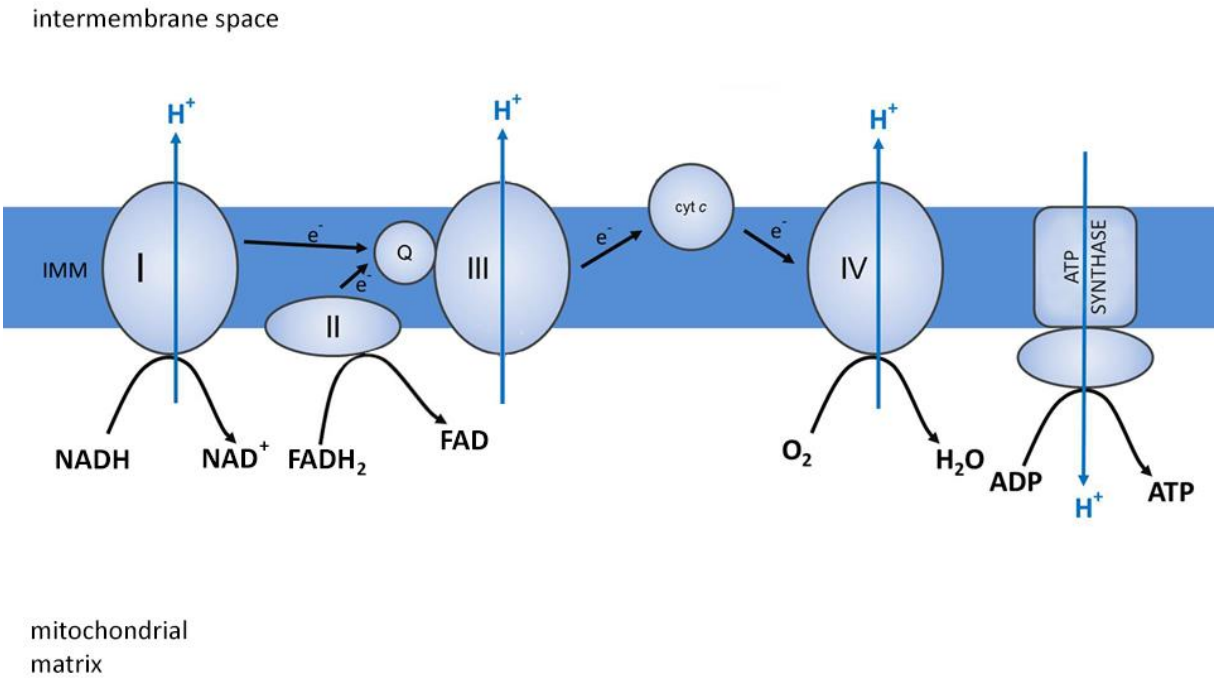

Figure 1.3 Respiratory chain complexes I-IV generate the proton gradient across IMM that drives ATP generation by ATP synthase. Electrons (e^-) from NADH and $FADH_2$ pass through complex I and complex II, respectively, and then to complex III via Q. Cytochrome *c* transfers electrons from complex III to complex IV, which reduces O_2 to H_2O. Flow of electrons is accompanied by H^+ transfer across IMM at complexes I, III and IV creating a proton electrochemical gradient ($\Delta\mu H^+$). Protons re-enter the mitochondrial matrix through ATP synthase, which uses the proton-motive force to generate ATP.

NADH-coenzyme Q oxidoreductase, also known as NADH dehydrogenase or complex I, is the first protein in the electron transport chain. Complex I is a giant enzyme with the mammalian complex I having 46 subunits and a molecular mass of about 1,000 kDa (Lenaz et al., 2006). The genes that encode the individual proteins are contained in both the cell nucleus and the mitochondrial genome, as is the case for many enzymes present in the

mitochondria. The reaction that is catalysed by complex I is the two-electron oxidation of NADH by Q, a lipid-soluble quinone that is found in IMM. The start of the reaction, and indeed of the entire electron chain, is the binding of a NADH molecule to complex I and the donation of two electrons. The electrons enter complex I via a prosthetic group attached to the complex, flavin mononucleotide (FMN). The addition of electrons to FMN converts it to its reduced form, $FMNH_2$. The electrons are then transferred through a series of iron–sulphur clusters, which are the second kind of prosthetic group present in the complex (Sazanov and Hinchliffe, 2006)**.** There are both [2Fe–2S] and [4Fe–4S] iron–sulphur clusters in complex I. As the electrons pass through this complex, four protons are pumped from the matrix into the intermembrane space. Finally, the electrons are transferred from the chain of iron–sulphur clusters to Q molecule in the membrane. Reduction of Q also contributes to the generation of a proton gradient, as two protons are taken up from the matrix as it is reduced to QH_2.

Succinate-Q oxidoreductase, also known as complex II or succinate dehydrogenase, is a second entry point to the electron transport chain (Cecchini, 2003). It is unusual because it is the only enzyme that is part of both the TCA cycle and the electron transport chain. Complex II consists of four protein subunits and contains a bound flavin adenine dinucleotide (FAD) cofactor, iron–sulphur clusters, and a heme group that does not participate in electron transfer to Q, but is believed to be important in decreasing production of ROS (Yankovskaya et al., 2003). Complex II oxidises succinate to fumarate and reduces Q. As this reaction releases less energy than the oxidation of NADH, complex II does not transport protons across IMM and does not contribute to $\Delta\mu H^+$.

Q-cytochrome *c* oxidoreductase is also known as cytochrome *c* reductase, cytochrome bc_1 complex, or simply complex III (Berry et al., 2000; Crofts, 2004). In mammals, this enzyme is a dimer, with each subunit complex containing 11 protein subunits, an [2Fe-2S] iron–sulphur cluster and three cytochromes: one cytochrome c_1 and two *b* cytochromes (Iwata et al., 1998). A cytochrome is a kind of electron-transferring protein that contains at least one heme group. The iron atoms inside complex III's heme groups alternate between a reduced ferrous (+2) and oxidised ferric (+3) state as the electrons are transferred through the protein. The reaction catalysed by complex III is the oxidation of one molecule of QH_2 and the reduction of two molecules of cytochrome *c*, a heme protein loosely associated with the mitochondrion. Unlike Q, which carries two electrons, cytochrome *c* carries only one electron. As only one of the electrons can be transferred from the QH_2 donor to a cytochrome *c* acceptor at a time, the reaction mechanism of complex III is more elaborate than those of the other respiratory complexes, and occurs in two steps called the Q cycle (Trumpower,

1990). In the first step, the enzyme binds three substrates, first, QH_2, which is then oxidised, with one electron being passed to the second substrate, cytochrome *c*. The two protons released from QH_2 pass into the intermembrane space. The third substrate is Q, which accepts the second electron from the QH_2 and is reduced to $Q^{-\bullet}$, which is the ubisemiquinone free radical. The first two substrates are released, but this ubisemiquinone intermediate remains bound. In the second step, a second molecule of QH_2 is bound and again passes its first electron to the cytochrome *c* acceptor. The second electron is passed to the bound ubisemiquinone, reducing it to QH_2 as it gains two protons from the mitochondrial matrix. This QH_2 is then released from the enzyme (Hunte et al., 2003). As Q is reduced to QH_2 on the inner side of the membrane and oxidised to Q on the other, a net transfer of protons across the membrane occurs, adding to the proton gradient. The rather complex two-step mechanism by which this occurs is important, as it increases the efficiency of proton transfer. If, instead of the Q cycle, one molecule of QH_2 were used to directly reduce two molecules of cytochrome *c*, the efficiency would be halved, with only one proton transferred per cytochrome *c* reduced.

Cytochrome *c* oxidase (COX), also known as complex IV, is the final protein complex in the electron transport chain (Calhoun et al., 1994). The mammalian enzyme has an extremely complicated structure and contains 13 subunits, two heme groups, as well as multiple metal ion cofactors; in all, three atoms of copper, one of magnesium and one of zinc (Tsukihara et al., 1996). This enzyme mediates the final reaction in the electron transport chain and transfers electrons to oxygen, while pumping protons across IMM (Yoshikawa et al., 2006). The final electron acceptor oxygen reduced to water in this step. Both the direct pumping of protons and the consumption of matrix protons in the reduction of oxygen contribute to $\Delta\mu H^+$. The reaction catalysed is the oxidation of cytochrome *c* and the reduction of oxygen.

ATP synthase is the final enzyme in the OXPHOS pathway (Leslie and Walker, 2000). The enzyme uses the energy stored in a proton gradient across a membrane to drive the synthesis of ATP from ADP and phosphate (P_i). This phosphorylation reaction is an equilibrium, which can be shifted by altering the proton-motive force ($\Delta\mu H^+$). In the absence of $\Delta\mu H^+$, the ATP synthase reaction will run hydrolysing ATP and pumping protons out of the matrix across the membrane. However, when the proton-motive force is high, the reaction is forced to run in the opposite direction; it allows protons to flow down their concentration gradient and turning ADP into ATP. ATP synthase is a massive protein complex. The mammalian ATP synthase contains 16 subunits and has a mass of ~600 kDa. The portion

embedded within the membrane is called F_O and contains a ring of *c* subunits and the proton channel. The stalk and the ball-shaped headpiece is called F_1 and is the site of ATP synthesis. The ball-shaped complex at the end of the F_1 portion contains six proteins of two different kinds (three α-subunits and three β-subunits), whereas the "stalk" consists of one protein: the γ-subunit, with the tip of the stalk extending into the ball of α- and β-subunits (Leslie and Walker, 2000). Both the α- and β-subunits bind nucleotides, but only the β-subunits catalyse the ATP synthesis reaction. Reaching along the side of the F_1 portion and back into the membrane is a long rod-like subunit that anchors the α- and β-subunits into the base of the enzyme. As protons cross the membrane through the channel in the base of ATP synthase, the F_O proton-driven motor rotates (Noji and Yoshida, 2001). Rotation might be caused by changes in the ionization of amino acids in the ring of *c*-subunits causing electrostatic interactions that propel the ring of *c* subunits past the proton channel (Capaldi and Aggeler, 2002). This rotating ring in turn drives the rotation of the central axle (the γ-subunit stalk) within the α- and β-subunits. The α- and β-subunits are prevented from rotating themselves by the side-arm, which acts as a stator. This movement of the tip of the γ-subunit within the ball of α- and β-subunits provides the energy for the active sites in the β-subunits to undergo a cycle of movements that produces and then releases ATP (Dimroth et al., 2006).

1.2.3.2 Calcium homeostasis

Mitochondria participate in intracellular Ca^{2+} homeostasis via several Ca^{2+} uptake and release pathways (Bernardi, 1999). In this context, mitochondria behave as a high-capacity, low-affinity transient Ca^{2+} store. An increase in cytosolic Ca^{2+} concentration induces Ca^{2+} entry across IMM and results in an elevation on the mitochondrial matrix Ca^{2+} concentration ($[Ca^{2+}]m$). Although this response serves primarily to buffer large, more pathophysiological changes in intracellular Ca^{2+} and may not be invoked by smaller transient changes that occur with physiological signalling, recent evidence indicates that mitochondria may act as a facilitation factor in the spreading of Ca^{2+} signals. These Ca^{2+}-regulating functions are supported by the observations of the close apposition between mitochondria and Ca^{2+}-release channels of ER, such a inositol 1,4,5-triphosphate [$Ins(1,4,5)P_3$] and ryanodine receptors, as well as proximity between mitochondria and plasma membrane (Camello-Almaraz, 2006).

1.3 Reactive oxygen species

Reactive oxygen species (ROS) is a term used to describe a variety of molecules and free radicals (chemical species with one unpaired electron) derived from molecular oxygen (Turrens, 2003). Molecular oxygen in the ground state is a bi-radical, containing two unpaired electrons in the outer shell (also known as triplet state). Since the two single electrons have the same spin, oxygen can only react with one electron at a time and therefore it is not very reactive with two electrons in a chemical bond. If one of the two unpaired electrons is excited and changes its spin, the resulting species (known as singlet oxygen) becomes a powerful oxidant as the two electrons with opposing spins can quickly react with other pairs of electrons, especially double bonds. The reduction of oxygen by one electron at time produces relatively stable intermediates. Superoxide anion ($O_2^{-\bullet}$), the product of a one-electron reduction of oxygen, is the precursor of most ROS and mediator in oxidative chain reactions. Dismutation of $O_2^{-\bullet}$ produces hydrogen peroxide (H_2O_2), which in turn may be fully reduced to water or partially reduced to hydroxyl radical (OH•), one of the strongest oxidant in nature. The formation of OH• is catalysed by reduced transition metals, which in turn may be re-reduced by $O_2^{-\bullet}$, propagating this process (Liochev and Fridovich, 1999). In addition, $O_2^{-\bullet}$ may react with others radicals including nitric oxide (NO•) in reaction controlled by the rate of diffusion of both radicals. The product, peroxynitrite is also powerful oxidant (Beckman and Koppenol, 1996; Radi et al., 2002). The oxidants derived from NO• is called reactive nitrogen species (RNS).

Oxidative stress is a various deleterious processes resulting from an imbalance between excessive formation of ROS and/or reactive nitrogen species (RNS) and limited antioxidant defences (Turrens, 2003). Sources of ROS production in the human tissue include the mitochondrial electron transport system, NADPH oxidases, xanthine oxidase, uncoupled nitric oxide synthase (NOS), and arachidonic acid metabolism pathways (12/15 lipoxygenase). These ROS sources vary in their pathological role and importance depend on the disease and the organ. Among them, the mitochondrial electron transport chain, NADPH oxidase, and xanthine oxidase are thought to be primary sources of ROS production in cardiomyocytes (Huynh et al., 2014), while NADPH oxidase, xanthine oxidase, and uncoupled NOS are thought to be primary sources of ROS production in vascular cells (Raaz et al., 2014).

1.3.1 Mitochondrial ROS production

Mitochondria reign as a major source of intracellular ROS. There are reports that between 0.2% and 2% of cellular mitochondrial oxygen consumption generates superoxide (Cadenas and Davies, 2000; Raha and Robinson, 2000). Multiple potential mitochondrial sites of ROS generation exist. These include the TCA cycle enzymes involved in redox reaction such α-ketoglutarate dehydrogenase and aconitase (Orrenius et al., 2007), glycerol-3-phosphate dehydrogenase from the glycerol-phosphate shuttle (Mracek et al., 2009), and monoamine oxidase (Bortolato et al., 2008; Vindis et al., 2001). Nevertheless, the huge majority of superoxide from mitochondria is produced, or modulated, by the complexes of the electron transport chain (Murphy, 2009).

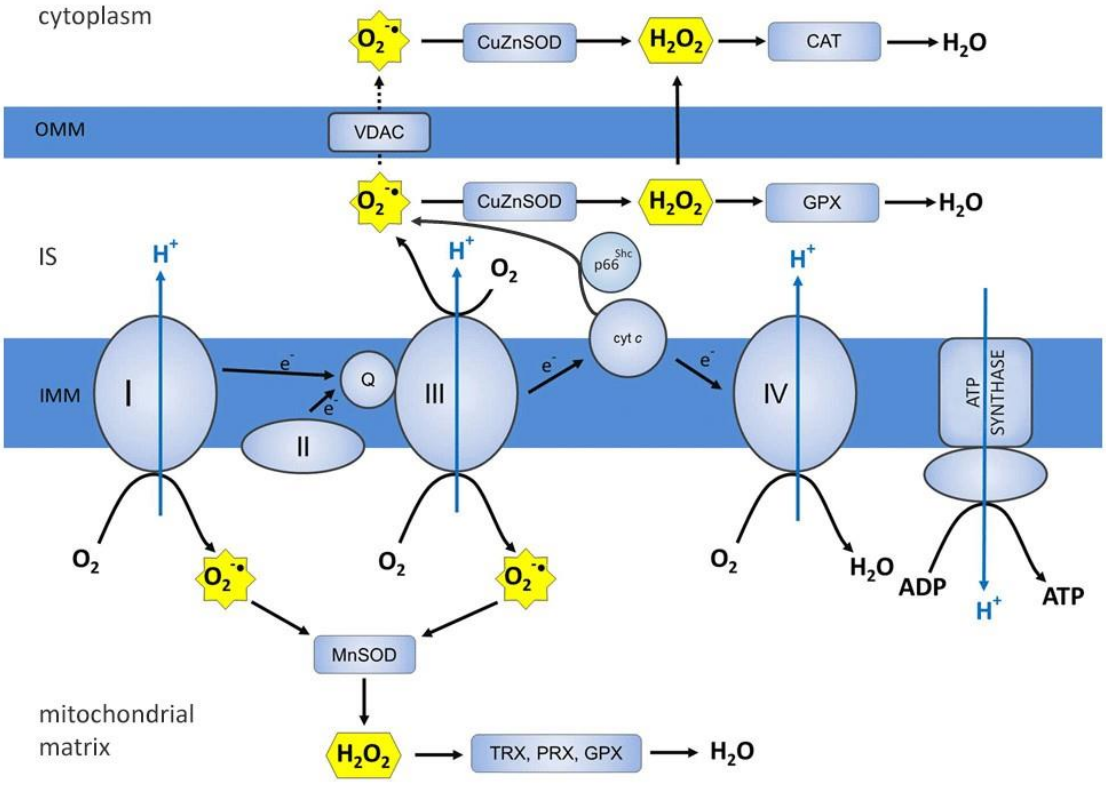

Figure 1.4 Electron transport chain and ROS production. The OXPHOS process receives reducing equivalents from the TCA cycle (NADH to complex I and $FADH_2$ to complex II) and passes these electrons down the transport chain, ultimately to reduce oxygen to water. Complex I leaks electrons to generate $O_2^{-\bullet}$ toward the matrix, whereas complex III generates $O_2^{-\bullet}$ toward both matrix and intermembrane space (IS). p66Shc in the IS subtracts electrons form cytochrome *c* to produce $O_2^{-\bullet}$. The voltage-dependent mitochondrial anion channel (VDAC) might serve as a conduit for intramembranous mitochondrial $O_2^{-\bullet}$ to pass through the outer mitochondrial membrane and into the cytoplasm. Superoxide is dismutated to H_2O_2 by manganese superoxide dismutase (Mn-SOD) in matrix and copper-zinc superoxide dismutase (CuZn-SOD) in IS and cytoplasm. H_2O_2 either may leave the mitochondria and react with mitochondria proteins, or may be reduced to H_2O by glutathione peroxidase (GPX), thioredoxin (TRX) or peroxiredoxin (PRX). In IS, H_2O_2 is reduced to H_2O by glutathione peroxidase (GPX), and in the cytoplasm by catalase (CAT) (Widlansky and Gutterman, 2011 - modified).

Superoxide anion can be produced at complex I, II and III of the mitochondrial electron transport chain (Turrens, 2003) (Figure 1.4). Complex I and II release $O_2^{-\bullet}$ into the mitochondrial matrix while complex III can release $O_2^{-\bullet}$ into either the mitochondrial intermembrane space or mitochondrial matrix (Muller et al., 2004). Notwithstanding, the mitochondrial electron transport chain generates $O_2^{-\bullet}$ primarily at complexes I and III (Zhang and Gutterman, 2007). In the past years, several studies have also demonstrated the role of complex II defect in formation of $O_2^{-\bullet}$. Among these, the groups of Quinlan et al. (Quinlan et al., 2012) and Siebles and Drose (Siebles and Drose, 2013) have studied ROS generation at complex II in artificial conditions, such a low concentration of succinate and inhibition of respiratory chain downstream to complex II. Additionally, ROS production by complex IV was demonstrated to be rather relevant in pathological conditions since hyperphosphorylation of complex IV on ischaemic hearts increases the electron leakage and, therefore the $O_2^{-\bullet}$ production (Prabu et al., 2006).

The relative contribution of every site to the overall $O_2^{-\bullet}$ production varies from organ to organ and also depends on whether mitochondria are actively respiring (phosphorylating state, state 3) or the respiratory chain is highly reduced (non-phosphorylating state, state 4) (Barja, 1999). The rate of $O_2^{-\bullet}$ formation by the respiratory chain is controlled by mass action, increasing both when electron flow slow down (increasing concentration of electron donors) and when the concentration of oxygen increases (Turrens et al., 1982). The energy released as electron flow through the respiratory chain is converted into a H^+ gradient through IMM (Mitchell, 1977). This gradient, in turn, drives ATP synthase and is responsible for ATP synthesis. In the absence of ADP, the movement of H^+ gradient builds up causing electron flow to slow down and the respiratory chain to become more reduced (state 4). As a results, the physiological steady state concentration of $O_2^{-\bullet}$ formation increases (Boveris et al., 1972). The formation of $O_2^{-\bullet}$ may be further increased in the presence of certain inhibitors (for example rotenone, an inhibitor of complex I, or antimycin, an inhibitor of complex III), which cause those carriers upstream form the site of inhibition to become fully reduced. In complex I, the primary source of $O_2^{-\bullet}$ appears to be one of the iron-sulphur clusters (Genova et al., 2001; Kushnareva et al., 2002). In complex III, most of the $O_2^{-\bullet}$ appears to be formed as a result of autoxidation of ubisemiquinone both on the outer and inner sides of IMM.

Complex III produces $O_2^{-\bullet}$ by autoxidation of ubisemiquinone radical intermediate ($QH^\bullet$), formed during Q cycle in the complex, with the Q_o site of the complex close to the

intermembrane space being the major site of $O_2^{-\bullet}$ production (Han et al., 2001). The Q_i site of complex III located close to matrix side is less likely to react with oxygen and form $O_2^{-\bullet}$ since the Q_i site firmly binds $QH^{\bullet}$ and stabilises it. Selective inhibitors of the Q_i portion of the cycle, such as antimycin A, prolong the lifetime of ubisemiquinone at the Q_o site and hence result in excess release of $O_2^{-\bullet}$. Inhibition of the proximal Q_o site by compounds such as myxothiazol inhibits the formation of ubisemiquinone at the Q_o site and thus reduces production of $O_2^{-\bullet}$. Complex III has the capacity to release $O_2^{-\bullet}$ to both sides of IMM, depending on the portion of the Q cycle involved (Han et al., 2001; Muller et al., 2004).

Complex I-derived $O_2^{-\bullet}$ seems to be predominately released into the matrix. Although precise mechanism of $O_2^{-\bullet}$ formation is unknown, it is suggested that complex I produces $O_2^{-\bullet}$ by reversible electron transfer from complex II upon succinate oxidation in the absence of NADH-linked substrates or in much lower amounts in the forward electron transfer from the NADH-linked substrates (Lenaz et al., 2006). Significant $O_2^{-\bullet}$ production from complex I was observed via reverse electron transfer, and this mechanism may account for more physiologically relevant ROS produced from mitochondria (Lambert and Brand, 2004). It is suggested that an iron-sulphur cluster distal in the electron transfer route of the complex could be the site of electron leak on $O_2^{-\bullet}$ production (Lenaz et al., 2006).

As a charged species, $O_2^{-\bullet}$ is not readily diffusible across mitochondrial membranes. However, mitochondrial PTP, containing the voltage-dependent mitochondrial anion channel (VDAC), might serve as a conduit for intramembranous mitochondrial $O_2^{-\bullet}$ to pass through the outer mitochondrial membrane and into the cytosol (Hand et al., 2003). Probably, a more important mechanism for transmembrane movement of reduced oxygen involves dismutation to hydrogen peroxide (H_2O_2) by superoxide dismutase (SOD). Once generated, the uncharged ROS, H_2O_2 can easily move across the membrane. H_2O_2 can generate the highly active hydroxyl radical via the Fenton reaction or the Haber-Weiss reaction. Hydroxyl radicals are short-lived, highly reactive, and contribute significantly to local organelle damage through protein modification.

1.3.2 Mitochondrial antioxidant defences

Superoxide is enzymatically converted to H_2O_2 by a family of metalloenzymes called superoxide dismutases (SOD) (Fridovich, 1995). There are three isoforms of SOD: copper-zinc SOD (CuZn-SOD or SOD1), manganese (Mn-SOD or SOD2), and an extracellular CuZn-SOD (EC-SOD or SOD3). CuZn-SOD is located in the cytosol, nucleus and intermembrane space of mitochondria (Okado-Matsumoto and Fridovich, 2001). Mn-SOD is

expressed solely in the mitochondrial matrix, and EC-SOD is found in the extracellular space. Each of them contributes to the reduction of $O_2^{-\bullet}$ to H_2O_2 (Figure 1.4). The physiological importance of Mn-SOD is demonstrated by the fact that, in contrast to other isoforms, genetic elimination of this isoform is embryonically lethal (Li et al., 1995). H_2O_2 can be further reduced by catalase and glutathione peroxidase. Glutathione peroxidase uses glutathione (GSH) to reduce H_2O_2 and lipid peroxides to water and corresponding alcohols, respectively. This is the primary mechanism for eliminating H_2O_2 in cytosol and mitochondria. Catalase is located mainly in peroxisomes and exclusively catalyses H_2O_2 to water. Catalase may be an important protective mechanism against a high concentration of H_2O_2 due to higher Km for H_2O_2 compared with glutathione peroxidase (Suttor et al., 1986). There are other enzymes such as thioredoxin (Zhang et al., 2004) and glutathione S-transferase, and antioxidant such as QH_2 and cytochrome *c*, that also help inactivate ROS produced from the mitochondria. Cytochrome *c* appears to have a detoxifying role against ROS. Ubiquinol (QH_2) has been shown to act as a reducing agent in the elimination of various peroxides in the presence of succinate (Binoldi et al., 1982; Eto et al., 1992). Thus, Q is a source of $O_2^{-\bullet}$ when partially reduced (semiquinone form) and an antioxidant when fully reduced (Beyer, 1990). Moreover, IMM contains vitamin E, a powerful antioxidant that interferes with propagation of free radical chain reaction (Ham and Liebler, 1995). Cytochrome *c* oxidase (complex IV) may also act as a peroxidase although, given the high Km to H_2O_2, the relevance of this reaction may be negligible (Orii, 1982).

1.3.3 Regulation of mitochondrial ROS production

The mitochondrial $\Delta\Psi$, intracellular Ca^{2+} and NO regulate or modulate mitochondrial ROS (mROS) production (Figure 1.5). As described above, $\Delta\Psi$ is the portion of the proton-motive force ($\Delta\mu H^+$) accounted for by the transfer of electrons through mitochondrial respiratory chain. Therefore, $\Delta\Psi$ is sensitive to mitochondrial respiratory chain substrate availability, pH and the fidelity of electron transport, with higher, more polarised $\Delta\Psi$ generally associated with greater mitochondrial superoxide production (Skulachev, 1998). When $\Delta\Psi$ is maximal, protons are less avidly pumped from the matrix to the intermembrane space, reducing mitochondrial respiratory chain flux and increasing the half-life of redox unstable intermediates (Thomas et al., 2008). Regulatory proteins in IMM also play a key role in modulating $\Delta\Psi$. Specifically, mitochondrial uncoupling proteins (UCPs) lead to membrane depolarisation and partial uncoupling of ATP synthesis from OXPHOS by reduction in the proton gradient. Suppression of UCP expression increases mROS production (Duval et al.,

2002), whereas overexpression of UCPs may attenuate mROS production, dependent on cellular ATP status (Fink et al., 2005).

The effects of elevated mitochondrial matrix Ca^{2+} concentration $[Ca^{2+}]m$ on mROS production are complex, and experimental findings are controversial (Brookes et al., 2004; Camello-Almaraz et al., 2006). Several mechanisms by which Ca^{2+} influence on mROS production have been suggested: (i) Ca^{2+} stimulates the TCA cycle and enhances electron flow into the respiratory chain; (ii) Ca^{2+} stimulates NO production by NO synthase, resulting in the inhibition of complex IV; (iii) and Ca^{2+} dissociates cytochrome *c* across the outer membrane (Brookes et al., 2004). Cytochrome *c* is a potent antioxidant, and its loss can result in more ROS liberation from mitochondria (Zhao et al., 2003). Under, some other conditions, mitochondrial Ca^{2+} uptake has no effect or slightly reduces mROS generation because, the increase in mitochondrial matrix Ca^{2+} concentration serves to collapse $\Delta\Psi$ (Brookes et al., 2004).

Nitric oxide is an inhibitor of the respiratory chain, and the relatively high basal concentration of NO in endothelial cells suggests that endothelial mitochondria respiration is restricted under basal conditions (Erusalimsky and Moncada, 2007). NO competes directly with O_2 at complex IV, reversibly inhibiting this complex and inducing mROS production (Cassina and Radi, 1996). NO also can inhibit complex I through S-nitrosylation (Burwell et al., 2006). Interaction between complex IV occurs rapidly and reversibly, playing an important role in short-term regulation of respiration and mROS production, whereas complex I inhibition by nitroso compounds is longer lasting, suggesting a greater role in long-term regulation of respiration and mROS production.

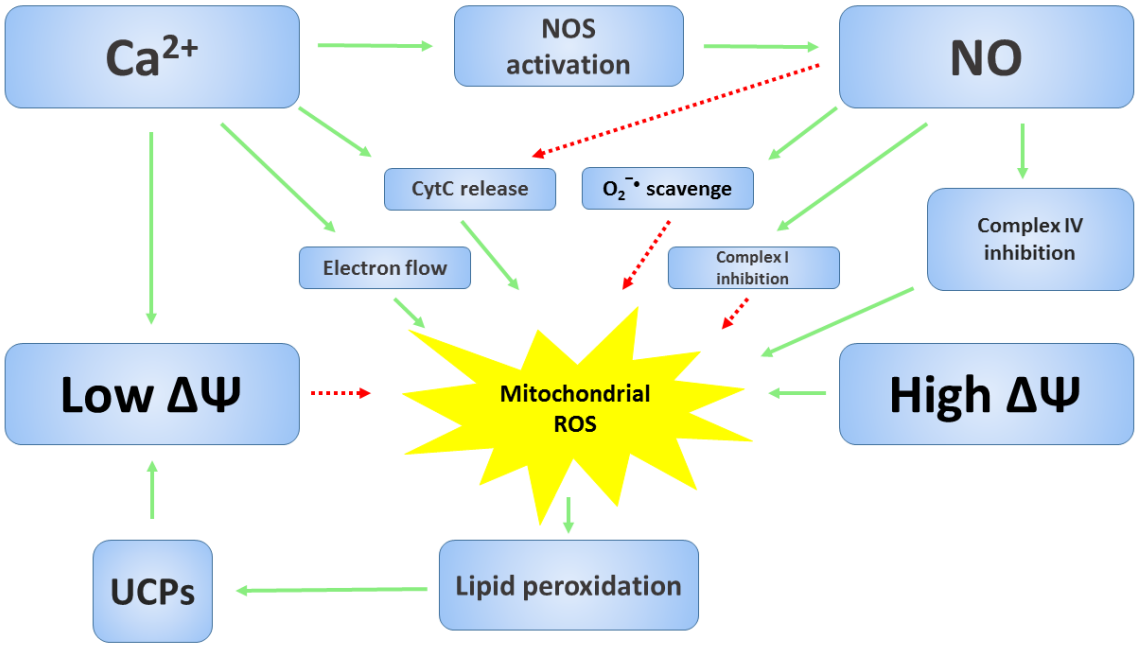

Figure 1.5 Regulation of mROS production by mitochondrial ΔΨ, Ca^{2+}, and NO. High ΔΨ favours the production of mROS, whereas low ΔΨ reduces. There is a negative feedback loop between mROS generation and membrane uncoupling. mROS increases lipid peroxidation, which in turn activates UCPs to induce mild uncoupling, thereby acting as a protective mechanism against excess mROS generation. Overall, Ca^{2+} seems to increase mROS production by 1) stimulation of the TCA cycle and enhancing the electron flow into the respiratory chain; 2) stimulation of NO production from NOS and consequent inhibition of complex IV; and 3) dissociation of cytochrome *c* (CytC) from IMM and higher concentration, including release of CytC across outer membrane. Under some conditions, Ca^{2+} may slightly decrease or exert no net effect on mROS production, possibly by lowering ΔΨ. NO in another important regulator of mROS. NO may either attenuate mROS production by inhibiting complex IV or attenuate mROS level by scavenging O_2^{-}• via peroxynitrite or CytC by inhibiting complex I. Solid green line, stimulatory pathway; dashed red line, inhibitory pathway (Zhang and Gutterman, 2007 – modified).

1.3.4 Non-mitochondrial ROS production

1.3.4.1 NADPH oxidase

Known as a member of the Nox family, NADPH oxidase is a multi-molecular enzyme composed of plasma membrane spanning cytochrome b_{558} (p22phox, gp91phox (Nox2)) and cytosolic components (rac, p47phox, p67phox, p40phox) (Kuroda et al., 2010). The major function of NADPH oxidase is to generate ROS, which sets it apart from other pathways that merely produce ROS as a by-product.

There are seven members of the Nox family (Nox1–5) and dual oxidase (Duox1–2) that have been identified, with Nox2 and Nox4 as the major myocardial isoforms (Kahles and Brandes, 2013). These have different cellular localizations, with Nox2 localised to the cell membrane, Nox4 to intracellular organelles around the nucleus. The intracellular localisation

reflects differences in their physiological, and by consequence pathological properties. Nox4 particularly has a mitochondrial localisation signal, and is expressed predominantly in the mitochondria of cardiac muscle cells (Ago et al., 2010). It has also been reported that the expression of Nox4 and the production of ROS are increased in pressure overloaded hearts (Kuroda et al., 2010). Disruption of Nox4 in cardiomyocyte significantly reduced cardiac hypertrophy, interstitial fibrosis and cardiomyocyte apoptosis in the presence of pressure overload, thereby improving cardiac dysfunction and reduced mitochondrial dysfunction (Kuroda et al., 2010). Moreover, infarct size after ischemia/reperfusion was also reduced in cardiomyocyte-specific Nox4 deletion mice compared to those of wild-type mice (Matsushima et al., 2013).

Several reports have also demonstrated increased activity of NADPH oxidase and expression of Nox4 in cardiomyocytes exposed to high glucose (Maalouf et al., 2012), as well as enhanced ROS production by NADPH oxidase in the heart of diabetic mouse models (Privratsky et al., 2003; Zhang et al., 2006). Furthermore, myocardial hypertrophy and fibrosis in type 1 diabetes mellitus is characterised by increased expression of Nox1 and Nox2 (Ritchie and Delbridge, 2006; Huynh et al., 2013). Similar increases in Nox have also been described in models of type 2 diabetes mellitus. Moreover, in the murine model of streptozotocin (STZ)-induced diabetes mellitus, a reduction in NADPH oxidase activation, due to Rac1 deficiency, has been shown to have beneficial effects upon myocardial remodelling (Shen et al., 2009). Taken together, these data suggest that NAPDH-generated ROS is associated with multiple cardiovascular complications in diabetes mellitus.

1.3.4.2 Xanthine oxidase

Xanthine oxidase is an enzyme present in the cytoplasm and catalyses oxidation of its substrates hypoxanthine and xanthine to uric acid using O_2 as an electron receptor and, in the process, produces $O_2^{-\bullet}$ and H_2O_2 (Kayama et al., 2015). These ROS are usually eliminated by antioxidant enzymes abundantly present in the cytoplasm (CuZn-SOD, GPx). However, hypoxanthine and xanthine oxidase are shown to react acutely with O_2 in ischemia/reperfusion states to produce a large amount of $O_2^{-\bullet}$ and H_2O_2, thus inducing cell damage as a consequence.

While this pathway is known to usually serve as an important source of ROS production in vascular endothelial cells, a similar role has been suggested for the xanthine oxidase pathway in cardiomyocytes as well (Ekelund et al., 1999). Administration of the

xanthine oxidase inhibitor, allopurinol, leads to improvements in cardiac as well as vascular function in a canine model of tachyarrhythmia-prone heart failure (Amado et al., 2005).

1.3.4.3 Lipoxygenases

Lipoxygenases (LOXs) constitute another important source of ROS production in both cardiomyocytes and vascular cells. LOXs are members of a family of lipid-peroxidising enzymes that oxidise free and esterified polyenoic FAs to form the corresponding hydroperoxy derivatives (Kuhn and O'Donnel, 2006). 12/15-LOX is a member of the LOX family that catalyses the step from arachidonic acid to 12(*S*)-hydroxyeicosatetraenoic acids (12(S)-HETE) and 15(*S*)-hydroperoxyicosatetraenoic acid (15(S)-HETE). Interestingly, while LOX metabolites of arachidonic acid mediate angiotensin II stimulation of NAD(P)H oxidase in cultured vascular smooth muscle cells (VSMC) (Zafari et al., 1999), arachidonic acid metabolism is itself another source of ROS production in vascular cells (Madamanchi, 2005). In addition, 12/15-LOX and its products, 12(S)-HETE and 15(S)-HETE, are implicated in the development of atherogenesis and heart failure (Bolick et al., 2006).

1.4 Endothelial mitochondria

In comparison with other cell types with higher energy requirements, mitochondrial content in endothelial cells is modest. In rat endothelial cells, for example, mitochondria compose 2-6% of the cell volume as opposed to 28% in hepatocytes and 32% in cardiac myocytes (Dromparis and Michelakis, 2013; Kluge et al., 2013). The low content of mitochondria in endothelial cells may indicate that mitochondrial-dependent OXPHOS is not that important for energy supplement. Endothelial cells obtain a large portion of their energy from anaerobic glycolytic metabolism of glucose. In cultured pig aortic endothelial cells, more than 75% of ATP is provided by glycolysis (Culic et al., 1997). Moreover, 99% of glucose is catabolised into lactate in isolated coronary microvascular endothelial cells, whole oxygen consumption is mainly attributable to oxidation of endogenous substrates (Spahr et al., 1989; Mertens et al., 1990). The relatively slight dependence of endothelial cells on OXPHOS has created the perception that mitochondria play no significant role in the endothelium and has thereby resulted in the neglect of their study in this context. However, several recent observations challenge this view by suggesting that mitochondria not only can contribute to ATP synthesis but also are centrally involved in maintaining the fine regulatory balance among mitochondrial calcium concentration, ROS production and NO (Davidson, 2010; Davidson and Duchen, 2007). Many questions must be addressed with respect to

understanding the physiological role that mitochondria play in endothelial cells and the contribution of endothelial mitochondria to vascular function and diseases.

1.4.1 Endothelial mitochondria as sensors of local environment

The positioning of the endothelial cells at the frontline in direct contact with the blood not only means that they are vulnerable to damaging molecules in the blood, but has them ideally situated for reconnaissance roles, sensing alternations in perfusate constituents and responding directly or transmitting reactive signals to nearby cells (Davidson and Duchen, 2007).

Rapid increase in endothelial production of NO and other vasodilatory molecules that occurs in response to even a modest decrease in arterial partial pressure of oxygen (PaO_2), causes vasodilation and increasing blood flow and O_2 supply (Davidson and Duchen, 2007). In various cell types, sensing of PaO_2 appears to be performed by ROS-producing system such as NADPH oxidase. Mitochondria have been proposed as the central oxygen sensors in the vasculature, particularly in the specialised case of hypoxic pulmonary vasoconstriction (HPV) via a mechanism, by which hypoxia causes an increase in the generation of mROS, which escape into the cytoplasm (Waypa and Schumacker, 2005). In coronary endothelial cells cultured in 5 mM glucose, O_2 does not decrease until PaO_2 drops below 3 mm Hg, and is half maximal at 0.8 mm Hg (Mertens et al., 1990) (compared with 1.6 mm Hg in resting cardiomyocytes (Rumsey et al., 1990)). ATP levels decrease in human umbilical vein endothelial cells (HUVEC) only when Po_2 is reduced to 3.5 mm Hg (Quintero et al., 2006). In cultured coronary endothelial cells, ATP levels remain constant even down to 0.1 mm Hg (either because of decreased ATP consumption or increased glycolysis) (Mertens et al., 1990). Inhibition of glycolysis can be tolerated by pig aortic endothelial cells for at least 3 hours, because of the fact that ATP-consuming pathways such as protein synthesis are co-ordinately downregulated when glycolysis is inhibited (Culic et al., 1997). When coronary endothelial cells are cultured with palmitate or glutamine to stimulate oxidative energy production, the adenine nucleotide contents decline rapidly at < 3 mm Hg oxygen (Martens et al., 1990). Mitochondrial ROS production is proportional to PaO_2, i.e., more mROS are generated at higher O_2 tension (Duchen, 2004). ROS production certainly does appear to increase during ischemia (Becker, 2004). Endothelial cells are the oxygen sensor of myocardium, they do, of course, respond to hypoxia by activating protective pathways common to many cell types. As the PaO_2 is reduced to 3.5 mm Hg, hypoxia-inducible factor (HIF1α) becomes stabilised in human microvascular endothelial cells (HMECs) (Quintero et al., 2006). NO produced by

human endothelial cells can regulate the activity of HIF1α and AMP-activated protein kinase (AMPK), thus affecting key response pathways to hypoxia and metabolic stress (Quintero et al., 2006). Endothelial cells respond to hypoxia by releasing Ca^{2+} from ER via inositiol-1,4,5-triposphate receptors (Peers et al., 2006). The mechanism involves ROS production and is suppressed when mitochondria are depolarised, suggesting that mitochondria may sense the hypoxia and transmit a signal to ER via mROS (Peers et al., 2006).

1.4.2 Endothelial mitochondria and diabetes

Type 2 diabetes entails hyperinsulinemia and hyperglycaemia and is also characterised by hyperlipidaemia. The progression of the disease is complicated by a number of secondary problems, in which the major target seems to be vascular, including a cardiomyopathy, increased occurrence of sudden death by cardiac infarction, and microvascular disease affecting the kidney and the retina (Poornima et al., 2006). The manifestation of vascular disease in the coronary arteries results in a greatly increased risk of heart failure in the diabetic population (Nesto et al., 2004; Beckman et al., 2002). Diabetes mellitus is associated with an increased risk of cardiovascular disease even in the presence of intensive glycaemic control. Vascular endothelial cells are an important target of hyperglycaemic damage. Mitochondrial dysfunction plays a central role in endothelial dysfunction in type II diabetes mellitus (Kizhakekuttu et al., 2012). In type II diabetes patients, mitochondrial function is impaired, which is evident from a lower mitochondrial O_2 consumption, $\Delta\Psi$, polymorphonuclear cell rolling velocity, and glutathione/glutathione disulphide (GSH/GSSG) ratio, and higher mROS production and rolling flux (Hernandez-Mijares et al., 2013). Hyperglycaemia-induced increase in the production of ROS by the mitochondrial electron transport chain in endothelial cells has been implicated in glucose-mediated vascular damage (Nishikawa et al., 2000; Brownlee, 2001; Du et al., 2003). Activation of AMPK reduces hyperglycaemia-induced mROS production and promotes mitochondrial biogenesis in HUVEC (Kukidome et al., 2006). In endothelial cells, AMPK activation by its agonists suppresses high-glucose-induced ROS generation by promoting mitochondrial biogenesis (Kukidome et al., 2006), inhibiting NADPH oxidase activity (Ceolotto et al., 2007), and inducing the expression of mitochondrial UCP2 (Xie et al., 2008) and MnSOD (Wang et al., 2011). Endothelium-selective activation of AMPK prevents diabetes mellitus-induced impairment in vascular function and re-endothelialisation (Li et al., 2012). In this regard, AMPK activator such as metformin could serve as candidate drug to improve mitochondria and subsequent endothelial function. Interestingly, a recent report has shown that mROS

enhances AMPK activation in the endothelium of patients with coronary artery disease and diabetes (Mackenzie et al., 2013). This finding may implicate that high glucose induces endothelial dysfunction by upregulating mROS, which in turn leads to the activation of AMPK. This feedback pathway may be a conserved pattern for the body to protect itself. Hyperglycaemia inhibits thioredoxin ROS-scavenging function through induction of thioredoxin-interacting protein (Txnip), which interacts with thioredoxin and serves as an endogenous inhibitor (Schulze et al., 2004; Li et al., 2009). Overexpression of Txnip increases oxidative stress, while Txnip gene silencing restores thioredoxin activity in hyperglycaemia (Schulze et al., 2004). In addition, Txnip induces inflammation through chromatin modification in retinal capillary endothelial cells under diabetic conditions (Perrone et al., 2009). Importantly, diabetic animals exhibit increased vascular expression of Txnip and reduced thioredoxin activity, which normalises with insulin treatment (Schulze et al., 2004). Mitochondria also contribute to hyperglycaemia-induced endothelial cells' apoptosis. In addition to mROS overproduction, other pathways have essential roles in this process. In human aortic endothelial cells, apoptosis-induced by hyperglycaemia involves mitochondrial depolarisation and mROS overproduction, which is prevented by the antioxidant N-acetyl-L-cysteine (Recchioni et al., 2002). The Ser/Thr Rho kinase 1 (ROCK1) is a potent regulator of mitochondrial dynamics in diabetic nephropathy and dynamin-related protein (Drp1) is a direct substrate for ROCK1. In hyperglycaemic conditions, ROCK1 phosphorylates Drp1 and leads to mitochondrial fission, mROS production, and subsequent release of cytochrome *c* (Wang et al., 2012). The mitochondrial permeability transition pore (PTP) is an oxidative stress-sensitive channel involved in cell death. Elevated glucose concentration leads to an oxidative stress that favours PTP opening and subsequent cell death in several endothelial cell types, and metformin prevents this PTP opening–related cell death (Detaille et al., 2005). There is some evidence suggesting that diabetic vascular disease results from oxidative stress. The endothelium is exposed directly to the blood and is therefore exposed directly to toxic metabolites and products such as oxidised low-density lipoprotein (oxLDL), which can cause damage directly by oxidative processes. Hyperglycaemia damages cells by causing increases in advanced glycation end products, increased hexosamine and polyol flux, and activation of classical isoforms of protein kinase C, via increased levels of oxidative stress (Brownlee, 2005). It has been shown that hyperglycaemia inhibits endothelial NOS (eNOS) activity and expression in aortic endothelial cells by increasing mitochondrial superoxide production (Srinivasan et al., 2004). Diabetes can lead to inhibition of endothelial NO production and derange normal vasodilation (Beckman, 2002). Hyperglycaemia may also affect

mitochondrial Ca^{2+} dynamics. Exposure of cultured endothelial cells to hyperglycaemic medium results in increased $[Ca^{2+}]m$ after histamine-mediated $[Ca^{2+}]c$ signalling, possibly as a consequence of altered mitochondrial morphology (Paltauf-Doburzynska et al., 2004). Hyperglycaemia may also induce endothelial apoptosis and contribute to the development of atherosclerosis (Du et al., 1998). The PTP may constitute part of the pathway toward endothelial cell death in diabetes as well as other pathologies. Conditions of oxidative stress or hyperglycaemia have been found to cause PTP opening in both HUVEC and bovine aortic endothelial cells (BAEC) (Detaille et al., 2005). Inhibition of PTP opening by exposure to cyclosporine A prevents this death (Detaille et al., 2005). Some antidiabetic drugs may have effects on the PTP. One of these drugs, metformin, appears to prevent opening of the PTP, although this may be secondary to metabolic effects of the drug (Detaille et al., 2005). In patients with inadequately controlled diabetes, myocardial energy utilisation shifts almost exclusively to the oxidation of free FAs. Although the consequence of this is extensively studied in cardiomyocytes, the effect on mitochondrial metabolism in endothelial cells has been largely disregarded because they are regarded as being primarily glycolytic. Activation of the fuel-sensing enzyme AMPK in endothelial cells promotes oxidation of FAs (but not glucose) as a source of ATP production, whereas dependence on glycolysis is decreased (Dagher et al., 2001). This suggests that in response to the metabolic disturbance associated with diabetes, the role of mitochondria as energy sources in endothelial cells might become significant. In a rat model of diabetes, HIF1α is increased, possibly indicating the existence of a state that has been termed “hyperglycaemic pseudohypoxia” (Williamson et el., 1993).

1.4.3 Mitochondrial ROS in cardiovascular diseases

At relatively low levels, mROS can be critical signalling molecules that support normal or compensatory function of the cell (Sena and Chandel, 2012). This fact means that mROS may increase even as part of normal signalling in the cell while the mitochondria themselves remain normal. Mitochondrial ROS are known to be biologically important in variety of physiological systems, including adaptation to hypoxia, regulation of autophagy, immunity, differentiation, and longevity. On the other hand, mROS have been implicated in the pathogenesis of cardiovascular diseases, such as atherosclerosis, hypertension, and diabetes. The mitochondrial dysfunction theory postulates that excess release of ROS from mitochondria is responsible for the inflammatory vascular reaction that leads to cardiovascular diseases (Ballinger, 2005; Puddu et al., 2005). Many cardiovascular risk factors, including hyperglycaemia and insulin resistance, hypercholesterolaemia and oxidation

of LDL, hyperhomocysteinemia, tobacco smoke exposure, and aging can adversely affect the function of endothelial cell mitochondria via various mechanisms, resulting in increased mROS generation. This increased mROS generation contributes to endothelial dysfunction and ultimately to the development of cardiovascular diseases. In addition, excessive mROS affect mitochondrial membranes, proteins and DNA, and cause further mitochondrial dysfunction through a vicious cycle. In addition to endothelial cells, increased production of mROS in other vascular cells (e.g., smooth muscle cells) may also contribute to the development of vascular lesions (Ballinger et al., 2002).

Most electrons flowing down the electron transport chain redox gradient ultimately reach ATP synthase. Moreover, 1-3% of electrons prematurely react with oxygen, at complexes I and III, to form superoxide and other types of ROS. In addition to complex I and III, other sources of mROS have been identified in endothelial cells (Tang et. al., 2014). One such example is the NADPH oxidase 4 (Nox4), which is highly expressed in endothelial cells and has been localised in mitochondria in other tissues. However, mitochondrial localisation in endothelial cells remains elusive. Nox4 is the most highly expressed the Nox family member in all cells of the cardiovascular system and is upregulated by a wide variety of agonists and cellular stresses. In endothelial cells, Nox4 is sensitive to mechanical forces. Nox4 and its homolog Nox2 are required for basal ROS production in endothelial cells' proliferation (Lassegue et al., 2012). Unlike Nox1, endogenous Nox4 predominantly produces H_2O_2 rather than $O_2^{-\bullet}$ (Dikalov et al., 2008). Current reports support that Nox4 is a protective ROS-generating vascular NADH oxidase partly through preventing endothelial dysfunction during ischemic and inflammatory stress (Schroder et al., 2012). Another example is the growth factor adaptor protein p66Shc, which functions in mitochondrial signalling. P66Shc facilitates the production of H_2O_2 by oxidising cytochrome *c* (Giorgio et al., 2005; Paneni et al., 2012).

Once excessive mROS is produced, cells rapidly response to oxidative stress by directly targeting the excessive ROS. Mn-SOD, which is predominant dismutase in mitochondria, is rapidly inducible and buffers the superoxide in the mitochondrial matrix by dismutating $O_2^{-\bullet}$ to H_2O_2. CuZnSOD buffers the $O_2^{-\bullet}$ that escapes into the intermembrane space and cytoplasm or even extracellularly. The levels of H_2O_2 are downregulated by antioxidant enzymes including catalase and peroxidases. Important mitochondrial peroxidases include thioredoxin-2, peroxididoxin-3, and glutaredoxin-2. Glutathione peroxidase-1 is located in both mitochondria and the cytoplasm of endothelial cells (Kluge et. al., 2013). Moreover, UCPs that are present in IMM decrease mROS production. UCP2 overexpression

in human aortic endothelial cells blocks FA-induced mROS generation (Lee et al., 2005). UCP2 preserves endothelial function through increasing NO bioavailability secondary to the inhibition of ROS production in endothelium of the obese diabetic mice (Tian et al., 2012). UCP2 upregulation also ameliorates hyperglycaemia-induced endothelial dysfunction (Sun et al., 2013).

Oxidative stress is closely associated with the pathogenesis of diabetes mellitus and results from overproduction of ROS (Kayama et al., 2015). ROS overproduction is associated with hyperglycaemia and metabolic disorders, such as impaired antioxidant function in conjunction with impaired antioxidant activity. Long-term exposure to oxidative stress in diabetes mellitus induces chronic inflammation and fibrosis in a range of tissues, leading to formation and progression of disease states. Indeed, markers for oxidative stress are overexpressed in patients with diabetes mellitus, suggesting that increased ROS may be primarily responsible for the development of diabetic complications. Diabetes mellitus and insulin resistance are characterised by elevated circulating levels of glucose and free FAs (Bogardus et al., 1984; Reaven et al., 1988). In endothelial cells, hyperglycaemia induces mitochondrial fission with subsequent development of excessive mROS production, reduced ATP production, and blunted cell growth (Yu et al., 2006). Endothelial cell-culture data demonstrate that exposure to high glucose (30 mM glucose for 7 days) increases endothelial ROS production. This phenomenon is primarily related to increases in mROS, because blunting of this effect occurs only with pharmacologic inhibition of complex II or exposure to MnSOD. Indicative of the cell-signalling capacity of mROS, mROS inhibitors also reduce nuclear factor kappa-light-chain-enhancer of activated B cells (NF-KB) and protein kinase C activation, and blunt the production of toxic advanced glycation end products and sorbitol (Nishikawa et al., 2000). Expression of cell-adhesion molecules on endothelial cell surface is dependent on mROS in the setting of high glucose (Srinivasan et al., 2003; Basta et al., 2005). Exposure to high concentration of free FAs (lysophosphatidylcholine and linoleic acid) increases $\Delta\Psi$, mROS, and NF-KB in human aortic endothelial cells (Lee et al., 2005). Each of this responses are inhibited by overexpression of UCP2, showing that reductions in mROS, linked to reduction in $\Delta\Psi$, are responsible for the observed improvement in endothelial function. Excessive mROS production in diabetes has been implicated as a “master switch” for activation of discrete pathologic signalling pathways leading to subsequent endothelial dysfunction through protein kinase C activation, increased age-related glycation end-product formation, and increased polyol and hexosamine pathway flux (Brownlee, 2001). In vivo, human studies have verified that hyperglycaemia induces such a state of endothelial

dysfunction through excessive oxidative stress. Hyperglycaemia has been shown to inhibit endothelial function in the forearm microvasculature through suppression of NO bioavailability (Williams et al., 1998). This reduced dilation during acute hyperglycaemia also is observed in patients with diabetes and can be improved by antioxidant therapy (Beckman et al., 2001).

1.4.4 Mitochondria and endothelial calcium homeostasis

The function of endothelial cells largely dependent on various extends on changes in intracellular Ca^{2+} concentration (Groschner et al., 2012). Although ER is the major storage site for calcium, 25% of cellular calcium is located in mitochondria. Mitochondria are also considered an important calcium buffering system. Mitochondria modulate Ca^{2+} signals by taking up, buffering, and releasing Ca^{2+} at key location near Ca^{2+} release or influx channels. The mitochondria and ER networks are very close proximity; actually, the two organelles communicate and corporate to regulate calcium trafficking and thereby orchestrate key aspects of endothelial function (Kluge et al., 2013). Calcium moving in and out of mitochondria is highly regulated. In endothelial cells, H_2O_2-induced increase in mitochondrial Ca^{2+} may depend partly on the decrease of Ca^{2+} extrusion via inhibiting the sodium/calcium exchanger (Jornot et al., 1999). UCP2 and UCP3 are fundamental for mitochondrial Ca^{2+} uniporter (MCU) activity in human endothelial cells (Trenker et al., 2007). Mitochondrial Ca^{2+} uptake controls intracellular Ca^{2+} signalling, cell metabolism, cell survival, and other cell-type specific functions by buffering Ca^{2+} levels and regulating mitochondrial effectors (Rizzuto et al., 2012). The very negative mitochondrial $\Delta\Psi$ allows mitochondria to sequester positive ions such as Ca^{2+} from the cytoplasm. Mitochondrial calcium is an important orchestrator of mitochondrial biogenesis per se and increases expression of peroxisome proliferator-activated receptor gamma coactivator 1α (PGC1α) (Szabadkai and Duchen, 2008). Physiological changes in the mitochondrial ($[Ca^{2+}]m$) and cytosolic ($[Ca^{2+}]c$) calcium concentrations have important regulatory effect on many aspects of mitochondrial functions, including mROS generation, energetics, motility, dynamics, and biogenesis (Davidson and Duchen, 2007; Kluge et al., 2013). There is increasing evidence that altered mitochondrial calcium contribute to endothelial response to pathophysiological stimuli. For example, mitochondrial calcium uptake stimulates NO production in mitochondria of bovine vascular endothelial cells (Dedkova et al., 2004). Elevated global endothelial concentration of Ca^{2+} promotes activation of eNOS, which, in turn, leads to the generation of NO (Katakam et al., 2013). Pharmacological depolarisation of endothelial mitochondria promotes activation of

eNOS by dual pathway involving elevated [Ca^{2+}]c as well as by phosphoinositide-3 kinase (PI3K)-induced eNOS phosphorylation. Depolarisation of mitochondria in endothelial cells promotes cerebral artery vasodilation (Katakam et al., 2013). Activation of tumor necrosis factor receptor 1 (TNFR1) ectodomain shedding by mitochondrial Ca^{2+} determines the severity of inflammation in mouse lung microvessels. This compensatory effect blunts the extent of endothelial activation under proinflammatory conditions (Rowlands et al., 2011). Moreover, the functions of many mitochondrial enzymes, including pyruvate dehydrogenase (PDH) are very calcium-dependent (Dromparis and Michelakis, 2013; Kluge et al., 2013). Calcium activates the TCA cycle enzymes and OXPHOS, thereby increasing ATP production. In addition to its direct effect on metabolic enzyme activity, a decrease in calcium influx hyperpolarises mitochondria, leading to mitochondrial and endothelial dysfunction.

1.4.5 Mitochondria and endothelial apoptosis

Mitochondria are implicated in cell death pathways, including apoptosis and necrosis. Supplementation of endothelial cells with mitochondrial targeted antioxidants inhibits peroxide-induced mitochondrial iron uptake, oxidative damage, and apoptosis (Dhansekaran et al., 2004). Ox-LDL induces dysfunction of the mitochondrial $\Delta\Psi$ leading to cytochrome *c* release into the cytosol, and thereby stimulates apoptosis of human endothelial cells. Apoptosis suppression by cyclosporine A (CSA) correlates with the prevention of mitochondrial dysfunction and thus indicates the importance of mitochondrial destabilisation in ox-LDL-induces apoptosis (Walter et al., 1998). Continuous oxidation of high-density lipoprotein (HDL) under hyperglycaemic conditions may induce endothelial apoptosis through mitochondrial dysfunction, following the deterioration of vascular function (Matsunaga et al., 2001). High glucose increases intracellular ROS and cell apoptosis through a mechanism involving interregulation between the cytosolic and mitochondrial ROS production. C-peptide activation of AMPKα inhibits high glucose-induced ROS production, mitochondrial fission, mitochondrial $\Delta\Psi$ collapse, and endothelial cell apoptosis (Bhatt et al., 2013). PGC-1α regulates ROS production and apoptosis in endothelial cells by increasing FA oxidation and enhancing ATP/ADP translocate activity (Won et al., 2010). Factors regulating the release of cytochrome *c* critically participate in mitochondria-dependent apoptosis of endothelial cells. A1, one of Bcl-2 family members, is localised to and functions in mitochondria. A1 is able to repress mitochondrial depolarisation, loss of cytochrome *c*, cleavage of caspase 9, a BH3 domain-containing proapoptotic Bcl2 family member (Bid), and poly(ADP-ribose) polymerase. A1 maintains temporary survival of endothelial cells in

response to TNF-α by maintaining mitochondrial viability and function (Duriez et al., 2000). Apoptosis signal-regulating kinase 1 (ASK1) mediates cytokines and ROS-induced apoptosis in a mitochondria-dependent pathway. Overexpression of thioredoxin-2 inhibits ASK1-induced apoptosis without effects on ASK1-induced JNK (c-Jun N-terminal protein kinase activation) in endothelial cells. Specific knockdown of thioredoxin-2 in endothelial cells increases TNFα, ASK1-induced cytochrome *c* release and cell death without increase in JNK activation, Bid cleavage, and Bcl-2 associated X protein (Bax) translocation (Zhang et al., 2004). In addition to apoptosis, mitochondria are also involved in necrosis. Mitochondria-mediated necrosis critically participates in cardiac myocyte dysfunction and cell death (Tait et al., 2013).

1.5 Uncoupling proteins

The uncoupling proteins (UCPs) are members of mitochondrial anion carrier family, which are present in IMM. They share a basic tripartite structure with six membrane-spanning α-helices divided by short helical domains in the matrix and loops in the intermembrane space (Rousset et al., 2004) (Figure 1.6). This family includes the adenine nucleotide translocase (ANT), an ATP/ADP antiporter, and multiple other metabolite and ion transporters. In contrast to basal leak, which is unregulated, UCPs can catalyse inducible proton leak that is sensitive to inhibitors.

UCP1, the first identified UCP, mediates non-shivering thermogenesis in brown adipose tissue (BAT) (Ricquier and Bouillaud, 2000). Four other members of this family were discovered: UCP2, UCP3, UCP4, and UCP5/brain mitochondrial carrier protein-1 (BMCP1). UCP2 and UCP3 are closest in amino acid identity to UCP1 (57% and 59% respectively) (Etchay et al., 2002). Whereas the UCP1 is detected mainly in brown adipocytes, UCP2 is present in many organs and cells types, and UCP3 is predominantly expressed in skeletal muscles and the heart. The tissue distribution of UCPs suggested a role other than adaptive thermogenesis. Following the discovery of various UCPs, they have become prominent in the fields of thermogenesis, obesity, diabetes, and free radical biology. UCPs have started to make an impact on the areas of degenerative, neurological, circulatory, and immunological diseases and aging. The proton conductance of UCPs is under tight control: inhibited by purine nucleotides and activated by free FAs.

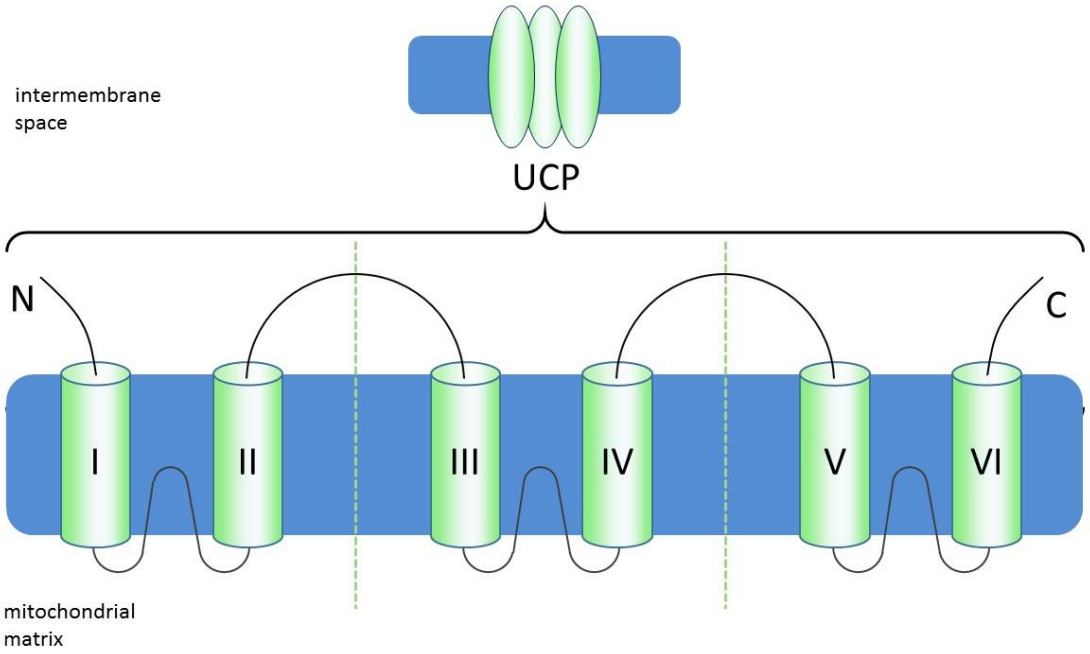

Figure 1.6 Model for UCPs and anion carriers of IMM. The protein is made of six transmembrane domains (numbers 1-6) linked by hydrophilic segments. The UCPs and mitochondrial anion transporters have a triplicated structure, with every third being made of two α-helices and a polar domain (Rousset et al., 2004 – modified).

1.5.1 Mechanism of UCP-mediated proton transport

The uncoupling activity of UCPs is explained by its ability to transport protons in particular when FAs bind to the protein. The question of the catalytic activity of UCPs is still debated between those who believe that UCP is a pure proton transporter activated by FAs (Klinbengerg, 1990), and others who consider that UCP mediates FA-induced uncoupling by trans-bilayer movement (flip-flop) of the protonated FA from the cytosolic to the matrix face of the inner membrane, with subsequent return of the anionic form to the cytosolic side (Skulachev, 1991) (Figure 1.7).

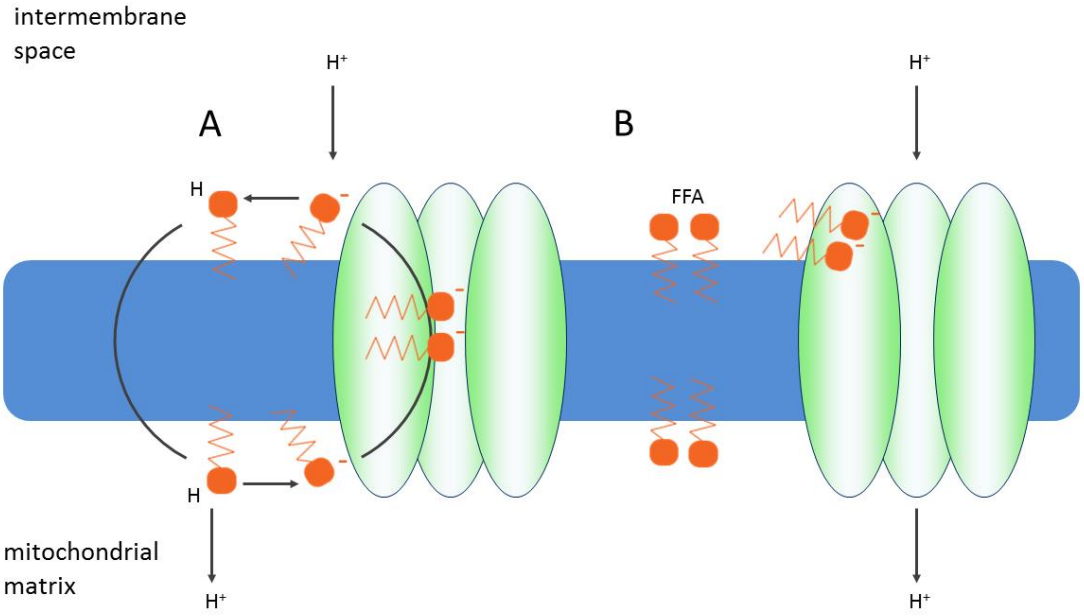

Figure 1.7 Schematic mechanism of proton transport by UCPs: proton release associated with cycling of free FA (FFA) (A), and direct proton translocation (B). (A) Illustrates the free diffusion of protonated FA through the membrane followed by a release of proton on the matricial side. Then, UCP returns the anionic form of FA through the membrane. (B) A direct transport of proton by UCP; the proton is provided by the carboxyl group of either amino acid residues or FA (Ricquier and Bouillaud, 2000 – modified).

The first hypothesis (Skuchalev, 1991) predicts the mechanism of FA cycling. UCPs and several other carriers are considered to conduct FA anions. The uniport of FA anions then leads to FA cycling, as FA anions can be protonated on a membrane trans-side and neutral FA can readily flip-flop back. FA dissociation releases H^+ and the resulting FA anion can enter the cycle again until all nonesterified FAs are depleted. The second hypothesis (the Klingenberg model) considers the existence of H^+ translocation pathway within the structure of UCPs and explain the observed FA-activation of UCP-mediated H^+ transport by local buffering (Kilngenberg, 1990). According to this hypothesis, ionised (anionic) FAs participate in jumps of H^+ over an array of sites, which form the H^+ translocation pathway.

1.5.2 Physiological role of UCPs

UCPs participate in various important physiological and pathological situations (Jezek, 2002). UCPs may contribute to body weight regulation, reduced ROS production, to various types of adaptive thermogenesis including fever, and to balancing apoptotic processes. Moreover, pathological implications in obesity, diabetes mellitus, and heart failure were revealed. Hormonal factors modulating the expression of UCPs have been described.

1.5.2.1 UCPs and prevention of ROS production

Mild uncoupling can be beneficial to cells and organism, as it causes a decrease in ROS formation (Skulachev, 1996). Mitochondrial ROS production is very sensitive to the proton-motive force ($\Delta\mu H^+$) set up across IMM by electron transport. Therefore, the mild uncoupling caused by activation of UCP2 and UCP3 might lower proton-motive force slightly, attenuate mROS production, and protect against oxidative stress (Skulachev, 1996; Kowaltowski et al., 1998; Etchay et al., 2002; Brand et al., 2002). Mild uncoupling implies a limited increase in proton conductance so that proton-motive force is slightly lowered and respiration rate is slightly increased, but ATP can still be produced. It differs from full uncoupling, where proton-motive force and ATP synthesis are abolished and respiration is maximal.

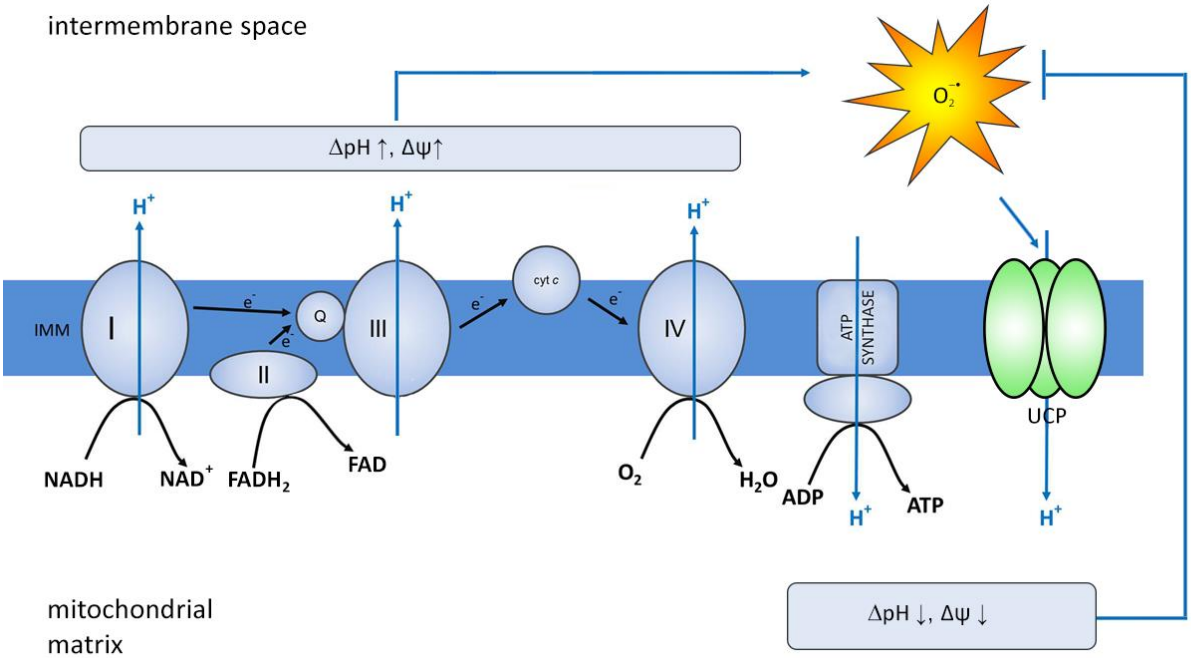

Figure 1.8 Antioxidative activity of UCPs. High ΔpH and ΔΨ of mitochondria will induce mROS production and thus oxidative damage; these mROS may activate UCPs and therefore cause a "mild uncoupling" and (as a negative feedback) will prevent further superoxide production and decrease oxidative damage (Liu et al., 2013 – modified).

1.5.2.2 UCPs and diabetes

Although two major types of diabetes have distinct aetiology, they lead to similar diabetic complications, and both of them are related to oxidative stress status. It is

demonstrated that activation of oxidative pathways plays a role in the development of not only the late complications (such as cardiovascular diseases, nephropathy, retinopathy, and amputations) in type 1 and 2 of diabetes mellitus, but also in the early stage such as insulin resistance (Maiese et al., 2007). Mitochondria are thought to be the main source of ROS generation in diabetes mellitus (Golbidi et al., 2012). The antioxidative activity of UCPs may be beneficial in diabetes mellitus and the complications. Uncoupling proteins may function as a sensor and a negative regulator of mROS generation under hyperglycaemia.

The relationship between UCP1 and diabetes mellitus has already been reported long before the other UCPs were discovered. Studies revealed that UCP1 mRNA and protein concentration in BAT were regulated by insulin (Geloen and Trayhurn, 1990; Burcelin et al., 1993). UCP1 has been proved to decrease $\Delta\Psi$, downregulate mROS production, and increase energy expenditure. Therefore, UCP1 gene is regarded as a candidate target gene in treatment of obesity or type 2 of diabetes mellitus. UCP1 had been thought to be expressed only in rodents and human infants for a long time. However, UCP1 protein and/or its mRNA expression were detected in human white adipose tissue, skeletal muscle, longitudinal smooth muscle layers, retinal cells, and islets cells (Carroll et al., 2005; Sale et al., 2007), although the physiological function of UCP1 in these tissue and organs are not established as well as in BAT. The imbalance between energy intake and expenditure is the underlying cause of obesity and diabetes mellitus. Brown adipose tissue consumes fuel for thermogenesis through tissue-specific UCP1. It was once thought that BAT had a functional role in rodents and human infants, but it has been shown that in response to mild cold exposure, adult human BAT consumes more glucose per gram than any other tissues (Orava et al., 2011). In addition to this nonshivering thermogenesis, human BAT may also combat weight gain by becoming more active in the setting of increased whole-body energy intake. These observations suggest that activation of BAT could be used as a safe treatment for obesity and metabolic dysregulation and further help to cure diabetes mellitus.

The mild uncoupling caused by activation of UCP2 may have a signalling role (Brand and Esteves, 2005). Activation of UCP2 may attenuate glucose-stimulated insulin secretion by pancreatic β cells. In the consensus model of the major route of glucose-stimulated insulin secretion by pancreatic β cells (Rutter, 2001), glucose catabolism increases the mitochondrial proton-motive force, the cytoplasmic ATP/ADP ratio rises, and plasma membrane K_{ATP} channels close, leading to depolarisation, opening the voltage-sensitive calcium channels, calcium influx, and insulin secretion. UCP2 could short-circuit this pathway by mild uncoupling, blunting the rise in proton motive force caused by raised glucose, and attenuating

insulin secretion (Chan et al., 1999). A plausible regulator of UCP2 function is FAs oxidation, which would rise β cell ROS production, activate the proton conductance of UCP2, and attenuate the insulin secretion (Brand et al., 2004; Lameloise et al., 2001), while hyperglycaemia may do the same pathologically (Zhang et al., 2001). UCP2 negatively regulate insulin secretion and is a major link between obesity, β-cell dysfunction, and type 2 of diabetes mellitus (Zhang et al., 2001).

UCP3 mRNA and protein levels are decreased in skeletal muscle od patients with type 2 of diabetes mellitus (Schrauwen et al., 2006). UCP3 content is reduced in prediabetes subjects (impaired glucose tolerance) and type 2 of diabetes mellitus, and eight weeks of rosiglitazone treatments significantly increases insulin sensitivity and restores skeletal muscle UCP3 protein in diabetic patients. Similar to UCP2, UCP3 has been found to be expressed in pancreatic β-cells, where it also influence of insulin secretion, although the physiological function of UCP3 in these cells is still not know (Li et al., 2008). UCP3 mRNA is expressed in human islets, but the relatively abundance of UCP2 is 8.1-fold higher. Immunohistochemical analysis has confirmed colocalisation of UCP3 protein with mitochondria in human β-cells. In human islets, UCP2 protein expression is increased approximately two-fold after high-glucose exposure, whereas UCP3 protein expression is decreased by ~40%. Moreover, UCP3 overexpression improves glucose-stimulated insulin secretion. Thus, UCP2 and UCP3 have distinct role in regulating β-cell functions; increased expression of UCP2 and decreased expression of UCP3 in humans with chronic hyperglycaemia may contribute to impaired glucose-stimulated insulin secretion (Li et al., 2008). The both, UCP2 and UCP3 can modulate cellular metabolism. The role of UCPs in the pathophysiology of chronic metabolic diseases such as type 2 of diabetes mellitus is highly dependent upon the specific UCP and its tissue of expression. Interesting, upregulation of UCP2 in pancreatic islets may lead to development of insulin insufficiency in type 2 of diabetes mellitus, while, in contrast, an increase in UCP3 expression in skeletal muscle could help to prevent the development of insulin resistance. Therefore, if the UCPs are to have any therapeutic relevance, strategies are required that incorporate acknowledgement of the need to upregulate UCP3 while decreasing activity of UCP2, tissue-specifically. In the case of UCP2, the treatment should not impact expression or activity in other tissues, like the brain, where it appears to confer cytoprotective effects.

1.5.2.3 Prospects: UCPs and drugs

Most cells seem to have one or more UCPs in their mitochondria. Therefore, this is very important to define the biological roles and biochemical function of particular UCPs, which must be better characterised and quantified in different tissues. UCPs seem to be related to lipid metabolism, and the relation between free FAs and UCPs needs to be defined, as does any role of UCPs in the metabolism of superoxide anions. UCPs' genes should be considered as putative targets of new drugs. Manipulation of the mitochondrial UCPs will be of interests for controlling the level of ROS in pathological situations. Any change in the level of coupling of mitochondria respiration to ADP phosphorylation has an effect on the production of free radicals and the cellular level of ROS (Skulachev, 1998; Nicholls and Budd, 2000).

1.5.2.4 UCPs and endothelial cells

Among the five mammalian UCPs isoforms, the expression of UCP2 and UCP3 is detected at the mRNA and protein level in various endothelial cells (Shimasaki et al., 2013). Increased UCP2 expression is common in highly proliferative cell types, including endothelial and cancer cells. UCP2 seems to be the primary UCP isoforms involved in regulation of endothelial metabolism. Exposure of endothelial cells to cellular stress: elevated ROS level or nutrient excesses, stimulates UCP2 expression, which involves a stress response coordinated by AMPK and PGC1α (Schulz et al., 2008; Valle et al., 2005). The ability to rapidly upregulate UCP2 expression may be important in protecting vascular endothelial cells from excess ROS formation. Although, the direct importance of UCP2 for the regulation of endothelial function has not be directly examined in humans, UCP2 may be related to human cardiovascular diseases. For instance, the 866G>A polymorphism is associated with increased UCP2 expression, decreased risk of coronary artery diseases in type 2 of diabetic men and is most likely associated with carotid artery atherosclerosis in middle-age women (Cheurfa et al., 2008; Oberkofler et al., 2005). It could be proposed that increased UCP2 expression in endothelial cells may aid in preventing the development and progression of vascular dysfunction. For instance, UCP2 could be a useful target in treating atherosclerosis or hypertension-related vascular events (Lee et al., 2005; Liu et al., 2013).

1.6 Mitochondria and hypoxia

Hypoxia (lack of oxygen) can occur in many ways:

- hypoxic hypoxia, caused by an insufficient oxygen concentration in the air in the lungs, which is common in during sleep apnoea, when the diffusion of oxygen to the blood is reduced or in high altitude sickness,
- hypoxemic hypoxia, which occur when the blood has reduced transport capacity as seen in carbon monoxide poisoning when haemoglobin cannot carry as much oxygen,
- stagnant hypoxia, occur when the cardiac output does not match the demands of the blood and the flow in not sufficient to deliver enough oxygenated blood to the tissue,
- sistotoxic hypoxia, when the cells cannot utilize the available oxygen, for instance during cyanide poisoning when oxygen cannot be used to produce ATP (Chan and Vanhoutte, 2013).

Moreover, hypoxia is observed in many diseases such as ischemia or cancer (Harris, 2002). Cells exposed to hypoxia respond acutely with endogenous metabolites and proteins promptly regulating metabolic pathways, but if hypoxia is prolonged, cells activate adapting mechanism, the master switch being HIF1. Activation of HIF1 is strictly related to the mitochondrial function, which in turns is related with the oxygen level. Moreover, under hypoxic conditions, mitochondria function as an oxygen sensor, convey signals to HIF1 directly or indirectly, contributing to cell redox potential, ion homeostasis and energy production.

1.6.1 Mechanisms of HIF activation

HIF1 is the heterodimeric transcription factor, which binds to hypoxia-responsive elements (HRE), activating the transcription of more than two hundred genes that allow cells adapt to hypoxic conditions (Semenza, 2003; Kaluz et al., 2008). HIF1 consists of an oxygen-sensitive HIF1α subunit that heterodimerises with the HIF1β subunit to bind DNA. In normal oxygen concentration, HIF1α is hydroxylated by prolyl hydroxylases (PHDs) using α-ketoglutarate derived from the TCA cycle. α-Ketoglutarate is required because the hydroxylation reaction is coupled to the decarboxylation of α-ketoglutarate to succinate. Hydroxylated HIF1α interacts with the von Hippel-Lindau protein (pVHL) (a critical member of an E3 ubiquitin ligase complex) that polyubiquitylates HIF. Then, it is catabolised by

proteasomes, such that HIF1α is continuously synthesised and degraded under normoxic conditions (Semenza, 2003) (Figure 1.9). Under hypoxic conditions, HIF1α hydroxylation does not occur stabilising HIF1.

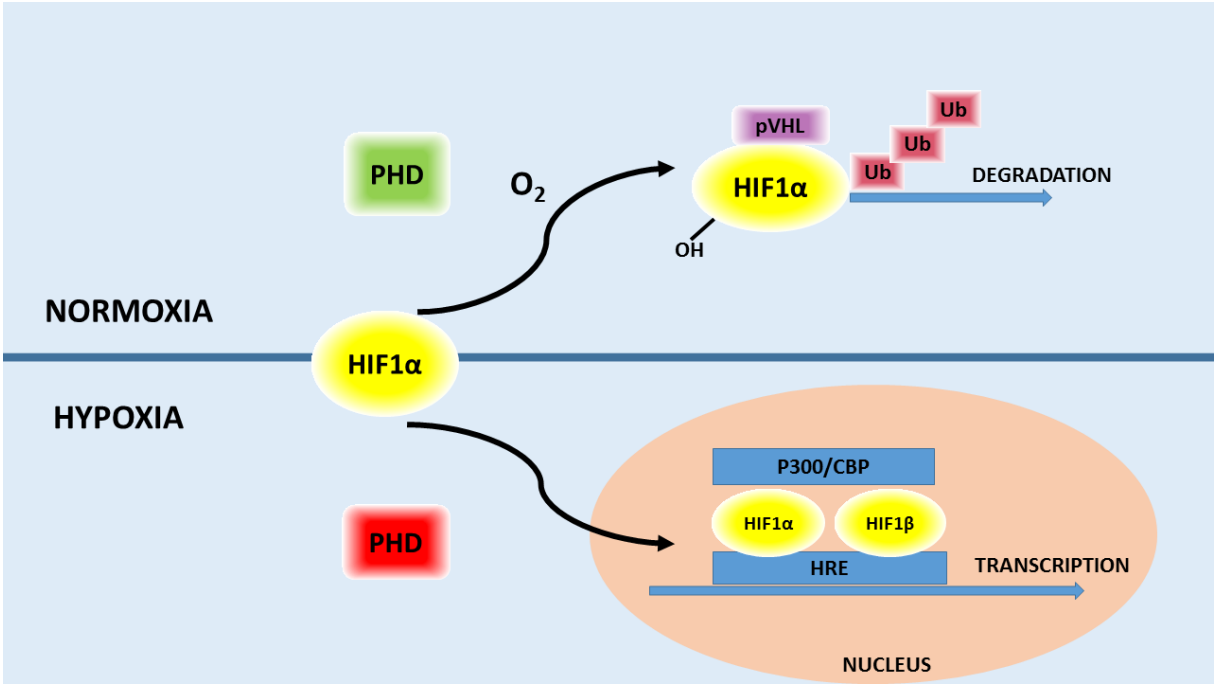

Figure 1.9 Hypoxia inducible factor HIF1α stabilisation in normoxia vs HIF1α degradation under hypoxia. Top: PHD in the presence of oxygen hydroxylates HIF1α. Which can then bind to von Hippel Lindau protein (pVHL). This event promotes the polyubiquitination of HIF1α followed by 26S-proteasomal degradation. Bottom: the lack of oxygen prevents the hydroxylation of HIF1α by PHD, leading to its stabilisation. HIF1α can then migrate to the nucleus and associate with HIF1β and the cofactor p300/CBP. The HIF1 complex binds to and induces the transcription of genes containing hypoxia-responsive elements (HRE) with core sequence 5'-ACGTG-3' in their promoter region (Balligand et al., 2009 – modified).

The active HIF1 complex binds to a core HRE in a wide array of genes involved in diversity of biological processes, and directly transactivates glycolytic enzyme genes (Semenza, 2007). Oxygen concentration, multiple mitochondrial products, including the TCA cycle intermediates and ROS can coordinate PHD activity, HIF stabilisation, hence the cellular response to oxygen deficiency (Pan et al., 2007; Lin et al., 2008). Impairment of the TCA cycle could be relevant for the metabolic changes occurring in mitochondria exposed to hypoxia, sine accumulation of succinate has been reported to inhibit PHDs (Koivunen et al., 2007). Moreover, it has been reported that ROS are crucial to activate HIF1 (Kietzmann and Gorlach, 2005).

1.6.2 Mitochondrial ROS and HIF regulation

As mentioned above, mROS regulate HIFs. There is a lot of evidence that hypoxia paradoxically increases ROS production (Duranteau et al., 1998; Chandel et al., 1998). Increased generation of ROS at complex III is required for HIF1α protein stabilisation during hypoxia (Klimova and Chandel, 2008). The overexpression of catalase abolished the HIF1α accumulation in response to hypoxia (Chandel et al., 2000). How ROS inhibit the hydroxylation of the HIF1α is currently unknown. The available data do not allow to definitely state a precise role of mROS in regulating HIF1α, but the pathway stabilising HIF1α appears undoubtedly mitochondrial-dependent (Pan et al., 2007). The hydroxylation reaction of HIF1α requires the reduced form of iron (Fe^{2+}). It is possible that hydrogen peroxide produced during hypoxia oxidises Fe^{2+} to Fe^{3+} (Gerald et al., 2004).

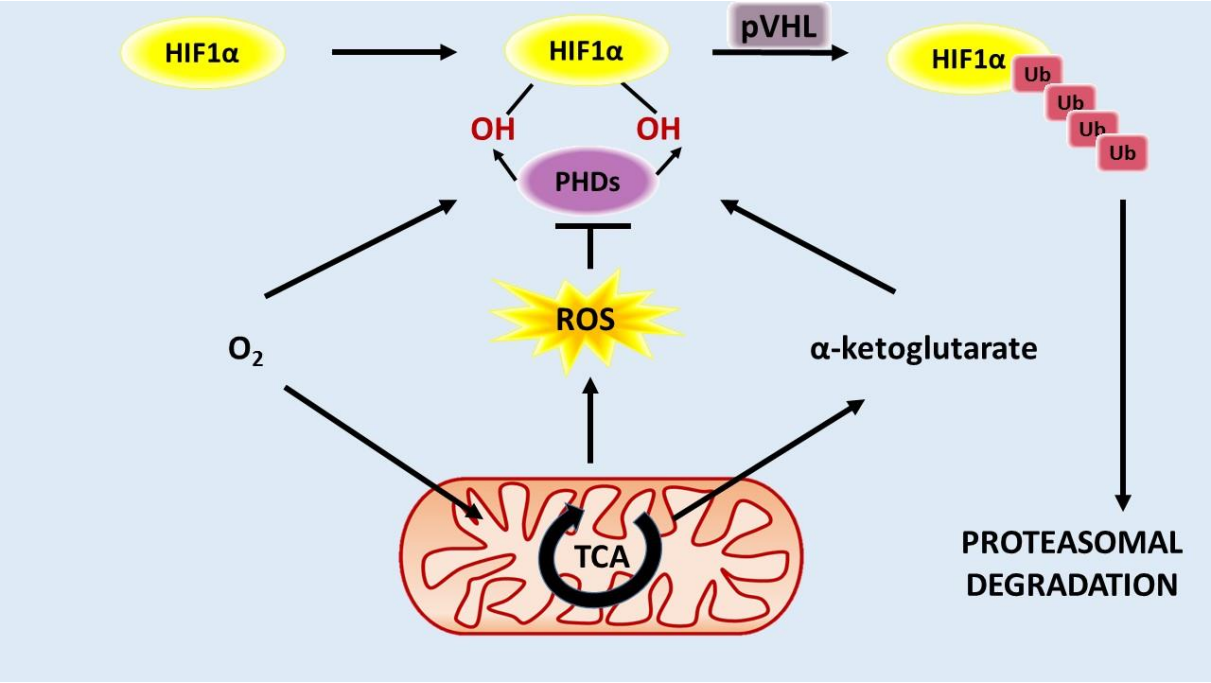

Figure 1.10 HIF1α proteins are hydroxylated at two distinct proline residues by prolyl hydroxylases (PHDs) under normoxic conditions. The hydroxylation directs HIF1α proteins for pVHL mediated ubiquitin dependent degradation. The hydroxylation reaction requires oxygen and α-ketoglutarate as substrates. Mitochondria can regulate hydroxylation by controlling availability of oxygen and the TCA cycle intermediate α-ketoglutarate to the PHDs. Under hypoxic conditions, the release of ROS from mitochondrial complex III results in prevention HIF1α proteins hydroxylation and stabilisation. Mitochondria regulate HIF1α proteins through ROS, oxygen, and α-ketoglutarate availability (Tormos and Chandel, 2010 - modified).

1.6.3 The TCA cycle intermediates and HIF regulation

The TCA cycle intermediates have the influence on HIF stabilisation (Tormos and Chandel, 2010). Prolyl hydroxylases (PHD) convert the TCA cycle intermediate α-ketoglutarate to succinate in order to hydroxylate the HIF1α subunit. Rise in succinate prevents hydroxylation. Succinate is normally converted into fumarate within the TCA cycle by succinate dehydrogenase, a membrane-bound enzyme that is also component of the mitochondrial electron transport chain (complex II). Moreover, fumarate could also regulate HIF activation (Pollard et al., 2005). Fumarate inhibits the forward hydroxylation reaction similar to succinate (Isaacs et al., 2005). Moreover, loss of fumarate hydratase results in ROS-dependent activation of HIF (Sudarshan et al., 2009). The fumarate hydratase mutations activate HIF by increases in the ROS and fumarate levels.

1.6.4 Effects of hypoxia on energy metabolism in cells

Without a doubt hypoxia (reduced oxygen level) affects energy metabolism in cells. There is a lot of data, which indicate that low oxygen reduces OXPHOS, the TCA cycle, and participates in the generation of NO, which also contributes to decreased respiration rate (Galkin et al., 2007; Brunori et al., 2004). Active HIF has effect on cellular energy homeostasis by inactivation of anabolism, activation of glycolysis, and inhibition of mitochondrial energy metabolism, i.e., the TCA cycle and OXPHOS. HIF1 activates transcription of genes encoding glucose transporters and glycolytic enzymes to further increase flux of reducing equivalents from glucose to lactate (Iyer et al., 1998; Lum et al., 2007). Pyruvate is normally converted to acetyl-CoA by the pyruvate dehydrogenase complex (PDC) and consumed by the TCA cycle. This process is regulated by pyruvate dehydrogenase kinase (PDK1), which phosphorylates pyruvate dehydrogenase and thus inhibits pyruvate dehydrogenase complex (Kolobova et al., 2001). PDK1 levels in hypoxic PC12 cells were elevated, indicating a decrease in pyruvate consumption in mitochondria and activation of pyruvate-to-lactate conversion (Zhandov et al., 2013). HIF1 regulates pyruvate supply to mitochondria through activation of PDK1 (Papandreou et al., 2006; Kim et al., 2006). Activation of HIF1α induces PDK1, which inhibits pyruvate dehydrogenase complex, suggesting that respiration is decreased by substrate limitation (Papandreou et al., 2006; Kim et al., 2006). Moreover, subunit composition of COX is altered by increased degradation of the COX4-1 subunit, which optimises COX activity under aerobic conditions, and increased expression of COX4-2 subunit, which optimises COX activity under hypoxic conditions (Semenza, 2007). On the other hand, direct assay of respiration rate in cells exposed to

hypoxia resulted in significant reduction in respiration (Zhang et al., 2008). According to this data, the respiration rate reduction has to be ascribed to mitochondrial autophagy, due to HIF1 mediated expression of BNIP3 (Bcl2/adenovirus E1B 19 kDa interacting protein 3). Moreover, there is a lot of data indicating a de-activation of complex I when oxygen is lacking, as it occurs in prolonged hypoxia (Galkin et al., 2009).

Hypoxia induces reprogramming of respiratory chain function and switching from oxidation of NAD-related substrates (complex I) to succinate oxidation (complex II). (Lukyanova, 1997, Lukyanova et al., 2013). The dissociation of complex I from the large supercomplexes occurs under hypoxic conditions, when succinate accumulates as a substrate for complex II (Sanborn et al., 1979; Acin-Perez et al., 2004; Althoff et al., 2011; Chen et al., 2012; Moreno-Lasters et al., 2012). Hypoxia is connected with activation of succinate dehydrogenase and succinate oxidation and with increased contribution of the latter to respiration and energy production (Acin-Perez et al., 2004; Althoff et al., 2011; Chen et al., 2012, Moreno-Lasters et al., 2012). The contribution of succinate dehydrogenase may reach 70-80% (Lukyanova et al., 2007). Under hypoxic conditions, complex II may function as an independent enzyme, whose activity is limited only by the substrate availability. The complex II driven electron flow is the primary way of mitochondrial membrane polarization under hypoxic conditions and the lack of succinate resulted in reversible $\Delta\Psi$ loss that could be restored by succinate supplementation (Nowak et al., 2008; Hawkins et al., 2010). Succinate dehydrogenase pathway is energetically more efficient under the hypoxic conditions (Hawkins et al., 2010). As mentioned above, proteasomic degradation of HIF1α in normoxic condition is coupled with utilisation of NAD-dependent substrate of the TCA cycle, α-ketogultarate, while another the TCA cycle substrate, succinate, is an allosteric inhibitor of this process (Semenza, 2002; Hewitson et al., 2010). Hypoxia inhibits the malate-aspartate bypass, which provides α-ketoglutarate to the cytosol, whereas succinate synthesis is intensified. Moreover, induction of HIF1α requires a low complex I activity and high complex II activity (potentiation of succinate oxidation) (Lukyanova et al., 2007; Lukyanova et al., 2011; Kirova et al., 2013; Lukyanova, 2014). However, the mentioned hypoxia-induced responses in aerobic metabolism are well documented mainly in cancer and brain cells. This issue has not been intensively studied in endothelial cells.

1.6.5 Endothelial mitochondria and hypoxia

Being the first cell layer in contact with blood, endothelial cells have to cope with all changes occurring within the blood. One of these changes is the variation in the oxygen

tension. Endothelial cell response to hypoxic stress can result in two different consequences in the surrounding tissues, depending on the duration of the exposure: short-term exposure causes physiological and reversible modulation of vascular tone and blood flow; chronic hypoxic stress results in irreversible remodelling of the vasculature and surrounding tissues, with smooth muscle proliferation and fibrosis (Faller, 1999). In endothelial cells, hypoxia initiates a number of responses that include cell growth and proliferation, increase in permeability, and changes in cell-surface adhesion molecules. Endothelial mitochondria may act as oxygen sensors in the signal cascade of hypoxic responses (Chandel and Schumacker, 2000). NO produced by human endothelial cells can regulate the activity of HIF1α and AMPK, thus affecting key response pathways to hypoxia and metabolic stress, respectively (Quintero et al., 2006). It has been reported that reoxygenation after hypoxia stimulates ROS production from complex III in HUVEC (Therade-Matharan et al., 2005). It remains unclear how mitochondria-derived ROS production in endothelial cells triggers ROS production from other cellular sources and activates AMPK, which can alter fuel selectivity and also protects cells from apoptosis during anoxia (Quintero et al., 2006, Davidosn, 2010). Some studies suggest that endothelial mitochondria regulate HIF1α and HIF2α stabilisation by releasing ROS to the cytosol (Davidson, 2010). It has also been suggested that endothelial mitochondria may sense the hypoxia and transmit via ROS a signal to ER that in turns releases Ca^{2+} (Peers et al., 2006). The influence of hypoxic exposure of endothelial cells (especially chronic exposure to hypoxia) in the aerobic metabolism, particularly mitochondrial oxidative function, has not been intensively studied. Many question must be addressed with respect to understanding the role of endothelial mitochondria in response to metabolic disturbances that relate to hypoxia.

1.7 Potassium channels and endothelial cells

Potassium channels are the most widely distributed and divers class of ion channels. They form potassium selective pores in cell membrane and control multiple cell function. Variety of ion channels is present in plasma membrane of endothelial cells. These includes the potassium channels such a Ca^{2+}-regulated K^+ channels (K_{Ca} channels), inwardly rectifying K^+ channels (K_{IR} channels), voltage-dependent K^+ channels (K_V channels), two-pore-domain potassium channels (K_{2P} channels), and also ATP-regulated potassium channels (K_{ATP} channels) (Feletou, 2009; Katnik and Adams, 1997; Nilius and Droogmans, 2001; Zaritsky et al., 2008). Endothelial potassium channels have been implicated in endothelium-dependent vasodilation. It is due to setting the $\Delta\Psi$ leading to modulation of endothelial Ca^{2+} signalling

and synthesis of vasodilating factors. The three subtypes of Ca^{2+}-regulated potassium channels (K_{Ca} channels) of large, intermediate and small conductance (BK_{Ca}, IK_{Ca}, and SK_{Ca}) are present in vascular wall. BK_{Ca}, channels are preferentially expressed in vascular smooth muscle cells, while IK_{Ca}, and SK_{Ca} are usually located in endothelial cells. Endothelial potassium channels are implicated in the control of vascular tone by several mechanisms, e.g., release of NO and endothelial-derived hyperpolarising factor.

Potassium-selective channels similar to these found in the plasma membrane have been also identified in IMM (Szabo et al., 2012). Potassium fluxes through IMM, which are involved in the regulation of mROS concentration, affect the mitochondrial volume and change both the mitochondrial $\Delta\Psi$ and the transport of Ca^{2+} into the mitochondria. Additionally, potassium flux across IMM into the mitochondrial matrix plays a key role in the cytoprotection of various mammalian cells.

1.7.1 Mitochondrial large conductance calcium-activated potassium channel

BK_{Ca} channels are present in the plasma membranes of different mammalian cell types. They are activated by changes in the concentration of free calcium and membrane depolarisation. The channels assemble as tetramers of the pore-forming α-subunit, which may be associated with distinct β-subunits (β1-β4), depending on the tissue. Together, these subunits determine the electrophysiological and pharmacological properties of the channel. The properties of mitochondrial large conductance Ca^{2+}-activated potassium ($mitoBK_{Ca}$) channels are similar to those of surface BK_{Ca} channels (Szewczyk et al., 2009). A mitochondrial large conductance Ca^{2+}-activated potassium channel ($mitoBK_{Ca}$) was originally described using patch-clamp technique in human glioma cell line LN229 (Siemen et al., 1999). It was observed in patch-clamp recording form mitoplasts of guinea pig ventricular cells that $mitoBK_{Ca}$ is stimulated by Ca^{2+}, potassium channel opener 1,3-dihydro-1-[2-hydroxy-5-(trifluoromethyl) phenyl]-5-trifluoromethyl)-2H-benzimidiazol-2-one (NS1619); blocked by charybtotoxin, iberiotoxin, and paxiline (Xu et al., 2002). Electrophysiological and pharmacological data from patch-clamp recordings of the mitoplasts of guinea pig ventricular cells have indicated that $mitoBK_{Ca}$ may protect guinea pig hearts from infarction (Xu et al., 2002). With the use of the patch-clamp technique, it has been shown that hypoxia increases $mitoBK_{Ca}$ activity of rat liver and astrocyte mitochondria (Cheng et al., 2008). Moreover, $mitoBK_{Ca}$ channels have been shown to contribute to the protection of cardiomyocytes isolated from chronically hypoxic rats (Borchert et al., 2011). Recently, with the use of planar lipid bilayers, two electrophysiologically different types of $mitoBK_{Ca}$

channels were observed in brain mitochondria (Fahanik-Babaei et al., 2011). To determine the subcellular localisation and distribution of the channel, rat brain fractions were examined by Western blot analysis, immunocytochemistry and immunogold electron microscopy (Douglas et al., 2006). These studies provide concrete morphological evidence for the existence mitoBK$_{Ca}$ channels (α-subunit) in IMM of rat brain cells. Moreover, rat skeletal muscle and brain mitochondria show immunoreactivity against antibodies targeting the BK$_{Ca}$ β4-subunit (Piwonska et al., 2008; Skalska et al., 2009; Skalska et al., 2008). These findings indicate a close molecular similarity between the mitoBK$_{Ca}$ channel and the plasma membrane BK$_{Ca}$ channel, suggesting that both channels are splice variants of the same gene product. Studies of BK$_{Ca}$ α-subunit in mitochondria revealed compartmentalisation in sensory cells, whereas heterologous expression of a BK-DEC splice variant cloned from cochlea revealed a BK mitochondrial candidate (Kathiresan et al., 2009). This channel may offer a link between cellular-mitochondrial calcium signalling and mitochondrial ΔΨ-dependent reactions. Altered mitochondrial calcium levels directly affects the potassium permeability of IMM, modulate ΔΨ thus can affect the efficiency of OXPHOS. The mitoBK$_{Ca}$ channel is expected to affect mitochondrial metabolism due to regulation of matrix volume (Halestrap, 1994). Moreover, it is reasonable to expect a possible cytoprotective effect of mitoBK$_{Ca}$ activation, probably in the presence of superoxide radicals (Stowe et al., 2006). It was also found, that cardioprotective effects of estradiol include the activation of mitoBK$_{Ca}$ in cardiac mitochondria (Ohya et al., 2005).

So far, no information has been reported about mitoBK$_{Ca}$ in endothelial mitochondria. This channel was described in some other mammalian mitochondria. Various observations suggest that mitochondria contributes to cytoprotective effects in various tissues. It seems that mitochondrial potassium channels such as Ca^{2+}-activated channels, play the important role in these effects. Mitochondrial potassium channels present in endothelium may be involved in protective mechanisms. Moreover, endothelial mitochondria may constitute an attractive target for potassium channel modulators. It seems to be very important to search for mitoBK$_{Ca}$ in the mitochondria of endothelial cells and to determine the electrophysiological and biochemical properties of this channel.

2 Aims

Mitochondria are found in most human cells; however, the synthesis of ATP in endothelial cells occurs primarily via a glycolytic pathway. The role of endothelial mitochondria as energy sources might become significant in response to metabolic disturbances. Many questions must be addressed with respect to understanding the physiological role that mitochondria play in endothelial cells and the contribution of endothelial mitochondria to vascular function and diseases. No previous studies have directly demonstrated that isolated endothelial mitochondria are efficient and well coupled.

The general goal of this doctoral thesis was to study the aerobic metabolism of endothelial cells under physiological and pathophysiological conditions.

The particular aims of the presented study were:

- to examine mitochondrial respiratory functions in endothelial EA.hy926 cells and isolated mitochondria,
- to assess the influence of chronic exposure to high-glucose levels on the aerobic metabolism of endothelial EA.hy926 cells,
- to characterise the UCP2 function in isolated endothelial mitochondria and endothelial cells, and to determine how this function is altered by long-term growth in high-glucose concentrations,
- to assess the influence of chronic hypoxia on the aerobic metabolism of endothelial EA.hy926 cells,
- to identify mitoBK$_{Ca}$ in the mitochondria of endothelial EA.hy926 cells and to determine the biochemical properties of this channel.

3 Material and methods

3.1 Cell culture

A permanent human endothelial cell line EA.hy926 (ATCC® CRL-2922™) was originally derived from a human umbilical vein. This line was derived by fusing human umbilical vein endothelial cells HUVEC with the permanent human cell line A549 (Edgell et al., 1983). Bioenergetic studies were conducted on isolated mitochondria, especially measurements of oxygen uptake, require large quantities of output material, i.e., at least a few grams of endothelial cells. Noteworthy is fact that one confluent 140 mm-diameter culture dish (75 cm^2), gives only 0.08-0.09 g of EA.hy926 cells. The obtaining of such amount of cells is very difficult in the case of primary cell lines, which are characterised by cell proliferation, which is limited to a small number of cell doublings. Therefore, the most suitable for the presented study seems to be permanent endothelial cell line EA.hy926.

The EA.hy926 cells were cultured in dishes of 140 mm in diameter until they reached ~90-100% confluence. Cells that were between passages 5 and 12 were used in this study. EA.hy926 cells were grown in DMEM (Dulbecco's modified Eagle's medium) supplemented with 10% foetal bovine serum (FBS), 1% L-glutamine, 2% HAT (hypoxanthine-aminopterin-thymidine medium), and 1% penicillin/streptomycin in a humidified atmosphere of 5% CO_2 at 37°C. During standard cell culture, O_2 concentration was 20%. During cell culture, the medium was changed every 3 days.

In high-glucose studies (Chapter 4.1 and Chapter 4.2), except for determination of a time-course of high-glucose-induced respiratory response (Figure 4.2), the EA.hy926 cells were cultured for 6 days in DMEM culture medium with either 5.5 or 25 mM D-glucose, representing normal- and high-glucose conditions, respectively. In some experiments, the culture medium with 5.5 mM D-glucose plus 19.5 mM L-glucose was used as an osmolality control.

In hypoxia studies (4.3), the EA.hy926 cells were cultured in DMEM culture medium with 5.5 mM D-glucose. The EA.hy926 cells were cultured for 6 days at two different oxygen concentrations, 20% and 1%, representing normoxic and chronic hypoxic conditions, respectively.

In mitoBK$_{Ca}$ studies (Chapter 4.4), the EA.hy926 cells were cultured for 6 days in a standard DMEM culture medium with 5.5 mM D-glucose and at 20% of O_2 tension.

3.2 Cell fraction preparation

The EA.hy926 cell cultures from 50 dishes were harvested with trypsin/EDTA, and rinsed twice with phosphate-buffered saline (PBS) (with 10% and 5% FBS, respectively), and centrifuged at 1,200 g for 10 min. Subsequently, the cells were washed in cold DMEJ medium containing 5.4 mM KCl, 0.8 mM $MgSO_4$, 110 mM NaCl, 44 mM $NaHCO_3$, 1.1 mM NaH_2PO_4, and 10 mM Na/Na buffer, pH 7.2, and were then centrifuged once again. The final cell pellet was resuspended in the same medium (1 g of cells per 2 ml medium) and kept on ice. The cells were counted prior to assays using a Burke haemocytometer. The yield of harvested cells did not differ significantly between the normal and high-glucose cells as 3.32 ± 0.24 g of cells (805,000 ± 78,000 cells) and 3.77 ± 0.14 g of cells (870,000 ± 104,000 cells) (S.E., n = 15), respectively, were harvested from 50 dishes of each culture. The yield of harvested cells differed significantly between the control and the hypoxia-treated cells. Namely, 4.3 ± 0.6 g and 3.8 ± 0.05 g of cells (SD, n = 25, $P < 0.05$), respectively, were harvested from 50 dishes of each culture (when cells were inoculated at the same density).

3.3 Mitochondria isolation

All of the subsequent steps were performed at 4^{o}C. After they were harvested and washed in PBS, EA.hy926 cells were resuspended in PREPI medium (0.25 M sucrose, 1.5 mM EDTA, 1.5 mM EGTA, 0.2% bovine serum albumin (BSA), and 15 mM Tris/HCl, pH 7.2) at a ratio of 3 ml of medium per 1 g of cells. The cells were then homogenised by 10 passes with a tight Dounce homogeniser, and the homogenates were subsequently centrifuged at 1,200 *g* for 10 min. The pellets were resuspended, and the cells were once again homogenised (eight passes) and centrifuged to collect the mitochondria remaining in the pellet. The supernatants were combined and centrifuged at 1,200 *g* for 10 min, and the resultant supernatants were then centrifuged at 12,000 *g* for 10 min. The mitochondrial pellets were washed with a PREPII medium containing 0.25 M sucrose and 15 mM Tris/HCl, pH 7.2, and centrifuged at 12,000 *g* (10 min). The final pellet was resuspended in a small volume of the same medium.

The yields of isolated mitochondria were equal to 3.9 ± 0.4, 2.9 ± 0.4 ($P < 0.05$), and 3.1 ± 0.3 ($P < 0.05$) (means ± SD; n = 15) mg of mitochondrial protein per g of cells for cells grown in control conditions (normal-glucose and normoxia), high-glucose conditions (25 mM glucose and normoxia), and hypoxic conditions (normal-glucose and 1% O_2), respectively.

3.4 Cytosolic fraction preparation

To obtain cytosolic fractions for enzymatic measurements, cells were homogenised in one step in the PREPII medium with the Polytron homogeniser (T18 basic, IKA) (8 times for 5 s, at 80% power). The homogenates were subsequently centrifuged at 1,200 *g* for 10 min. After spinning down the unbroken cells and cell debris, the supernatants were collected for measurements of activities of citrate synthase (CS), cytochrome *c* oxidase (COX), and lactate dehydrogenase (LDH).

3.5 Mitoplast preparation

Mitoplasts were prepared from the mitochondrial fraction by a swelling procedure. The mitochondria were added to a hypotonic solution containing 5 mM HEPES (pH 7.2) and 100 μM $CaCl_2$ for 1 min to induce swelling and breakage of the mitochondrial outer membrane. Afterwards, the suspension was added to a hypertonic solution composed of 750 mM KCl, 100 μM $CaCl_2$, and 30 mM HEPES (pH 7.2) to restore the sample to an isotonic condition. The mitoplast suspension was centrifuged at 12,000 *g* (10 min) and the final pellet was resuspended in a small volume of the latter medium.

3.6 Measurement of cell respiration

The mitochondrial respiration in detached EA.hy926 cells was determined polarographically as previously described for the extracellular flux analysis in adherent bovine aortic endothelial cells (BAEC) (Dranka et al., 2010). Measurements were performed in 0.7 ml of PBS or DMEJ medium with 0.5-0.7 mg of cell protein with a Hansatech oxygen electrode at 37°C. To estimate the ATP-linked oxygen consumption rate (OCR) and non-ATP-linked OCR (proton leak) components of the basal respiratory rate, oligomycin (1 μg/ml) was added to inhibit ATP synthesis (Figure 3.1). Subsequently, the proton ionophore (uncoupler) carbonyl cyanide 4-(trifluoromethoxy) phenylhydrazone (FCCP, 0.4 μM) was added to determine the maximal OCR that the cells can sustain. Finally, cyanide (0.5 mM) was added to inhibit complex IV (COX) and thereby block the entire mitochondrial cytochrome pathway. In the presence of cyanide, no residual (non-mitochondrial) respiration was observed. The following substrates were used: 5 mM pyruvate, 5.5 mM D-glucose, 25 mM D-glucose, 5 mM pyruvate, 3-5 mM L-glutamine, or 0.3 mM palmitate.

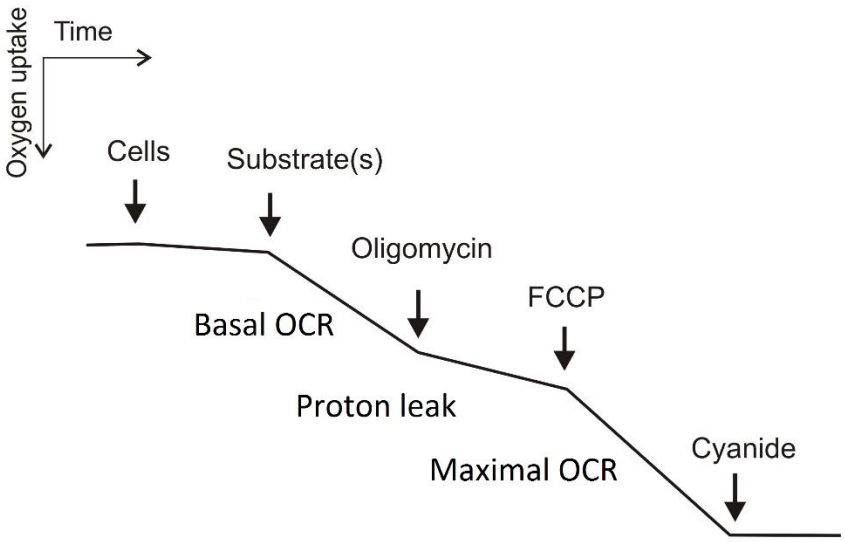

Figure 3.1 A scheme for the OCR measurements with the sequential addition of respiratory substrate(s), oligomycin (1 µg/ml), FCCP (0.4 µM), and cyanide (0.5 mM).

3.7 Measurement of mitochondrial respiration and membrane potential

Oxygen uptake was determined polarographically using a Rank Bros. (Cambridge UK) oxygen electrode or a Hansatech oxygen electrode in either 1.4 ml or 2.8 ml of standard incubation medium (37°C), which consisted of: 150 mM sucrose, 2.5 mM KH_2PO_4, 1-2 mM $MgCl_2$, 20 mM Tris/HCl, pH 7.2, and 0.1% BSA, with either 0.7 or 2 mg of mitochondrial protein (isolated mitochondria). ΔΨ was measured simultaneously with oxygen uptake using a tetraphenylphosphonium (TPP^+)-specific electrode. The TPP^+-electrode was calibrated by four sequential additions (0.4, 0.4, 0.8, and 1.6 µM) of TPP^+. After each run, 0.5 µM FCCP was added to release TPP^+ for base-line correction. For the calculation of the ΔΨ value, the matrix volume of endothelial mitochondria was assumed to be 2.0 µl × mg^{-1} protein. The calculation assumes that the TPP^+ distribution between mitochondria and medium followed the Nernst equation. The values of ΔΨ were corrected for TPP^+ binding using the apparent external and internal partition coefficients of TPP^+ (Woyda-Ploszczyca et al., 2011). The correction shifted the calculated value ΔΨ s to lower values (approx. 30 mV-shift), but it did not influence the changes in the resulting ΔΨ (relative changes). O_2 uptake values are presented in nmol O_2 × min^{-1} × mg^{-1} protein. The values of ΔΨ are given in mV.

Phosphorylating (state 3) respiration was measured using 0.12-0.15 mM (pulse) or 1 mM ADP, and uncoupled respiration was measured using 0.25-0.5 µM FCCP. Non-

phosphorylating (resting, state 4) respiration measurements were performed in the absence of exogenous ADP and the presence of 1.8 μM carboxyatractyloside and 0.5 μg/ml oligomycin, which inhibited the activities of an ATP/ADP antiporter and ATP synthase, respectively. During OXPHOS studies, the inhibitors were omitted.

The 5 mM TCA cycle substrates (malate, succinate in the presence or absence of 1-2 μM rotenone, pyruvate, α-ketoglutarate, and isocitrate), 5 mM glutamate, and 0.3 mM palmitoylcarnitine were used as respiratory substrates. When succinate was used as a respiratory substrate, measurements were performed in the presence of 0.05-0.15 mM ATP to activate succinate dehydrogenase.

Only high-quality mitochondria preparations, i.e., with an ADP/O value of ~1.3 and a respiratory control ratio (RCR) of ~2.5-3.2 (during succinate oxidation), and with an ADP/O value of ~2.3 and RCR of 3.6-4.2 (during malate oxidation), were used in the presented experiments.

3.7.1 Measurement of UCP2 activity

To induce UCP2 activity, palmitic acid (up to 21 μM) or linoleic acid (up to 32 μM) were used. To inhibit UCP2 activity, 2-4 mM GTP was applied.

The proton leak UCP-mediated measurements were performed as previously described (Swida-Barteczka et al., 2009; Tian et al., 2012). Respiratory rate and ΔΨ measurements of isolated endothelial mitochondria were carried out with 5-10 mM succinate (plus 1-2 μM rotenone) as an oxidisable substrate, in the presence of 1.8 μM carboxyatractyloside and 0.5 μg/ml oligomycin. The response of proton conductance to its driving force can be expressed as the relationship between the oxygen uptake rate and ΔΨ (flux-force relationship) when varying the potential by titration with respiratory chain inhibitors. To decrease the rate of the Q-reducing pathway, succinate dehydrogenase was titrated with malonate (up to 5 mM). To decrease the rate of the QH_2-oxidising pathway, succinate dehydrogenase was titrated with cyanide (up to 20 μM).

3.7.2 Measurement of mitoBK$_{Ca}$ activity

The mitoBK$_{Ca}$ activity was determined during respiratory rate and ΔΨ measurements of isolated endothelial mitochondria. Oxygen uptake was determined polarographically using a Rank Bros. oxygen electrode (Cambridge, UK) in 2.8 ml standard incubation medium, which consisted of 70 mM sucrose, 50 mM KCl, 2.5 mM KH_2PO_4, 2 mM $MgCl_2$, 10 mM Tris-HCl, 10 mM HEPES (pH 7.2), and 0.2% BSA, at 37°C. ΔΨ was measured

simultaneously with oxygen uptake using a tetraphenylphosphonium (TPP^+)-specific electrode. All measurements were performed with 2 mg of mitochondrial protein in the presence of 0.15 mM ATP (to activate succinate dehydrogenase) and 10 μM glibenclamide (to inhibit mitoK_{ATP}). Succinate (5 mM) plus rotenone (2 μM) was used as a respiratory substrate. Resting, non-phosphorylating respiratory rate measurements were performed in the presence of 1.8 μM carboxyatractyloside and 0.5 μg/ml oligomycin. Phosphorylating respiration was measured using 120 μM ADP.

1,3-Dihydro-1-[2-hydroxy-5-(trifluoromethyl)phenyl]-5-(trifluoromethyl)-2H-benzimidazole-2-one (NS1619) (Sigma, St. Louis, Mo, USA) and 1-(3,5-bis-trifluoromethyl-phenyl)-3-[4-bromo-2-(1H-tetrazol-5-yl)-phenyl]-thiourea (NS11021) (NeuroSearch A/S, Ballerup, Denmark), which were dissolved in methanol, were used to induce mitoBK_{Ca} activity. Up to 2 μM iberiotoxin (Bachem AG, Bubendorf, Switzerland) (dissolved in water) or 10 μM paxilline (Sigma, St. Louis, Mo, USA) (dissolved in methanol) were used to inhibit the channel activity.

3.8 Determination of ROS production

3.8.1 Determination of superoxide anion formation with NBT

Superoxide anion production was detected by nitroblue tetrazolium (NBT) assay with EA.hy926 cells and isolated mitochondria. NBT (yellow water-soluble) was reduced by superoxide to formazan-NBT (dark-blue water insoluble). The assay was performed by incubating detached cells (0.2 mg of protein in 1 ml DMEM medium) with 0.2% NBT under agitation for 1 h (37°C) in the presence or absence of 10 μM diphenyleneiodonium (DPI) (an inhibitor of NADPH oxidase and endothelial eNOS, enzymes involved in endothelial ROS formation). In high-glucose studies, DMEM medium with 5.5 or 25 mM glucose (for the normal-glucose and high-glucose cells, respectively) was used. The cells were centrifuged (1,200 *g* for 10 min at 4°C), the supernatant was removed, and formazan-NBT was dissolved in 200 μl 50% acetic acid by sonication (three pulses of 10 s each; Bandelin electronic). The samples were briefly centrifuged (spun down), and the absorbance of the supernatant was determined at 560 nm using a UV 1620 Shimadzu spectrophotometer.

In isolated endothelial mitochondria, the level of superoxide anion release was determined spectrophotometrically at 560 nm (UV 1602, Shimadzu) by measuring the rate of NBT (0.07 mg/ml) reduction at 37°C. Mitochondria (0.2 mg) were incubated in 0.7 ml of the standard incubation medium (Chapter 3.7) in the presence of succinate (5 mM) plus rotenone

(2 μM) as a respiratory substrate. Under non-phosphorylating conditions, measurements were performed in the presence 1.8 μM carboxyatractyloside and 0.5 μg/ml oligomycin. Measurements were performed in the absence or presence of superoxide dismutase (SOD, Sigma-Aldrich (20 units). The difference between these measurements has been used to present results.

3.8.2 Determination of superoxide anion formation with MitoSox

In EA.hy926 cells, mitochondrial superoxide formation was measured with MitoSox Red (Invitrogen), a specific fluorescent mitochondrial superoxide indicator. In high-glucose studies, cells grown in 96-well plates were loaded with 5 μM MitoSox in PBS containing 5.5 mM D-glucose (normal glucose cells) or 25 mM D-glucose (high-glucose cells), or 5.5 mM D-glucose plus 19.5 mM L-glucose (an osmolality control) for 10 min. at 37°C. In hypoxia studies, the assay was performed by incubating adherent cells (grown in 96-well plates) with 5 μM MitoSox in PBS containing 5.5 mM D-glucose and 5 mM pyruvate for 10 min at 37°C. Cells were washed twice with PBS. Fluorescence emission at 595 nm under 510 nm excitation was recorded using an Infinite M200 PRO Tecan multimode reader.

3.8.3 Determination of hydrogen peroxide formation with Amplex Red

Mitochondrial (H_2O_2) production was measured by the Amplex Red-horseradish peroxidase method (Invitrogen) (Zhou M et al., 1997). Horseradish peroxidase (0.1 units/ml) catalyses the H_2O_2-dependent oxidation of non-fluorescent Amplex Red (5 μM) to fluorescent resorufin red. Fluorescence was kinetically followed for 15 min at an excitation wavelength of 545 nm and an emission wavelength of 590 nm using an Infinite M200 PRO Tecan multimode reader. Isolated mitochondria (0.1-0.2 mg of mitochondrial protein) were incubated in 0.5 ml of the standard incubation medium (Chapter 3.7) with 5 mM succinate plus or minus 2 μM rotenone, 5 mM malate, or both 5 mM succinate and 5 mM malate, in the absence (non-phosphorylating state 4 conditions) or presence of 150 μM ADP (phosphorylating state 3 conditions). Under non-phosphorylating conditions, measurements were performed in the absence or presence of 1.8 μM carboxyatractyloside and 0.5 μg/ml oligomycin. Reactions were monitored with constant stirring and calibrated with known amounts of H_2O_2. H_2O_2 production rates were determined from slopes calculated from readings obtained along several 15-min repeated measurements.

3.9 UCP2 silencing

Small interfering RNA (siRNA) transfections were carried out using commercial siRNA constructs (sc-42682, Santa Cruz Biotechnology) according to the manufacturer's protocol. EA.hy926 cells were transfected with target-specific siRNA oligonucleotides designed to knockdown UCP2 expression. Scrambled siRNA was used as control (sc-37007, Santa Cruz Biotechnology).

3.10 Trypan blue cell viability assay

In high-glucose studies, cells grown with 5.5 or 25 mM glucose and with or without knockdown of UCP2 by UCP2 siRNA were incubated (after reaching 100% confluence) in the absence or presence of 1.8 mM H_2O_2 for 24 h (at 37°C). In hypoxia studies, cells were cultured for 6 days under two different oxygen concentrations, 20% and 1%, (representing normoxia and hypoxia conditions, respectively). After 6 days of culture, both living and dead EA.hy926 cells were harvested from cultures (Chapter 3.2). Afterwards, 0.4% trypan blue solution was added (1:1 v/v) to the cell suspension, and cell viability was determined with a Countess Automated Cell Counter (Invitrogen). In a Trypan Blue exclusion assay, cells that take up the dye are either necrotic or apoptotic.

3.11 Measurements of cellular and mitochondrial Q10 concentrations and mitochondrial Q reduction level

The cellular and mitochondrial concentrations of coenzyme Q10 (Q) and the mitochondrial Q reduction level were determined by an extraction technique followed by high-performance liquid chromatography (HPLC) detection (Van den Bergen et al., 1994). Coenzyme Q extraction were conducted during measurement of oxygen uptake (endothelial cells) with a Hansatech oxygen electrode (Chapter 3.6) or during simultaneous measurement of $\Delta\Psi$ and oxygen uptake (isolated mitochondria) using a tetraphenylphosphonium (TPP^+)-specific electrode and a Clark-type oxygen electrode (Chapter 3.7). Endothelial cells (0.5-0.7 mg of cell protein) or isolated mitochondria (2 mg of mitochondrial protein) were chemically quenched with 4 ml of 0.4 M $HClO_4$ (in methanol, at -20ºC). Ubiquinones were subsequently extracted when the obtained mixture was added to 3 ml of petroleum, ether and all components were vigorously mixed with a vortex for 1 min. Afterwards, centrifugation at 990 *g* for 2 min resulted in a clear phase partitioning with the oxidised and reduced Q forms

present in the upper petroleum ether phase. The petroleum phase solution was evaporated to dryness with a stream of nitrogen and samples were stored at -80ºC.

A LiChrosorb RP-18 column (4.6 mm x 250 mm) was used for the separation of the oxidised and reduced Q10 forms. The column was equilibrated with nitrogen-purged ethanol/methanol solvent (3:2 v:v.) and this mixture was used as the mobile phase (Reed and Ragan, 1987). The flow rate was 1 ml/min (Van den Bergen et al., 1994). The HPLC detection was performed with an AKTA chromatograph (Amersham Pharmacia Biotech). The dried samples were dissolved in 150 µl of nitrogen-purged ethanol and an aliquot of 100 µl was injected using a microsyringe (Hamilton) into the injection chamber. Detection of the reduced (QH_2) and oxidised (Q) Q10 forms was performed at 290 nm and 275 nm, respectively. The amount of Q and QH_2 were calculated from the peak area taking into account the molar extinction coefficient (ε) (Lenaz and Esposti, 1985):

- Q5-Q10 (oxidised form dissolved in ethanol): λ_{max} = 275 nm, ε = 14,7 mM^{-1}
- $Q5H_2$-$Q10H_2$ (reduced form dissolved in ethanol): λ_{max} = 290 nm, ε = 4,1 mM^{-1}.

For the calibration and quantification of the Q10 peaks, commercial coenzyme Q (Sigma) was used. The mitochondrial Q reduction levels are expressed as the percentage of total mitochondrial Q (QH_2/Qtot). HPLC grade solvents of methanol, ethanol, $HClO_4$, and petroleum ether were used.

3.12 Measurement of citrate synthase activity

The activity of CS was determined by tracking the formation of DTNB-CoA at 412 nm (Freitas et al., 2010). Suspensions of detached cells were placed in SET buffer (0.32 M sucrose, 1 mM EDTA, 10 mM Tris-HCl, pH 7.4) (1-1.2 mg pr/ ml) and homogenised with Polytron (3 x 2 sec). All of the steps were performed at 4^{o}C. After a short (30 sec) centrifugation of unbroken cells and cell debris, the supernatant was collected for the determination of CS activity. The reaction mixture (1 ml) contained 100 µM Tris, pH 8.0; 100 µM acetyl-Co; 100 mM 5,5'-di-thiobis-(2-nitrobenzoic acid) (DTNB); 0.1% triton X-100; and 40-60 µg supernatant protein. The reaction was initiated with 100 µM oxaloacetate and monitored at 412 nm (UV 1620 Shimadzu) for 3 min at 37^{o}C.

3.13 Measurement of cytochrome *c* oxidase activity

The COX maximal activity was assessed with 2 mg of cell protein or 0.25 mg of mitochondrial protein without exogenously added respiratory substrate and in the presence of sequentially added antimycin A (10 µM), 8 mM ascorbate, 0.06% cytochrome *c*, and up to 2

mM N,N,N'N'-tetramethyl-*p*-phenylenediamine (TMPD) (Figure 3.2). The oxygen consumption was measured in 0.7 ml of DMEJ medium or PBS (cellular respiration) or in 0.7 ml of a standard incubation medium (Chapter 3.7) (isolated mitochondria respiration).

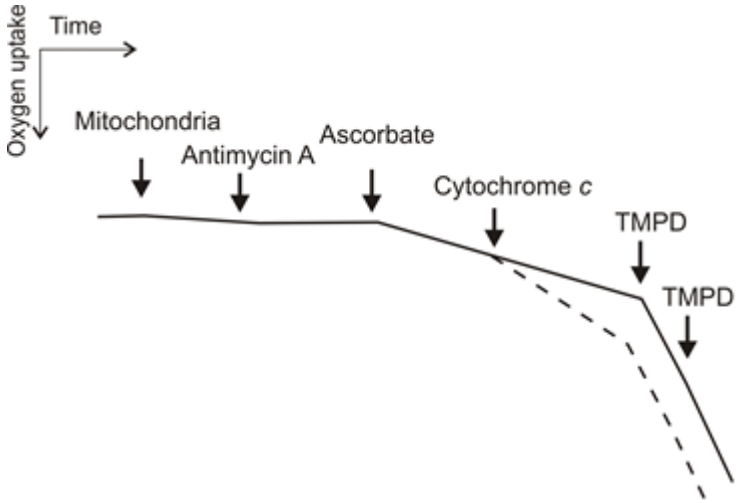

Figure 3.2 Assessment of the COX maximal activity and testing the integrity of the outer mitochondrial membrane. The COX maximal activity was assessed with 0.25 mg of mitochondrial protein without exogenously added respiratory substrate and in the presence of sequentially added antimycin A (10 µM), 8 mM ascorbate, 0.06% cytochrome *c*, and up to 2 mM TMPD. The rate of oxygen consumption following the addition of TMPD reflected the maximal O_2 consumption by COX. Exogenous cytochrome *c* was added to assess the outer membrane integrity. An increase in oxygen consumption with exogenous cytochrome *c* is apparent if the outer mitochondrial membrane is damaged (a broken line). A full line illustrates a preparation where membrane integrity is high.

The rate of oxygen consumption following the addition of TMPD reflected the maximal O_2 consumption by COX (complex IV). The estimation of outer mitochondrial membrane integrity was based on impermeability of the membrane to exogenous cytochrome *c*. A preparation induced damage of the outer mitochondrial membrane and as a result, subsequent loss of cytochrome *c* can be detected by a stimulation of respiration (the COX activity) after the addition of cytochrome *c*. Thus, the percentage of the activity that is latent, (hidden by a membrane) can be determined. Therefore, the integrity of outer membrane of isolated mitochondria was assayed as the latency of COX activity during oxygen uptake measurements in the absence and presence of exogenous cytochrome *c* (Figure 3.2). The same additions, i.e., 10 µM antimycin A, 8 mM ascorbate, 0.06% cytochrome *c*, and up to 2 mM TMPD, were applied. No or slight acceleration of respiration by addition of exogenous cytochrome *c* prior to addition of TMPD indicated a high outer membrane integrity. The integrity was calculated from OCRs in the presence of given chemicals using the following equation: $[TMPD_{OCR} - \text{cytochrome } c_{OCR}] / [TMPD_{OCR} - \text{ascorbate}_{OCR}] \times 100\%$.

3.14 Measurement of lactate dehydrogenase activity

The activity of LDH was measured spectrophotometrically at 340 nm (UV 1620 Shimadzu) by following the oxidation of NADH (150 μM) mixed with pyruvate (10 mM) in 50 mM Tris/HCl (pH 7.3). The activity of LDH was measured in 50 μg of protein from the cytosolic fractions.

3.15 Determination of protein levels through immunoblotting

RIPA buffer (150 mM NaCl, 1% Triton X-100, 0.5% Na deoxycholate, 0.1% SDS, and 50 mM Tris, pH 8.0) was used to lyse the cells. The cellular and mitochondrial fractions were isolated as described in Chapter 3.2 and Chapter 3.3, respectively, in the presence of protease inhibitors (Sigma-Aldrich). Before loading, 20-100 μg protein samples were mixed (1:1 v:v) with a Laemmli sample buffer (2x concentrate, Sigma-Aldrich) and incubated for 5 min at 95ºC. The spectra^{TM} Multicolor Broad Range Protein Ladder (Fermentas) was used as a molecular weight marker. The proteins were separated on an 8% to 14% SDS-PAGE gel. For SDS-PAGE gel preparation the following components were used: 40% acrylamide/bis-acrylamide solution (19:1 v:v), deionised water, 10% dodecylsulfate-Na-salt (SDS) (w/v), 1.5 M Tris-HCl, pH 8.8, 0.5 M Tris-HCl, pH 6.8, 10% ammonium persulfate (APS) (w/v), and N,N,N′,N′-tetramethylethylenediamine (TEMED) (Sigma-Aldrich) (Table 3.1 and Table 3.2).

Electrophoresis was performed in a running buffer containing 25 mM Tris, 192 mM glycine, and 0.1% SDS for 1-2 h at 100-200 V in a Mini-PROTEAN® Tetra Cell electrophoresis chamber (Bio-Rad) at room temperature. Separated proteins were then transferred from the gel into nitrocellulose membrane (AMERSHAM^{TM} PROTAN^{TM} 0.45 μm) in a transfer buffer containing 25 mM Tris-HCl, 192 mM glycine, and 20% methanol. Wet transfer was performed in the Mini-PROTEAN® Tetra Cell chamber (Bio-Rad) at 350 mA for 1.5 h on ice. Semi-dry transfer was performed in a Large Semi-Dry Blotter (APELEX) at 250 mA for 2 h at room temperature.

Nitrocellulose membrane was blocked for 1 h at room temperature with a gentle agitation or overnight at 4ºC in TBS-T buffer (137 mM NaCl, 0.1% Tween-20, and 20 mM Tris, pH 7.6) containing 5% non-fat dried milk.

Gel (%)	Deionized water (ml)	Acrylamide/Bis-acrylamide (ml)	Tris-HCl pH 8.8 (ml)	SDS (ml)	APS (µl)	TEMED (µl)
8%	5.4	2.0	2.5	0.1	50	5
10%	4.9	2.5	2.5	0.1	50	5
12%	4.4	3.0	2.5	0.1	50	5
14%	3.9	3.5	2.5	0.1	50	5

Table 3.1 Resolving gel preparation (for 10 ml).

Gel (%)	Deionized water (ml)	Acrylamide/Bis-acrylamide (ml)	Tris-HCl pH 6.8 (ml)	SDS (ml)	APS (µl)	TEMED (µl)
8%	5.4	2.0	2.5	0.1	50	10
10%	4.9	2.5	2.5	0.1	50	10
12%	4.4	3.0	2.5	0.1	50	10
14%	3.9	3.5	2.5	0.1	50	10

Table 3.2 Stacking gel preparation (for 10 ml).

After blocking, membrane was incubated for 1 h at room temperature with an appropriate primary antibody in TBS-T buffer containing 5% non-fat dried milk. Afterwards, membrane was washed 3 times for 10 min with TBS-T buffer with a gentle agitation. After washing with TBS-T buffer, membrane was incubated for 1 h at room temperature with an appropriate horseradish peroxidase (HRP)-linked secondary antibody in TBS-T buffer containing 5% non-fat dried milk. After final washing, protein bands were visualised using the Amersham ECL system and digitally quantified using the GeneTools 4.03 software package.

The following primary antibodies were used: mouse monoclonal anti-β actin (42 kDa) (CP01, Calbiochem), mouse monoclonal anti-hexokinase I (HK I, 120 kDa) (sc-80978, Santa Cruz Biotechnology), purified goat polyclonal anti-acyl-coenzyme A dehydrogenase (ACADS, 44 kDa) (sc-107371 Santa Cruz Biotechnology), mouse monoclonal lactate dehydrogenase (LDH, 35 kDa) (sc-133123 Santa Cruz Biotechnology), purified goat polyclonal anti-E3-binding protein of pyruvate dehydrogenase (E3BP) (54 kDa, sc-79236, Santa Cruz Biotechnology), purified goat polyclonal anti-UCP2 (35 kDa) (sc-6525, Santa Cruz Biotechnology), purified goat polyclonal anti-mitochondrial superoxide dismutase

(SOD2, 25 kDa) (sc-18503, Santa Cruz Biotechnology), rabbit polyclonal anti-citrate synthase (CS, 52 kDa) (ab-96600, Abcam), mouse monoclonal anti-mitochondrial marker (MTC02, 60 kDa), the MitoProfile® total OXPHOS human antibody cocktail (MS601, MitoScience) containing antibodies raised against subunit of complex I (20 kDa subunit NDUFB8), complex II (30 kDa subunit), complex III (subunit Core 2, 47 kDa), complex IV (COXII, 24 kDa) and ATP synthase (subunit α, 57 kDa), rabbit polyclonal anti-UCP3 (34 kDa) (ab3477, Abcam), mouse monoclonal anti-intercellular adhesion molecule 1 (ICAM1, 89 kDa) (ab53013, Abcam), rabbit monoclonal anti-hypoxia-inducible factor 1-alpha (HIF1α, 93 kDa) (ab51608, Abcam), rabbit polyclonal anti-superoxide dismutase 1 (SOD1, 18 kDa) (ab-13498, Abcam), rabbit polyclonal anti-$K_{Ca}1.1$ and anti-$slo\beta_2$ antibodies (APC-107 and APC-034, Alomone Laboratories) in the presence or absence of blocking peptide, mouse monoclonal anti-plasma membrane Na/K-ATPase (α-subunit) (MA3-929, ThermoFisher Scientific), rabbit polyclonal anti-calnexin (ER membrane marker, 67 kDa) (ab10286, Abcam), and rabbit polyclonal anti-glyceraldehyde 3-phosphate dehydrogenase (GAPDH, 40 kDa) (ab-9485, Abcam). Appropriate horseradish peroxidase-conjugated secondary antibodies were used: Amersham ECL mouse IgG, HRP-linked whole antibody (from sheep) (NA931), goat anti-rabbit IgG (H + L)-HRP-conjugated (1706515, Bio-Rad), and donkey anti-Goat IgG-HRP (sc-2020, Santa Cruz Biotechnology).

The expression levels of COXII or mitochondrial marker (for the mitochondrial fractions) and of β-actin or GAPDH (for the cell fractions) were used as loading normalisation controls.

3.16 Protein concentration determination

Protein concentrations of the cellular, cytosolic, mitochondrial, and mitoplast fractions were determined following the Bradford's protocol-based Bio-Rad protein assay (Bio-Rad). Defatted BSA (Sigma-Aldrich) was used as a standard for a calibration curve. Dye reagent was prepared by dilution of 1 part of dye reagent concentrate with 4 parts of distilled, deionized water. 48 µl of 100 mM NaOH was added to 2 µl of protein sample (in triplicate) and vortexed. Afterwards, 2.5 ml of dye reagent solution was added to all samples, vortexed and left at room temperature for 10 min. The absorbance was measured spectrophotometrically at 595 nm (UV 1620 Shimadzu). Simultaneously, five dilutions of a protein standard (BSA) were prepared and measured in the same way as described above. The linear range of BSA concentrations was within 5 to 25 mg/ml. The protein concentration was calculated from the equation of the linear standard curve.

3.17 Statistical analysis

In Chapter 4.1, results are presented as the means ± SE obtained from at least 5-10 independent experiments (cell suspension preparations or mitochondrial isolations), and each determination was performed at least in duplicate. An unpaired two-tailed Student's t-test was used to identify significant differences; in particular, differences were considered to be statistically significant if $P < 0.05$ (*), $P < 0.01$ (**), or $P < 0.001$ (***). In Chapters 4.2, 4.3 and 4.4, results are presented as the means ± SD obtained from at least 5-10 independent cellular or mitochondrial isolations, in which each determination was performed at least in duplicate. ANOVA followed by post-hoc Tukey's test for pair-wise comparisons was used to identify significant differences; in particular, differences were considered to be statistically significant if $P < 0.05$ (*), $P < 0.01$ (**), or $P < 0.001$ (***).

4 Results and discussion

4.1 The influence of high-glucose exposure on the aerobic metabolism of EA.hy926 cells

4.1.1 Mitochondrial oxidative metabolism of high-glucose-exposed endothelial cells

4.1.1.1 Establishment of experimental model of chronic exposure to high-glucose levels

All measurements with detached EA.hy926 cells were performed within 4 h because the detachment of cells may results in anoikis, which is associated with increased ROS and mitochondrial damage (Li et al., 1999). During this period, cell viability was retained.

An optimal number of detached EA.hy926 cells and the equivalent concentration of total cell protein needed to obtain a measurable OCR. Cellular oxygen consumption was proportional to cell concentration; in particular, the range of 10×10^6-40×10^6 cells per ml was equivalent to 1-4 mg of protein per ml, independent of the respiratory substrates (Figure 4.1). For subsequent experiments, a cell protein concentration of 2 mg per ml (equivalent to ~20×10^6 cells per ml) was selected for the optimal detection of changes in the OCR of cells.

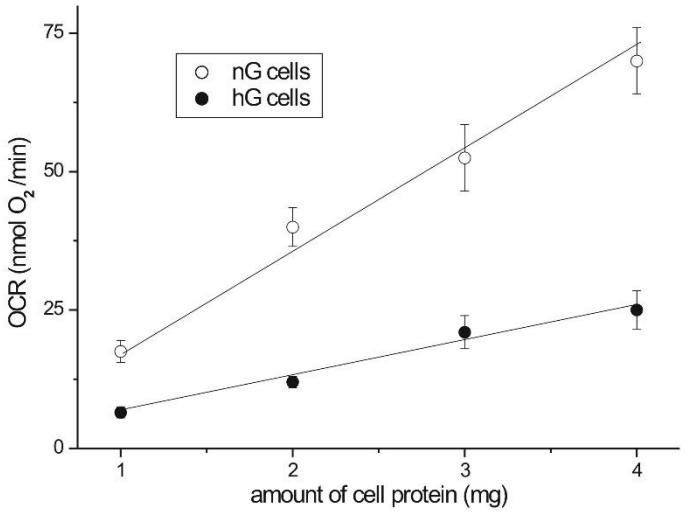

Figure 4.1 The basal OCR plotted as a function of the amount of cell protein. EA.hy926 cells cultured in normal-glucose (nG cells) and high-glucose (hG cells) concentrations were used. Means ± SE; *n* = 9.

To establish the time-course of respiratory response induced by excess glucose, basal OCR of EA.hy926 cells after 3, 6, and 9 days of treatment with 5.5 or 25 mM glucose was

measured (Figure 4.2). A statistically significant decrease in basal OCR was observed in cells grown in high glucose for at least 6 days or longer. These measurements indicate that the respiratory response of endothelial cells to glucose depends on the duration of exposure to elevated glucose concentrations. The greatest difference (the greatest decrease) in respiration between both types of cells was observed for 6-day exposure. Therefore, further experiments were performed with EA.hy926 cells grown for 6 days in the normal-glucose or high-glucose levels.

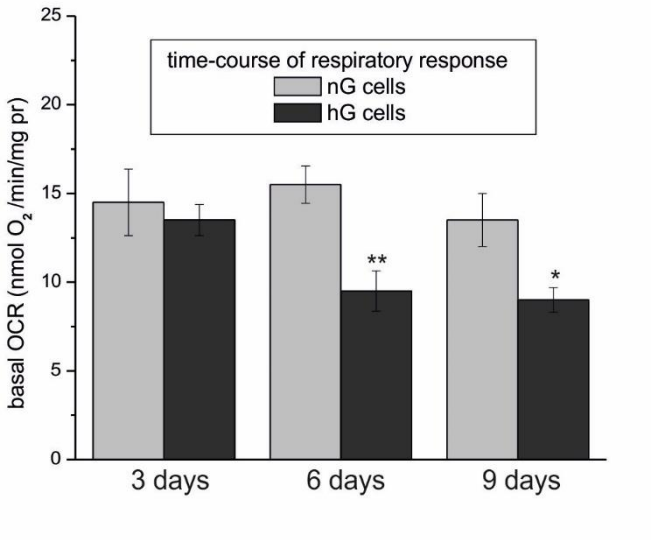

Figure 4.2 Time-course of cell respiratory response induced by excess glucose. EA.hy926 cells were cultured for 3, 6 and 9 days in normal-glucose concentration (nG cells) or high-glucose concentration (hG cells). The basal OCR was measured with 5 mM pyruvate. Means ± SE; *n* = 9.

4.1.1.2 Characteristics of mitochondrial respiratory function in endothelial cells levels

To examine how EA.hy926 cells grown in normal or high glucose respond to simple change in respiratory substrates, mitochondrial respiratory function were measured with the following substrates: pyruvate alone, 5.5 mM glucose alone, 25 mM glucose alone, a combination of pyruvate and either 5.5 mM or 25 mM glucose, glutamine, or palmitate (Figure 4.3).

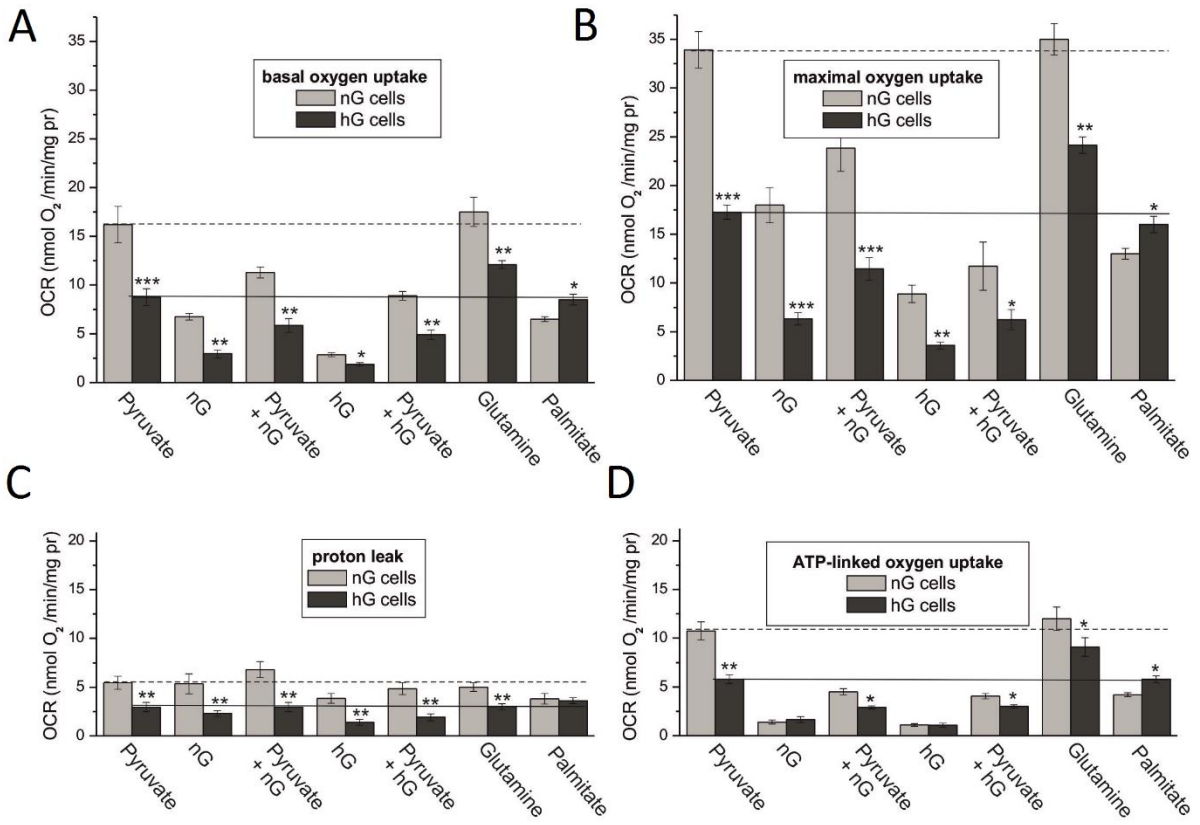

Figure 4.3 Mitochondrial function of EA.hy926 cells grown in normal-glucose concentrations (nG cells) or high-glucose concentrations (hG cells). Substrate-dependent changes in the basal OCR (A), maximal OCR (B), proton leak (C), and ATP-dependent OCR (D). Substrates: 5 mM pyruvate, 5.5 mM D-glucose (nG), 25 mM D-glucose (hG), 5 mM pyruvate, 3 mM L-glutamine, or 0.3 mM palmitate. Means ± SE; *n* = 6.

Under basal conditions (basal OCR) (Figure 4.3 A), FCCP-stimulated conditions (maximal OCR) (Figure 4.3 B), and the presence of oligomycin (the oligomycin-resistant OCR, ATP-linked OCR) (Figure 4.3 D), both types of cells demonstrated the highest OCR with pyruvate alone or glutamine and the lowest OCR with 25 mM glucose alone. However, in the cells grown in high glucose, the OCR with glutamine was significantly higher than the OCR with pyruvate, whereas in the cells grown at normal glucose, both of these substrates were oxidised at a similar level. Moreover, in the high-glucose cells, the OCR with palmitate was similar to the OCR with pyruvate, whereas in the normal-glucose cells, the OCR with palmitate was much lower than the OCR with pyruvate. These results indicate an increased oxidation of glutamine and palmitate in the cells cultured under high-glucose conditions. Among the tested OCRs, the proton leak (non-ATP-linked OCR) exhibited the least dependence on the type of substrate that was applied (Figure 4.3 C). For both types of EA.hy926 cells, the highest (at least five-fold) difference between respiration with pyruvate as the sole substrate and

respiration with 25 mM glucose alone was observed in the ATP-linked OCR and the basal OCR (Figure 4.3).

In general, for all of the examined conditions during measurements of mitochondrial respiratory function, glucose decreased the OCR of both types of cells in a concentration-dependent manner. Moreover, the Crabtree effect (the decreased OCR in the presence of glucose) was observed during the sequential addition of glucose to the medium of pyruvate-oxidising cells under basal conditions. Figure 4.4 shows the representative oxygen uptake measurement with EA.hy926 cells (using nG cells as an example), illustrating the Crabtree effect.

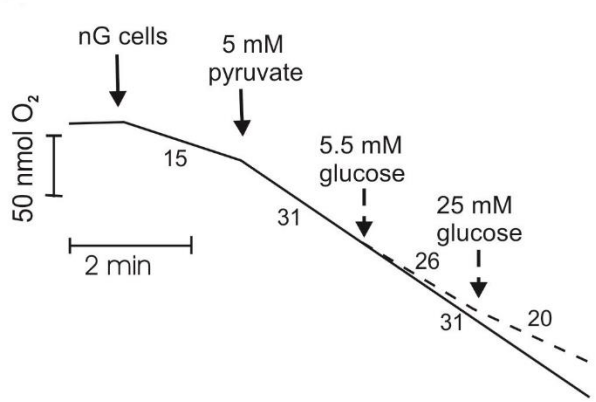

Figure 4.4 The representative oxygen uptake measurement with EA.hy926 cells (using nG cells as an example), illustrating the Crabtree effect. The numbers on the traces refer to the OCR in nmol^{-1} O_2 x min^{-1} x mg protein. nG cells, cells grown in normal-glucose concentrations.

4.1.1.3 High-glucose levels and mitochondrial oxidation of reducing fuels in cells

As was shown above, under all conditions and with respect to all substrates except palmitate, the EA.hy926 cells grown at high-glucose concentrations displayed significantly lowered mitochondrial function relative to the cells exposed to normal-glucose concentrations (Figure 4.3). In particular, the high-glucose cells exhibited at least two-fold lower maximal mitochondrial respiratory capacity with pyruvate alone, glucose alone (either 5.5 mM or 25 mM), or any combination of these substrates (Figure 4.3 B). For glutamine oxidation, a less dramatic decrease (only ~1.4-fold decrease) in the maximal OCR was observed. By contrast, the oxidation of palmitate was significantly higher in the high-glucose cells, and similar results were observed using stearic acid, another free FA (data not shown). These results

indicate that there is a greater contribution from FAs as fuels of endothelial respiration under high-glucose conditions. Interestingly, no significant differences in ATP-linked OCR were observed between both types of cells during the oxidation of glucose alone (either 5.5 mM or 25 mM), indicating similar low levels of mitochondrial OXPHOS during carbohydrate catabolism (Figure 4.3 D).

Thus, in endothelial cells, growth in high-glucose concentrations lowered mitochondrial respiration during carbohydrate and glutamine oxidation, and increased respiration with FAs.

4.1.1.4 High-glucose levels and mitochondrial biogenesis and respiratory capacity

The next step was measurement of mitochondrial key enzyme activities (CS and COX) (Figure 4.5), estimation of the cellular Q10 concentration (Figure 4.5), and determination of cellular protein levels of CS, COX (subunit II), mitochondrial marker, HKI (hexokinase I), and LDH (Figure 4.6) in EA.hy926 cells grown in normal- and high-glucose concentrations.

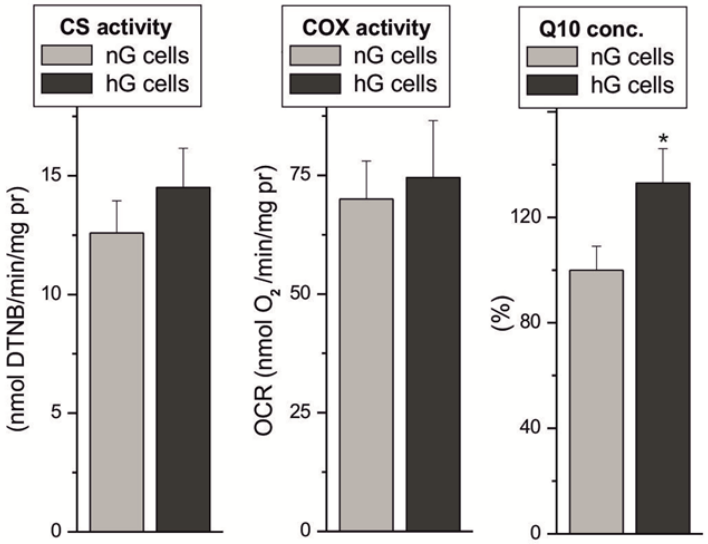

Figure 4.5 The COX activity, CS activity, and cellular concentration of Q10 (expressed as the percentage of Q10 concentration in nG cells) in endothelial EA.hy926 cells grown in normal-glucose concentrations (nG cells) or high-glucose concentration (hG cells). DTNB, 5,5'-di-thiobis-(2-nitrobenzoic acid). Means ± SE; *n* = 4-8.

The endothelial cells cultured in the normal-glucose or high-glucose conditions exhibited similar CS and COX activities (Figure 4.5), indicating that the different growth conditions did not change the capacity of the TCA cycle or the mitochondrial respiratory

chain. Moreover, no differences in the expressions of mitochondrial marker, COXII, and CS were detected (Figure 4.6), indicating unaltered mitochondrial biogenesis. Additionally, a significantly greater cellular Q10 content was found in the cells grown under high-glucose conditions (Figure 4.5).

A significant upregulation of HKI and LDH was observed in the cells grown in high-glucose concentrations (Figure 4.6), indicating that these cells displayed intensified anaerobic glucose oxidation through a glycolic pathway and lactate fermentation.

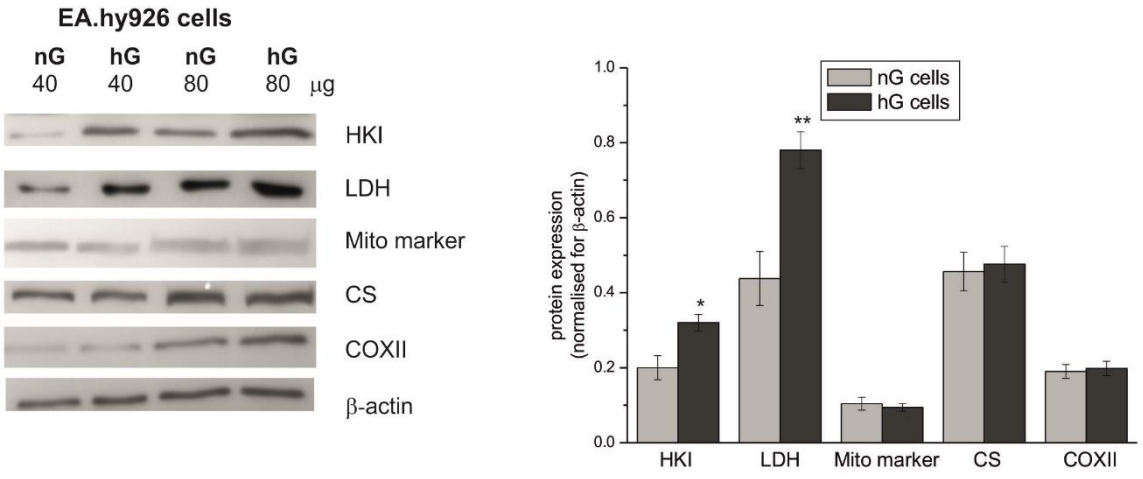

Figure 4.6 Determination of protein levels in EA.hy926 cells grown in normal-glucose (nG cells) or high-glucose (hG cells) concentration. Representative Western blots and analyses of the protein expression of HKI, LDH, mitochondrial marker (Mito marker), CS, and COXII. Expression levels normalised for β actin protein abundance are shown. Means ± SE; *n* = 10.

Thus, in EA.hy926 cells grown in high-glucose levels, the Crabtree effect (the decreased OCR in the presence of glucose) (Figure 4.4) was accompanied by the increased expression of both HKI, the enzyme catalysing the first rate-limiting step of the glycolytic pathway, and LDH, the enzyme catalysing the interconversion of pyruvate to lactate. These results indicate the increased anaerobic and decreased aerobic (mitochondrial) breakdown of glucose in EA.hy926 cells grown under high-glucose conditions.

4.1.1.5 High-glucose levels and intracellular and mitochondrial ROS formation

As shown in Figure 4.7, compared with cells cultured under normal-glucose conditions, exposure of EA.hy926 cells to high-glucose concentrations caused approximately two-fold increase in intracellular ROS generation. Moreover, DPI, a flavoprotein inhibitor of NADPH oxidase, inhibited significantly high-glucose-induced ROS generation. The DPI-

insensitive ROS generation was significantly higher in the high-glucose cells, indicating an elevated mitochondrial respiratory chain-derived ROS generation. Thus, in EA.hy926 cells, high-glucose-induced ROS appears to be produced through the enzyme NADPH oxidase and from mitochondrial sources.

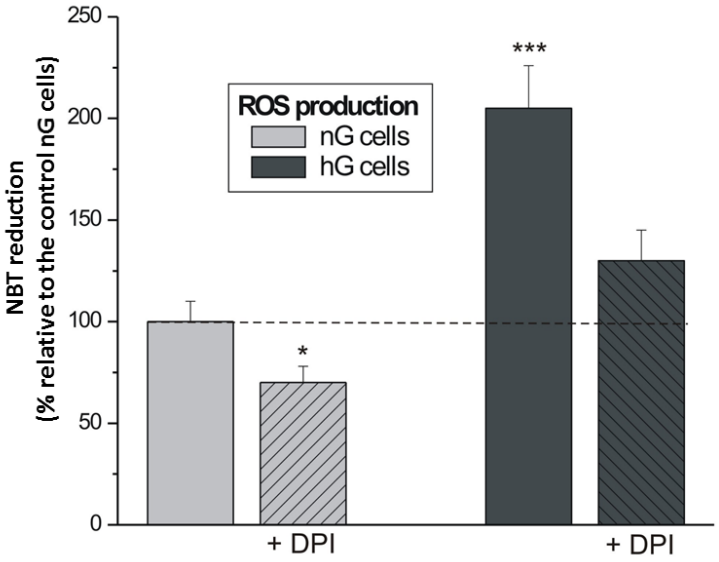

Figure 4.7 Determination of superoxide anion generation in EA.hy926 cells grown in normal-glucose (nG cells) or high-glucose levels (hG cells). NBT reduction in the absence or presence of 10 µM DPI is shown. Means ± SE; *n* = 7.

4.1.2 Functional characteristics of mitochondria isolated from high-glucose-exposed endothelial cells

The efficient procedure of mitochondria isolation from EA.hy926 cells, which was elaborated in this study (Chapter 3.3) produces highly active and well-coupled mitochondria (Figure 4.8). The mitochondria isolated from both types of cells exhibited good coupling parameters, i.e., high ADP/O and RCR with malate or succinate. These results indicate that mitochondrial electron transport through the respiratory chain of isolated endothelial mitochondria is coupled well with ATP synthesis when complex I and complex II substrates are applied. Moreover, the mitochondria were quite stable for 6-7 h and their outer mitochondrial membrane exhibited good integrity (97-99%).

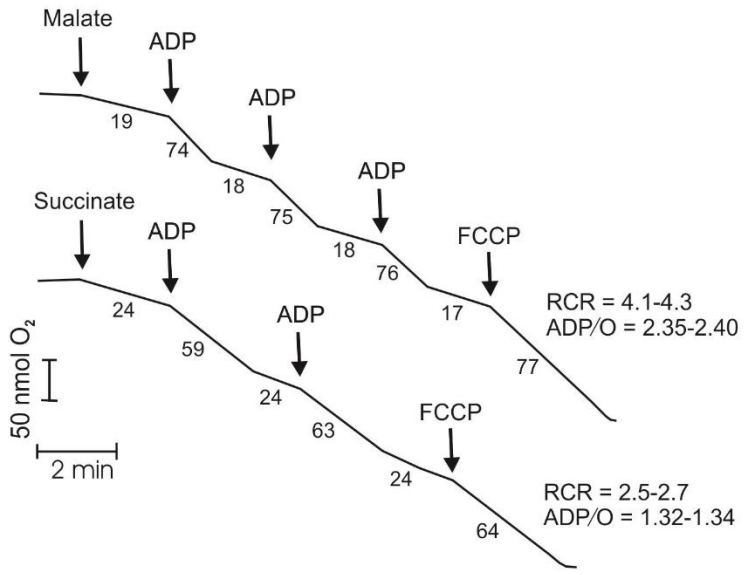

Figure 4.8 Representative oxygen uptake measurements of non-phosphorylating respiration, phosphorylating respiration, and uncoupled respiration, as well as the obtained coupling parameters, ADP/O and RCR. Mitochondria isolated from cells grown in normal-glucose levels are shown as an example. Malate (10 mM) and 10 mM succinate (plus 1 µM rotenone) were used as respiratory substrates. The numbers on the traces refer to OCR in nmol O_2 x min^{-1} x mg^{-1} protein. Means ± SE; *n* = 6.

4.1.2.1 High-glucose levels and mitochondrial respiratory activity and protein levels

Next step was to study functional characteristics of endothelial mitochondria isolated from normal-glucose and high-glucose cells. The highest maximal mitochondrial respiration (phosphorylating or uncoupled respiration) was observed with malate, either alone or supplemented with pyruvate, glutamate or a combination of succinate and glycerol-3-phospate, and with succinate alone (Figure 4.9). Malate oxidation appeared to saturate the capacity of the mitochondrial respiratory chain, as the addition of the other reducing substrate(s) to malate did not further increase mitochondrial respiration. Interestingly, the apparent maximal mitochondrial respiration comprised ~27% of the apparent capacity of complex IV (COX) (Figure 4.10). Glutamate (an intermediate of amino acid metabolism), glycerol-3-phosphate and palmitoylcarnitine (lipid breakdown intermediates) were more weakly oxidised by EA.hy926 mitochondria than were malate or succinate (the TCA cycle intermediates) (Figure 4.9). Interestingly, the oxidation of pyruvate alone was not very intense compared with the oxidation of these two TCA cycle substrates.

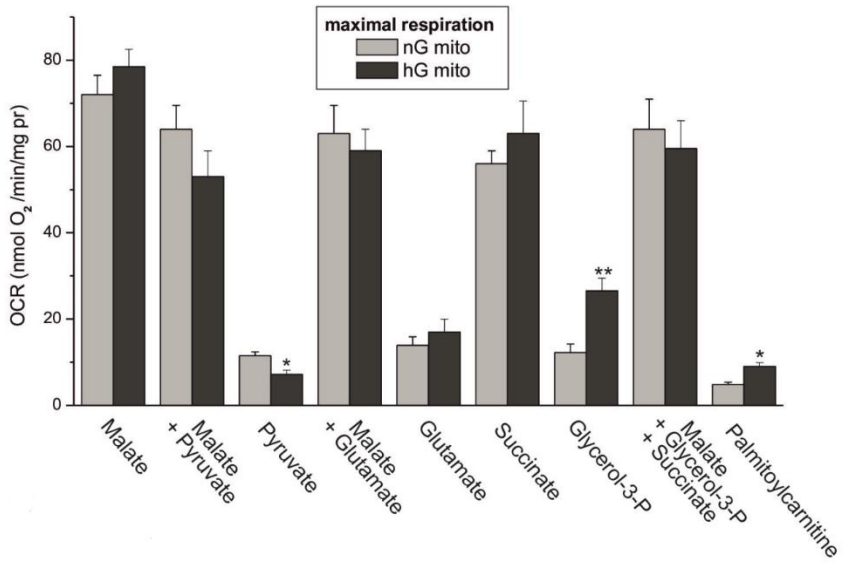

Figure 4.9 The maximal respiration (phosphorylating respiration or uncoupled respiration) of mitochondria isolated from cells grown in normal-glucose (nG mito) and high-glucose (hG mito) levels. Respiratory substrates: 10 mM malate, 10 mM pyruvate, 10 mM glutamate, 10 mM succinate, 3 mM glycerol-3-phosphate (glycerol-3-P), and 0.3 mM palmitoyl-DL-carnitine. Means ± SE; *n* = 6.

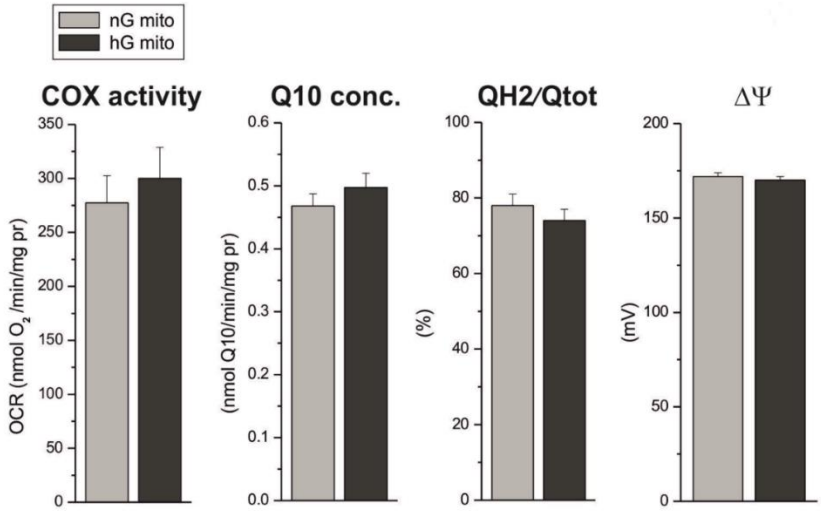

Figure 4.10 The COX activity, concentration of Q10 in mitochondria, and mitochondrial Q reduction level (QH_2/Qtot), and ΔΨ during non-phosphorylating oxidation of succinate. Measurements were performed with mitochondria isolated from cells grown in normal-glucose (nG mito) and high-glucose (hG mito) levels. Means ± SE; *n* = 6.

In high-glucose-exposed cells, the cytochrome pathway activity, COX activity, and OXPHOS efficiency did not change, and the mitochondrial ΔΨ and Q reduction level of the resting state (with succinate as an oxidisable substrate) were also unaffected (Figure 4.9 and

Figure 4.10). The expression levels of subunits of ATP synthase (α) and the four respiratory chain complexes, namely, complex I (NDUFB8), complex II (subunit 30 kDa), complex III (Core2), and complex IV (COXII) (Figure 4.11), as well as the Q10 content of the mitochondria (Figure 4.10), were not affected by high-glucose growth. In addition, no change in the expression level or activity of CS was observed (Figure 4.5, Figure 4.6, and Figure 4.12), indicating that high-glucose conditions produced no discernible change at the level of the TCA cycle.

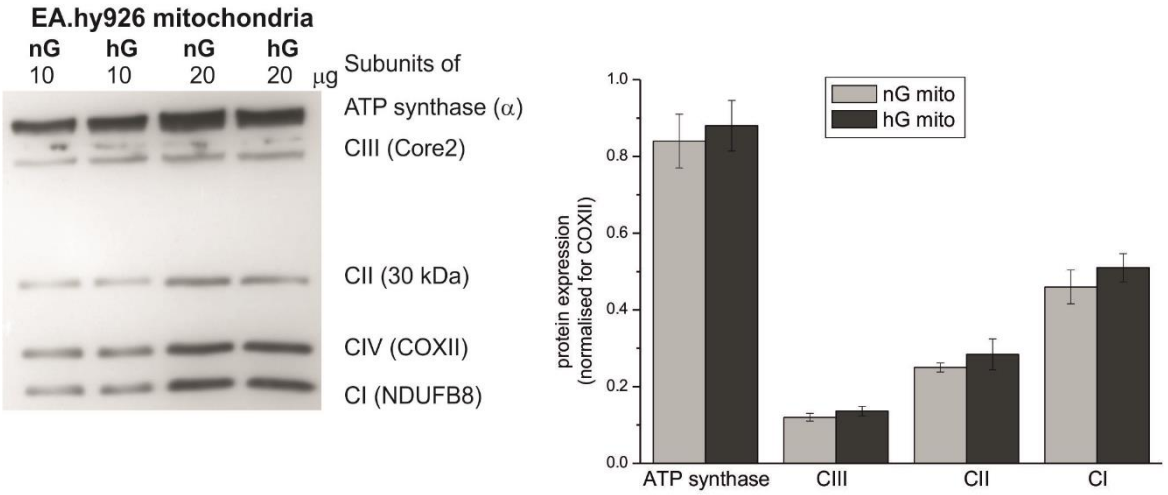

Figure 4.11 Determination of protein levels in mitochondria isolated from EA.hy926 cells grown in normal-glucose (nG, nG mito) or high-glucose (hG, hG mito) concentrations. Representative Western blots and analyses of the protein expression of particular subunits of ATP synthase, complex III (CIII), complex II (CII), and complex I (CI). Expression levels normalised for COXII protein abundance are shown. Means ± SE; *n* = 10.

In endothelial mitochondria isolated from high-glucose cultured EA.hy926 cells, an increased level of expression of acyl-CoA dehydrogenase (ACADS), which catalyses the initial step of FA β-oxidation, was observed (Figure 4.12). This finding is consistent with the greater oxidation of palmitoylcarnitine and glycerol-3-phosphate that was observed in mitochondria isolated from the high-glucose cells (Figure 4.9), indicating the greater oxidation of reducing substrates not originating from the TCA cycle. By contrast, these mitochondria demonstrated significantly decreased expression of the E3BP component of the pyruvate dehydrogenase complex (Figure 4.12) and significantly decreased pyruvate oxidation relative to mitochondria from cells cultured under normal-glucose levels (Figure 4.9).

Thus, these results indicate that growth of endothelial cells in high-glucose level induced an increase in mitochondrial oxidation of palmitoylcarnitine and glycerol-3-

phosphate, and a decrease in pyruvate oxidation, whereas the TCA cycle and respiratory chain remained unaffected (Figure 4.9, Figure 4.10, and Figure 4.11). Growth under high-glucose concentrations did not influence the activity (Figure 4.9 and Figure 4.10) or composition (Figure 4.11) of basic respiratory chain components in EA.hy926 mitochondria.

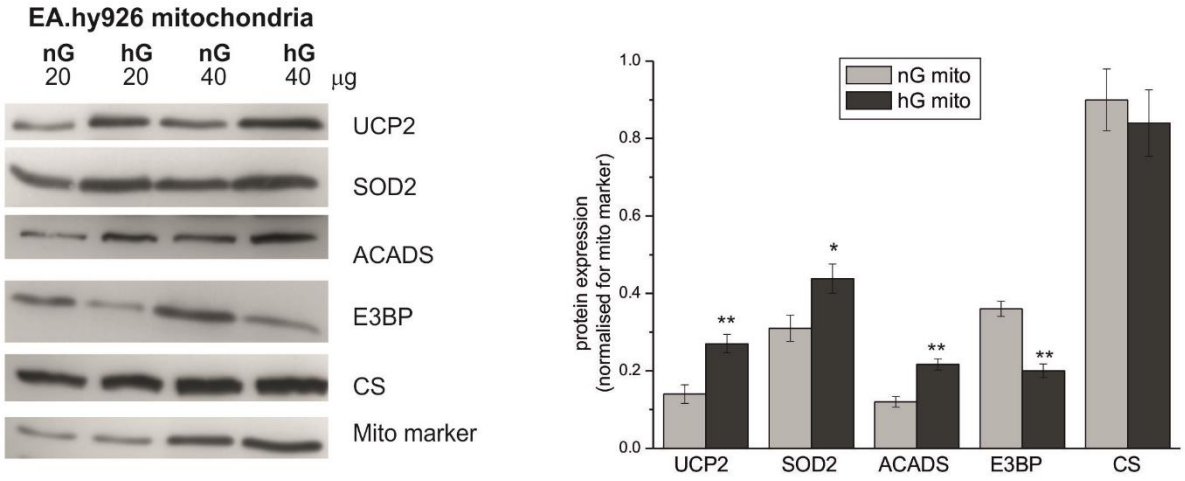

Figure 4.12 Determination of protein levels in mitochondria isolated from EA.hy926 cells grown in normal-glucose (nG, nG mito) or high-glucose (hG, hG mito) concentrations. Representative Western blots and analyses of the protein expression of UCP2, SOD2, ACADS, E3BP, and CS. Expression levels normalised for mitochondrial marker (mito marker) protein abundance are shown. Means ± SE; *n* = 10.

4.1.2.2 High-glucose levels and UCP2 upregulation

As shown in Figure 4.12, in response to high-glucose conditions, the upregulation of the expression of mitochondrial antioxidant proteins, such as SOD2 and UCP2, was observed. Therefore, the next goal of this study was to determine whether UCP2 is functionally active in endothelial mitochondria. The activation of UCP2 by free FAs (palmitic acid) and the inhibition by GTP was evaluated in isolated EA.hy926 mitochondria. In non-phosphorylating mitochondria isolated from cells grown in high-glucose conditions, the maximal rate of the respiration induced by palmitic acid, which presented UCP2 activity, was two-fold higher (Figure 4.13). Similarly, a two-fold greater decrease in the $\Delta\Psi$ and Q reduction level was observed upon maximal activation of UCP2 by palmitic acid. The addition of 2 mM GTP partially reversed the changes induced by palmitic acid in both types of mitochondria.

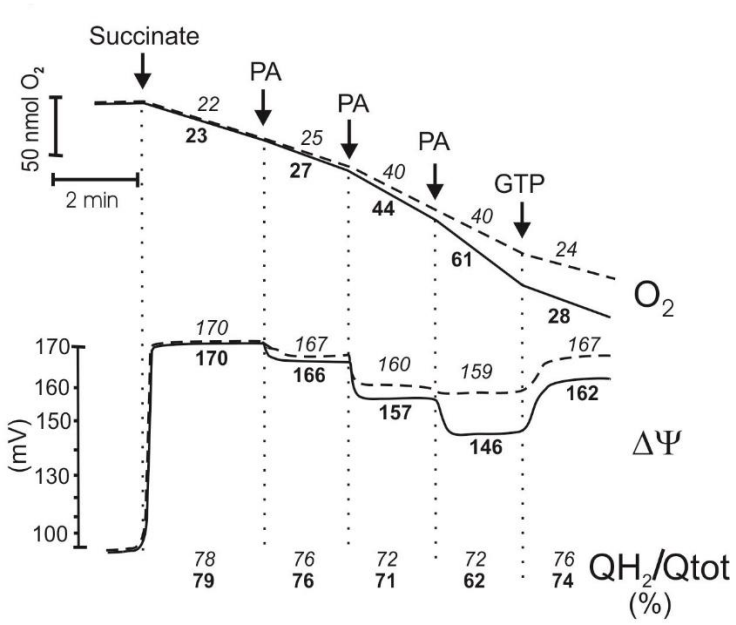

Figure 4.13 The effects of UCP2 activation by palmitic acid (PA) (7 µM per addition), and UCP2 inhibition by 2 mM GTP on the oxygen uptake, ΔΨ, and Q reduction level. The mitochondria from normal-glucose cells (nG mito) are represented by broken lines and numbers in italics, and the mitochondria from high-glucose cells (hG mito) are represented by solid lines and bold numbers. The numbers on the traces refer to OCR in nmol O_2 x min^{-1} x mg^{-1} protein, ΔΨ in mV, and Q reduction level in %. Succinate (with 1 µM rotenone) was used as and oxidisable substrate. Means ± SE; *n* = 6.

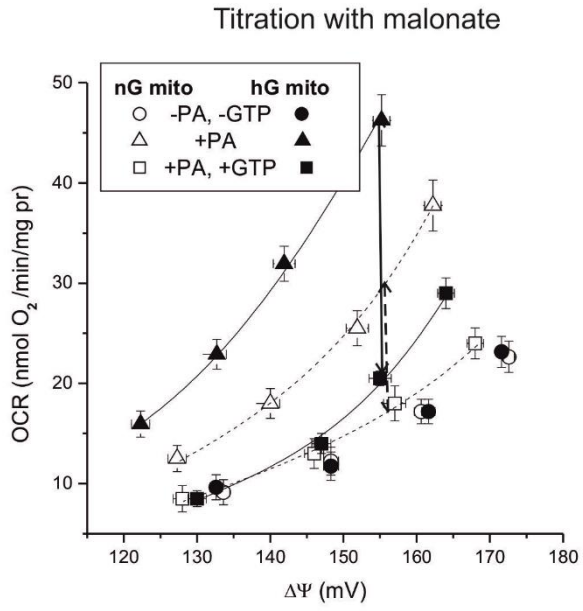

Figure 4.14 The relationship between the respiratory rate and ΔΨ (proton leak kinetics) during non-phosphorylating succinate oxidation titrated with malonate. The palmitic acid (PA)-induced, GTP-inhibited, UCP2-mediated proton leak at the same ΔΨ (155 mV) is indicated as vertical lines. Broken lines indicate the mitochondria from normal-glucose cells (nG mito) and solid lines indicate the mitochondria from high-glucose cells (hG mito). The mitochondria were incubated in the absence or presence of 14 µM PA and/or 2 mM GTP. Means ± SE; *n* = 6.

Furthermore, a proton leak kinetics study (Figure 4.14) indicates that for given palmitic acid (14 μM) and GTP (2 mM) concentrations, the palmitic acid-induced GTP-inhibited UCP2-mediated proton leak at the same ΔΨ (155 mV) was also two-fold higher in the mitochondria from the high-glucose cells.

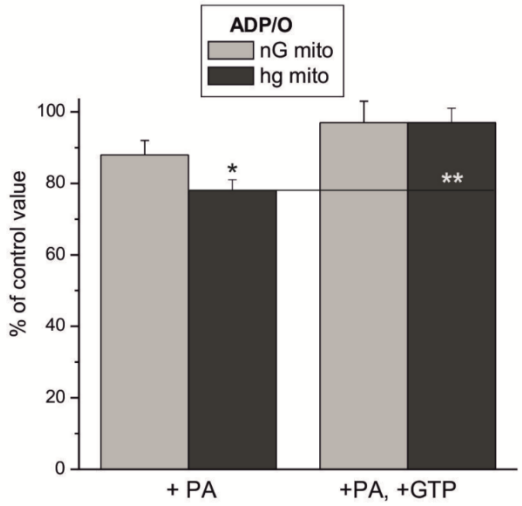

Figure 4.15 The influence of palmitic acid (PA) and GTP on the ADP/O ratio during the phosphorylating respiration. Measurements were performed with mitochondria isolated from cells grown in normal-glucose (nG mito) and high-glucose (hG mito) levels. Relative changes compared with the control values (in the absence of PA and GTP) are shown. Succinate (with 1 μM rotenone) was used as and oxidisable substrate. The mitochondria were incubated in the absence or presence of 14 μM PA and/or 2 mM GTP. Means ± SE; *n* = 6.

Under phosphorylating conditions, the augmented activity of UCP2 in the mitochondria from the high-glucose cells led to a significantly greater reduction in the OXPHOS yield (Figure 4.15). For given palmitic acid (14 μM) and GTP (2 mM) concentrations, the palmitic acid-induced GTP-reversed drop in the ADP/O ratio was almost two-fold greater in the mitochondria from the high-glucose cells than in the mitochondria from the normal-glucose cells.

Thus, these results indicate that EA.hy926 mitochondria possess UCP2 activity that is stimulated by free FAs and inhibited by purine nucleotides. Moreover, UCP2 activity is two-fold greater in mitochondria isolated from EA.hy926 cells cultured in high-glucose conditions.

4.1.3 Discussion and conclusions

The comparison between the mitochondrial respiratory functions of endothelial EA.hy926 cells cultured in medium with either high- or normal-glucose concentration indicate that chronic high-glucose conditions induced a reduction in mitochondrial respiration with carbohydrate catabolism intermediates (glucose, pyruvate, or a combination of both of these substrates) and glutamine, whereas OCR with palmitate (an intermediate in lipid metabolism) was increased (Figure 4.3). The Crabtree effect was also observed in both types of cells when the influence of 5.5 mM or 25 mM glucose on pyruvate oxidation was studied (Figure 4.3 and Figure 4.4). In the cells grown in high glucose, the OCR with glutamine was significantly higher than the OCR with pyruvate (Figure 4.3). These results indicate that high-glucose levels lower the contribution of carbohydrate oxidation to the aerobic metabolism of EA.hy926 cells, whereas the contributions of amino acid oxidation and lipid oxidation increase. Interestingly, it has been shown previously that in HUVEC, FAs can serve as an important energy source; moreover, the activation of the fuel-sensing enzyme AMPK favours the oxidation of FAs as the source of ATP production and reduces dependence on glycolysis (Dagher et al., 2001). The high-glucose EA.hy926 cells examined in this study seem to undergo a shift of aerobic metabolism towards the oxidation of lipids that resembles the change in the myocardial energy utilisation that is induced by high-glucose levels. In particular, diabetes is associated with a switch in myocardial substrate utilisation that results in decreased glucose oxidation and increased FA oxidation (Teagtmeyer et al., 2002). The present study shows for the first time that a shift to a predominant oxidation of FAs, which accompanies diabetic changes in metabolism, could also occur in endothelial cells. Manipulation of proteins that are upregulated in endothelial cells under high-glucose conditions (LDH, HKI, UCP2, and SOD2) by overexpression or siRNA could pinpoint in the future the molecules responsible for the described switch in oxidative metabolism.

In EA.hy926 cells grown for 6 days in 25 mM glucose concentration, the Crabtree effect (the decreased OCR in the presence of glucose) was accompanied by the increased expression of both HKI (the enzyme catalysing the first step, which is the rate-limiting step, of the glycolytic pathway) and LDH (the enzyme that catalyses the interconversion of pyruvate and lactate) (Figure 4.6). These results indicate the increased anaerobic and decreased aerobic (mitochondrial) breakdown of glucose in EA.hy926 cells grown under chronic high-glucose conditions. It has been shown that HUVEC and bovine retinal endothelial cells (BREC) grown in high-glucose for 7 days exhibit elevated lactate production

(La Selva et al., 1996). A short (up to 45 min) exposure of human microvascular endothelial cells (HMEC) to 25 mM glucose appears to produce no change in lactate production or OCR, although increased levels of a glycolytic intermediate, glucose 6-phosphate, have been observed (Sweet et al., 2009). Therefore, it appears that the respiratory response of endothelial cells to high glucose depends on the period of the exposure to elevated glucose (Figure 4.2). A clear decrease in respiration was observed in EA.hy926 cells grown in high-glucose levels for at least 6 days or longer. Therefore, the present study describing a chronic exposure to elevated glucose does not reflect the effect of short-term high-glucose levels on endothelial cells.

The presented results indicate the increased oxidative stress in EA.hy926 cells grown under chronic high-glucose conditions. A significantly higher intracellular and mitochondrial ROS generation (Figure 4.7) and upregulation of the expression of mitochondrial antioxidative system proteins such as SOD2 and UCP2 (Figure 4.12) were observed. The increased expression levels of SOD2 and UCP2 in response to high glucose have previously been observed for other endothelial cells (Zheng et al., 2009; Cui et al., 2006). Numerous reports also indicate that the exposure of endothelial cells to high glucose levels leads to increased intracellular and mitochondrial ROS production and therefore produces excessive oxidative stress (Cui et al., 2006; Du et al., 2000; Giardnio et al., 1996; Nascimento et al., 2006; Nishikava et al., 2000; Srinivasan et al., 2004; Xie et al., 2008; Zheng et al., 2009 and Zheng et al., 2010). Mitochondrial contribution to high-glucose-induced ROS production was also observed in BAEC, BREC, HUVEC and retinal capillary endothelial cells, including cells chronically exposed to elevated glucose (Cui et al., 2006; Du et al., 2000; Nishikawa et al., 2000; Xie et al., 2008; Zheng et al., 2009 and Zheng et al., 2010). In EA.hy926 endothelial cells, high-glucose-induced ROS appears to be produced through the enzyme NADPH oxidase and from mitochondrial sources. However, these results indicate that glucose-fuelled oxidative metabolism cannot rather mediate oxidative stress because OCR with carbohydrate catabolism intermediates (glucose, pyruvate, or a combination of both of these substrates) was impaired in the EA.hy926 cells grown in high-glucose levels (Figure 4.3). Furthermore, mitochondria isolated from the high-glucose cells demonstrated significantly decreases in both pyruvate oxidation (Figure 4.9) and the expression of the E3BP component of the pyruvate dehydrogenase complex (Figure 4.12). Thus, it appears that the supply of energy to the TCA cycle from pyruvate, a key intermediate in several metabolic pathways, is impaired in EA.hy926 cells grown in high-glucose levels. This finding is consistent with previously promulgated suggestions that the accumulation of glucose 6-phosphate during the incubation

of endothelial cells under high-glucose concentrations indicates that downstream metabolic steps are rate-limiting (Sweet et al., 2009).

The greater contribution of lipid oxidation to the aerobic metabolism of the EA.hy926 cells grown in high glucose is indicated by the increased expression of ACADS (Figure 4.12) and the higher oxidation of palmitoylcarnitine and glycerol-3-phosphate in the mitochondria that were isolated from these cells (Figure 4.9). Glycerol-3-phosphate serves as a major link between carbohydrate metabolism and lipid metabolism, and the glycerol-3-phosphate shuttle is an important electron supply to the animal mitochondrial respiratory chain. Thus, the increased level of reducing substrates originating from lipid metabolism likely mediates the endothelial oxidative stress induced by excess glucose. In general, mROS generation is associated with increased levels of reduction of respiratory chain components (complex I and complex III) that may be due to the increased oxidation of mitochondrial fuels and/or the impairment of the QH_2-oxidising pathway (Turrens et al., 2003). The impaired production of NO (a competitive inhibitor of complex IV, COX) observed in endothelial cells exposed to acute or chronic high-glucose levels (Du et al. 2000, Srinivasan et al. 2004) does not account for the latter possibility. However, eNOS, as being a source of ROS through other mechanism, cannot be excluded under experimental conditions of this study. The operation of the Crabtree effect would decrease the contribution of ROS produced by mitochondria and favour the contributions from other steps of glucose metabolism in the cell, including increased NADPH oxidase activity (Sweet et al., 2009). Under high-glucose conditions, endothelial mitochondria could stimulate the overall intracellular production of ROS; despite the fact, these mitochondria may not generally be a major source of ROS (Davidson, 2010). In high-glucose EA.hy926 cells, a higher cellular content of Q10 (in contrast to the mitochondrial Q10 content) (Figure 4.5 and Figure 4.10) may indicate an increased need for this lipid-soluble antioxidant, given that an elevated level of Q10 has been observed to be a protective response to excessive oxidative stress in certain diseases, including endothelial dysfunction (Littaru and Tain, 2007).

Recent studies of mitochondrial function through extracellular flux analysis in adherent primary BAEC have indicated that endothelial mitochondria are highly coupled to ATP synthesis and possess a considerable bioenergetic reserve, although exposure to sublethal oxidative stress reduces this reserve capacity (Dranka et al., 2010). In EA.hy926 cells, the apparent mitochondrial reserve capacity did not differ for any of the tested substrates between cells grown in normal and high glucose. The present study provided the first measurement of endothelial mitochondrial function, directly demonstrating that in isolated

EA.hy926 mitochondria, electron transport is coupled well with ATP synthesis. Thus, despite the fact that endothelial cells are primarily glycolytic and do not generate significant contributions to cellular ATP production through OXPHOS, they possess active and well-coupled mitochondria.

The foregoing results indicate that EA.hy926 mitochondria possess UCP2 activity that is stimulated by free FAs and inhibited by purine nucleotides. Furthermore, UCP2 activity is two-fold greater in mitochondria isolated from EA.hy926 cells cultured in high-glucose concentrations. More details about the physiological role of UCP2 in endothelial cells under high-glucose conditions are presented in subsequent Chapter 4.2.

It can be concluded that although in endothelial cells, the synthesis of ATP occurs primarily via a glycolytic pathway (Davidson, 2010; Davidson and Duchen, 2007), they possess highly active and well-coupled mitochondria with a functioning energy-dissipating pathway that involves UCP2. The growth of endothelial cells under high-glucose conditions induces numerous changes in the cells' aerobic metabolism, particularly with respect to the Crabtree effect, as well as a shift towards the oxidation of lipids and amino acids. These results indicate the role of endothelial mitochondria in response to metabolic disturbances that relate to hyperglycaemia.

4.2 The influence of high-glucose exposure on UCP2 function and activity in EA.hy926 cells

The results presented in the previous chapter (Chapter 4.1) induced questions with respect to understanding the physiological role that UCP2 plays in endothelial mitochondria. The present chapter describes in more details the functional characteristics of UCP2 in isolated endothelial mitochondria and endothelial cells, and how UCP2 function is altered by long-term growth in glucose concentrations that are well above the physiological range. To address this issue, the UCP2 functions were studied in human endothelial EA.hy926 cells cultured in media with either high (25 mM) or normal (5.5 mM) D-glucose concentrations, representing high-glucose and normal-glucose levels.

4.2.1 High-glucose levels and expression of UCP2 and UCP3

Using western blot analysis, the expression of UCP2 and UCP3, but not UCP1, could be detected in EA.hy926 cells (Trenken et al., 2007). In the present study, the endothelial EA.hy926 cells cultured under normal- or high-glucose conditions exhibited a similar UCP3 expression level (Figure 4.16 A and Figure 4.16 B). On the other hand, as presented previously (Figure 4.12), a significantly higher expression of UCP2 was observed in the cells grown in high-glucose concentrations (Figure 4.16 A and Figure 4.16 B).

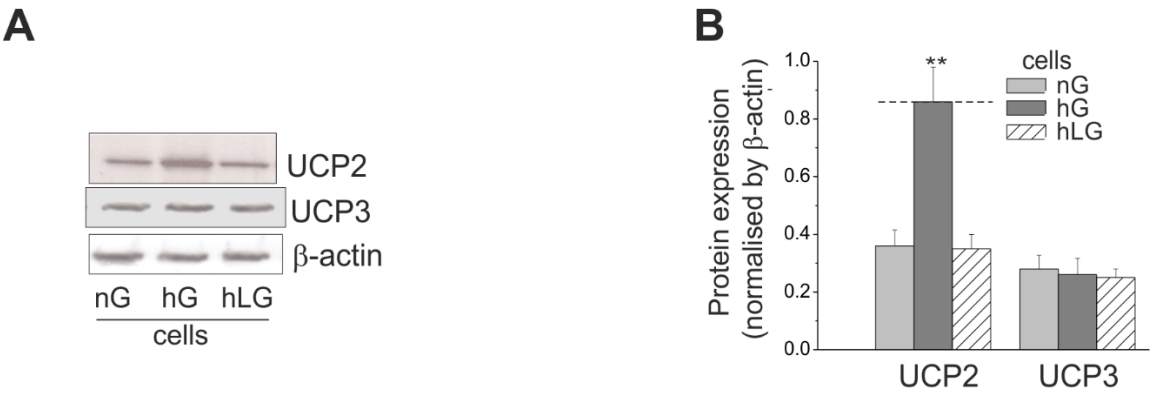

Figure 4.16 A: UCP2 and UCP3 protein levels in cells grown in normal glucose (5.5 mM D-glucose, nG cells), high glucose (25 mM D-glucose, hG cells) or high non-metabolised glucose (5.5 mM D-glucose plus 19.5 mM L-glucose, hLG). The same amounts of proteins (40 μg) were loaded into each lane. B: Expression levels normalised by β actin protein abundance are shown. Means ± SD; *n* = 7-8.

To verify whether the upregulation of UCP2 was not due to the high osmolality, the effect of treatment with 19.5 mM L-glucose plus 5.5 mM D-glucose, providing an equivalent osmolality as 25 mM D-glucose, was studied (Figure 4.16). The analysis suggests that

osmolality control did not significantly change the expression of UCP2 protein, and that the observed upregulation of UCP2 is specific for metabolised 25 mM D-glucose. Furthermore, it seems that UCP2 is the only UCP involved in high glucose-induced modifications in EA.hy926 cells. Therefore, the high-glucose-induced changes in UCP activity (Chapter 4.1.2.2 and Chapter 4.2) can be attributed to UCP2.

4.2.2 High-glucose levels and UCP2 activity under non-phosphorylating and phosphorylating conditions

To determine UCP2 function in endothelial mitochondria, the activation of UCP2 by free FAs (linoleic acid) and its inhibition by purine nucleotides (GTP) were studied in mitochondria isolated from EA.hy926 cells. Figure 4.17 A presents examples of oxygen consumption and $\Delta\Psi$ measurements for non-phosphorylating mitochondria respiring with succinate as a reducing substrate. In non-phosphorylating mitochondria isolated from cells grown in high-glucose conditions, the respiratory rate and $\Delta\Psi$ were observed to be more sensitive to 16 μM linoleic acid (i.e., a greater stimulation of respiratory rate and a greater decrease in $\Delta\Psi$) and a subsequent addition of 4 mM GTP (i.e., a more pronounced recoupling effect), indicating a higher level of UCP activity (mainly UCP2 activity) compared to that of the control mitochondria isolated from cells grown in normal-glucose conditions.

Moreover, a proton leak kinetics study obtained with cyanide titration (Figure 4.17 B) indicates that for given linoleic acid (16 μM) and GTP (4 mM) concentrations, the linoleic acid-induced, GTP-inhibited, UCP2-mediated proton leak at the same $\Delta\Psi$ (154 mV) was two-fold greater in the mitochondria from high-glucose cells. These observations are consistent with the proton kinetics study obtained with malonate titration, when palmitic acid was applied to activate UCP2 (Figure 4.14). Thus, a much higher UCP2 activity was observed after exposure of endothelial cells to high-glucose levels independent of the type of respiratory chain titration (Q-reducing pathway titration or QH_2-oxidising pathway titration). Interestingly, the obtained proton leak kinetics (Figure 4.17 B and Figure 4.14) indicate the dependence of UCP2 inhibition by GTP on the Q reduction level. Namely, a full inhibition of UCP2-mediated proton leak was observed at lower Q reduction levels (titration with malonate) (Figure 4.14), while attenuation of this inhibition was observed at higher Q reduction levels (titration with cyanide) (Figure 4.17).

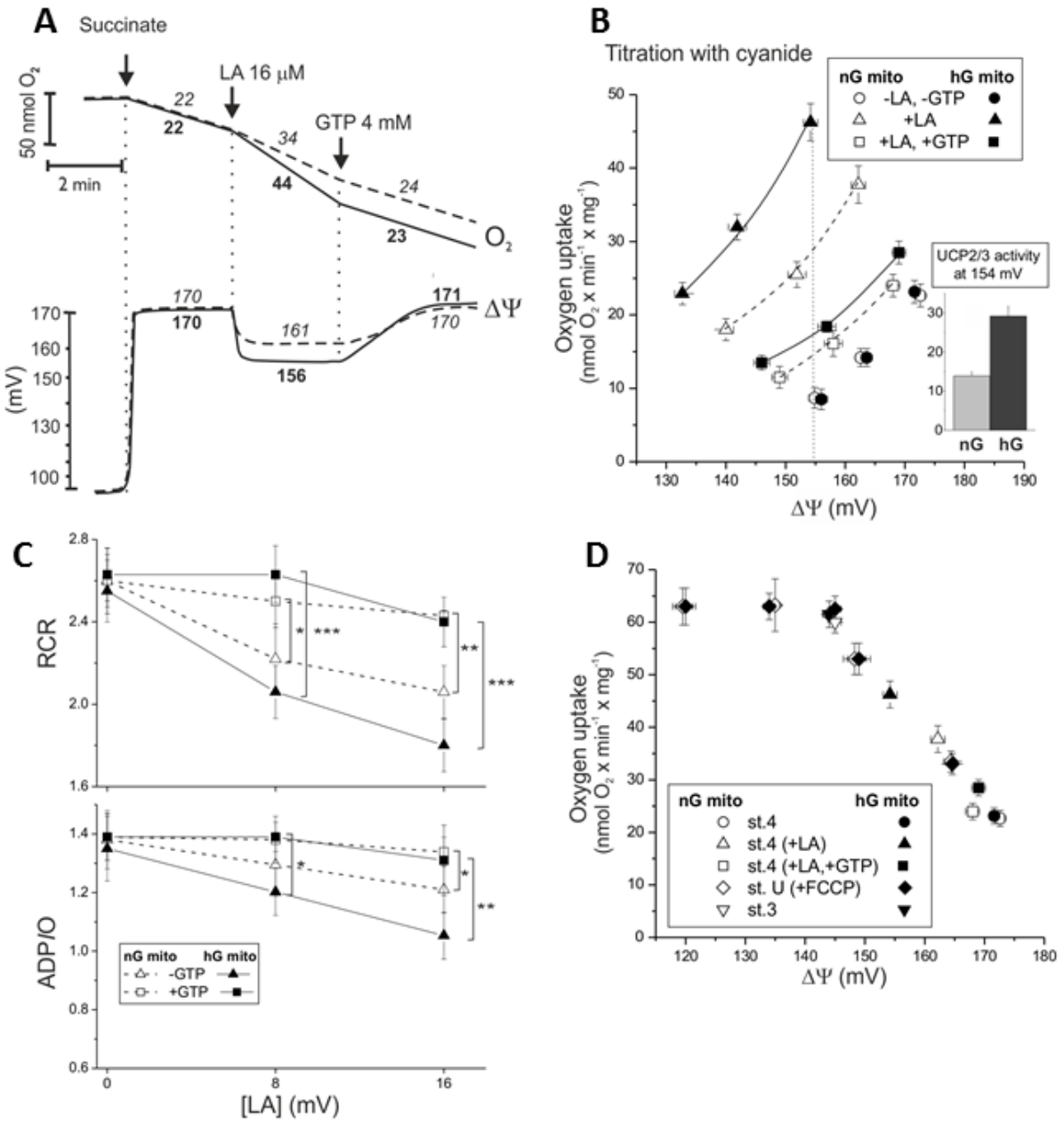

Figure 4.17 Linoleic acid (LA)-induced GTP-inhibited UCP2 activity in endothelial mitochondria. A: The effects of UCP2 activation by LA and UCP inhibition by GTP on oxygen uptake and ΔΨ. The mitochondria from normal-glucose cells (nG mito) are represented by broken lines and numbers in italics, and the mitochondria isolated from high-glucose cells (hG mito) are represented by solid lines and bold numbers. B: The relationship between the respiratory rate and ΔΨ during non-phosphorylating succinate oxidation titrated with cyanide. The LA-induced GTP-inhibited UCP-mediated proton leak at the same ΔΨ (154 mV) is indicated in the inset image. C: Effects of LA-induced GTP-inhibited UCP activity on the ADP/O ratio and RCR (phosphorylating respiration vs non-phosphorylating respiration). Concentrations used: 0, 8 and 16 μM LA, and 4 mM GTP. D: The relationship between the respiratory rate and ΔΨ during non-phosphorylating respiration (state 4, st.4) in the absence or presence of LA and/or GTP, uncoupled respiration (st.U) in the presence of increasing concentrations of FCCP (up to 0.3 μM) and phosphorylating respiration (st.3) in the presence of 0.4 mM ADP. Means ± SD; *n* =7.

Under phosphorylating conditions, a direct consequence of UCP activity is a decrease in the amount of ATP synthesised per oxygen consumed, i.e., the yield of mitochondrial OXPHOS. As shown in Figure 4.17 C, in both types of endothelial mitochondria, linoleic acid-induced GTP-inhibited UCP activity was able to divert energy from oxidative phosphorylation, indicating an energy-dissipating function during phosphorylating respiration. The increased activity of UCP2 in phosphorylating mitochondria from high-glucose cells led to a significantly greater reduction in the OXPHOS yield (ADP/O ratio) and RCR (Figure 4.17 C). For given linoleic acid (8 or 16 μM) and GTP (4 mM) concentrations, the linoleic acid-induced, GTP-reversed drops in the ADP/O ratio and RCR were approximately two-fold greater in the mitochondria from high-glucose cells. Similar results were observed when 14 μM palmitic acid and 2 mM GTP were used to modulate UCP2 activity (Figure 4.15). Thus, a greater contribution of UCP2 activity to phosphorylating respiration was observed in the mitochondria from high-glucose cells compared to the mitochondria from normal-glucose cells.

The voltage dependence of the electron flux (Figure 4.17 D) shows that the linoleic acid-induced GTP-inhibited respiration (for 16 μM linoleic acid and 4 mM GTP) only occurs due to UCP-mediated proton recycling, as it corresponds to a pure protonophoretic effect of linoleic acid that is not distinguishable from the effect of a well-known protonophore FCCP. Indeed, for both types of mitochondria, couples of respiratory rate and ΔΨ measurements in resting (state 4) respiration with increasing concentrations of FCCP or in the presence of 16 μM linoleic acid (with or without 4 mM GTP), as well as in phosphorylating state 3 respiration, constituted a single flow-force relationship. Thus, a modulation of the force (ΔΨ), either by phosphorylation potential, linoleic acid or protonophore led to the same modification of the flow (respiratory rate). Results presented in Figure 4.17 D indicate that linoleic acid (at 16 μM concentration) did not interact with the respiratory chain of endothelial mitochondria and that the growth of endothelial cells under high-glucose conditions did not disturb the voltage dependence of the electron flux in the respiratory chain of these mitochondria.

4.2.3 High-glucose levels and UCP2 control of respiratory rate, ΔΨ, and mROS

The next step was to determine the effect of UCP2 activation on respiratory rate, ΔΨ, and mROS formation in mitochondria isolated from EA.hy926 cells grown in the high-glucose and normal-glucose conditions. In mitochondria from normal-glucose and high-glucose cells, respiration rates and ΔΨ during the oxidation of succinate were similar in the

absence of linoleic acid (Figure 4.18 A, B, and C). The maximal linoleic acid concentration required to obtain a simultaneous increase in oxygen consumption and a decrease in ΔΨ was determined for non-phosphorylating endothelial mitochondria from both studied types of cells (Figure 4.18). All measurements were performed in the presence of defatted BSA to exclude UCP activation by endogenous free FAs. Moreover, to exclude uncoupling mediated by an adenine nucleotide carrier, all measurements were performed in the presence of carboxyatractyloside.

Figure 4.18 shows the influence of four different concentrations of linoleic acid (8, 16, 24 and 32 μM) on the respiratory rate (Figure 4.18 A) and the ΔΨ (Figure 4.18 B). As shown in Figure 4.18 A, in mitochondria from normal-glucose cells, the maximal linoleic acid-induced uncoupling effect was observed with 16 μM linoleic acid, which increased the respiration rate by ~55%. In mitochondria from high-glucose cells, the maximal linoleic acid-induced uncoupling effect was observed with 24 μM linoleic acid, with which the respiration rate increased significantly by ~160%. These increases in respiration were accompanied by a decrease in ΔΨ of ~11 mV and ~23 mV for mitochondria from normal-glucose and high-glucose cells, respectively (Figure 4.18 B). Results presented in Figure 4.18 affirm a much greater linoleic acid-induced uncoupling in mitochondria from high-glucose cells at any linoleic acid concentration up to 16 μM. Moreover, at 24 μM linoleic acid, there was decrease (in mitochondria from normal-glucose cells) and no further increase (in mitochondria from high-glucose cells) in oxygen consumption compared to that at 16 μM linoleic acid. At 32 μM linoleic acid, an inhibition of respiration was also revealed in mitochondria from high-glucose cells. Thus, an inhibition of the respiratory chain occurred at a higher linoleic acid concentration in mitochondria from cells exposed to high-glucose levels, indicating less sensitivity to the inhibitory excess of FA.

The determination of superoxide anion formation showed that in the absence of linoleic acid, mROS production was similar in both types of mitochondria respiring with succinate (Figure 4.18 C). With increasing linoleic acid concentrations up to 16 μM or 24 μM superoxide generation was gradually reduced in mitochondria from normal-glucose and high-glucose cells, respectively.

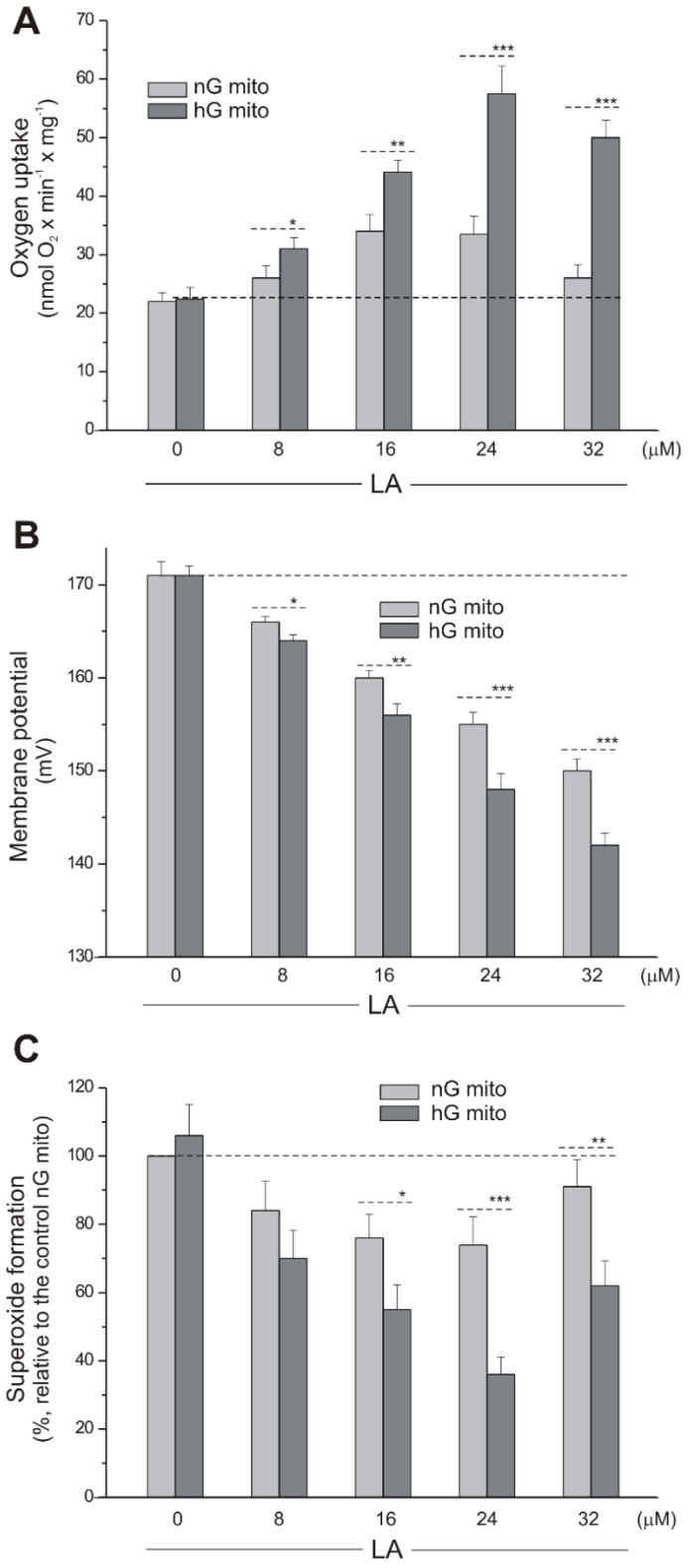

Figure 4.18 The influence of increasing concentrations of linoleic acid (LA, 0-32 µM) on the respiratory rate (A), ΔΨ (B), and superoxide formation (C) of endothelial non-phosphorylating mitochondria from normal-glucose (nG mito) and high-glucose (hG mito) cells. Measurements were performed in the presence of 1.8 µM carboxyatractyloside and 0.5 µg/ml oligomycin. Means ± SD; *n* = 7-8.

However, for a given linoleic acid concentration (up to 16 μM), the linoleic acid-induced attenuation of mROS formation was significantly stronger in mitochondria from high-glucose cells. In mitochondria from normal-glucose and high-glucose cells, concentrations of linoleic acid higher than 16 μM and 24 μM, respectively, caused an increase in superoxide formation compared to that, which occurred in the presence of lower FA concentrations.

The foregoing results indicate that when concentrations of FA were too high, an inhibition of the mitochondrial respiratory chain was observed, which was revealed by a decreased respiratory rate and $\Delta\Psi$, and increased mROS. However, in the case of mitochondria from high-glucose cells, less sensitivity to the inhibitory excess of FA was observed. Compared to non-phosphorylating conditions in both types of endothelial mitochondria, production of superoxide (Figure 4.19 B) and H_2O_2 (Figure 4.19 C) was considerably reduced by 30-50% under phosphorylating (in the presence of ADP) and uncoupled (in the presence of FCCP) conditions. In the presence of GTP, superoxide formation during uncoupled respiration did not change (Figure 4.19 B). When the non-induced or linoleic acid-induced changes in mitochondrial function, including mROS production, are sensitive to purine nucleotides, they can be considered to indicate UCP activation. The effects of UCP2 activation (by linoleic acid) or inhibition (by GTP) on mROS formation in non-phosphorylating mitochondria in the presence of OXPHOS inhibitors were measured (Figure 4.19 A and C). In the presence of oligomycin and carboxyatractyloside, the highest level of mROS formation was observed.

Moreover, in both types of mitochondria, the addition of GTP, which blocks linoleic acid-induced UCP2 activity, increased superoxide formation in a concentration-dependent manner (Figure 4.19 A). The inhibitory effect of GTP on inducible UCP2 activity and thereby on UCP2 antioxidant activity was much greater in mitochondria from high-glucose cells. Furthermore, in the presence of 4 mM GTP, superoxide formation was restored to the level that was detected before FA addition. Similar effects of linoleic acid (i.e., decrease in mROS formation) and GTP (i.e., re-increase in mROS formation), more pronounced in high-glucose cells, were observed during H_2O_2 production measurement in non-phosphorylating mitochondria (Figure 4.19 C).

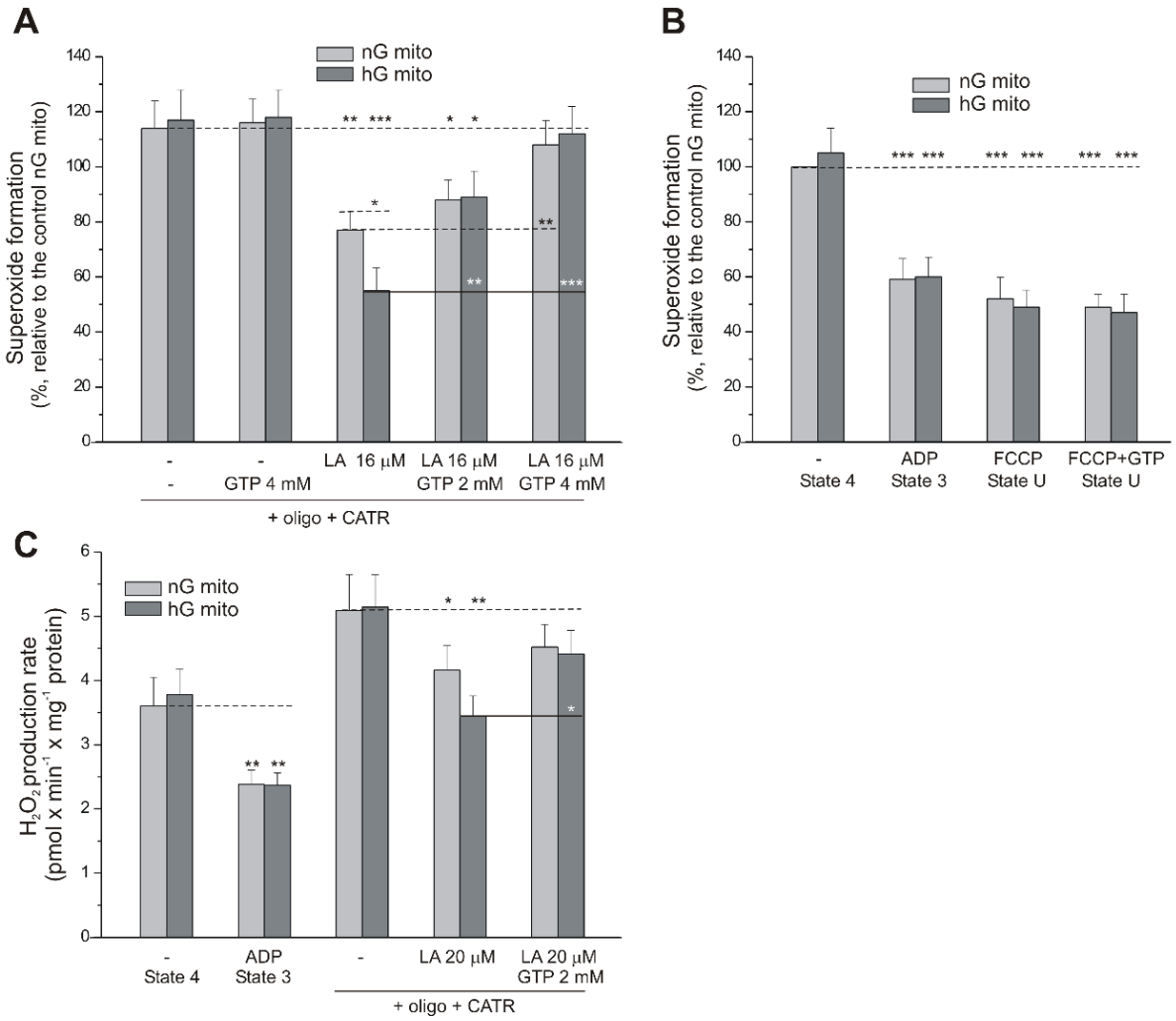

Figure 4.19 Effect of UCP activation and inhibition on mROS formation in endothelial mitochondria isolated from normal-glucose (nG mito) and high-glucose (hG mito) cells. In measurements of non-phosphorylating mitochondria, 1.8 μM carboxyatractyloside (CATR) and 0.5 μg/ml oligomycin (oligo) were added. Measurements of mitochondrial superoxide formation (with NBT) (A-B) and mitochondrial H_2O_2 formation (with Amplex Red) (C). Additions (where indicated): linoleic acid (LA, 16 μM), GTP (2 or 4 mM). Measurements under non-phosphorylating (state 4), phosphorylating (state 3, in the presence of 0.4 mM ADP), uncoupled (state U, in the presence of 0.6 μM FCCP and in the presence or absence of 4 mM GTP) conditions. A-B: Superoxide formation is shown as relative to the control nG mitochondria in state 4 in the absence of carboxyatractyloside and oligomycin (100%) (the first bar in B). Means ± SD; *n* = 7-8.

These results show for the first time that FA-induced GTP-inhibited UCP2 activity lowers mROS formation in isolated endothelial mitochondria and that this mROS-decreasing protective function of UCP2 is much more pronounced in mitochondria from cells grown under elevated-glucose concentrations. Furthermore, these results clearly indicate that the UCP2 control of respiratory rate, $\Delta\Psi$, and mROS is more pronounced in mitochondria isolated from high-glucose-treated cells compared to control mitochondria.

4.2.4 High-glucose levels and effect of UCP2 silencing on inflammation and ROS

To explicate a physiological role for UCP2 in endothelial cells, EA.hy926 cells cultured under normal-glucose (normal UCP2 level) and high-glucose (UCP2 upregulation) conditions (cells with control siRNA) were cultured with cells that had been treated with UCP2 siRNA to knock down UCP2 (no UCP2 cells). In the normal-glucose and high-glucose cells, the efficiency of knockdown was confirmed by a lack of UCP2 detection in UCP2-null cells (Figure 4.20). Moreover, UCP3 expression did not change in both types of endothelial cells independent of UCP2 silencing. The immunodetection of ICAM1 protein indicated an increased level of the inflammation marker in high-glucose cells compared to normal-glucose cells. This result was independent of the presence of UCP2. Thus, in both types of cells, the lack of UCP2 led to increased ICAM1 expression, although the increase was much greater in the high-glucose cells. These results indicate that in the high-glucose-treated cells, lack of UCP2 induces ameliorated inflammation compared to the control cells.

As shown in Figure 4.21, compared to UCP2-expressing cells cultured in normal-glucose conditions, the exposure of UCP2-expressing cells to high-glucose concentrations caused a significant increase in total (Figure 4.21 A) and mitochondrial (Figure 4.21 A and B) superoxide generation. Mitochondrial superoxide generation was estimated in endothelial cells either as DPI-insensitive NBT reduction (Figure 4.21 A) or MitoSOX oxidation (Figure 4.21 B). These results are consistent with previous observations (Figure 4.7), indicating that in EA.hy926 cells, high-glucose-induced ROS appear to be produced by the enzyme NADPH oxidase and from mitochondrial sources (including DPI-insensitive sources). To affirm that the high-glucose-induced enhancement of superoxide formation was not due to the high osmolality, the effect of treatment with 19.5 mM L-glucose plus 5.5 mM D-glucose, providing an equivalent osmolality as 25 mM D-glucose, was studied (Figure 4.21 B). The osmolality control did not show a significant change in superoxide production between cells grown with 19.5 mM L-glucose plus 5.5 mM D-glucose compared to cells grown with 25 mM D-glucose. This result indicates that the observed high-glucose-induced enhancement of superoxide formation is specific for metabolised 25 mM D-glucose. Thus, in normal-glucose and high-glucose cells, the absence of UCP2 caused a significant increase in total and mitochondrial superoxide formation (Figure 4.21). However, the enhancement of superoxide formation in UCP2-deficient cells was much more pronounced in high-glucose cells than in normal-glucose cells, indicating an increased need for the antioxidative activity of UCP2 under high-glucose conditions.

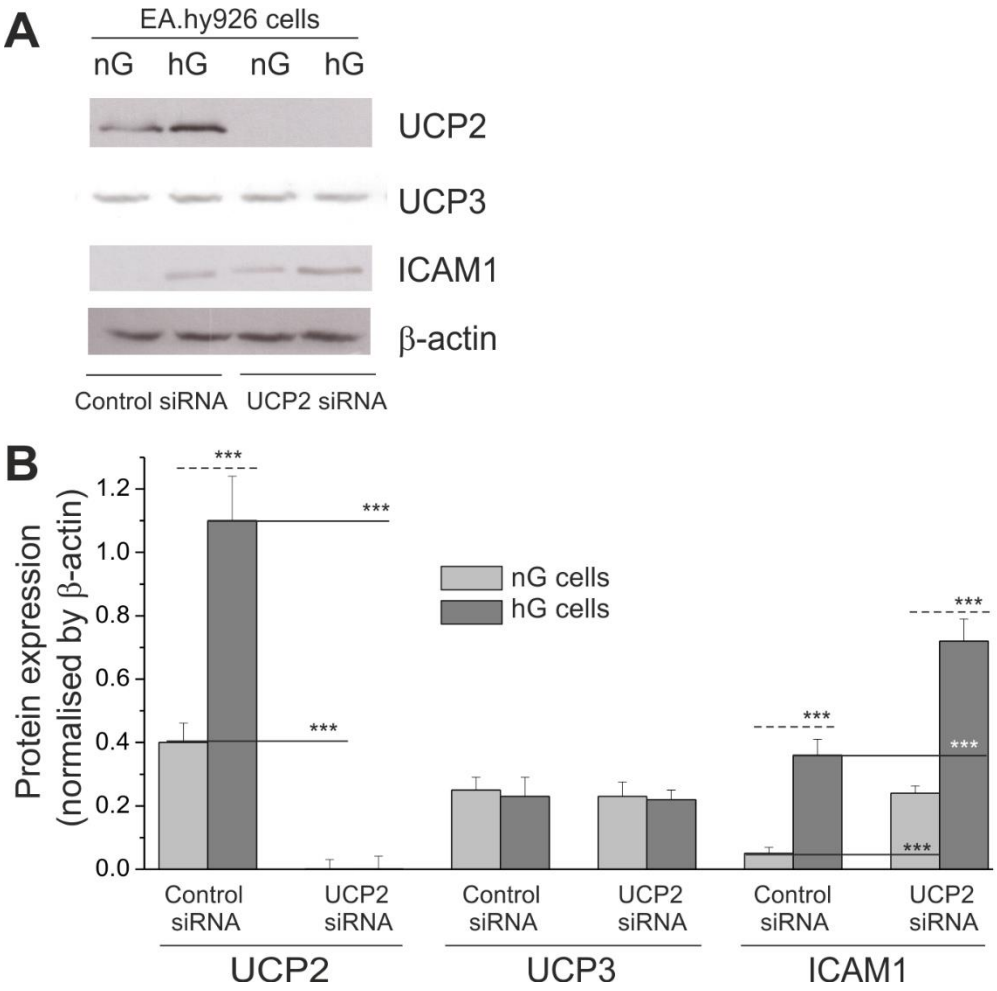

Figure 4.20 Effect of UCP2 silencing on the UCP2, UCP3, and ICAM1 protein levels in EA.hy926 cells grown in normal-glucose (nG cells) or high-glucose (hG cells) conditions expressing either UCP2 targeting (UCP2 knockdown) or scrambled (control) siRNAs. A: Examples of immunoblots (using samples from 7 different cellular fraction preparations) are shown. The same amounts of proteins (80 μg) were loaded into each lane. B: Expression levels normalised by β actin protein abundance are shown. Means ± SD; *n* = 7.

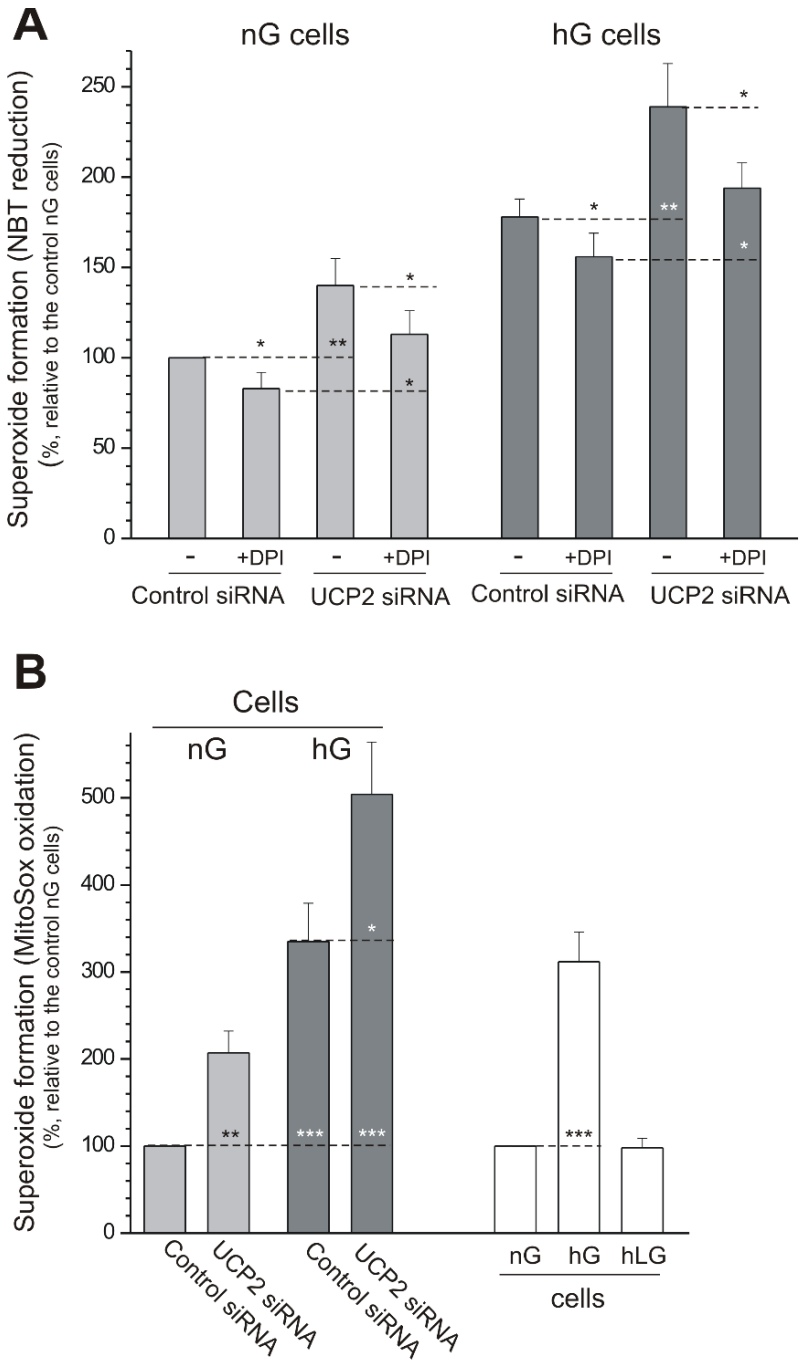

Figure 4.21 Superoxide formation in normal-glucose (5.5 mM, nG cells) or high-glucose (25 mM, hG cells) endothelial cells expressing either UCP2 targeting (UCP2 knockdown) or scrambled (control) siRNAs. A: Measurements of superoxide formation (with NBT) were performed in the absence or presence of 10 μM DPI. B: Measurements of superoxide formation (with MitoSox probe) were performed in cells grown in normal glucose (5.5 mM D-glucose, nG cells), high glucose (25 mM D-glucose, hG cells) or high non-metabolised glucose (5.5 mM D-glucose plus 19.5 mM L-glucose, hLG, an osmolality control). Means ± SD; *n* = 7-8.

4.2.5 High-glucose levels and effect of UCP2 silencing on cell viability and resistance to oxidative stress

Despite increased ICAM1 expression (Figure 4.20) and pronounced ROS generation (Figure 4.21), endothelial cells grown under high-glucose conditions revealed a similar viability compared to normal-glucose cells (Figure 4.22).

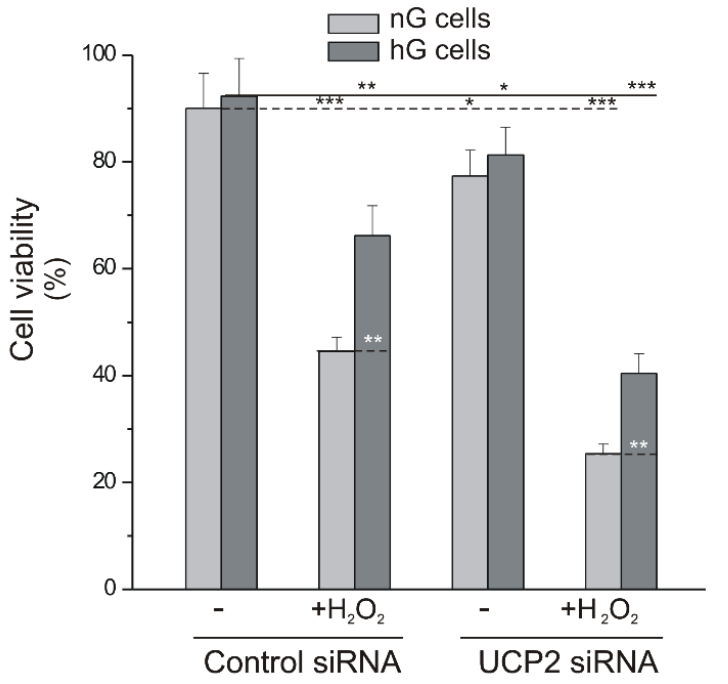

Figure 4.22 Viability of EA.hy926 cells grown under normal-glucose (nG cells) or high-glucose (hG cells) conditions with (UCP2 siRNA) or without (control siRNA) knockdown of mitochondrial UCP2. Cells were incubated in the absence or presence of 1.8 mM H_2O_2 for 24 h. Means ± SD; *n* = 7.

Furthermore, UCP2 silencing led to a similar (~12%) decrease in cell viability in both types of cells grown in the absence of H_2O_2 (Figure 4.22). In order to verify whether the lack of UCP2 and/or high-glucose conditions had an impact on endothelial cell resistance to stress, the normal-glucose and high-glucose cells were incubated with 1.8 mM H_2O_2 for 24 h. Their survival was evaluated relative to that of controls without H_2O_2 treatment. As shown in Figure 4.22, peroxide significantly impaired cell viability in normal-glucose and high-glucose cells (by ~45% and ~26% in UCP2-expressing cells and by ~52% and ~40% in UCP2 knocked down cells, respectively). Moreover, high-glucose cells were significantly less sensitive to peroxide than normal-glucose cells independent of UCP2 expression. UCP2 silencing led to slightly more impaired stress resistance to peroxide in high-glucose cells compared to normal-

glucose cells (~26% reduction and ~19% reduction vs high-glucose and normal-glucose UCP2-expressing cells, respectively) (Figure 4.22).

These results indicate that UCP2 influences endothelial cell viability and resistance to oxidative stress. Moreover, in endothelial cells exposed to high-glucose concentrations, increased expression of UCP2 led to improved stress resistance. In high-glucose-treated cells, the increased activity of UCP2, and thereby increased antioxidant defence led to improved stress resistance and protection against acute oxidative stress.

4.2.6 Discussion and conclusions

In the present study, the effect of UCP2 on mitochondrial function was studied in mitochondria isolated from endothelial cells exposed to high-glucose levels. The results indicate that in isolated endothelial mitochondria, high-glucose conditions induced an increase in free FA-induced GTP-inhibited UCP2 activity under both non-phosphorylating and phosphorylating conditions (results shown in Chapter 4.1.2.2 and Chapter 4.2.2). In non-phosphorylating mitochondria from high-glucose endothelial cells, the increased UCP2 activity had a bigger impact on the mitochondrial respiratory rate, $\Delta\Psi$, and ROS generation. The presented results show that UCP2-mediated uncoupling modulates the proton leak across IMM of endothelial mitochondria. The observed antioxidative activity of endothelial UCP2 was dependent on its effect on $\Delta\Psi$. The high-glucose-induced UCP2-mediated uncoupling caused an increased antioxidative efficiency (increased mROS attenuation) in mitochondria from high-glucose-exposed cells. However, the high-glucose-induced increase in the activity of UCP2 led to a greater reduction in the OXPHOS yield. These findings indicate that under high-glucose-induced oxidative stress, the maintenance of ATP synthesis efficiency is not as important as the attenuation of mROS production, especially given that endothelial mitochondria are not particularly dependent on OXPHOS.

In endothelial mitochondria from both normal-glucose and high-glucose cells, an excess of linoleic acid inhibited the respiratory chain, no further activating mitochondrial uncoupling through UCP2 (Figure 4.18). As shown in the previous chapter (Chapter 4.1), high-glucose exposure induces a shift in endothelial aerobic metabolism from carbohydrate oxidation towards the oxidation of lipids and amino acids. Therefore, in hyperglycaemic endothelial cells, the increased oxidation of FAs by mitochondria may protect the mitochondrial respiratory chain against the inhibitory effect of excess levels of FAs. On the other hand, in endothelial mitochondria with high-glucose-induced increased levels of UCP2, lower levels of FAs may still activate UCP2-mediated uncoupling largely than in

mitochondria from normal-glucose cells. The results presented in this chapter indicate that the mitochondrial respiratory chain in high-glucose cells is less sensitive to free FA inhibition due to UCP2 upregulation.

The exposure of endothelial cells to high-glucose levels leads to increased intracellular and mitochondrial ROS production and therefore produces excessive oxidative stress (Du et al., 2000; Giardino et al., 1996; Nacsimento et al., 2006; Nishikava et al., 2000; Srinivasan et al., 2004; Zhang and Gutterman, 2007). Under our experimental conditions, the increased oxidative stress in EA.hy926 cells grown under chronic high-glucose conditions was revealed by significantly higher intracellular and mitochondrial ROS generation and the upregulation of UCP2 as a mitochondrial antioxidative system protein. The increased expression levels of UCP2 in response to high-glucose levels have previously been observed in other endothelial cell lines (such as HUVEC, BREC, and HMEC) (Cui et al., 2006; Dymkowska et al., 2014; Quian et al., 2011; Zheng et al., 2010) and endothelial cells isolated from animal models of diabetes (for example, diabetic mice) (Sun et al., 2013; Xie et al., 2008). In EA.hy926 endothelial cells, high-glucose-induced ROS appear to be produced by the enzyme NADPH oxidase and by mitochondrial sources (Figure 4.21 and Figure 4.21). In general, mROS generation is associated with an increased reduction of respiratory chain components that may be caused by the increased oxidation of mitochondrial fuels and/or the impairment of the QH_2-oxidising pathway. These results indicate that under high-glucose-induced oxidative stress conditions, UCP2 activity may attenuate mROS production by lessening the reduction level of mitochondrial respiratory chain complexes. A greater enhancement in superoxide formation was observed in UCP2-deficient EA.hy926 cells that were exposed to high-glucose concentrations compared to UCP2-deficient control cells (Figure 4.21), indicating an increased need for antioxidative UCP2 activity under high-glucose conditions. Our studies show that endothelial UCP2 participates in the control of mitochondria-derived ROS.

As shown in Figure 4.22, UCP2 influenced cell viability both in high-glucose and normal-glucose EA.hy926 cells. There was a significant difference in viability of UCP2-expressing and also UCP2-knocked down cells after H_2O_2 treatment between normal-glucose and high-glucose conditions (Figure 4.22), although UCP2 siRNA reduced UCP2 protein to similar very low levels in both types of endothelial cells (Figure 4.20)**.** UCP2 silencing only slightly more impaired stress resistance in high-glucose cells compared to normal-glucose cells. These findings indicate the presence of additional UCP2-independent mechanisms of endothelial cell injury induced by high-glucose conditions. They could involve high-glucose-induced UCP2-independent mitochondrial changes and non-mitochondrial alternations that

influence endothelial cell viability. However, high-glucose cells were significantly more resistant to peroxide independent of UCP2 expression. Thus, in endothelial cells exposed to high-glucose concentrations, the increased activity of energy-dissipating protein, i.e., UCP2, and thereby increased antioxidant defence led to improved stress resistance and protection against acute oxidative stress. These results indicate that in endothelial cells, hyperglycaemia could be involved in the hormetic induction (Cypser and Johnson, 2002) of antioxidant defence and stress resistance. Moreover, inhibition of high-glucose-induced apoptosis by lentivirus-mediated UCP2 overexpression has been observed in HUVEC cells (He et al., 2014). Thus, our data highlight and support the importance of mitochondrial UCP2-mediated uncoupling in endothelial stress resistance.

Several studies have shown that in response to hyperglycaemia, endothelial UCP2 may function as a sensor and negative regulator of mROS overproduction, which is an initiating cause in the pathogenesis of diabetic complications, such as diabetic retinopathy, hypertension, or atherosclerosis. In diabetic mice, AMPK activation increases UCP-2 expression, resulting in the inhibition of both superoxide and prostacyclin synthase nitration and thus attenuation of oxidative stress (Xie et al., 2008). In diet-induced obese mice, UCP2 protects endothelial function through increasing NO bioavailability secondary to the inhibition of ROS formation (Tian et al., 2012)**.** Similarly, in diabetic *ob*/*ob* mice, vascular benefit is likely to result from the upregulation of UCP2 expression, which reduces oxidative stress and increases the level of NO (Sun et al., 2013). For example, this effect accounts for the endothelium-dependent relaxation observed in capsaicin-treated *db*/*db* mice. Thus, the results of present study showing a greater UCP2-mediated decrease in mROS generation, an improved antioxidative role for UCP2, and improved resistance to oxidant stress-induced cell death in association with increased UCP2 expression and activity in endothelial cells exposed to high-glucose levels, support studies on diabetes-induced vascular disease. The increase in UCP2 expression in endothelial cells may aid in preventing the development and progression of vascular dysfunction. For instance, UCP2 could be a useful target in treating atherosclerosis or hypertension-related vascular events (Lee et al., 2005; Liu et al., 2014). However, many questions must be addressed with respect to understanding the physiological role that UCP2 plays in endothelial mitochondria and its contribution to vascular function and disease.

It can be concluded that UCP2 influences endothelial cell viability and resistance to oxidative stress. Endothelial cells exposed to high glucose concentrations are significantly more resistant to peroxide. In these cells, the increased activity of UCP2 leads to improved

stress resistance and protection against acute oxidative stress. These results indicate that endothelial UCP2 may function as a sensor and negative regulator of mROS production in response to exposure of endothelial cells to high-glucose levels.

4.3 The influence of chronic hypoxia on the aerobic metabolism of EA.hy926 cells

The influence of hypoxic exposure of endothelial cells, especially chronic exposure to hypoxia, on the mitochondrial oxidative function has not been intensively studied. To study acute hypoxia-induced changes, endothelial EA.hy926 cells were cultured for 6 days at 1% O_2 tension. The aim of this study was to elucidate the effects of chronic hypoxia on the aerobic metabolism of endothelial cells at the cellular and mitochondrial levels. Cell viability, superoxide formation, and mitochondrial respiratory function, including the respiratory response to different reducing fuels and mitochondrial oxidative capacity, were determined in hypoxic cells (grown at 1% O_2) and normoxic cells (grown at 20% O_2). Moreover, the effect of the chronic exposure of growing endothelial cells to hypoxia on their mitochondria was studied by measuring mitochondrial respiratory activities with complex I and complex II substrates, ATP synthesis, $\Delta\Psi$, protein-mediated uncoupling, and mROS formation.

4.3.1 Mitochondrial oxidative metabolism of hypoxia-exposed endothelial cells

4.3.1.1 Hypoxia and anaerobic metabolism, mitochondrial biogenesis, and aerobic respiratory capacity

In endothelial EA.hy926 cells exposed to chronic 6-day hypoxia, significantly elevated expression levels of HKI, the enzyme catalysing the first rate-limiting step of the glycolytic pathway, and LDH, the enzyme catalysing the interconversion of pyruvate and lactate, were observed in addition to an increased level of HIF1α (Figure 4.23). The changes were accompanied by a considerable ~60% increase in LDH activity (Figure 4.24 B), indicating that cells grown under hypoxic conditions display an intensified anaerobic glucose oxidation via the glycolytic pathway and lactic acid fermentation. Noteworthy, cell viability was unaltered in chronically hypoxic cells compared to normoxic cells (Figure 4.24 A). Moreover, EA.hy926 cells cultured under normoxic and hypoxic conditions exhibited similar activities (Figure 4.24 C and D) and expression levels (Figure 4.23) of CS and COX, indicating no change in the capacities of the TCA cycle or the mitochondrial respiratory chain and unaltered mitochondrial biogenesis (mitochondrial content).

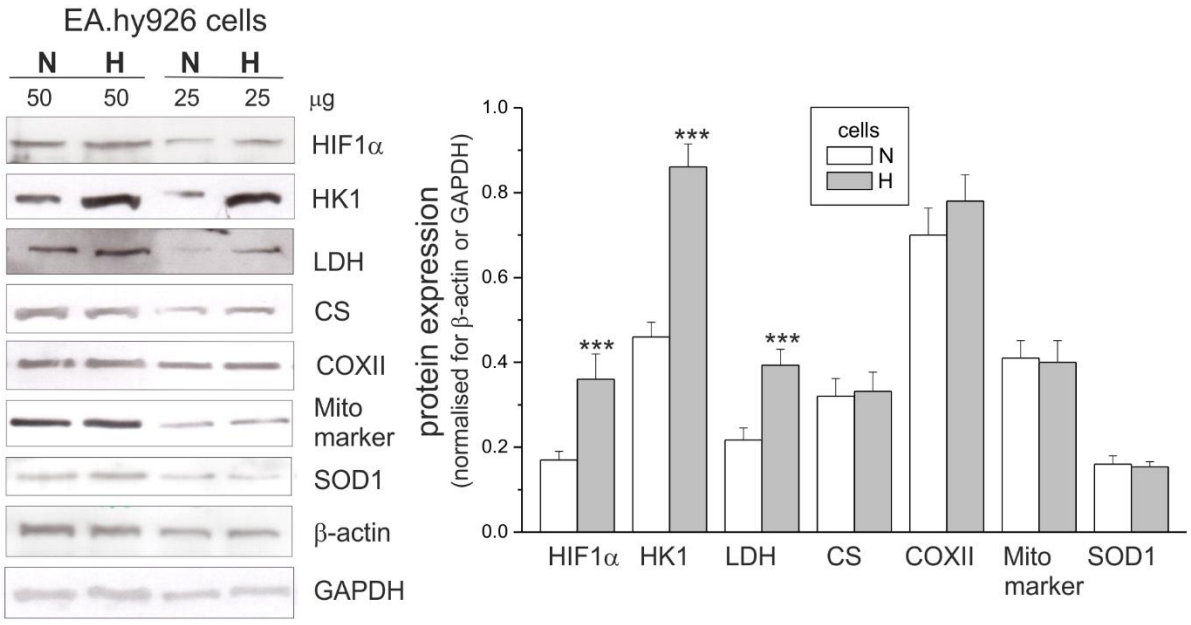

Figure 4.23 Representative Western blots (left) and analyses of the protein expression (right) in endothelial cells grown for 6 days under normoxic (N) and hypoxic (H) conditions. Detected proteins: HIF1α, HKI, LDH, CS, COX (subunit II), SOD1, and mitochondrial marker (mito marker). Means ± SD; *n* = 10.

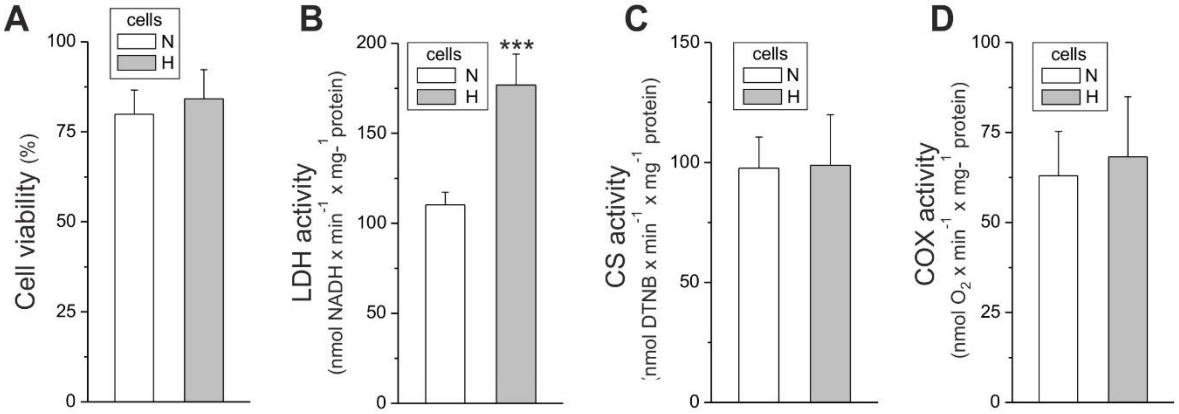

Figure 4.24 Cell viability (A) and maximal activities of marker enzymes of aerobic (C, D) and anaerobic catabolism (B) of EA.hy926 cells grown in normoxia (N) or chronic hypoxia (H). DTNB, 5,5'-di-thiobis-(2-nitrobenzoic acid). Means ± SD; *n* = 8.

4.3.1.2 Hypoxia and mitochondrial oxidation of reducing fuels in cells

As shown in Figure 4.25, under basal conditions (basal OCR) (Figure 4.25 A), FCCP-stimulated conditions (maximal OCR) (Figure 4.25 C), and in the presence of oligomycin (oligomycin-resistant, ATP-linked OCR) (Figure 4.25 D), in both types of cells, the highest

OCR was observed with pyruvate or glutamine. The non-ATP-linked OCR (proton leak) exhibited the least dependence on the type of reducing substrate present (Figure 4.25 C).

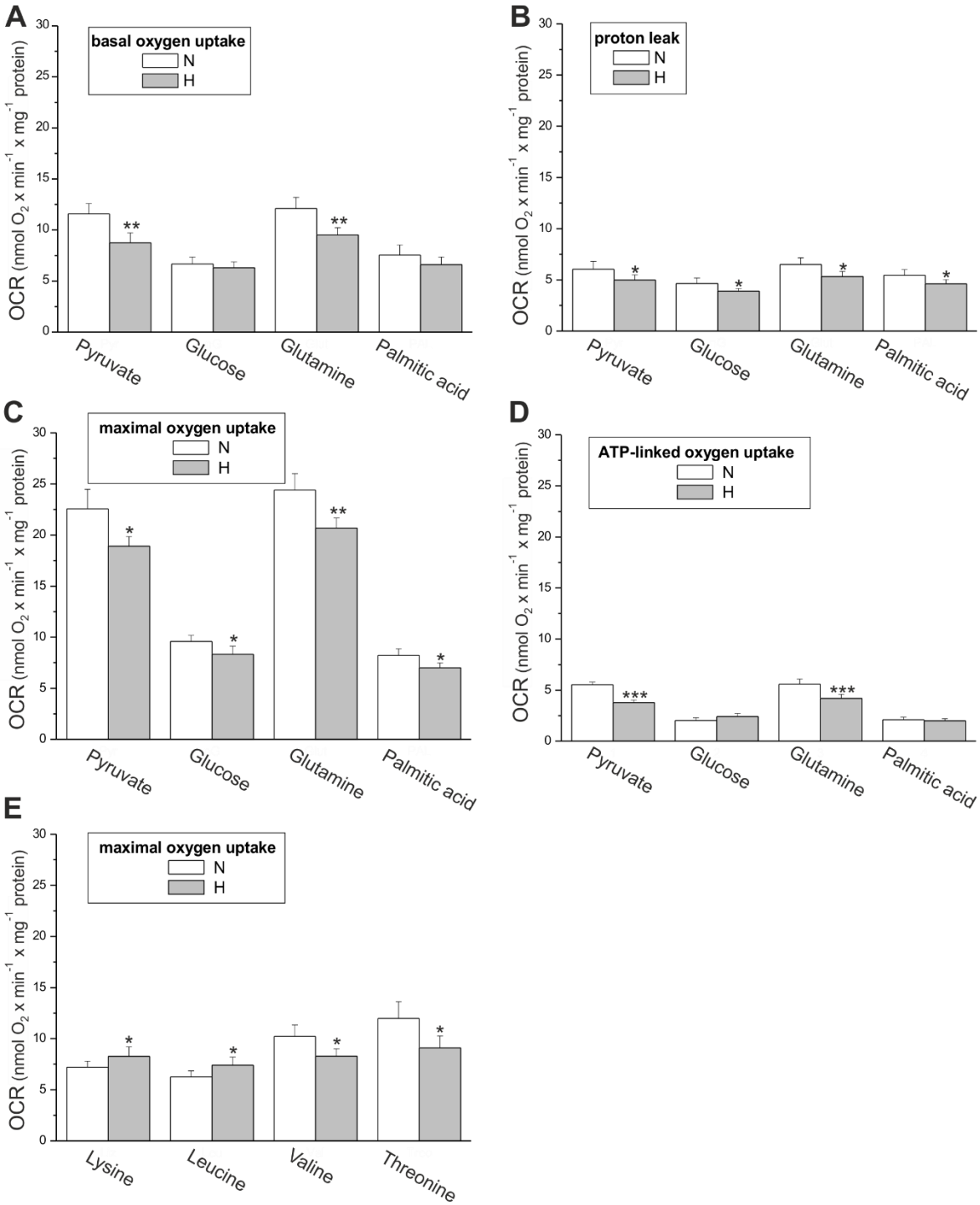

Figure 4.25 Oxidative metabolism of EA.hy926 cells grown in normoxia (N) or chronic hypoxia (H). Substrate-dependent changes in basal OCR (A), proton leak (B), maximal oxygen uptake (C, E), and ATP-dependent oxygen uptake (D). Substrates: 5 mM pyruvate, 5.5 mM glucose, 5 mM amino acids, or 0.3 mM palmitate. Means ± SD; *n* = 6.

To determine how aerobic metabolism in endothelial EA.hy926 cells was altered by long-term cell growth at 1% O_2, the cellular oxygen consumption was measured with different reducing fuels. In general, under all respiratory conditions and with respect to all reducing fuels except lysine and leucine (exclusively ketogenic amino acids), hypoxic cells displayed reduced mitochondrial function (Figure 4.25). In particular, cells exposed to hypoxia exhibited ~13-25% reductions in their maximal mitochondrial respiratory capacity in the presence of pyruvate, glucose, palmitic acid, or amino acids (glutamine, valine, and threonine) (Figure 4.25 C and E). Similarly, with pyruvate and glutamine, significantly reduced ATP-linked OCR was observed in hypoxic cells, indicating diminished levels of mitochondrial OXPHOS (Figure 4.25 D). Interestingly, a significant reduction of non-ATP-linked OCR was also found during oxidation of all substrates (Figure 4.25 B), indicating decreased proton leak in hypoxic cells. Thus, mitochondrial respiratory measurements indicate a general reduction in mitochondrial respiration during carbohydrate, FA, and glucogenic amino acid oxidation in hypoxia-exposed endothelial cells. In contrast, the maximal oxidation of lysine and leucine was significantly higher in hypoxic cells (Figure 4.25 E), indicating a greater contribution from exclusively ketogenic amino acids as a fuel source for endothelial respiration during growth under hypoxic conditions.

4.3.1.3 Hypoxia and intracellular and mitochondrial superoxide anion generation

To examine the influence of hypoxia on mitochondrial and non-mitochondrial ROS generation, superoxide anion formation was measured in hypoxic and normoxic cells. Compared with normoxic cells, the exposure of EA.hy926 cells to chronic hypoxia caused a significant elevation in total (~80% increase) and mitochondrial (~75-100% increase) superoxide generation (Figure 4.26). Mitochondrial superoxide generation was measured as either DPI-insensitive NBT reduction (Figure 4.26 A) or MitoSOX oxidation (Figure 4.26 B). The results indicate that in hypoxic cells, DPI, a flavoprotein inhibitor of NADPH oxidase and eNOS, significantly inhibited (~30% reduction) hypoxia-induced superoxide generation (Figure 4.26 A). Thus, in endothelial cells, hypoxia-induced ROS production appears to occur via enzyme sources and mitochondrial sources (including DPI-insensitive respiratory chain sources).

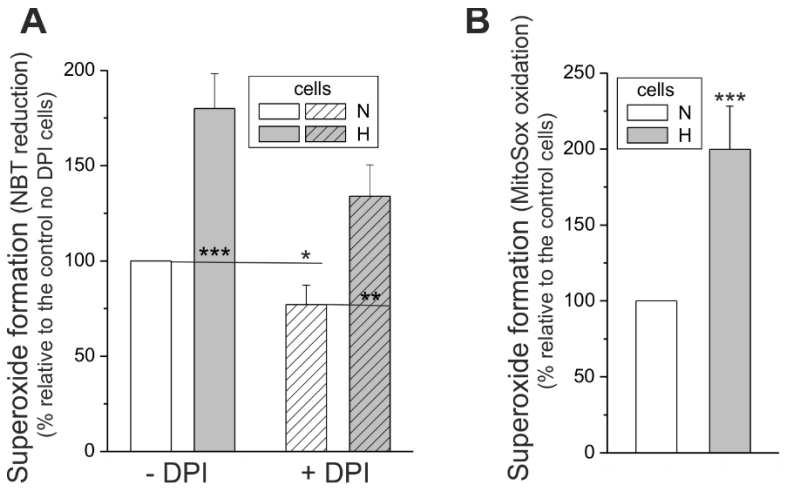

Figure 4.26 Cellular and mitochondrial superoxide formation in endothelial cells grown in normoxia (N) or chronic hypoxia (H). Measurements of superoxide formation with NBT in the absence or presence of DPI (A) and with the MitoSox probe (B). Means ± SD; *n* = 7.

4.3.2 Functional characteristics of mitochondria isolated from hypoxia-exposed cells

4.3.2.1 Hypoxia and mitochondrial oxidative phosphorylation system

To determine the effect of hypoxia on respiratory activity at the mitochondrial level, the maximal respiratory rate with various reducing substrates was measured in isolated endothelial mitochondria (Figure 4.27). In mitochondria from normoxic cells, the highest maximal respiration was observed with malate or a mixture of NAD-linked substrates (malate, α-ketoglutarate, and isocitrate), which saturate the capacity of the endothelial respiratory chain. In mitochondria from hypoxic cells, a significant ~30% decrease in malate-sustained complex I activity was observed (Figure 4.27 A), which was accompanied by ~30% reduction in complex I expression level (Figure 4.28). In addition, reduced (by ~20%) respiration with the mixture of NAD-linked substrates was found (Figure 4.27 A). Interestingly, in mitochondria from hypoxic cells, the maximal oxidation of α-ketoglutarate alone or isocitrate alone was significantly increased but did not exceed malate oxidation, which seems to saturate the decreased capacity of complex I.

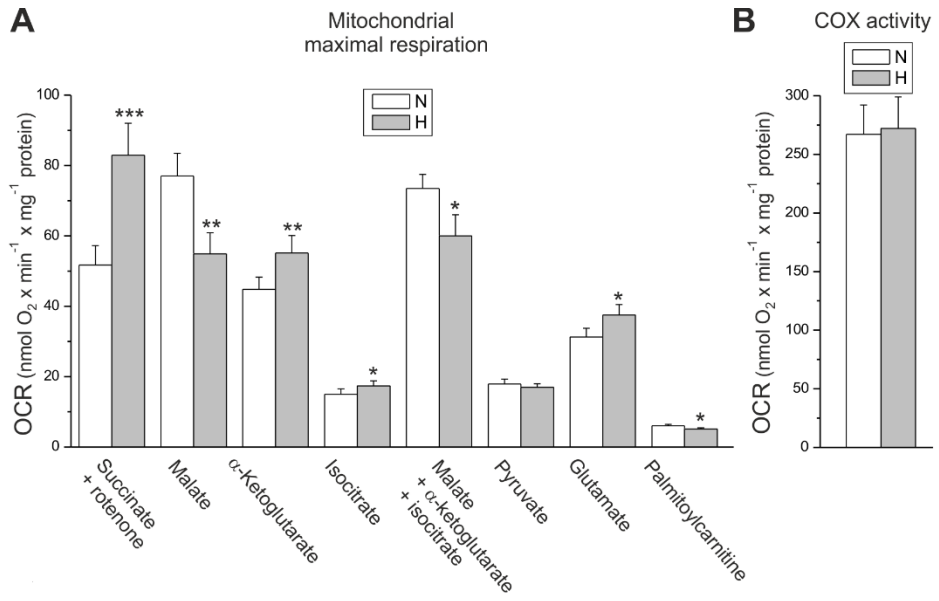

Figure 4.27 Functional characteristics of endothelial mitochondria isolated from cells grown in normoxia (N) or chronic hypoxia (H). The maximal (phosphorylating or uncoupled) respiration with various respiratory substrates (A). The 5 mM TCA substrates (malate, succinate in the presence or absence of 2 μM rotenone, pyruvate, α-ketoglutarate, and isocitrate), 5 mM glutamate, and 0.3 mM palmitoylcarnitine were used. The COX activity (B). Means ± SD; *n* = 4-8.

In mitochondria from hypoxic endothelial cells, the reduced activity of complex I was displayed by significantly decreased respiratory rates and ΔΨ during phosphorylating and non-phosphorylating oxidation of malate (Table 4.1). In contrast to reduction of activity and expression of complex I, the exposure of endothelial cells to hypoxia caused in mitochondria a significant ~60% increase in succinate oxidation (Figure 4.27 A) accompanied by ~100% elevation of complex II expression level (Figure 4.28). In mitochondria from hypoxic cells, the elevated activity of complex II was displayed by significantly increased respiratory rates and ΔΨ during phosphorylating and non-phosphorylating oxidation of succinate in the presence of rotenone (Table 4.1). Despite changes in activities of complex I and complex II, the efficiency of OXPHOS (the ADP/O ratio) during oxidation of malate or succinate was not significantly changed, although displayed a slight decreasing or increasing tendency, respectively. Except complex I and complex II, the expression of other components of the OXPHOS system and CS in mitochondria form hypoxic cells was unaltered (Figure 4.28). Moreover, the maximal COX activity was also unaffected (Figure 4.27 B). However, in mitochondria isolated from hypoxic cells, the oxidation of glutamate was significantly elevated, whereas the oxidation of palmitoylcarnitine was reduced (Figure 4.27 A). This latter change was accompanied by a downregulation in mitochondria of the expression of ACADS (Figure 4.28), the enzyme which catalyses the initial step of FA β-oxidation.

	Succinate + rotenone		Malate	
	N	H	N	H
State 3 rate	51.8 ± 4.8	↑ 82.9 ± 5.4 ***	74.0 ± 7.0	↓ 52.5 ± 4.2 *
State 3 ΔΨ	152.3 ± 0.7	↑ 160.4 ± 1.1 **	161.3 ± 1.2	↓ 152.6 ± 0.9 **
State 4 rate	19.6 ± 2.2	18.6 ± 1.8	17.3 ± 1.2	↓ 13.7 ± 1.4 *
State 4 ΔΨ	168.9 ± 0.9	↑ 172.9 ± 1.5 *	175.1 ± 1.5	↓ 170.4 ± 1.2 *
RCR	2.64 ± 0.16	↑ 4.46 ± 0.28 ***	4.28 ± 0.26	↓ 3.84 ± 0.24 *
ADP/O	1.34 ± 0.08	1.42 ± 0.07	2.39± 0.11	2.30 ± 0.07

Table 4.1 Respiratory rates and ΔΨ were measured in the absence (state 4, non-phosphorylating respiration following phosphorylating respiration) or presence (state 3, phosphorylating respiration) in mitochondria isolated from endothelial cells grown in normoxic (N) and hypoxic (H) conditions. RCR is equal to the ratio of state 3 to state 4 respiration. Means ± SD; *n* = 15.

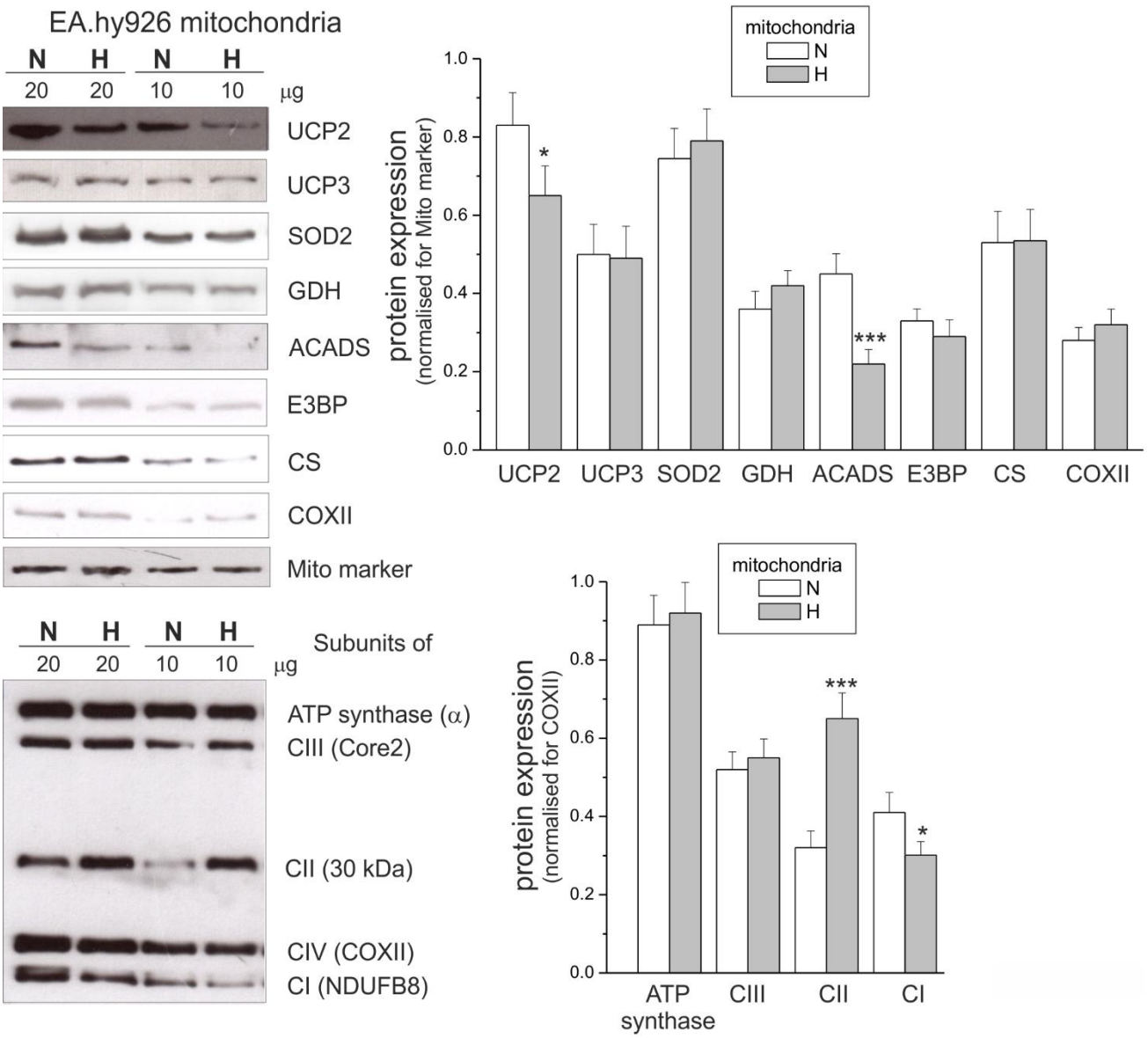

Figure 4.28 Representative Western blots (left) and analyses of the protein expression (right) in mitochondria isolated from cells grown for 6 days under normoxic (N) and hypoxic (H) conditions. Detected proteins: HKI, COX (subunit II), SOD1, SOD2, UCP2, UCP3, glutamate dehydrogenase (GDH), ACADS, E3BP, ATP synthase (*α*-subunit), and subunits of respiratory chain complexes (CI-CIV), mitochondrial marker (mito marker), and GAPDH. Means ± SD; *n* = 10.

4.3.2.2 Hypoxia and mitochondrial ROS formation

In mitochondria isolated from hypoxic endothelial cells, the reduced activity of complex I led to a significantly decreased by ~10-14% H_2O_2 formation during malate oxidation under non-phosphorylating and phosphorylating conditions (Figure 4.29).

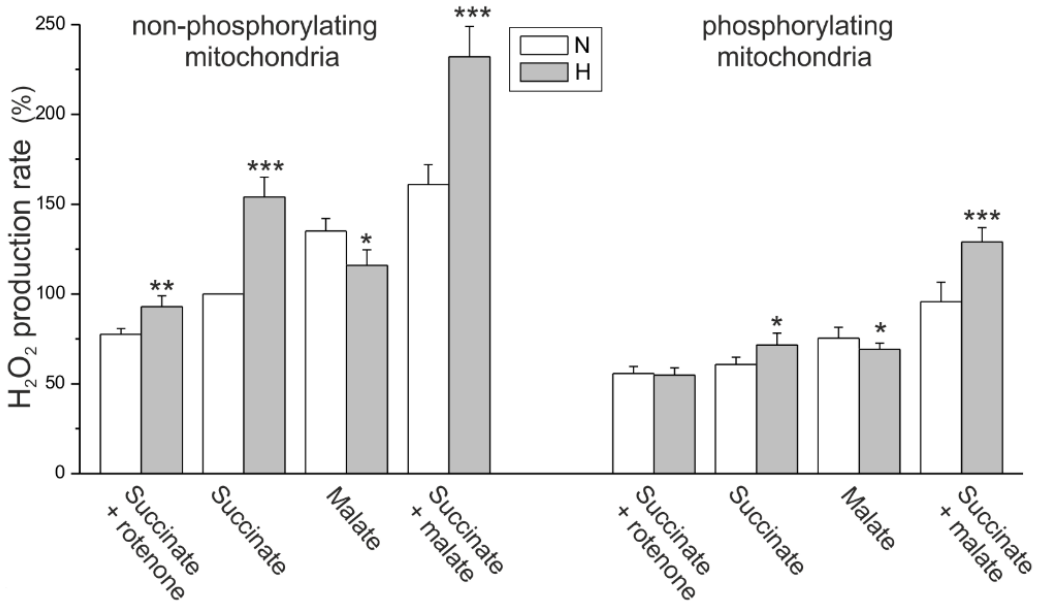

Figure 4.29 H_2O_2 production by endothelial mitochondria isolated form cells grown in normoxia (N) or chronic hypoxia (H) with various substrates. Percentage relative to the control (N) mitochondria oxidising succinate alone (100%). Means ± SD; *n* = 4-8.

However, when malate and succinate were oxidised together, a considerable ~35-45% elevation of H_2O_2 formation was observed in mitochondria from hypoxia-exposed cells. This elevation was caused by the increase in complex II activity resulting in elevated mROS formation involving complex III and mainly the complex I-mediated reverse electron transfer. Namely, a ~20% increase in H_2O_2 formation was observed for non-phosphorylating mitochondria from hypoxic cells during succinate oxidation in the presence of rotenone (an inhibitor of complex I). No changes with succinate (plus rotenone) under phosphorylating conditions were found. In mitochondria from hypoxic cells, a greater elevation of H_2O_2 formation was observed, both under non-phosphorylating (~50% increase) and phosphorylating (~20% increase) conditions, compared to mitochondria from normoxic cells, when succinate was oxidised in the absence of rotenone. These results indicate that in mitochondria after exposure of endothelial cells to hypoxia, the decreased activity of complex I may produce (i) less mROS when supplied by NAD-linked substrate, and (ii) more mROS when reverse electron transport is supplied by upregulated complex II activity.

4.3.2.3 Hypoxia and UCP2

The analysis of UCP2 protein expression (Figure 4.28) showed a slight ~20% down-regulation of the protein in mitochondria isolated from hypoxic cells relative to those isolated

from control cells. No change in the UCP3 expression level was found. Therefore, the hypoxia-induced changes in UCP activity, described below, can be attributed to UCP2.

To determine whether UCP2 activity is changed due to the growth of EA.hy926 cells in hypoxia, the activation of UCP2 by linoleic acid and the inhibition by GTP was evaluated in isolated endothelial mitochondria (Figure 4.30). In general, in non-phosphorylating mitochondria isolated from hypoxic cells, the stimulatory effect of linoleic acid and the inhibitory effect of GTP were weaker than the effects observed in control mitochondria. An analysis of the proton leak kinetics indicates that for specific linoleic acid (14 μM) and GTP (4 mM) concentrations, the linoleic acid-induced GTP-inhibited UCP2-mediated proton leak (UCP2 activity) at the same ΔΨ (162 mV) was ~18% lower in mitochondria from the hypoxic cells than it was in the control mitochondria (Figure 4.30, right panel). Despite slightly decreased UCP2 activity and protein levels, the expression level of SOD2, another mitochondrial antioxidant protein, was unaltered in mitochondria from hypoxic cells (Figure 4.28).

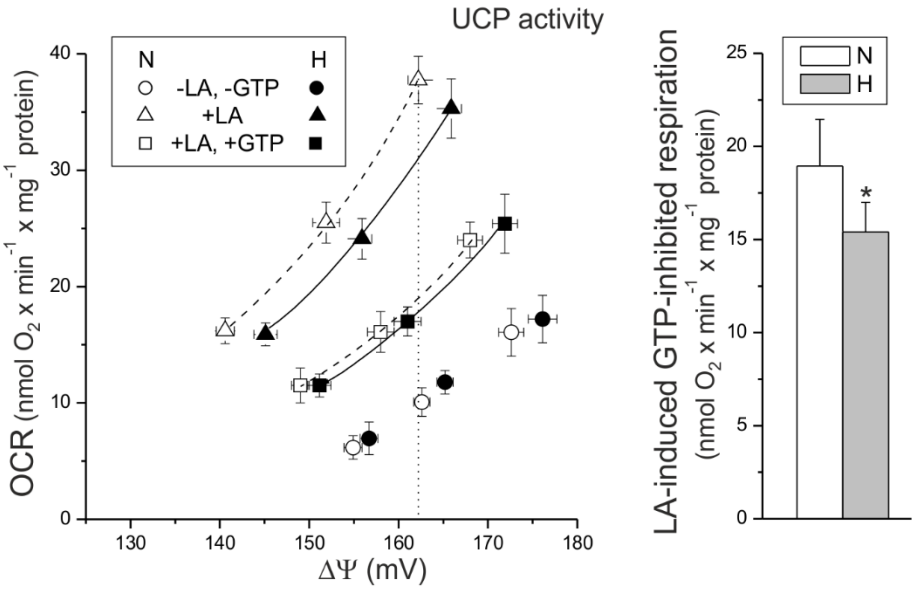

Figure 4.30 UCP activity in endothelial mitochondria isolated from cells grown in normoxia (N) or chronic hypoxia (H). The relationship between the respiratory rate and ΔΨ (proton leak kinetics) during non-phosphorylating succinate oxidation titrated with cyanide (left). The linoleic acid (LA)-induced, GTP-inhibited, UCP-mediated proton leak at the same ΔΨ (162 mV) (right). Means ± SD; *n* = 4-8.

4.3.3 Discussion and conclusions

The hypoxia-induced responses in aerobic metabolism are well documented, for instance for cancer or brain cells (Lin et al., 2008; Eales et al., 2016; Lukyanova and Kirova, 2015; Tormos and Chandel, 2010), but this issue has not been intensively studied in endothelial cells. Therefore, the aim of this study was to determine for the first time the effects of chronic hypoxia on mitochondrial oxidative metabolism in endothelial cells, including the effects on isolated endothelial mitochondria. The hypoxia-induced endothelial metabolism changes were supported by a significantly increased level of HIF1α (Figure 4.23). The comparison of the mitochondrial respiratory functions of EA.hy926 cells cultured in hypoxia or normoxia demonstrate that deficiency in O_2 tension induces a general reduction in mitochondrial respiration supplied with carbohydrate catabolic intermediates (glucose or pyruvate), lipid metabolism intermediate (palmitic acid), and amino acids (glutamine, valine, or threonine), whereas cellular respiration with exclusively ketogenic amino acids (lysine or leucine) was significantly increased (Figure 4.25). The increased oxidation of exclusively ketogenic amino acids, which are directly degraded to acetyl-CoA, suggests that the TCA cycle is not impaired in hypoxic endothelial cells in contrast to pyruvate-dependent oxidation. Moreover, in EA.hy926 mitochondria from hypoxic cells, the mitochondrial oxidation of palmitoylcarnitine and the expression of ACADS were significantly decreased, confirming hypoxia-induced decrease in FA metabolism. Thus, similar to cancer cells (Huang et al., 2014), in endothelial cells, hypoxia inhibits FA β-oxidation, another major source of acetyl-CoA. In present study, in mitochondria from hypoxic endothelial cells, the oxidation of pyruvate and the expression of the E3BP component of pyruvate dehydrogenase complex were unaltered, suggesting that the other factors downregulate pyruvate-linked oxidation. It has been previously proposed that activation of HIF1α induces pyruvate dehydrogenase kinase 1 (PDK1), which inhibits pyruvate dehydrogenase complex, and respiration is decreased by substrate limitation (Papandreou at al., 2006; Kim et al., 2006). Metabolic responses observed in this study indicate that this HIF1α-coordinated regulatory pathway decreasing the TCA cycle activity under hypoxic exposure seems to occur also in endothelial cells. Limitation of mitochondrial fuel oxidation may provide some metabolic advantages to endothelial cells exposed to hypoxia, including diversion of pyruvate into anabolic pathways, or reduction of apoptosis by hyperpolarised $\Delta\Psi$.

In EA.hy926 cells grown for 6 days in hypoxia, the decreased respiration in the presence of glucose (Figure 4.25) was accompanied by an elevated expression of HKI (Figure

4.23) and an elevated expression (Figure 4.23) and activity of LDH (Figure 4.24). Thus, in addition to the reduction in aerobic glucose oxidation, endothelial hypoxic cells display an enhanced anaerobic glycolysis, which seems to be an important energy source under hypoxic conditions. The results obtained with endothelial cells are consistent with previous observations from other cells that hypoxia affects energy metabolism and HIF1α activates transcription of genes encoding glycolytic enzymes to further increase flux of reducing equivalents from glucose to lactate (Lum et al., 2007).

It has been well documented that the exposure of endothelial cells to hypoxia leads to increased intracellular ROS production and therefore oxidative stress (Quintero et al., 2006; Davidson 2010; Paternotte et al., 2008). Under experimental conditions of present study, a significant increase in intracellular ROS and mROS generation was also observed. However, the hypoxia-induced oxidative stress seems not to be excessive for endothelial cells because they maintained cell viability. Moreover, no changes in the expression levels of the cytosolic and mitochondrial SODs (SOD1 and SOD2, respectively) and UCP2, thus proteins of the antioxidative systems, were observed. Thus, there was no need for protection against the overwhelming oxidative stress and increased level of ROS may be involved in endothelial signalling. Increased mROS are now known to be biologically important in a variety of physiological systems, including adaptation to hypoxia (Tang et al., 2014; Sena and Chandel, 2012). For instance, cells can utilise an acute increase in mROS to stabilise HIF under hypoxia conditions and subsequently restrain mROS production in chronic hypoxia to avoid cellular damage (Sena and Chandel, 2012). The present study indicates that the observed decrease in mitochondrial oxidative metabolism of endothelial cells may help mROS in not exceeding the buffering capacity of SODs. Therefore, cell viability of endothelial cells exposed to chronic hypoxia remains unchanged.

Because the activities of COX and CS (Figure 4.24) and the expression level of mitochondrial marker proteins (Figure 4.28) remained unchanged, it appears that the chronic growth of EA.hy926 cells in hypoxia did not change their maximal aerobic respiration capacity or mitochondrial biogenesis. However, measurements of mitochondrial function in isolated endothelial mitochondria indicate that hypoxia induced an important remodelling of OXPHOS system at the level of respiratory chain dehydrogenases. In mitochondria from hypoxic endothelial cells, the considerably elevated protein expression (Figure 4.28) and activity of complex II (Figure 4.27, Table 4.1) contribute to an increase in $\Delta\Psi$ and succinate-sustained mROS formation mainly through increased reverse electron transport. It has been previously reported that in endothelial cells, complex II-driven electron flow is the primary

means by which the mitochondrial membrane is polarised under hypoxic conditions (Hawkins et al., 2010). Another interesting finding of this study is that in mitochondria from hypoxic endothelial cells, a reduction of expression (Figure 4.28) and maximal malate-sustained activity of complex I (Figure 4.27 and Table 4.1) was accompanied by an increase in oxidation of α-ketoglutarate or isocitrate, other but weaker than malate NAD-linked substrates (Figure 4.27). Thus, the hypoxia-induced reduction of OXPHOS system of endothelial mitochondria was found only during malate-sustained complex I activity. Interestingly, it has been reported that in many cells lack of oxygen deactivates mitochondrial complex I (Galkin et al., 2009; Lukyanova and Kirova, 2015). It has also been proposed that hypoxia induces reprogramming of respiratory chain function and switching from oxidation of complex I substrates to succinate oxidation (complex II) (Lukyanova and Kirova, 2015; Schonenberger and Kovacs, 2015). The dissociation of complex I from the large mitochondrial supercomplexes has been observed under hypoxic conditions, when succinate accumulates as a substrate for complex II (Chen et al., 2012; Moreno-Lastres et al., 2012). It is well documented that in mammalian cells hypoxia is connected with activation of succinate dehydrogenase and succinate oxidation, and with increased contribution of the latter to respiration and energy production (Eales et al., 2016; Lukyanova and Kirova, 2015; Tormos and Chandel, 2010). Under hypoxic conditions, complex II may function as an independent enzyme whose activity is limited only by the substrate availability. Hypoxia inhibits the malate-aspartate shuttle, which provides α-ketoglutarate to the cytosol, whereas succinate synthesis is intensified.

In the previous chapter (Chapter 4.2), it has been shown that one physiological role of UCP2 in endothelial cells could be the attenuation of mROS production under conditions of excessive oxidative stress such as exposure to high-glucose levels. The results of present chapter indicate that, in response to hypoxia during endothelial cell growth, UCP2 activity and protein levels were slightly but statistically significantly decreased in mitochondria even intracellular and mROS formation was increased. Reduction in UCP2 activity leads to higher $\Delta\Psi$ and consequently increased mROS production. Thus, in hypoxic endothelial cells, one physiological role of UCP2 could be the ensuring of efficient OXPHOS yield rather that the attenuation of mROS production.

In mammalian cells, multiple mitochondrial products, including the TCA cycle intermediates and mROS can coordinate PHD activity and thereby HIF stabilisation, hence the cellular response to oxygen deficiency (Pan et al., 2007; Lin et al., 2008). Accumulation of succinate and fumarate inhibits PHDs leading to elevated level of HIF, whereas α-

ketoglutarate facilitates PHD action leading to HIF degradation (Koivunen et al., 2007). In present study, in hypoxic endothelial cells, no change in activity of CS, a pace-making enzyme of the first step of the TCA cycle was observed (Figure 4.24). However, the observed increase in mitochondrial oxidation of isocitrate, α-ketoglutarate and glutamate (up-stream of succinate oxidation) and the decrease in malate oxidation (down-stream of succinate oxidation) could be relevant for maintaining the high levels of succinate and fumarate despite the elevated activity of succinate dehydrogenase (complex II). Moreover, a significantly ameliorated mitochondrial oxidation of α-ketoglutarate may lead to suppression of cytosolic α-ketoglutarate accumulation in endothelial cells exposed to hypoxia. It has been reported that in mammalian cells, especially in cancer cells or other highly proliferating cells, ROS including mROS are crucial to activate HIF1 (Kietzmann and Gorlach, 2005). A precise role of mROS in regulating HIF1α is unclear, but the pathway stabilising HIF1α appears undoubtedly mitochondrial-dependent (Pan et al., 2007). The present study indicates that under hypoxic conditions, endothelial mitochondria also function as oxygen sensors and convey signals to HIF1 likely through elevated mROS, accumulation of succinate and decreased level of α-ketoglutarate. Thus, it seems that in endothelial cells, coordinated signalling between HIFs (at least HIF1α) and the mitochondria regulate cellular response to chronic hypoxia.

In conclusion, the growth of endothelial cells under hypoxic conditions induces numerous changes in their aerobic metabolism, particularly a general decrease in mitochondrial respiration except for the increased oxidation of exclusively ketogenic amino acids. The hypoxia-induced increases in intracellular and mROS production do not lead to overwhelming oxidative stress because cell viability and antioxidant systems (SODs and UCPs) are not upregulated. The hypoxia-induced increase in mROS formation could result from decreased mitochondrial UCP2-mediated uncoupling, and mainly from remodelling of mitochondrial respiratory chain function with elevated activity of complex II and decreased activity of complex I. In mitochondria from hypoxic cells, the increased activity of complex II results in increase in succinate-sustained mROS formation mainly through increased reverse electron transport. These observations highlight the role of endothelial mitochondria in response to metabolic adaptations related to hypoxia.

4.4 Functional characteristics of mitoBK$_{Ca}$ in mitochondria of endothelial EA.hy926 cells

So far, no information has been reported about potassium channels in endothelial mitochondria, such as the mitoBK$_{Ca}$ described in some other mammalian mitochondria. Therefore, the next goal was to search for mitoBK$_{Ca}$ in the mitochondria of endothelial EA.hy926 cells and to determine the biochemical properties of this channel. With this purpose, the effects of BK$_{Ca}$ channel activators (Ca^{2+}, NS1619, and NS11021) and inhibitors (iberiotoxin and paxilline) on $\Delta\Psi$ and respiration in isolated mitochondria were studied. Moreover, to detect the presence of mitoBK$_{Ca}$ subunits in endothelial mitochondria, immunological experiments were performed.

4.4.1 Immunological detection of mitoBK$_{Ca}$ protein

Immunoblotting of total mitochondrial and mitoplast proteins allowed for the immunological detection of the human endothelial mitoBK$_{Ca}$ channel. The immunoblotting was performed with antibodies raised against the mammalian plasma membrane BK$_{Ca}$ pore (α-subunit K$_{Ca}$1.1) and auxiliary β-subunits. In the endothelial mitochondrial and mitoplast fractions, a protein band with a molecular mass of ~125 kDa was detected using the anti-K$_{Ca}$1.1 antibody (Figure 4.31 A). Moreover, the anti-*slo*β2 antibody cross reacted with a single band of ~44 kDa (Figure 4.31 B). No reactivity was observed with the anti-*slo*β1 or anti-*slo*β4 antibodies (data not shown). Using the anti-K$_{Ca}$1.1 and anti-*slo*β2 antibodies (Figure 4.31 A and B), much stronger signals were obtained for the mitoplast fraction than for the mitochondrial fraction (for lanes with equal total protein concentration loaded on the SDS-PAGE), proving that the detected proteins localised to the endothelial IMM. Moreover, specific blocking peptides blocked the antibody-antigen interaction, demonstrating the specificity of the reaction in the immunoblotting assays. Additionally, immunological analysis with antibodies raised against a plasma membrane marker (Na/K-ATPase) was performed (Figure 4.31 C)**.** In contrast to a fraction containing total cells protein, mitochondrial (isolated mitochondria and mitoplasts) fractions displayed no signal with these antibodies. These results indicate the absence of surface membrane contamination in the endothelial mitochondrial fraction. Moreover, the immunodetection with antibody against ER marker (calnexin) revealed a presence of mitochondria-associated ER membrane (MAM) only in the mitochondrial fraction but not in the mitoplast fraction (Figure 4.31 D). These results strengthen the identification of α and β2 subunits of mitoBK$_{Ca}$ in IMM of EA.hy926 cells.

Therefore, it can be concluded that the endothelial mitoBK$_{Ca}$ may contain subunits that are similar to the surface α-subunit K$_{Ca}$1.1 and the β-subunit *slo*β2.

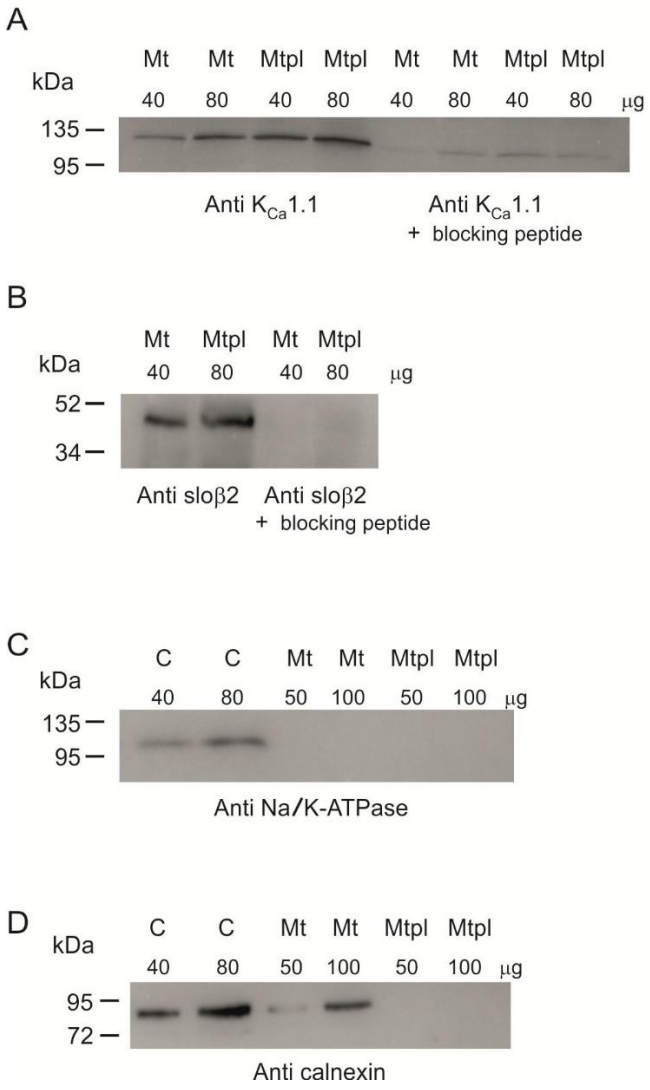

Figure 4.31 Western blot analysis of mitochondria and mitoplast fractions from endothelial EA.hy926 cells using anti-KCa1.1 (A) and anti-sloβ2 (B) antibodies raised against the mammalian BK$_{Ca}$ proteins in the absence or presence of a specific blocking peptide. C, Detection of Na/K-ATPase subunit α. D, Detection of calnexin, ER membrane marker. C, cells; Mt, mitochondria; Mtpl, mitoplasts. Different amounts of protein were loaded into each lane (as indicated). Means ± SD; *n* = 3-4.

4.4.2 Effects of mitoBK$_{Ca}$ modulators on the respiratory rate and ΔΨ

At the beginning, the possible effects of Ca^{2+} on the potassium permeability of the mitochondria isolated from EA.hy926 cells were studied. Mitochondrial non-phosphorylating (resting) respiration and ΔΨ in potassium-containing medium in the presence of 100 µM $CaCl_2$, using succinate as an oxidisable substrate, were studied. Figure 4.32 A presents an example of simultaneous measurements of the respiratory rate and ΔΨ. The addition of Ca^{2+}

led to an accumulation of the ions into mitochondrial matrix. A significant transient increase in the respiratory rate from 22 to 39 nmol $O_2 \times min^{-1} \times mg^{-1}$ protein and a decrease in $\Delta\Psi$ from 170 to 150 mV (Figure 4.32 A, left panel, dashed line) were observed. Compared to the initial values before Ca^{2+} addition, after transient Ca^{2+} accumulation, the resulting respiratory rate was increased by ~14% (to 27 nmol $O_2 \times min^{-1} \times mg^{-1}$ protein) and $\Delta\Psi$ was decreased by 3 mV (to 167 mV). Subsequent addition of 2 μM iberiotoxin into the respiring mitochondria caused an inhibition of mitoBK$_{Ca}$, leading to a decrease in the respiratory rate by 26% and an increase in $\Delta\Psi$ by 4 mV. Almost two-fold weaker effect of the inhibitor in the absence of Ca^{2+} was observed (Figure 4.32 A, left panel, solid line). The foregoing results indicate that Ca^{2+} stimulates iberiotoxin-sensitive K^+ flux into endothelial mitochondria, decreasing $\Delta\Psi$ and thus accelerating the mitochondrial respiration rate. The iberiotoxin-sensitive changes in the respiratory rate and $\Delta\Psi$ represent the mitoBK$_{Ca}$ activity (i.e., the channel-mediated K^+ flux). The highest activity of mitoBK$_{Ca}$ was observed in the presence of exogenous Ca^{2+} (100 μM) and the lowest activity was observed in the presence of 1 mM EGTA (a chelator of Ca^{2+}).

Moreover, similar to calcium ions, the potassium channel openers NS1619 and NS11021 stimulated non-phosphorylating oxygen uptake (Figure 4.32 B and C, left panel) and decreased non-phosphorylating $\Delta\Psi$ (Figure 4.32 B and C, right panel) in isolated EA.hy926 mitochondria. Figure 4.32 shows the effect of increasing concentrations of NS1619 up to 80 μM or NS11021 up to 4 μM on the respiratory rate and $\Delta\Psi$. The addition of NS1619 up to 50 μM or NS11021 up to 2.5 μM resulted in an increase in the rate of respiration by ~100% (by ~20-21 nmol $O_2 \times min^{-1} \times mg^{-1}$ protein) and ~64% (by ~14-15 nmol $O_2 \times min^{-1} \times mg^{-1}$ protein) in the absence or presence of 2 μM iberiotoxin, respectively (Figure 4.32 B, right panel). At the same time, $\Delta\Psi$ decreased after the addition of up to 50 μM NS1619 or up to 2.5 μM NS11021 by ~24 and 20 mV in the absence or presence of iberiotoxin, respectively (Figure 4.32 B, right panel). As shown in Figure 4.32 B, only at 10 μM NS1619 or 2.5 μM NS11021, 2 μM iberiotoxin almost completely abolished the NS-induced respiration and $\Delta\Psi$ depolarisation. In the presence of 20 to 50 μM NS1619 or 1 to 2.5 μM NS11021, iberiotoxin partially blocked NS-induced respiration and $\Delta\Psi$ depolarisation, indicating a non-specific uncoupling effect of both activators on isolated endothelial mitochondria. Moreover, concentrations of NS1619 above 50 μM and NS11021 above 2.5 μM caused a decrease in respiration and a further decrease in $\Delta\Psi$, indicating an impairment of the respiratory chain by higher concentrations of the potassium channel openers. Thus, it can be concluded that in

endothelial mitochondria, NS1619 (at 10 μM) and NS11021 (at 0.5 μM) stimulate the iberiotoxin-sensitive K^+ flux, decrease ΔΨ, and thus accelerate the mitochondrial respiratory rate.

Figure 4.32 C exemplifies the comparison of the efficiency of iberiotoxin and paxilline in the inhibition of mitoBK$_{Ca}$ activity under NS-stimulated conditions. An example of the effect of increasing concentrations of the two inhibitors on NS1619-induced respiration and ΔΨ depolarisation is shown (Figure 4.32 C, left panel). A subsequent increase in the concentrations of iberiotoxin (above 2 μM) and paxilline (above 20 μM) did not led to any additional effects (data not shown). NS1619-induced respiration was blocked by 2 μM iberiotoxin by 100% and by 20 μM paxilline by 72% (Figure 4.32 C, left panel). Iberiotoxin almost completely restored NS1619-induced ΔΨ depolarisation (an increase by 4 mV), while paxilline only partially restored this parameter (an increase by 1.5 mV). The difference in the sensitivity of the endothelial mitoBK$_{Ca}$ to iberiotoxin and paxilline was also evident when the NS-induced inhibitor-blocked changes in the respiratory rate and ΔΨ were compared (Figure 4.32 C, right panel). A weaker inhibitory effect of paxilline compared to iberiotoxin was observed with 10 μM NS1619, 0.5 μM NS11021 (Figure 4.32 C, right panel), and Ca^{2+}-induced mitoBK$_{Ca}$ activity (data not shown), indicating a lower sensitivity of mitoBK$_{Ca}$ activity to paxilline in isolated endothelial mitochondria. However, Ca^{2+} (100 μM), NS1619 (10 μM) or NS11021 (0.5 μM), when applied separately, induced similar iberiotoxin-sensitive mitoBK$_{Ca}$ activities, i.e., an ~7 nmol $O_2 \times min^{-1} \times mg^{-1}$ protein increase in respiratory rate and an ~4 mV ΔΨ depolarisation (Figure 4.32 A and C, right panel). On the other hand, when 100 μM Ca^{2+} and 10 μM NS1619 (or 0.5 μM NS11021) were applied simultaneously, no further increase in the iberiotoxin-sensitive mitoBK$_{Ca}$ activity was observed (data not shown).

The above bioenergetic analysis of the effects of the known mitoBK$_{Ca}$ modulators on the respiratory rate and ΔΨ in respiring endothelial mitochondria indicated the presence of Ca^{2+}- and NS-induced, iberiotoxin- and paxilline-inhibited K^+ flux. To exclude the influence of the applied modulators (Ca^{2+}, NS1619, iberiotoxin, and paxilline) on succinate dehydrogenase (complex II) activity, experiments with malate as a respiratory substrate were also performed (data not shown). The results obtained with the NAD-linked complex I substrate confirmed the observations from the experiments described in (Figure 4.32) for the FAD-linked substrate (succinate).

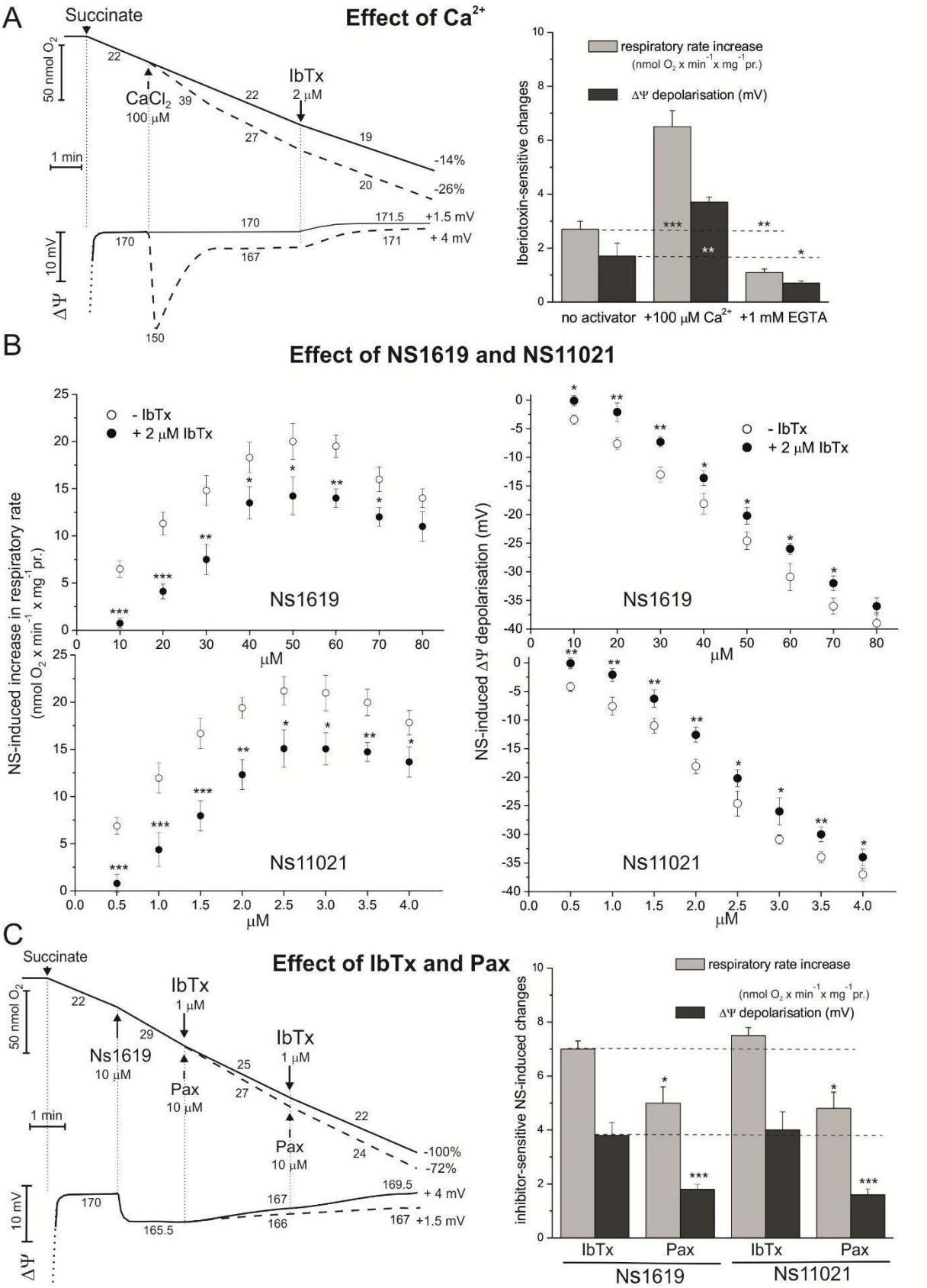

Figure 4.32 Influence of mitoBK$_{Ca}$ modulators on the non-phosphorylating respiratory rate and ΔΨ in mitochondria isolated from EA.hy926 cells. A, Effect of Ca^{2+}. Left panel, Additions as indicated: 5 mM succinate, 100 μM $CaCl_2$, and 2 μM iberiotoxin (IbTx). The solid line trace shows the measurement

obtained in the absence of activator (Ca^{2+}). Right panel, The IbTx-induced changes in the non-phosphorylating respiratory rate and ΔΨ were calculated as the difference between the respective values measured in the absence and presence of 2 µM IbTx. Conditions: no additions (no activator), plus 100 µM $CaCl_2$, and plus 1 mM EGTA. Statistical comparison vs control value (no additions). B, Effect of increasing concentrations of NS1619 or NS11021 on non-phosphorylating respiratory rate (left panel) and ΔΨ (right panel) in the absence or presence of 2 µM IbTx. IbTx was added prior to activator addition. C, Effect of IbTx and paxilline (Pax). Left panel, Additions as indicated: 5 mM succinate, 10 µM NS1619, and two doses of 1 µM IbTx (solid line) or 10 µM Pax (dashed line). Right panel, the inhibitor-sensitive changes in non-phosphorylating respiratory rate and ΔΨ were calculated as the difference between respective values measured in the absence and presence of 2 µM IbTx or 20 µM Pax. The mitoBK$_{Ca}$ activity was induced by 10 µM NS1619 or 0.5 µM NS11021. Statistical comparison vs value obtained with NS1619 and IbTx. A and C, numbers on the traces refer to the O_2 uptake rates in nmol O_2 × min^{-1} × mg^{-1} protein or to the ΔΨ values in mV. Means ± SD; *n* = 8.

4.4.1 Cation selectivity

Cation selectivity of endothelial mitoBK$_{Ca}$ was studied by determination of the effect of NS1619 and iberiotoxin on isolated EA.hy926 mitochondria that were respiring (with succinate) in incubation media containing different monovalent cations (chloride salts) compared to those incubated in the presence of K^+ or in the absence of any monovalent cations.

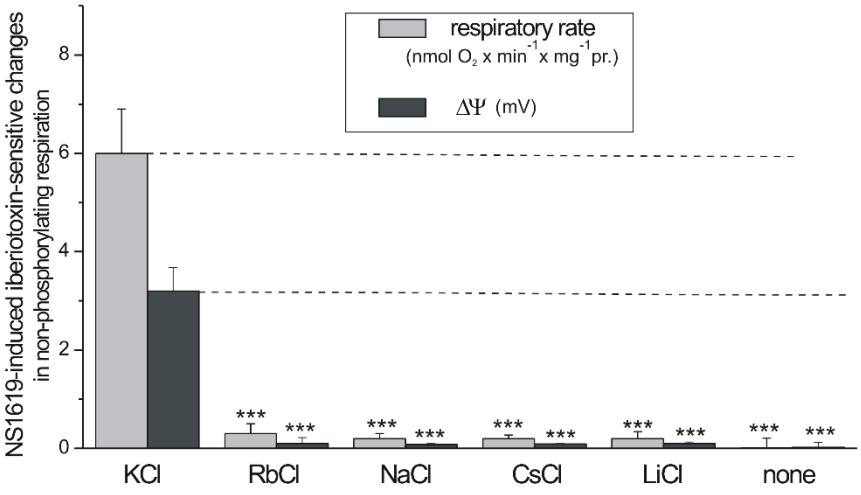

Figure 4.33 Cation selectivity; the influence of monovalent cations on the NS1619-induced, iberiotoxin-sensitive non-phosphorylating respiratory rate and ΔΨ. Mitochondria were incubated in the standard incubation medium (Chapter 3.7.2), except that 2.5 mM KH_2PO_4 was replaced with 2.5 mM $TrisH_2PO_4$ and 50 mM KCl was replaced with 50 mM of another chloride salt: NaCl, LiCl, CsCl, or RbCl (as indicated). The changes in the non-phosphorylating respiratory rate and ΔΨ induced by a given chloride salt relative to the initial values of respiration or ΔΨ are shown as the difference between the respective values measured in the presence of 10 µM NS1619 and the values measured in the presence of NS1619 and 2 µM iberiotoxin. Means ± SD; *n* = 8. Statistical comparison vs values obtained in the presence of KCl.

Figure 4.33 presents the influence of 50 mM KCl, NaCl, LiCl, RbCl, and CsCl in the incubation media on the NS1619-induced, iberiotoxin-sensitive increase in non-phosphorylating respiration and ΔΨ depolarisation (i.e., the difference between the respective values obtained in the presence of 10 μM NS1619 and those obtained in the presence of NS1619 and 2 μM iberiotoxin). These results indicate that the influence of potassium channel modulators (NS1619 and iberiotoxin) on the isolated endothelial mitochondria can be significantly attributed to K^+ influx through IMM. Similar results were obtained when iberiotoxin was replaced with 20 μM paxilline (data not shown).

4.4.2 Effect of mitoBK$_{Ca}$ activity on phosphorylating mitochondria

The effect of mitoBK$_{Ca}$ activity on phosphorylating endothelial mitochondria was studied by determination of the ADP/O ratio and RCR, the best parameters to estimate OXPHOS efficiency, in the absence or presence of the channel activator (10 μM NS1619) and/or the channel inhibitor (2 μM iberiotoxin) (Table 4.2).

	State 4	State 3	RCR	ADP/O	ΔΨ4	ΔΨ3
No additions	22 ± 3	64 ± 5	2.9 ± 0.3	1.34 ± 0.12	170 ± 1	141 ± 4
+ NS1619	29 ± 3*	63 ± 4	2.2 ± 0.2*	1.18 ± 0.11*	165 ± 2*	140 ± 4
+ NS1619, IbTx	23 ± 2	64 ± 3	2.7 ± 0.2	1.30 ± 0.11	168 ± 2	140 ± 4

Table 4.2 Effect of mitoBKCa activity on the respiratory rates, ΔΨ, and coupling parameters of isolated EA.hy926 mitochondria. Mitochondria were incubated in standard incubation medium in the presence of 5 mM succinate (plus rotenone) and in the absence or presence of mitoBK$_{Ca}$ modulators: 2 μM iberiotoxin (IbTx) (inhibitor), and 10 μM NS1619 (activator). Comparisons were made between the results of separate experiments. ΔΨ3 and ΔΨ4, ΔΨ under phosphorylating and non-phosphorylating conditions (respectively) presented in mV. The respiratory rates in state 3 and state 4 are given in nmol O_2 × min^{-1} × mg^{-1} protein. Means ± SD; *n* = 6.

In the presence of the mitoBK$_{Ca}$ modulators, phosphorylating (state 3) respiration and ΔΨ (ΔΨ3) remained unchanged. However, when the mitoBK$_{Ca}$ was activated by NS1619, NS1619-induced mitochondrial uncoupling was observed, as the ADP/O ratio and RCR were significantly lowered, non-phosphorylating (state 4) respiration significantly increased, and non-phosphorylating ΔΨ (ΔΨ4) significantly decreased. The effect of NS1619 on the coupling parameters was concentration-dependent up to 50 μM (data not shown). When NS1619-induced mitoBK$_{Ca}$-mediated uncoupling was inhibited by iberiotoxin, the ADP/O

ratio, RCR, non-phosphorylating respiration and ΔΨ (ΔΨ4) were clearly restored (Table 4.2). The foregoing results clearly indicate that NS1619-induced, iberiotoxin-inhibited uncoupling diverts energy from ATP synthesis during phosphorylating respiration in endothelial EA.hy926 mitochondria.

4.4.3 Discussion and conclusions

The results of Chapter 4.4 present for the first time the functional properties of mitoBK$_{Ca}$ in endothelial mitochondria. These studies were performed in collaboration with Prof. Szewczyk's group from Nencki Institute in Warsaw. Above described in details biochemical experiments were performed in Department of Bioenergetics UAM Poznan. The Warsaw group performed electrophysiological experiments (Bednarczyk et al., 2013). The electrophysiological properties of mitoBK$_{Ca}$ were studied in IMM of endothelial EA.hy926 mitochondria, using a patch clamp technique in the mitoplast-attached mode. Large conductance (270 ± 10 pS), voltage dependence, a higher open-state probability at positive potentials, sensitivity to Ca^{2+}, NS1619 (a BK$_{Ca}$ channel opener), and paxilline and iberiotoxin (BK$_{Ca}$ channel inhibitors) (Bednarczyk et al., 2013) indicate the similarity of endothelial mitoBK$_{Ca}$ to the mammalian mitoBK$_{Ca}$ channels previously reported in glioma (Siemen et al., 1999), skeletal muscle (Skalska at al., 2008), brain (Fahanik-Babaei et al., 2011), and cardiac (Xu et al., 2002) cells. Interestingly, mitoBK$_{Ca}$ with similar electrophysiological properties (although with a much higher conductance of 502-605 pS) has also been described in non-mammalian (potato tuber) mitochondria (Koszela-Piotrowska et al., 2009). The mitoBK$_{Ca}$ channel of slime mode *Dictyostelium discoideum* displays conductance (~260 pS) (Laskowski et al., 2015) similar to that of human endothelial channel (Bednarczyk et al., 2013).

In EA.hy926 cells, the mRNA expression of BK$_{Ca}$ α-subunit has been previously detected, while the mRNA and protein expression of the BK$_{Ca}$ channel β-subunit, corresponding to the β4-subunit, has been undetectable (Papassotiriou et al., 2000). β2-subunit has not been searched in these cells until now. The immunodetection of mitoBK$_{Ca}$ subunits in the mitochondria of EA.hy926 cells (Figure 4.31) indicates cross-reactivity with antibodies raised against the K$_{Ca}$1.1 α-subunit of BK$_{Ca}$ and the β2-subunit of the sloβ2 BK$_{Ca}$ channel. However, the existence of β2-subunit of plasma membrane BK$_{Ca}$ in EA.hy926 cells cannot be excluded. The mRNA transcript for β2-subunit has been shown by RT-PCR in porcine basilar and middle cerebral arteries (Wulf et al., 2009). Immunological detection of

mitoBK$_{Ca}$ subunits (Figure 4.31) indicates that the channel present in the endothelial IMM may be structurally similar to the plasma BK$_{Ca}$. Specifically, it may be formed by the principle pore-forming α-subunit that interacts with an auxiliary β2-subunit. The predominant β2-subunit may determine the mitoBK$_{Ca}$. activity, including Ca^{2+} and ΔΨ sensitivity, as in the case of the plasma BK$_{Ca}$. The relative molecular mass of the detected endothelial mitoBK$_{Ca}$ proteins (~125 and ~44 kDa for the α- and β2-subunits, respectively) are the same as those of the mammalian proteins from the plasma membrane (Douglas et al., 2006; Wulf et al., 2009) and mitochondria (Piwonska et al., 2008). The β2-subunit of mitoBK$_{Ca}$ has been detected in astrocyte mitochondria (Piwonska et al., 2008) and potato tuber mitochondria (Koszela-Piotrowska et al., 2009). The molecular identity (gene and protein sequences) of mitoBK$_{Ca}$ still awaits elucidation. It has been recently shown that SLO2 coded for by a member of the BK$_{Ca}$ gene family underlies mitoBK$_{Ca}$ activity and anaesthetic preconditioning-induced protection in both *Caenorhabditis elegans* and perhaps in mouse hearts, as well (*Slo2*) (Wojtovich et al., 2011).

In isolated EA.hy926 mitochondria, 10 μM NS1619 and 0.5 μM NS11021 induced a similar mitoBK$_{Ca}$ activity, which was revealed as an ~7 nmol $O_2 \times min^{-1} \times mg^{-1}$ protein iberiotoxin-sensitive increase in non-phosphorylating respiration and an ~4 mV iberiotoxin-sensitive decrease in non-phosphorylating ΔΨ (Figure 4.32). These results indicate that in isolated endothelial mitochondria, NS11021 works at concentrations 20 times lower compared to NS1619. Thus, NS11021 seems to be much more efficient activator of mitoBK$_{Ca}$ (Figure 4.32) and BK$_{Ca}$ (Bentzen et al., 2007). In endothelial mitochondria, 2 μM iberiotoxin completely abolished the NS-induced respiration and ΔΨ depolarisation only at concentrations of openers not higher than 10 μM (with NS1619) or 0.5 μM (with NS11021) (Figure 4.32). When compared to the full inhibitory effect of iberiotoxin on Ca^{2+}-induced respiration and ΔΨ depolarisation, this observation could indicate a non-specific uncoupling effect of NS1619 and NS11021 within the concentration range of 20 μM to 50 μM and 1 μM to 2.5 μM (respectively) on isolated endothelial mitochondria (when 0.7 mg of mitochondrial protein is used) rather than the low sensitivity of the channel to iberiotoxin. Similarly, in some isolated mammalian mitochondria, the sensitivity of NS1619- or NS11021-induced respiration and ΔΨ depolarisation to mitoBK$_{Ca}$ blockers (iberiotoxin, charybdotoxin, and paxilline) is not complete (Aon et al., 2010; Heinen et al., 2007; Skalska el al., 2009; Skalska et al., 2008). Furthermore, in mitochondria isolated from EA.hy962 cells, concentrations of NS1619 above 50 μM and NS11021 above 2.5 μM caused a decrease in

respiration and a further decrease in ΔΨ, indicating an impairment of the respiratory chain by higher concentrations of the potassium channel openers. Biochemical analysis presented in this chapter indicates that the application of NS1619 and NS11021 to isolated mitochondria requires some caution because above a given concentration of these compounds, non-specific mitochondrial uncoupling or even impairment of the respiratory chain may take place.

Under non-phosphorylating conditions, potassium channel activators, Ca^{2+} (100 μM), NS1619 (10 μM), and NS11021 (0.5 μM), were able to modulate the respiratory rate (stimulation) and ΔΨ (depolarisation) in isolated endothelial mitochondria (Figure 4.32). Conversely, mitochondrial respiratory rate inhibition and ΔΨ repolarisation were observed when mitoBK$_{Ca}$ inhibitors, iberiotoxin and paxilline, were applied. These effects were markedly dependent on the presence of K^+ in the incubation medium. Furthermore, this study shows for the first time that the activation of mitoBK$_{Ca}$ leads to a decrease in the yield of OXPHOS. Namely, in the phosphorylating mitochondria of EA.hy926 cells, NS1619-induced iberiotoxin-inhibited uncoupling decreased ATP synthesis (Table 4.2). Thus, endothelial mitoBK$_{Ca}$ can potentially modulate the tightness of coupling between respiration and ATP synthesis in mitochondria, thereby contributing to the maintenance of a balance between energy supply and demand in the cell. The observed effects of mitoBK$_{Ca}$ modulators indicate the activation of electrogenic potassium transport through IMM of human endothelial EA.hy926 cells, as K^+ influx into the matrix led to a decrease in ΔΨ and a stimulation of the respiratory rate. Thus, endothelial mitoBK$_{Ca}$ may function as a possible signalling link between intramitochondrial calcium levels and mitochondrial ΔΨ and ROS. It has been previously observed that potassium channels affect mitochondrial matrix swelling, regulate the concentration of ROS, change the mitochondrial ΔΨ and the transport of Ca^{2+} into mitochondria (O'Rourke 2007; Szabo et al., 2012; Szewczyk et al., 2009). Interesingly, recent studies have shown that endothelial mitoBK$_{Ca}$ can be activated by CO, a product of heme degradation by heme oxygenases (Kaczra et al., 2015).

The presented results show identification and characterisation of mitoBK$_{Ca}$ in IMM of endothelial EA.hy926 cells using immunoblotting and functional measurements of oxygen uptake and ΔΨ with isolated mitochondria. It can be concluded that functional and molecular properties of mitoBK$_{Ca}$ of human endothelial cells are similar to those of the plasma membrane BK$_{Ca}$ channels and mitoBK$_{Ca}$ channels of other mammalian cells. However, the physiological role of mitoBK$_{Ca}$ in endothelial mitochondria, which seems to significantly modulate mitochondrial metabolism, awaits exploration.

5 General conclusions

The results presented in this doctoral thesis demonstrate that primarily glycolytic endothelial cells possess highly active mitochondria with functioning energy-dissipating pathways UCP2 and mitoBK$_{Ca}$. The growth of endothelial EA.hy926 cells under pathophysiological conditions, i.e., under high-glucose or hypoxic conditions, induces numerous changes in their aerobic metabolism.

High-glucose exposure induced a shift of the endothelial aerobic metabolism from the carbohydrate oxidation towards the oxidation of lipids and amino acids. Moreover, high-glucose-exposed endothelial cells may display intensified anaerobic glucose oxidation through a glycolic pathway and lactate fermentation. The presented results indicate the increased anaerobic and decreased aerobic (mitochondrial) breakdown of glucose in endothelial cells grown under high-glucose conditions. However, high-glucose levels did not change mitochondrial biogenesis or aerobic respiratory capacity of endothelial cells. No changes were also observed in the mitochondrial OXPHOS system. Mitochondria isolated from high-glucose-exposed cells displayed a greater oxidation of reducing substrates not originating from the TCA cycle (palmitoylcarnitine and glycerol-3-phospate). The entry to the TCA cycle was decreased as revealed by the decreased oxidation of pyruvate and the decreased expression of E3BP. High-glucose conditions induced an elevation of intracellular and mROS formation that was accompanied by the increased expression of mitochondrial antioxidant proteins SOD2 and UCP2. Figure 5.1 presents observed effects of chronic high-glucose concentrations on endothelial cells and their mitochondria.

Endothelial UCP2 may function as a sensor and negative regulator of mROS production in response to high-glucose levels. Under non-phosphorylating and phosphorylating conditions, UCP2 activity was significantly higher in mitochondria isolated from high-glucose-treated cells. A more pronounced control of the respiratory rate, $\Delta\Psi$ and mROS by UCP2 was observed in these mitochondria. A greater UCP2-mediated decrease in mROS generation indicates an improved antioxidative role for UCP2 under high-glucose conditions. Mitochondrial and non-mitochondrial ROS generation was significantly higher in high-glucose cells independent of UCP2 expression. UCP2 gene silencing led to elevated mROS formation and ICAM1 expression, especially in high-glucose-cultured cells. UCP2 influenced endothelial cell viability and resistance to oxidative stress. Endothelial cells exposed to high-glucose concentrations were significantly more resistant to peroxide. In these

cells, the increased activity of UCP2 led to improved stress resistance and protection against acute oxidative stress (Figure 5.1).

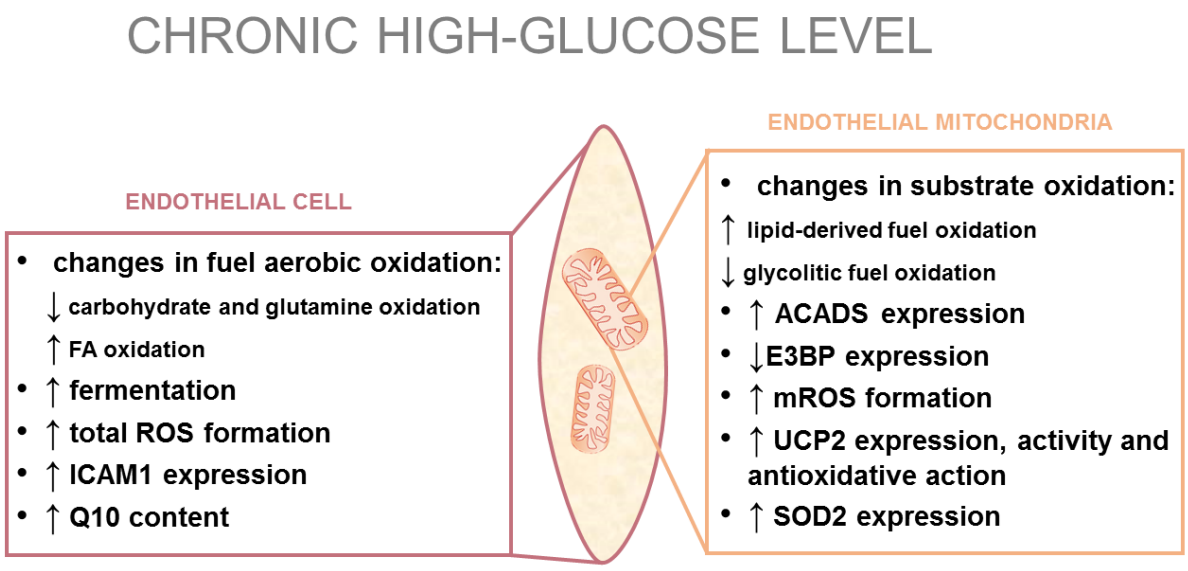

Figure 5.1 Schematic summary of effects of chronic high-glucose exposure on human endothelial EA.hy926 cells and their mitochondria. ↑, increase; ↓, decrease.

In endothelial EA.hy926 cells, the growth of endothelial cells under hypoxic conditions induced a shift in catabolic metabolism from aerobic toward anaerobic. A general decrease in mitochondrial respiration was observed except for the increased oxidation of exclusively ketogenic amino acids. The hypoxia-induced non-excessive increase in intracellular and mROS formation may be involved in endothelial signalling of hypoxic responses. The hypoxia-induced increase in mROS formation could result from decreased mitochondrial UCP2-mediated uncoupling and mainly from remodelling of mitochondrial respiratory chain functions with the elevated activity of complex II and decreased activity of complex I. In mitochondria from hypoxic cells, the increased activity of complex II resulted in an amelioration of succinate-sustained mROS formation mainly through increased reverse electron transport. The presented results indicate an important role of succinate, complex II and reverse electron transport in hypoxia-induced adjustments of endothelial cells. These observations highlight the role of endothelial mitochondria in response to metabolic adaptations related to hypoxia. Figure 5.2 presents observed effects of chronic hypoxia on endothelial cells and their mitochondria.

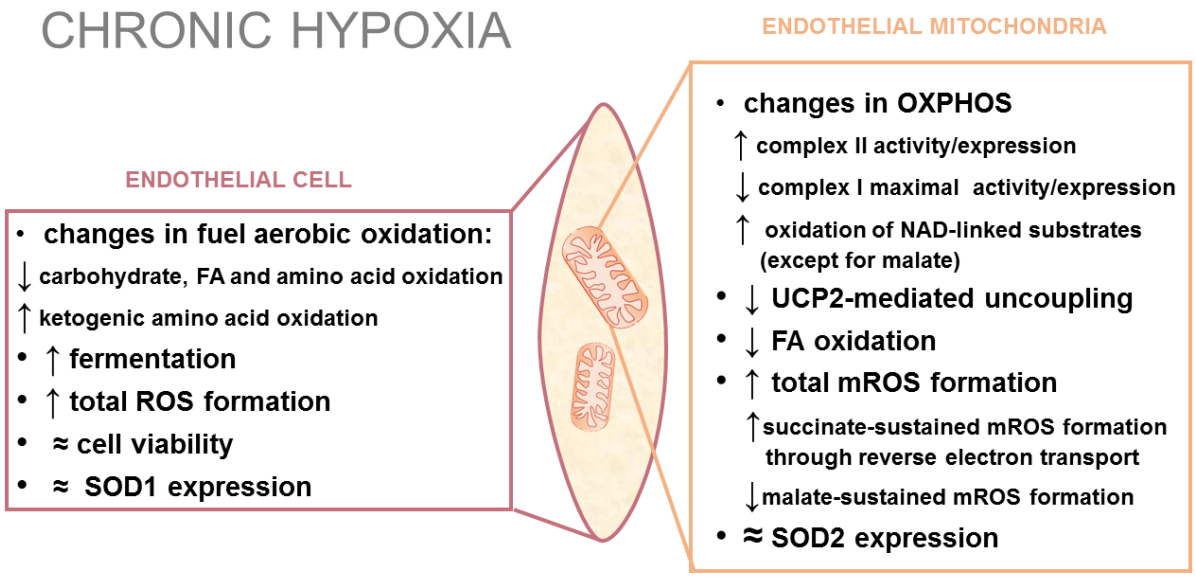

Figure 5.2 Schematic summary of effects of chronic hypoxia on human endothelial EA.hy926 cells and their mitochondria. ↑, increase; ↓, decrease; ≈, no change.

Large conductance Ca^{2+}-activated potassium channel (mitoBK$_{Ca}$) functions in mitochondria of endothelial EA.hy926 cells. Its functional and molecular properties are similar to those of the plasma membrane BK$_{Ca}$ channels and mitoBK$_{Ca}$ channels of other mammalian cells. Substances known to modulate BK$_{Ca}$ channel activity influence the bioenergetics of endothelial mitochondria. Activators of mitoBK$_{Ca}$ such as Ca^{2+}, NS1619, and NS11021 depolarise $\Delta\Psi$ and stimulate non-phosphorylating respiration. These effects are blocked by iberiotoxin and paxilline in a potassium-dependent manner (Figure 5.3). The endothelial mitoBK$_{Ca}$ can potentially modulate the tightness of coupling between respiration and ATP synthesis in mitochondria, thereby contributing to the maintenance of a balance between energy supply and demand in the cell. The endothelial mitoBK$_{Ca}$ may be formed by the principle pore-forming α-subunit that interacts with an auxiliary β2-subunit.

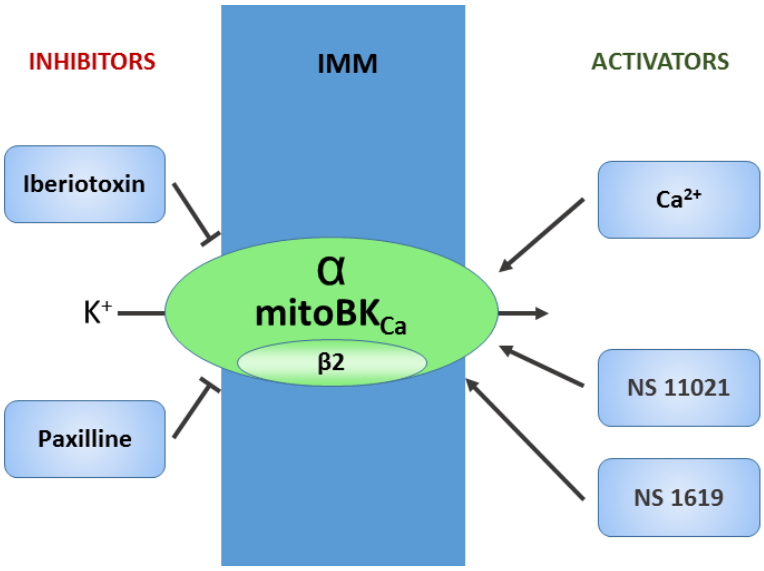

Figure 5.3 Schematic summary presenting effects of activators and inhibitors of mitoBK$_{Ca}$ of human endothelial mitochondria.

Summary

1. The present study highlights the role of endothelial mitochondria in response to metabolic adaptations related to pathophysiological conditions such as high-glucose levels and hypoxia.
2. The high-glucose and hypoxia conditions induce numerous changes in their aerobic metabolism of endothelial cells including changes in reducing fuel oxidation at different steps of oxidative catabolism.
3. The high-glucose-induced and hypoxia-induced increases in mROS formation may be involved in endothelial signalling of metabolic responses related to oxidative stress (high-glucose levels) and non-excessive ROS levels (hypoxia).
4. Endothelial UCP2 may function as a sensor and negative regulator of mROS production in response to high-glucose levels, antagonising oxidative stress-induced endothelial cell dysfunction. Downregulation of UCP2 under hypoxic conditions also indicates its involvement in modifications of mitochondrial function resulting from hypoxia-induced metabolic adjustments.
5. Energy-dissipating pathways UCP2 and mitoBK$_{Ca}$ may contribute to the maintenance of energy balance in the endothelial cell.

6 Streszczenie

Śródbłonek naczyniowy tworzy pojedynczą warstwę komórek wyścielającą naczynia krwionośne stanowiąc jednocześnie pierwszą linię kontaktu z warunkami panującymi we krwi. Prawidłowe funkcjonowanie śródbłonka przekłada się na prawidłowe działanie układu krążenia a w konsekwencji całego organizmu. Dysfunkcja śródbłonka związana jest z rozwojem wielu chorób sercowo-naczyniowych. W komórkach śródbłonka synteza ATP zachodzi głównie drogą glikolityczną. Stosunkowo niewielka zależność komórek śródbłonka od mitochondrialnego dostarczania energii może sugerować nieznaczną rolę mitochondriów w tych komórkach. Jednakże ostatnie badania pokazują, że mitochondria śródbłonka nie tylko uczestniczą w procesie wytwarzania ATP na drodze fosforylacji oksydacyjnej, ale również odgrywają rolę wewnątrzkomórkowego buforu jonów wapnia oraz są istotnym miejscem wytwarzania reaktywnych form tlenu (ROS) i tlenku azotu (NO). Mitochondria komórek śródbłonka mogą pełnić rolę czujnika zmian zachodzących w lokalnym środowisku (krwi) oraz wpływać na przeżywanie tych komórek w warunkach stresu oksydacyjnego. Celem rozprawy doktorskiej było zbadanie metabolizmu tlenowego komórek śródbłonka EA.hy926 w warunkach fizjologicznych i patofizjologicznych. Zmiany w metabolizmie tlenowym (mitochondrialnym) badano na poziomie całych komórek śródbłonka oraz mitochondriów izolowanych z tych komórek.

Realizacja projektu wymagała opracowania procedury hodowli komórek śródbłonka (unieśmiertelniona linia z ludzkiej żyły pępowinowej EA.hy926) na bardzo dużą skalę oraz opracowania procedury izolacji z tych komórek dużej ilości aktywnych, dobrze sprzężonych mitochondriów. Przedstawione wyniki pokazują, że komórki śródbłonka, mimo głównie glikolitycznego dostarczania energii, posiadają bardzo aktywne, sprzężone mitochondria.

Pierwszym celem przeprowadzonych badań było określenie wpływu chronicznego, wysokiego stężenia glukozy na metabolizm tlenowy komórek śródbłonka. Komórki śródbłonka EA.hy926 hodowano w mediach zawierającym 5.5 mM lub 25 mM glukozę, co reprezentuje odpowiednio normalne i wysokie stężenie glukozy. Zmiany w oddychaniu obserwowano w komórkach śródbłonka rosnących co najmniej 6 dni w 25 mM glukozie. Hodowla komórek śródbłonka w warunkach wysokiej glukozy powoduje znaczne obniżenie mitochondrialnego oddychania podczas utleniania pirogronianu i glukozy (katabolizmu węglowodanów), mniej wyraźne obniżenie mitochondrialnego oddychania z glutaminą (katabolizmu aminokwasów) oraz istotne zwiększenie mitochondrialnego oddychania z

palmitynianem (katabolizmu tłuszczy). Efekt Crabtree obserwowano w obu typach komórek. Komórki śródbłonka rosnące w warunkach wysokiego stężenia wykazują większą ilość koenzymu Q10 oraz podwyższoną produkcję ROS. Ponadto ekspozycja komórek śródbłonka na wysokie stężenie glukozy indukuje wzrost ekspresji heksokinazy I (HK1), dehydrogenazy mleczanowej (LDH), dehydrogenazy acetylo-CoA (ACADS), białka rozprzęgającego 2 (UCP2), dysmutazy ponadtlenkowej 2 (SOD2), oraz obniżoną ekspresję podjednostki E3 kompleksu dehydrogenazy pirogronianowej (E3BP).W mitochondriach izolowanych z komórek śródbłonka hodowanych w warunkach wysokiego stężenia glukozy obserwowano wzrost utleniania palmitylo-karnityny i glicerolo-3-fosforanu oraz obniżenie utleniania pirogronianu. Przeprowadzone badania wskazują, że w komórkach śródbłonka chroniczne, wysokie stężenie glukozy prowadzi do przesunięcia metabolizmu tlenowego w stronę utleniania tłuszczy i aminokwasów.

Występujące we wewnętrznej błonie mitochondrialnej białka rozprzęgające (UCPs) katalizują przeciek protonów prowadzący do zmniejszenia protonowego gradientu elektrochemicznego wytworzonego przez mitochondrialny łańcuch oddechowy. UCPs są aktywowane przez wolne kwasy tłuszczowe a ich allosterycznymi inhibitorami są nukleotydy purynowe. UCPs poprzez rozpraszanie użytecznej energii swobodnej pochodzącej z utleniania substratów oddechowych stanowią ważny punkt kontrolny gospodarki energetycznej komórki oraz mitochondrialnej produkcji reaktywnych from tlenu (mROS). Przedstawione badania charakteryzują funkcjonowanie i antyoksydacyjną rolę UCP2 w komórkach śródbłonka oraz w izolowanych z nich mitochondriach. Badania opisują zmiany w funkcjonowaniu UCP2 wywołane długotrwałą ekspozycją komórek śródbłonka na wysokie stężenie glukozy. Ludzkie komórki śródbłonka EA.hy926 hodowano w medium zawierającym wysokie (25 mM) lub normalne (5.5 mM) stężenie glukozy. W warunkach fosforylujących oraz niefosforylujących, aktywność UCP2 jest znacznie wyższa w mitochondriach izolowanych z komórek śródbłonka rosnących w warunkach wysokiej glukozy. Ponadto obserwowano zwiększoną kontrolę przez UCP2 szybkości oddychania, potencjału błonowego oraz produkcji mROS. Wydajniejsze obniżanie produkcji mROS za pośrednictwem UCP2 wskazuje na zwiększoną antyoksydacyjną rolę UCP2 w mitochondriach izolowanych z komórek rosnących w warunkach wysokiego stężenia glukozy. Mitochondrialna oraz komórkowa produkcja ROS jest znacznie wyższa w komórkach śródbłonka rosnących w warunkach wysokiej glukozy niezależnie od ekspresji UCP2. Wyciszenie ekspresji genu UCP2 prowadzi do znacznie większej produkcji mROS oraz zwiększonej ekspresji ICAM1 (cząsteczki adhezyjnej będącej markerem stanu

zapalnego), szczególnie w komórkach rosnących w wysokim stężeniu glukozy. Badania wykazały, że UCP2 wpływa na żywotność komórek śródbłonka oraz ich odporność na stres oksydacyjny. Komórki śródbłonka wystawione na podwyższony poziom glukozy są znacznie bardziej odporne na nadtlenek wodoru. W komórkach tych, wzrost aktywności UCP2 prowadzi do znacznie zwiększonej odporności na stres oksydacyjny. Przedstawione wyniki pokazują, że UCP2 może służyć jako czujnik oraz negatywny regulator produkcji mROS w odpowiedzi komórek śródbłonka na podwyższony poziom glukozy.

Kolejnym celem przeprowadzonym badań było określenie wypływu niskiego stężenia tlenu w hodowli na metabolizm oksydacyjny ludzkich komórek śródbłonka. Komórki śródbłonka EA.hy926 hodowano w warunkach 1% lub 20% stężenia tlenu, reprezentujących odpowiednio hipoksję oraz normoksję. Badania pokazały, że 6-dniowa ekspozycja komórek śródbłonka na 1% stężenie tlenu powoduje liczne zmiany w ich metabolizmie tlenowym na poziomie komórek oraz izolowanych mitochondriów. Hipoksja powoduje zwiększoną fermentację, jednocześnie nie doprowadzając do zmian w biogenezie mitochondriów oraz w ich pojemności oddechowej. W komórkach śródbłonka chroniczna hipoksja obniża utlenianie węglowodanów, kwasów tłuszczowych i aminokwasów z wyjątkiem aminokwasów ketogennych. Hipoksja prowadzi do wzrostu całkowitej i mitochondrialnej produkcji ROS, jednakże białka systemu antyoksydacyjnego (SOD1, SOD2, UCP2) nie ulegają zwiększonej ekspresji. Ekspozycja komórek śródbłonka na niedotlenienie prowadzi do znaczącej re-aranżacji mitochondrialnego łańcucha oddechowego z przeciwstawną regulacją dwóch najważniejszych dehydrogenaz (zwiększona aktywność kompleksu II, zmniejszona aktywność kompleksu I). Zwiększonej aktywności kompleksu II towarzyszy zwiększona produkcja mROS, głównie poprzez odwrócony transport elektronów. Wzrost komórek śródbłonka w warunkach chronicznej hipoksji prowadzi do obniżenia aktywności oraz ekspresji UCP2. Wyniki te pokazują, że (i) wzrost komórek śródbłonka w warunkach chronicznego niedotlenienia powoduje przesunięcie katabolizmu z tlenowego na beztlenowy; (ii) w mitochondriach komórek poddanych chronicznej hipoksji, kompleks II pełni istotną rolę w produkcji mROS, głównie poprzez odwrócony transport elektronów; oraz (iii) indukowany hipoksją zwiększony poziom mROS stanowi ważny element sygnalizacyjny w metabolicznej odpowiedzi komórek śródbłonka na warunki obniżonego stężenia tlenu.

W przedstawionej pracy scharakteryzowano kanał potasowy regulowany jonami wapnia o dużym przewodnictwie (BK_{Ca}) mitochondriów komórek śródbłonka EA.hy926. Przy użyciu przeciwciał skierowanych na podjednostki kanału BK_{Ca} błony plazmatycznej, zidentyfikowano w wewnętrznej błonie mitochondriów śródbłonka tworzącą por kanału

podjednostkę α oraz podjednostkę regulatorową β2. Substancje znane jako modulatory aktywności kanału BK_{Ca} wpływają na bioenergetykę mitochondriów izolowanych z komórek śródbłonka. W warunkach niefosforylujących, aktywatory: 100 μM Ca^{2+}, 10 μM NS1619 oraz 0.5 μM NS11021 depolaryzują mitochondrialny potencjał błonowy oraz stymulują oddychanie. Efekt ten jest blokowany przez paksylinę i iberiotoksynę w sposób zależny od obecności jonów potasu. Wyniki te pokazują po raz pierwszy, że w wewnętrznej błonie mitochondriów ludzkich komórek śródbłonka EA.hy926 obecny jest kanał potasowy regulowany jonami wapnia o dużym przewodnictwie mający właściwości podobne to kanału obecnego w błonie plazmatycznej.

7 List of author's publications

Publications presenting results included in the doctoral thesis:

Koziel A, Woyda-Ploszczyca A, Kicinska A, Jarmuszkiewicz W. 2012 The influence of high glucose on the aerobic metabolism of endothelial EA.hy926 cells. Pflügers Archiv – European Journal of Physiology 464(6):657-669. doi: 10.1007/s00424-012-1156-1. (**Chapter 4.1**)

Bednarczyk P, **Koziel A**, Jarmuszkiewicz W, Szewczyk A. 2013 Large-conductance Ca^{2+}-activated potassium channel in mitochondria of endothelial EA.hy926 cells. American Journal of Physiology – Heart and Circulatory Physiology 304(11):H1415-H1427. doi: 10.1152/ajpheart.00976.2012. (**Chapter 4.4**)

Koziel A, Sobieraj I, Jarmuszkiewicz W. 2015 Increased activity of mitochondrial uncoupling protein 2 improves stress resistance in cultured endothelial cells exposed in vitro to high glucose levels. American Journal of Physiology – Heart and Circulatory Physiology 309(1):H147-56. doi: 10.1152/ajpheart.00759.2014. (**Chapter 4.3**)

Koziel A, Jarmuszkiewicz W. Hypoxia and aerobic metabolism adaptations of human endothelial cells. Submitted (**Chapter 4.2**)

Additional publications:

Woyda-Ploszczyca A*, **Koziel A*,** Antos-Krzeminska N, Jarmuszkiewicz W. 2011 Impact of oxidative stress on Acanthamoeba castellanii mitochondrial bioenergetics depends on cell growth stage. Journal of Bioenergetics and Biomembranes 43(3):217-225. doi: 10.1007/s10863-011-9351-x. *equal authors contribution.

Jarmuszkiewicz W, Woyda-Ploszczyca A*, **Koziel A*,** Majerczak J, Zoladz JA. 2015 Temperature controls oxidative phosphorylation and reactive oxygen species production through uncoupling in rat skeletal muscle mitochondria. Free Radical Biology and Medicine 83:12-20. doi: 10.1016/j.freeradbiomed.2015.02.012. * equal authors contribution.

Broniarek I, **Koziel A**, Jarmuszkiewicz W. 2016 The effect of chronic exposure to high palmitic acid concentrations on the aerobic metabolism of human endothelial EA.hy926 cells. Pflügers Archiv - European Journal of Physiology 468(9):1541-1554. doi: 10.1007/s00424-016-1856-z.

Zoladz JA, **Koziel A**, Woyda-Ploszczyca A, Celichowski J, Jarmuszkiewicz W. 2016 Endurance training increases the efficiency of rat skeletal muscle mitochondria. Pflügers Archiv - European Journal of Physiology. doi:10.1007/s00424-016-1867-9.

Reviews:

Koziel A, Jarmuszkiewicz W. 2013 Aerobic metabolism and reactive oxygen species in endothelial cells. Postepy Biochemi 59(4):386-394. Article in Polish.

Szewczyk A, Jarmuszkiewicz W, **Koziel A,** Sobieraj I, Nobik W, Lukasiak A, Skup A, Bednarczyk P, Drabarek B, Dymkowska D, Wrzosek A, Zablocki K. 2015 Mitochondrial mechanisms of endothelial dysfunction. Pharmacological Reports 67(4):704-710. doi: 10.1016/j.pharep.2015.04.009.

8 References

Acin-Perez R, Bayona-Bafaluy MP, Fernandez-Silva P, Moreno-Loshuertos R, Perez-Martos A, Bruno C, Moraes CT, Enriquez JA. **2004** Respiratory complex III is required to maintain complex I in mammalian mitochondria. Molecular Cell 13(6):805-815.

Ago T, Kuroda J, Pain J, Fu CX, Li H, Sadoshima J. **2010** Upregulation of Nox4 by hypertrophic stimuli promotes apoptosis and mitochondrial dysfunction in cardiac myocytes. Circulation Research 106(7):1253-1264.

Alberts B, Johnson A, Lewis J, Raff M, Roberts K, Walter P. **2002** Molecular Biology of the Cell 4th edition. New York: Garland Science.

Aley PK, Porter KE, Boyle JP, Kemp PJ, Peers C. **2005** Hypoxic modulation of Ca^{2+} signaling in human venous endothelial cells. Multiple role for reactive oxygen species. Journal of Biological Chemistry 280(14):13349-13354.

Althoff T, Mills DJ, Popot JL, Kühlbrandta W. **2011** Arrangement of electron transport chain components in bovine mitochondrial supercomplex I1III2IV1. EMBO Journal 30(22):4652-4664.

Amado LC, Saliaris AP, Raju SV, Lehrke S, St John M, Xie JS, Stewart G, Fitton T, Minhas KM, Brawn J, Hare JM. **2005** Xanthine oxidase inhibition ameliorates cardiovascular dysfunction in dogs with pacing-induced heart failure. Journal of Molecular and Cellular Cardiology 39(3):531-536.

Aon MA, Cortassa S, Wei AC, Grunnet M, and O'Rourke B. **2010** Energetic performance is improved by specific activation of K^+ fluxes through K_{Ca} channels in heart mitochondria. Biochimica et Biophysica Acta - Bioenergetics 1797(1):71-80.

Balligand JL, Feron O, Dessy C. **2009** eNOS Activation by Physical Forces: From Short-Term Regulation of Contraction to Chronic Remodeling of Cardiovascular Tissues. Physiological Reviews Published 89(2):481-534.

Ballinger SW, Patterson C, Knight-Lozano CA, Burow DL, Conklin CA, Hu Z, Reuf J, Horaist C, Lebovitz R, Hunter GC, McIntyre K, Runge MS. **2002** Mitochondrial integrity and function in atgerogenesis. Circulation 106(5):544-549.

Ballinger Sw. 2005 Mitochondrial dysfunction in cardiovascular diseases. Free Radical Biology and Medicine 38(10):1278-1295.

Barja G. 1999 Mitochondrial oxygen radical generation and leak: sites of productions in states 4 and 3, organ specificity and relation to aging and longevity. Journal of Bioenergetics and Biomembranes 31(4):347-366.

Basta G, Lazzerini G, Del Turco S, Ratto GM, Schmidt AM, De Caterina R. **2005** At least 2 distinct pathways generating reactive oxygen species mediate vascular cell adhesion molecule-1 induction by advanced glycation end products. Arteriosclerosis, Thrombosis, and Vascular Biology 25(7):1401-1407.

Bayer RE. 1990 The participation of coenzyme Q in free radical production and antioxidation. Free Radical Biology and Medicine 8(6):545-565.

Becker LB. 2004 New concepts in reactive oxygen species and cardiovascular reperfusion physiology. Cardiovascular Research 61(3):461-470.

Beckman JA, Creager MA, Libby P. **2002** Diabetes and atherosclerosis: epidemiology, pathophysiology and management. Journal of the American Medical Association 287(19):2570-2581.

Beckman JA, Goldfine AB, Gordon MB, Creager MA. **2001** Ascorbate restores endothelium-dependent vasodilation impaired by acute hyperglycemia in humans. Circulation 103(12):1618-1623.

Beckman JS and Koppenol WH. 1996 Nitric oxide and peroxynitrite: the good the bad and the ugly. American Journal of Physiology 271(5Pt1):C1424-C1437.

Bednarczyk P, Koziel A, Jarmuszkiewicz W, Szewczyk A. **2013** Large-conductance Ca^{2+}-activated potassium channel in mitochondria of endothelial EA.hy926 cells. American Journal of Physiology: Heart and Circulatory Physiology 304(11):H1415-H1427.

Bentzen BH, Nardi A, Calloe K, Madsen LS, Olesen SP, and Grunnet M. **2007** The small molecule NS11021 is a potent and specific activator of Ca $^{2+}$-activated big-conductance K^+ channels. Molecular Pharmacology 72(4):1033-1044.

Beresiewicz A, Maczewski M, Duda M. **2004** Effect of classic preconditioning and diazoxide on endothelial function and superoxide and NO generation in the post-ischemic guinea-pig heart. Cardiovascular Research 63(1):118-129.

Bernardi P. 1999 Mitochonsrial transport of cations: channels, exchangers and permability transition. Physiological Review 79(4):1127-1155.

Berry EA, Guergova-Kuras M, Huang LS, Crofts AR. **2000** Structure and function of cytochrome bc complexes. Annual Review of Biochemistry 69:1005-1075.

Bhatt MP, Lim YC, Kim YM, Ha KS. **2013** C-Peptide activates AMPKα and prevents ROS-mediated mitochondrial fission and endothelial apoptosis in diabetes. Diabetes 62(11):3851-3862.

Binoldi A, Cavallini L, Jocelyn P. **1982** Mitochondrial lipid peroxidation by cumene hydroperoxide and its prevention by succinate. Biochimica et Biophysica Acta 681(3):496-503.

Bogardus C, Lillioja S, Howard BV, Reaven G, Mott D. **1984** Relationship between insulin secretion, insulin action, and fasting plasma glucose concentration in nondiabetic and noninsulin-dependent diabetic subject. Journal of Clinical Investigation 74(4):1238-1246.
Bolick DT, Srinivasan S, Whetzel A, Fuller LC, Hedrick CC. **2006** 12/15 lipoxygenase mediates monocyte adhesion to aortic endothelium in apolipoprotein E-deficient mice through activation. Arteriosclerosis, Thrombosis, and Vascular Biology 26:1260-1266.
Borchert GH, Yang C, Kolár F. **2011** Mitochondrial BK_{Ca} channels contribute to protection of cardiomyocytes isolated from chronically hypoxic rats. American Journal of Physiology - Heart and Circulatory Physiology 300(2):H507-H513.
Bortolato M, Chen K, Shih JC. **2008** Monoamine oxidase inactivation: from physiology to therapeutics. Advanced Drug Delivery Reviews 60(13-14):1527-1533.
Boveris A, Oshino N, Chance B. **1972** The cellular production of hydrogen peroxide. Biochemical Journal 128(3):617-630.
Brand MD and Esteves TC. 2005 Physiological function of the mitochondrial uncoupling proteins UCP2 and UCP3. Cell Metabolism 2(2):85-93.
Brand MD, Affourtit C, Esteves TC, Green K, Lambert AJ, Miwa S, Pakay JL, Parker N. **2004** Mitochondrial superoxide: production, biological effects, and activation of uncoupling proteins. Free Radical Biology and Medicine 37(6):755-767.
Brand MD, Pamplona R, Portero-Otin M, Requena JR, Roebuck SJ, Buckingham JA, Clapham JC, Cadenas S. **2002** Oxidative damage and phospholipid fatty acyl composition in skeletal muscle mitochondria from mice underexpressing and overexpressing uncoupling protein 3. Biochemical Journal 368(Pt2):597-603.
Brookes PS, Yoon Y, Robotham JL, Andres MW, Sheu SS. **2004** Calcium, ATP and ROS: a mitochondrial love-hate triangle. American Journal of Physiology - Cell Physiology 287(4):C817-C833.
Brownlee M. 2001 Biochemistry and molecular cell biology of diabetic complications. Nature 414(6865):813-820.
Brownlee M. 2005 The pathobiology of diabetic complications: A unifying mechanism. Diabetes 54(6):1615-1625.
Brunori M, Giuffrè A, Forte E, Mastronicola D, Barone MC, Sarti P. **2004** Control of cytochrome c oxidase activity by nitric oxide. Biochimica et Biophysica Acta 1655(1-3):365-371.
Budinger GR, Duranteau J, Chandel NS, Schumacker PT. **1998** Hibernation during hypoxia in cardiomyocytes. Role of mitochondria as the O_2 sensor. Journal of Biological Chemistry 273(6):3320-3326.
Burcelin B, Kande J, Ricquier D, Girard J. **1993** Changes in uncoupling protein and GLUT4 glucose transporter expressions in interscapular brown adipose tissue of diabetic rats: relative roles of hyperglycaemia and hypoinsulinaemia. Biochemical Journal 291(1):109-113.
Burwell LS, Nadtochiy SM, Tompkins AJ, Young S, Brookes PS. **2006** Direct evidence for S-nitrosation of mitochondrial complex I. Biochemical Journal 394(Pt 3): 627–634.
Cadenas E and Davies KJ. 2000 Mitochondrial free radical generation, oxidative stress, and aging. Free Radical Biology and Medicine 29(3-4):222-230.
Calhoun MW, Thomas JW, Gennis RB. **1994** The cytochrome oxidase superfamily of redox-driven proton pumps. Trends in Biochemical Sciences 19(8):325-330.
Camello-Almaraz C, Gomez-Pinilla PJ, Pozo MJ, Camello P. **2006** Mitochondrial reactive species and Ca^{2+} signaling. American Journal of Physiology - Cell Physiology 291(5):C1082-C1088.
Cannon B and Nedergaard J. 2004 Brown adipose tissue: function and physiological significance. Physiological Reviews 84(1):277-359.
Capaldi RA and Aggeler R. 2002 Mechanism of the F_1F_0-type ATP synthase, a biological rotary motor. Trends in Biochemical Sciences 27(3):154-160.
Carroll AM, Haines LR, Pearson TW, Fallon PG, Walsh CM, Brennan CM, Breen EP, Porter RK. **2005** Identification of a functioningmitochondrial uncoupling protein 1 in thymus. Journal of Biological Chemistry 280(16):15534-15543.
Cassina A and Radi R. 1996 Differential inhibitory action of nitric oxide and peroxynitrite on mitochondrial electron transport. Archives of Biochemistry and Biophysics 328(2):309-316.
Ceaser EK, Ramachandran A, Levonen AL, Arley-Usmar VM. **2003** Oxidized low-density lipoprotein and 15-deoxy-delta 12,14-PGJ2 increase mitochondrial complez I activity in endothelial cells. American Journal of Physiology - Heart and Circulatory Physiology 285(6):H2298-H2308.
Cecchini G. 2003 Function and structure of complex II of the respiratory chain. Annual Review of Biochemistry 72:77–109.
Ceolotto G, Gallo A, Papparella I, Franco L, Murphy E, Iori E, Pagnin E, Fadini GP, Albiero M, Semplicini A, Avogaro A. **2007** Rosiglitazone reduces glucose-induced oxidative stress mediated by NAD(P)H oxidase via AMPK-dependent mechanism. Arteriosclerosis, Thrombosis, and Vascular Biology 27(12):2627-2633.

Chan CB, MacDonald PE, Saleh MC, Johns DC, Marbàn E, Wheeler MB. **1999** Overexpression of uncoupling protein 2 inhibits glucose-stimulated insulin secretion from rat islets. Diabates 48(7):1482-1486.
Chan CK and Vanhoutte PM. 2013 Hypoxia, vascular smooth muscles and endothelium. Acta Pharmaceutica Sinica B 3(1):1-7.
Chan DC. 2006 Mitochondria: Dynamic Organelles in Disease, Aging, and Development. Cell 125(7):1241-1252.
Chandel NS and Schumacker PT. 2000 Cellural oxygen sensing by mitochondria: old question, new insight. Journal of Applied Physiology 88(5):1880-1889.
Chandel NS, Maltepe E, Goldwasser E, Mathieu CE, Simon MC, Schumacker PT. **1998** Mitochondrial reactive oxygen species trigger hypoxia-induced transcription. Proceedings of the National Academy of Sciences of the United States of America 95(20):11715-11720.
Chandel NS, McClintock DS, Feliciano CE, Wood TM, Melendez JA, Rodriguez AM, Schumacker PT. **2000** Reactive oxygen species generated at mitochondrial complex III stabilize hypoxia-inducible factor-1alpha during hypoxia: a mechanism of O_2 sensing. Journal of Biological Chemistry 275(33):25130-25138.
Chen YC, Taylor EB, Dephoure N, Heo JM, Tonhato A, Papandreou I, Nath N, Denko NC, Gygi SP, Rutter J. **2012** Identification of a protein mediating respiratory supercomplex stability. Cell Metabolism 15(3)348-360.
Cheng Y, Gu XQ, Bednarczyk P, Wiedemann FR, Haddad GG, Siemen D. **2008** Hypoxia increases activity of the BK-channel in the inner mitochondrial membrane and reduces activity of the permeability transition pore. Cellular Physiology and Biochemistry 22(1-4):127-36.
Cheurfa N, Dubois-Laforgue D, Ferrarezi DA, Reis AF, Brenner GM, Bouche C, Le Feuvre C, Fumeron F, Timsit J, Marre M, Velho G. **2008** The common -866G>A variant in the promoter of UCP2 is associated with decreased risk of coronary artery disease in type 2 diabetic men. Diabetes 57(4):1063-1068.
Chipuk JE, Bouchier-Hayes L, Green DR. **2006** Mitochondrial outer membrane permeabilization during apoptosis: the innocent bystander scenario. Cell Death and Differentiation 13(8):1396–1402.
Cines DB, Pollak ES, Buck CA, Loscalzo J, Zimmerman GA, McEver RP, Pober JS, Wick TM, Konkle BA, Schwartz BS, Barnathan ES, McCrae KR, Hug BA, Schmidt AM, Stern DM. **1998** Endothelial cells in physiology and in the pathophysiology of vascular disorders. Blood Journal 91(10):3527-3561.
Clementi E, Brown GC, Feelisch M, Moncada S. **1998** Persistent inhibition of cell respiration by nitrix oxide: crucial role of S-nitrosylation of mitochondrial complex I and protective action of glutathione. Proceedings of the National Academy of Sciences of the United States of America 95(13):7631-7636.
Crofts AR. 2004 The cytochrome bc1 complex: function in the context of structure. Annual Review of Physiology 66:689-733.
Cui Y, Xu X, Bi H, Zhu Q, Wu J, Xia X, Qiushi R, Ho PCP. **2006** Expression modification of uncoupling proteins and MnSOD in retinal endothelial cells and pericytes induced by high glucose: The role of reactive oxygen species in diabetic retinopathy. Experimental Eye Research 83(4):807-816.
Culic O, Decking UK, Schrader J. **1999** Metabolic adaptation of endothelial cells to substrate deprivation. American Journal of Physiology 276(5Pt1):C1061-C1068.
Culic O, Gruwel M, Schrader J. **1997** Energy turnover of vascular endothelial cells. American Journal of Physiology 273(1Pt1):C205-C213.
Cypess AM, White AP, Vernochet C, Schulz TJ, Xue R, Sass CA, Huang TL, Roberts-Toler C, Weiner LS, Sze C, Chacko AT, Deschamps LN, Herder LM, Truchan N, Glasgow AL, Holman AR, Gavrila A, Hasselgren PO, Mori MA, Molla M, Tseng YH. **2013** Anatomical localization, gene expression profiling and functional characterization of adult human neck brown fat. Nature Medicine 19(5):635-639.
Cypser JR and Johnson TE. 2002 Multiple stressors in Caenorhabditis elegans induce stress hormesis and extended longevity. Journals of Gerontology - Series A Biological Sciences and Medical Sciences 57(3):B109-B114.
Dagher Z, Ruderman N, Tornheim K, Ido Y. **2001** Acute regulation of fatty acid oxidation and amp-activated protein kinase in human umbilical vein endothelial cell. Circulation Research 88(12):1276-1282.
Davidson SM and Duchen MR. 2007 Endothelial mitochondria: Contributing to vascular function and disease. Circulation Research 100(8):1128-1141.
Davidson SM. 2010 Endothelial mitochondria and heart disease. Cardiovascular Research 88(1):58-66.
Dedkova EN, Ji X, Lipsius SL, Blatter LA. **2004** Mitochondrial calcium uptake stimulates nitric oxide production in mitochondria of bovine vascular endothelial cells. American Journal of Physiology - Cell Physiology 286(2):C406-C415.
Detaille D, Guigas B, Chauvin C, Batandier C, Fontaine E, Wiernsperger N, Leverve X. **2005** Metformin prevents high-glucose-induced endothelial cell death thrugh a mitochondrial permability teransition dependent process. Journal of Diabetes 54(7):1172-1181.
Dhanasekaran A, Kotamraju S, Kalivendi SV, Matsunaga T, Shang T, Keszler A, Joseph J, Kalyanaraman B. **2004** Supplementation of endothelial cells with mitochondria-targeted antioxidants inhibit peroxide-induced

mitochondrial iron uptake, oxidative damage, and apoptosis. Journal of Biological Chemistry 279(36):37575-37587.
Dikalov SI, Dikalova AE, Bikineyeva AT, Schmidt HH, Harrison DG, Griendling KK. **2008** Distinct roles of Nox1 and Nox4 in basal and angiotensin II-stimulated superoxide and hydrogen peroxide production. Free Radical Biology and Medicine 45(9):1340-1351.
Dimroth P, von Ballmoos C, Meier T. **2006** Catalytic and mechanical cycles in F-ATP synthases. Fourth in the Cycles Review Series EMBO Reports 7(3):276-282.
Douglas RM, Lai JCK, Bian S, Cummins L, Moczydlowski E, and Haddad GG. **2006** The calcium-sensitive large-conductance potassium channel (BK/MAXI K) is present in the inner mitochondrial membrane of rat brain. Neuroscience 139(4):1249-1261.
Dranka BP, Hill BG, Darley-Usmar VM. **2010** Mitochondrial reserve capacity in endothelial cells: Impact of nitric oxide and reactive oxygen species. Free Radical Biology and Medicine 48(7):905-914.
Dromparis P and Michelakis ED. 2013 Mitochondria in vascular health and disease. Annual Review of Psychology 75:95-126.
Du X, Matsumura T, Edelstein D, Rossetti L, Zsengeller Z, Szabo C, Brownlee M. **2003** Inhibition of GAPDH activity by poly(ADP-ribose) polymerase activates three major pathways of hyperglycemic damage in endothelial cells. Journal of Clinical Investigation 112(7):1049-1057.
Du XL, Edelstein D, Rossetti L, Fantus IG, Goldberg H, Ziyadeh F, Wu J, Brownlee M. **2000** Hyperglycemia-induced mitochondrial superoxide overproduction activates the hexosamine pathway and induces plasminogen activator inhibitor-1 expression by increasing Sp1 glycosylation. Proceedings of the National Academy of Sciences of the United States of America 97(22):12222-12226.
Du XL, Sui GZ, Stockklauser-Farber K, Weiss J, Zink S, Schwippert B, Wu QX, Tschope D, Rosen P. **1998** Introduction of apoptosis by high-proinsulin and glucose in cultured human umbilical vein endothelial cells is mediated by reactive oxygen species. Diabetologia 41(3):249-256.
Duchen MR. 2004 Roles of Mitochondria in Health and Disease. Diabetes 53(1):96-102.
Duranteau J, Chandel NS, Kulisz A, Shao Z, Schumacker PT. **1998** Intracellular signaling by reactive oxygen species during hypoxia in cardiomyocytes. Journal of Biological Chemistry 276(19):11619-11624.
Duriez PJ, Wong F, Dorovini-Zis K, Shahidi R, Karsan A. **2000** A1 functions at the mitochondria to delay endothelial apoptosis in response to tumor necrosis factor. Journal of Biological Chemistry 275(24):18099–18107.
Duval C, Negre-Salvayre A, Dogilo A, Salvayre R, Penicaud L, Casteilla L. **2002** Increased rective oxygen species production with antisense oligonucleotides directed against uncoupling protein 2 in murine endothelial cells. Biochemistry and Cell Biology 80(6):757-764.
Dymkowska D, Drabarek B, Podszywalow-Bartnicka P, Szczepanowska J, and Zablocki K. **2014** Hyperglycaemia modifies energy metabolism and reactive oxygen species formation in endothelial cells in vitro. Archives of Biochemistry and Biophysics 542:7-13.
Eales KL, Hollinshead KE, Tennant DA. **2016** Hypoxia and metabolic adaptation of cancer cells. Oncogenesis 5:e190.
Edgell CJS, McDonald CC, Graham JB. **1983** Permanent cell line expressing human factor VIII-related antigen established by hybridization. Proceedings of the National Academy of Sciences of the United States of America 80(12):3734-3737.
Ekelund UE, Harrison RW, Shokek O, Thakkar RN, Tunin RS, Senzaki H, Kass DA, Marbán E, Hare JM. **1999** Intravenous allopurinol decreases myocardial oxygen consumption and increases mechanical efficiency in dogs with pacing-induced heart failure. Circulation Reserarch 85(5):437–445.
Erusalimsky JD and Moncada S. 2007 Nitric oxide and mitochondrial signaling: from physiology to pathophysiology. Arteriosclerosis, Thrombosis, and Vascular Biology 27(12):2524-2531.
Esposti M and Lenaz G. 1985 A clarification of the effects of DCCD on the electron transfer and antimycin binding of the mitochondrial bc1 complex. Journal of Bioenergetics and Biomembranes 17(2):109-121.
Etchay KS, Roussel D, St-Pierre J, Jekabsons MB, Cadenas S, Stuart JA, Harper JA, Roebuck SJ, Morrison A, Pickering S, Clapham JC, Brand MD. **2002** Superoxide activates mitochondrial uncoupling proteins. Nature 415(6867):96-99.
Eto Y, Kang D, Hasegawa E, Takeshige K, Minakami S. **1992** Succinate-dependent lipid peroxidation by reduced ubiquinone in beef heart submitochondrial particles. Archives of Biochemistry and Biophysics 295(1):101-106.
Fahanik-Babaei J, Eliassi A, Saghiri R. **2011** How many types of large conductance Ca^{+2}-activated potassium channels exist in brain mitochondrial inner membrane: evidence for a new mitochondrial large conductance Ca^{2+}-activated potassium channel in brain mitochondria. Neuroscience 199:125-132.
Faller DV. 1999 Endothelial cell responses to hypoxic stress. Clinical and Experimental Pharmacology and Physiology 26(1):74-84.

Feletou M. 2009 Calcium-activated potassium channels and endothelial dysfunction: therapeutic options? British Journal of Pharmacology 156(4):545-562.
Feng J and Zuo Z. 2011 Isoflurane preconditioning increases endothelial cell tolerance to in-vitro simulated ischaemia. Journal of Pharmacy and Pharmacology 63(1):106-110.
Fink BD, Reszka KJ, Herlein JA, Mathahs MM, Sivitz WI. **2005** Respiratory uncoupling by UCP1 and UCP2 and superoxide generation in endothelial cel mitochondria. American Journal of Physiology - Endocrinology and Metabolism 288(1):E71-E79.
Freitas TP, Rezin GT, Gonçalves CL, Jeremias GC, Gomes LM, Scaini G, Teodorak BP, Valvassori SS, Quevedo J, Streck EL. **2010** Evaluation of citrate synthase activity in brain of rats submitted to an animal model of mania induced by ouabain. Molecular and Cellular Biochemistry 341(1-2):245-249.
Fridovich I. 1995 Superoxide radical and superoxide dismutases. Annual Review of Biochemistry 64:97-112.
Galkin A, Abramov AY, Frakich N, Duchen MR, Moncada S. **2009** Lack of oxygen deactivates mitochondrial complex I: implications for ischemic injury? Journal of Biological Chemistry 284(52):36055-36061.
Galkin A, Higgs A, Moncada S. **2007** Nitric oxide and hypoxia. Essays in Biochemistry 43:29-42.
Geloen A and Trayhurn P. **1990** Regulation of the level of uncoupling protein in brown adipose tissue by insulin. American Journal of Physiology - Regulatory Integrative and Comparative Physiology 258(2):R418-R424.
Genova ML, Ventura B, Giuliano G, Bovina C, Formiggini G, Parenti CG, Lenaz G. **2001** The site of production of superoxide radical in mitochondria Complex I is not a bound ubisemiquinone but presumably iron-sulfur cluster N2. FEBS Letters 505(3):364-368.
Gerald D, Berra E, Frapart YM, Chan DA, Giaccia AJ, Mansuy D, Pouysségur J, Yaniv M, Mechta-Grigoriou F. **2004** JunD reduces tumor angiogenesis by protecting cells from oxidative stress. Cell 118(6):781-794.
Giardino I, Edelstein D, Brownlee M. **1996** BCL-2 expression or antioxidants prevent hyperglycemia-induced formation of intracellular advanced glycation endproducts in bovine endothelial cells. Journal of Clinical Investigation 97(6):1422-1428.
Giorgio M, Migliaccio E, Orsini F, Paolucci D, Moroni M, Contursi C, Pelliccia G, Luzi L, Minucci S, Marcaccio M, Pinton P, Rizzuto R, Bernardi P, Paolucci F, Pelicci PG. **2005** Electron transfer between cytochrome c nad p66Shc generates reactive oxygen species that trigger mitochondrial apoptosis. Cell 122(2):221-233.
Golbidi S, Badran M, Laher I. **2012** Antioxidant and anti-inflammatory effects of exercise in diabetic patients. Experimental Diabetes Research vol. 2012 Article ID 941868.
Groschner LN, Waldeck-Weiermair M, Malli R, Graier WF. **2012** Endothelial mitochondria-less respiration, more integration. Pflugers Archiv European Journal of Physiology 464(1):63-76.
Guyton AC and Hall JE. 2015 Textbook of Medical Physiology. Thirteen Edition.
Halestrap AP. 1994 Regulation of mitochondrial metabolism through changes in matrix volume. Biochemical Society Transactions 22(2):522-529.
Ham AJ and Liebler DC. 1995 Vitamin E oxidation in rat liver mitochondria. Biochemistry 34(17):5754-5761.
Han D, Antunes F, Canali R, Rettori D, Cadenas E. **2003** Voltage- ependent anion channels control the release of superoxide anion from mitochondria to cytosol. Journal of Biological Chemistry 278(8):5557-5563.
Han D, Williams E, Cadenas E. **2001** Mitochondrial respiratory chain-dependent generation of superoxide anion and its release into the intermembrane space. Biochemical Journal 353(2):411-416.
Harris AL. 2002 Hypoxia–a key regulatory factor in tumour growth. Nature Reviews Cancer 2(1):38-47.
Hawkins BJ, Levin MD, Doonan PJ, Petrenko NB, Davis CW, Patel VV, Madesh M. **2010** Mitochondrial complex II prevents hypoxic but not calcium- and proapoptotic Bcl-2 protein-induced mitochondrial membrane potential loss. Journal of Biological Chemistry 285(34):26494-26505.
Hayashi T, Rizzuto R, Hajnoczky G, Su TP. **2009** MAM: more than just a housekeeper. Trends Cell Biology 19(2):81-88.
He Y, Wang N, Shen Y, Zheng Z, Xu X. **2014** Inhibition of high glucose-induced apoptosis by uncoupling protein 2 in human umbilical vein endothelial cells. International Journal of Molecular Medicine 33(5):1275-1281.
Heinen A, Camara AKS, Aldakkak M, Rhodes SS, Riess ML, Stowe DF. **2007** Mitochondrial $Ca2^{+}$-induced K^{+} influx increases respiration and enhances ROS production while maintaining membrane potential. American Journal of Physiology - Cell Physiology 292(1):C148-C156.
Hernandez-Mijares A, Rocha M, Rovira-Llopis S, Bañuls C, Bellod L, de Pablo C, Alvarez A, Roldan-Torres I, Sola-Izquierdo E, Victor VM. **2013** Human leukocyte/endothelial cell interactions and mitochondrial dysfunction in type 2 diabetic patients and their association with silent myocardial ischemia. Diabetes Care 36(6):1695-1702.
Hewitson KS, Lienard BM, McDonough MA, Clifton IJ, Butler D, Soares AS, Oldham NJ, McNeill LA, Schofield CJ. **2007** Structural and mechanistic studies on the inhibition of the hypoxia-inducible transcription

factor hydroxylases by tricarboxylic acid cycle intermediates. Journal of Biological Chemistry 282(5):3293-3301.
Hoffman DL, Salter JD, Brookes PS. **2007** Response of mitochondrial reactive oxygen species generation to steady-state oxygen tension: implication for hypoxic cell signaling. American Journal of Physiology - Heart and Circulatory Physiology 292(1):H101-H108.
Huang D, Li T, Li X, Zhang L, Sun L, He X, Zhong X, Jia D, Song L, Semenza GL, Gao P, Zhang H. **2014** HIF-1-mediated suppression of acylo-CoA dehydrogenases and fatty acid oxidation is critical for cancer progression. Cell Reports 8(6):1930-1942.
Hunte C, Palsdottir H, Trumpower BL. **2003** Protonmotive pathways and mechanisms in the cytochrome bc1 complex. FEBS Letters 545(1):39-46.
Huynh K, Bernardo BC, McMullen JR, Ritchie RH. **2014** Diabetic cardiomyopathy: Mechanisms and new treatment strategies targeting antioxidant signaling pathways. Pharmacology and Therapeutics 142(3):375-415.
Huynh K, Kiriazis H, Du XJ, Love JE, Gray SP, Jandeleit-Dahm KA, McMullen JR, Ritchie RH. **2013** Targeting the upregulation of reactive oxygen species subsequent to hyperglycemia prevents type 1 diabetic cardiomyopathy in mice. Free Radical Biology and Medicine 60:307-317.
Isaacs JS, Jung YJ, Mole DR, Lee S, Torres-Cabala C, Chung YL, Merino M, Trepel J, Zbar B, Toro J, Ratcliffe PJ, Linehan WM, Neckers L. **2005** HIF overexpression correlates with biallelic loss of fumarate hydratase in renal cancer: novel role of fumarate in regulation of HIF stability. Cancer cell 8(2):143-153.
Iwata S, Lee JW, Okada K, Lee JK, Iwata M, Rasmussen B, Link TA, Ramaswamy S, Jap BK. **1998** Complete structure of the 11-subunit bovine mitochondrial cytochrome bc1 complex. Science 281(5373):64–71.
Iyer NV, Kotch LE, Agani F, Leung SW, Laughner E, Wenger RH, Gassmann M, Gearhart JD, Lawler AM, Yu AY, Semenza GL. **1998** Cellular and developmental control of O_2 homeostasis by hypoxia-inducible factor 1 alpha. Genes and Development 21(2):149-162.
Jezek P and Hlavata L. 2005 Mitochondria in homeostasis of reactive oxygen species in cell, tissues, and organism. International Journal of Biochemistry and Cell Biology 37(12):2478-2503.
Jezek P. 2002 Possible physiological roles of mitochondrial uncoupling proteins-UCPn. The International Journal of Biochemistry and Cell Biology 34(10):1190-1206.
Jornot L, Maechler P, Wollheim CB, Junod AF. **1999** Reactive oxygen metabolites increase mitochondrial calcium in endothelial cells: implication of the Ca^{2+}/Na^{+} exchanger. Journal of Cell Science 112:1013-1022.
Kaczara P, Motterlini R, Rosen GM, Augustynek B, Bednarczyk P, Szewczyk A, Foresti R, Chlopicki S. **2015** Carbon monoxide released by CORM-401 uncouples mitochondrial respiration and inhibits glycolysis in endothelial cells: A role for mitoBKCa channels. Biochimica et Biophysica Acta 1847(10):1297-1309.
Kahles T and Brandes RP. 2013 Which NADPH Oxidase Isoform Is Relevant for Ischemic Stroke? The Case for Nox 2. Antioxidants and Redox Signaling 18(12):400-1417.
Kaluz S, Kaluzová M, Stanbridge EJ. **2008** Rational design of minimal hypoxia-inducible enhancers. Biochemical and Biophysical Research Communications 370(4):613-618.
Katakam PVG, Wappler EA, Katz PS, Rutkai I, Institoris A, Domoki F, Gaspar T, Grovenburg SM, Snipes JA, Busija DW. **2013** Depolarization of mitochondria in endothelial cells promotes cerebral artery vasodilation by activation of nitric oxide synthase. Arteriosclerosis, Thrombosis, and Vascular Biology 33(4):752-759.
Kathiresan T, Harvey M, Orchard S, Sakai Y, Sokolowski B. **2009** A protein interaction network for the large conductance Ca^{2+}-activated K^{+} channel in the mouse cochlea. Molecular and Cellular Proteomics 8(8):1972-1987.
Katnik C and Adams DJ. 1997 Characterization of ATP-sensitive potassium channels in freshly dissociated rabbit aortic endothelial cells. American Journal of Physiology 272(5 Pt 2):H2507-H2511.
Kayama Y, Raaz U, Jagger A, Adam M, Schellinger IN, Sakamoto M, Suzuki H, Toyama K, Spin JM, Tsao PS. **2015** Diabetic Cardiovascular Disease Induced by Oxidative Stress. International Journal of Molecular Sciences 16(10): 25234-25263.
Kietzmann T and Gorlach A. 2005 Reactive oxygen species in the control of hypoxia-inducible factor-mediated gene expression. Seminars in Cell and Developmental Biology 16(4-5):474-486.
Kim JW, Tchernyshyov I, Semenza GL, Dang CV. **2006** HIF-1-mediated expression of pyruvate dehydrogenase kinase: a metabolic switch required for cellular adaptation to hypoxia. Cell Metabolism 3(3):177-185.
Kirova Y, Germanova E, Lukyanova L. **2013** Phenotypic Features of the Dynamics of HIF-1alpha Levels in rat neocortex in different hypoxia regimens. Bulletin of Experimental Biology and Medicine154(6):718-722.
Kizhakekuttu TJ, Wang J, Dharmashankar K, Ying R., Gutterman DD, Vita JA, et al. **2012** Adverse alterations in mitochondrial function contribute to type 2 diabetes mellitus–related endothelial dysfunction in humans. Arteriosclerosis, Thrombosis, and Vascular Biology 32(10):2531-2539.
Klingenberg M. 1990 Mechanism and evolution of the uncoupling protein of brown adipose tissue. Trends in Biochemical Sciences 15(3):108-112.
Kluge AM, Fetterman JL, Vita JA. **2013** Mitochondria and endothelial function. Circulation Research 112(8): 1171-1188.

Koivunen P, Hirsila M, Remes AM, Hassinen IE, Kivirikko KI, Myllyharju J. **2007** Inhibition of hypoxia-inducible factor (HIF) hydroxylases by citric acid cycle intermediates: possible links between cell metabolism and stabilization of HIF. Journal of Biological Chemistry 282(7):4524-4532.
Kolobova E, Tuganova A, Boulatnikov I, Popov KM. **2001** Regulation of pyruvate dehydrogenase activity through phosphorylation at multiple sites. Biochemical Journal 358(Pt 1):69-77.
Koszela-Piotrowska I, Matkovic K, Szewczyk A, Jarmuszkiewicz W. **2009** A large-conductance calcium-activated potassium channel in potato (Solanum tuberosum) tuber mitochondria. Biochemical Journal 424(2):307-316.
Kowaltowski AJ, Costa AD, Vercesi AE. **1998** Activation of the potato plant uncoupling mitochondrial protein inhibits reactive oxygen species generation by the respiratory chain. FEBS Letters 425(2):213-216.
Koziel A, Sobieraj I, Jarmuszkiewicz W. **2015** Increased activity of mitochondrial uncoupling protein improves stress resistance in cultured endothelial cells exposed in vitro to high glucose levels. American Journal of Physiology – Heart and Circulatory Physiology 309(1):H147-H156.
Koziel A, Woyda-Ploszczyca A, Kicinska A, Jarmuszkiewicz W. **2012** The influence of high glucose on the aerobic metabolism of endothelial EA.hy926 cells. Pflugers Archiv European Journal of Physiology: 464(6)657-669.
Kuhlbrandt W. 2015 Structure and function of mitochondrial membrane protein complexes. BMC Biology 13:89.
Kuhn H and O'Donnell VB. 2006 Inflammation and immune regulation by 12/15-lipoxygenases. Progress in Lipid Research 45(4):334-356.
Kukidome D, Nishikawa T, Sonoda K, Imoto K, Fujisawa K, Yano M, Motoshima H, Taguchi T, Matsumura T, Araki E. **2006** Activation of AMP-activated protein kinase reduces hyperglycemia-induced mitochondrial reactive oxygen species production and promotes mitochondrial biogenesis in human umbilical vein endothelial cells. Diabetes 55(1):120–127.
Kuroda J, Ago T, Matsushima S, Zhai ZY, Schneider MD, Sadoshima J. **2010** NADPH oxidase 4 (Nox4) is a major source of oxidative stress in the failing heart. Proceedings of the National Academy of Sciences of the United States of America 107(35):15565-15570.
Kushnareva Y, Murphy AN, Andreyev A. **2002** Complex I-mediated reative oxygen species generation: modulation by cytochrome c and $NAD(P)^+$ oxidation-reduction state. Biochemical Journal 368(2):545-553.
La Selva M, Beltramo1 E, Pagnozzi F, Bena E, Molinatti PA, Molinatti GM, Porta M. **1996** Thiamine corrects delayed replication and decreases production of lactate and advanced glycation end-products in bovine retinal and human umbilical vein endothelial cells cultured under high glucose conditions. Diabetologia 39(11):1263-1268.
Lambert AJ and Brand MD. 2004 Inhibitors of the quinone-binding site allow repid superoxide production from mitochondrial NADH:ubiquinone oxidoreductase (complex I). Journal of Biological Chemistry 279(38):39414-39420.
Lameloise N, Muzzin P, Prentki M, Assimacopoulos-Jeannet F. **2001** Uncoupling protein 2: a possible link between fatty acid excess and impaired glucose-induced insulin secretion? Diabetes 50(4):803-809.
Laskowski M, Kicinska A, Szewczyk A, Jarmuszkiewicz W. **2015** Mitochondrial large-conductance potassium channel from *Dictyostelium discoideum*. International Journal of Biochemistry and Cell Biology 60:167-175.
Lassegue B, Martin AS, Griendling KK. **2012** Biochemistry, physiology and pathophysiology of NADPH oxidases in the cardiovascular. Circulation Research 110(10):1364-1390.
Lee KU, Lee IK, Han J, Song DK, Kim YM, Song HS, Kim HS, Lee WJ, Koh EH, Song KH, Han SM, Kim MS, Park IS, Park JY. **2005** Effects of recombinant adenovirus-mediated uncoupling protein 2 overexpression on endothelial function and apoptosis. Circulation Reserarch 96(11):1200-1207.
Lee KU, Lee IK, Han J, Song DK, Kim YM, Song HS, Kim HS, Lee WJ, Koh EH, Song KH, Han SM, Kim MS, Park IS, Park JY. **2005** Effects of recombinant adenovirus-mediated uncoupling protein 2 overexpression in endothelial function and apoptosis. Circulation Research 96(11):1200-1207.
Lenaz G, Fato R, Genova ML, Bergamini C, Bianchi C, Biondi A. **2006** Mitochondrial Complex I: structural and functional aspects. Biochimica et Biophysica Acta 1757(9-10):1406-1420.
Lenaz G. 1998 Role of mitochondria in oxidative stress and ageing. Biochimica et Biophisica Acta-Bioenergetics 1366(1-2):53-67.
Leslie AG and Walker JE. 2000 Structural model of F1-ATPase and the implications for rotary catalysis. Philosophical Transactions of the Royal Society B: Biological Sciences 355(1396):465-71.
Li AE, Ito H, Rovera II, Kim K-S, Takeda K, Yu Z-Y, Ferrans VJ, Finkel T. **1999** A role for reactive oxygen species in endothelial cell anoikis. Circulation Research 85(4):304-310.
Li FYL, Lam KSL, Tse HF, Chen C, Wang Y, Vanhoutte PM, Xu A. **2012** Endothelium-selective activation of AMP-activated protein kinase prevents diabetes mellitus–induced impairment in vascular function and reendothelialization via induction of heme oxygenase-1 in mice. Circulation 126(10):1267-1277.

Li JM, Gall NP, Grieve DJ, Chen M, Shah AM. **2002** Activation of NADPH oxidase during progression of cardiac hypertrophy to failure. Hypertension 40(4):477-484.
Li X, Rong Y, Zhang M, Wang XL, LeMaire SA, Coselli JS, Zhang Y, Shen YH. **2009** Up-regulation of thioredoxin interacting protein (Txnip) by p38 MAPK and FOXO1 contributes to the impaired thioredoxin activity and increased ROS in glucose-treated endothelial cells. Biochemical and Biophysical Research Communications 381(4):660-665.
Li Y, Huang TT, Carlson EJ, Melov S, Ursell PC, Olson JL, Noble LJ, Yoshimura MP, Berger C, Chan PH, Wallace DC, Epstein CJ. **1995** Dilated cardiomyopathy and neonatal lethality in mutant mice lacking manganese superoxide dismutase. Nature Genetics 11(4):376-381.
Li Y, Maedler K, Haataja L. **2008** UCP-2 and UCP-3 proteins are differentially regulated in pancreatic beta-cells. PLoS ONE 3(1):e1397.
Libby P, Ridker PM, Hansson GK. **2011** Progress and challenges in translating the biology of atherosclerosis. Nature 473(7347):317-325.
Lin X, David CA, Donnelly JB, Michaelides M, Chandel NS, Huang X, Warrior U, Weinberg F, Tormos KV, Fesik SW, Shen Y. **2008** A chemical genomics screen highlights the essential role of mitochondria in HIF-1 regulation. Proceedings of the National Academy of Sciences of the United States of America 105(1):174-179.
Liochev SI and Fridovich I. 1999 Superoxide and iron: partners in crime. IUBMB Life 48(2):175-161.
Littaru GP and Tain L. 2007 Bioenergetic and antioxidant properties of coenzyme Q10: recent developments. Molecular Biotechnology 37(1):31-37.
Liu J, Li J, Li WJ, Wang CM. **2013** The role of uncoupling proteins in diabetes mellitus. The Journal of Diabetes Research 2013:585897.
Liu L, Liu J, Tian XY, Wong WT, Lau CW, Xu A, Xu G, Ng CF, Yao X, Gao Y, Huang Y. **2013** Uncoupling protein-2 mediates DPP-4 inhibitor-induced restoration of endothelial function in hypertension through reducing oxidative stress. Antioxidant and Redox Signaling 21(11):1571-1581.
Logan DC. 2006 The mitochondrial compartment. Journal of Experimental Botany 56(6):1225-1234.
Lukanova L, Dudchenko AM, Tsybina TA, Germanova EL, Tkachuk EN, Erenburg IV. **2008** Effect of intermittent hypoxia on kinetic properties of mitochondrial enzymes. Bulletin of Experimental Biology and Medicine 144(6):795-801.
Lukanova L, Germanova EL, Kirova YI. **2011** The signal function of succinate and free radicals in mechanism of preconditioning and long-term adaptation to hypoxia. The Adaptation Biology and Medicine. Cell Adaptation and Challenges 6:257-277.
Lukyanova L. 1997 Bioenergy hypoxia: concept, mechanisms, correction. Bulletin of Experimental Biology and Medicine 124(9):244-254.
Lukyanova L. 2014 Mitochondria signaling in adaptation to hypoxia. International Journal of Physiology and Pathophysiology 5:363-381.
Lukyanova LD and Kirova YI. 2015 Mitochondria-controlled signaling mechanisms of brain protection in hypoxia. Frontiers in Neuroscience 9:320.
Lukyanova LD, Dudchenko AM, Tsybina TA, Germanova EL, Tkachuk EN, Erenburg IV. **2007** Effect of intermittent normobaric hypoxia on kinetic properties of mitochondrial enzymes. Bulletin of Experimental Biology and Medicine 144(6):795-801.
Lukyanova LD, Kozlov LV, Bichucher AM, Kirova YI, Germanova EL. **2011** Urgent reaction of the complement system to hypoxic exposure in rats sensitive to hypoxia. Bulletin of Experimental Biology and Medicine 150(6):685-689.
Lukyanova LD, Sukoyan GV, Kirova YI. **2013** Role of proinflammatory factors, nitric oxide, and some parameters of lipid metabolism in the development of immediate adaptation to hypoxia and HIF-1α accumulation. Bulletin of Experimental Biology and Medicine 154(5):597-601.
Lum JJ, Bui T, Gruber M, Gordan JD, DeBerardinis RJ, Covello KL, Simon MC, Thompson CB. **2007** The transcription factor HIF-1alpha plays a critical role in the growth factor-dependent regulation of both aerobic and anaerobic glycolysis. Genes and Development 21(9):1037-1049.
Ma ZA, Zhao Z, Turk J. **2012** Mitochondrial dysfunction and β-cell failure in type 2 diabetes mellitus. Experimental Diabetes Research 2012:703538.
Maalouf RM, Eid AA, Gorin YC, Block K, Escobar GP, Bailey S, Abboud HE. **2012** Nox4-derived reactive oxygen species mediate cardiomyocyte injury in early type 1 diabetes. American Journal of Physiology - Cell Physiology 302(3):C597-C604.
Mackenzie RM, Salt IP, Miller WH, Logan A, Ibrahim HA, Degasperi A, Dymott JA, Hamilton CA, Murphy MP, Delles C, Dominiczak AF. **2013** Mitochondrial reactive oxygen species enhance AMP-activated protein kinase activation in the endothelium of patients with coronary artery disease and diabetes. Clinical Sciences 124(6):403-411.
Madamanchi NR, Vendrov A, Runge MS. **2005** Oxidative stress and vascular disease. Arteriosclerosis, Thrombosis, and Vascular Biology 25(1):29-38.

Maiese K, Morhan SD, Zhao ZC. **2007** Oxidative stress biology and cell injury during Type 1 and Type 2 diabetes mellitus. Current Neurovascular Research 4(1)63-71.
Matsunaga T, Iguchi K, Nakajima T, Koyama I, Miyazaki T, Inoue I, et al. **2001** Glycated high-density lipoprotein induces apoptosis of endothelial cells via a mitochondrial dysfunction. Biochemical and Biophysical Research Communications. 287(3):714-720.
Matsushima S, Kuroda J, Ago T, Zhai, PY, Ikeda Y, Oka S, Gong GH, Tian R, Sadoshima J. **2013** Broad suppression of NADPH oxidase activity exacerbates ischemia/reperfusion injury through inadvertent downregulation of hypoxia-inducible factor-1alpha and upregulation of peroxisome proliferator-activated receptor-alpha. Circulation Research 112(3):1135-1149.
McMillin JB and Dowhan W. **2002** Cardiolipin and apoptosis. Biochimica et Biophysica Acta 1585(2-3):97-107.
Mertens S, Noll T, Spahr R, Krutzfeldt A, Piper HM. **1990** Energetic response of coronary endothelial cells to hypoxia. American Journal of Physiology 258(3Pt2):H689-H694.
Millet L, Vidal H, Andreelli F, Larrouy D, Riou JP, Ricquier D, Laville M, Langin D. **1997** Increased uncoupling protein-2 and -3 mRNA expression during fasting in obese and lean humans. Journal of Clinical Investigation 100(11):2665-2670.
Mitchell P. 1961 Coupling of phosphorylation to electron and hydrogen transfer by a chemi-osmotic type of mechanism. Nature 191(4784):144-148.
Mitchell P. 1977 Vectorial chemiosmotic precesses. Annual Review of Biochemistry 46:966-1005.
Moreno-Lastres D, Fontanesi F, García-Consuegra I, Martín MA, Arenas J, Barrientos A, Ugalde C. **2012** Mitochondrial complex I plays an essential role in human respirasome assembly. Cell Metabolism 15(3):324-335.
Mracek T, Pecionova A, Vrbacky M, Drahota Z, Houstek J. **2009** High efficiency of ROS production by glycerolphosphate dehydrogenase in mammanial mitochondria. Archives of Biochemistry and Biophysics 481(1):30-36.
Muller FL, Liu Y, Van Rammen H. **2004** Complex III release superoxide to both sites of the inner mitochondrial membrane. Journal of Biological Chemistry 279(47):49064-49073.
Murphy MP. 2009 How mitochondria produce reactive oxygen species. Biochemical Journal 417(1):1-13.
Murray CB and Lopez AD. 1997 Global mortality, disability, and the contribution of risk factors: Global Burden of Diseaeses Study. Lancet 349(9063):1436-1442.
Nascimento NRF, Lessa LMA, Kerntopf MR, Sousa CM, Alves RS, Queiroz MGR, Price J, Heimark DB, Larner J, Du X, Brownlee M, Gow A, Davis C, and Fonteles MC. **2006** Inositols prevent and reverse endothelial dysfunction in diabetic rat and rabbit vasculature metabolically and by scavenging superoxide. Proceedings of the National Academy of Sciences of the United States of America 103(1):218-223.
Nesto RW. 2004 Correlation between cardiovascular disease and diabetes mellitus: current concepts. American Journal of Medicine 116(5A):11S-22S.
Nicholls DG and Budd SL. 2000 Mitochondrial and neuronal survival. Psyhological Review 80:315-360.
Nicholls DG and Ferguson SJ. 2002 Bioenergetics. Academis Press London Thrid edition.
Nilius B and Droogmans G. 2001 Ion channels and their functional role in vascular endothelium. Physiological Reviews 81(4):1415-59.
Nishikawa T, Edelstein D, Du XL, Yamagishi S, Matsumura T, Kaneda Y, Yorek MA, Beede D, Oates PJ, Hammes HP, Giardino I, Brownlee M. **2000** Normalizing mitochondrial superoxide production blocks three pathways of hyperglycemia damage. Nature 404(6779):787-790.
Noji H and Yoshida M. **2001** The rotary machine in the cell, ATP synthase. Journal of Biological Chemistry 276 (3):1665–1668.
Nowak G, Clifton GL, Bakajsova D. **2008** Succinate ameliorates energy deficits and prevents dysfunction of complex I in injured renal proximal tubular cells. Journal of Pharmacology and Experimental Therapeutics 324(3):1155-1162.
Oberkofler A, Iglseder B, Klein K, Unger J, Haltmayer M, Krempler F et al. **2005** Association of the UCP2 gene locus with asymptomatic carotid atherosclerosis in midde-aged women. Arteriosclerosis, Thrombosis, and Vascular Biology 25(3):604-610.
Ohya S, Kuwata Y, Sakamoto K, Muraki K, Imaizumi Y. **2005** Cardioprotective effects of estradiol include the activation of large-conductance Ca^{2+}-activated K^{+} channels in cardiac mitochondria. American Journal of Physiology - Heart and Circulatory Physiology 289(4):H1635-H1642.
Okado-Matsumoto A, Fridovich I. 2001 Subcellural distribution of superoxide dismutases (SOD) in rat liver: CuZn-SOD in mitochondria. Journal of Biological Chemistry 276(6Pt1):38388-38393.
Orava J, NuutilaP, Lidell ME et al. **2011** Different metabolic responses of human brown adipose tissue to activation by cold and insulin. Cell Metabolism 14(2):272-279.
Orii Y. 1982 The cytochrome c peroxidase activity of cytochrome oxidase. Journal of Biological Chemistry 257(16):9246-9248.

O'Rourke B. 2007 Mitochondrial ion channels. Annual Review of Physiology 69:19-49.
Orrenius S, Gogvadze V, Zhivotovsky B. **2007** Mitochondrial oxidative stress: implications for cell death. Annual Review of Pharmacology and Toxicology 47:143-183.
Paltauf-Doburzynska J, Malli R, Graier WF. **2004** Hyperglycemic conditions affect shape and Ca^{2+} homeostasis of mitochondria in endothelial cell. Journal of Cardiovascular Pharmacology 44(4):423-436.
Pan Y, Mansfield KD, Bertozzi CC, Rudenko V, Chan DA, Giaccia AJ, Simon MC. **2007** Multiple factors affecting cellular redox status and energy metabolism modulate hypoxia-inducible factor prolyl hydroxylase activity in vivo and in vitro. Molecular and Cellular Biology 27(3):912-925.
Panei F, Mocharla P, Akhmedov A, Costantino S, Osto E, Volpe M, Lüscher TF, Cosentino F. **2012** Gene silencing of the mitochondrial adaptor p66Shc suppresses vascular hyperglycemic memory in diabetes. Circulation Research 111(3):278-289.
Papandreou I, Cairns RA, Fontana L, Lim AL, Denko NC. **2006** HIF-1 mediates adaptation to hypoxia by actively downregulating mitochondrial oxygen consumption. Cell Metabolism 3(3):187-197.
Papassotiriou J, Kohler R, Prenen J, Krause H, Akbar M, Eggermont J, Paul M, Distler A, Nilius B, and Hoyer J. **2000** Endothelial K^+ channel lacks the Ca^{2+} sensitivity-regulating b subunit. FASEB Journal 14(7):885-894.
Paternotte E, Gaucher C, Labrude P, Stoltz JF, Menu P. **2008** Review: behaviour of endothelial cells faced with hypoxia. Bio-Medical Materials and Engineering 18(4-5):295-299.
Pauw De, Tajerina S, Raes M, Keijer J, Arnould T. 2009 Mitochondrial (dys)function in adipocyte (de)differentiation and systemic metabolic alterations. American Journal of Pathology 175(3):927-939.
Pearlstein DP, Ali MH, Mungai PT, Hynes KL, Gewertz BI, Schumacker PT. **2002** Role of mitochondrial oxidant generation in endothelial cell response to hypoxia. Arteriosclerosis, Thrombosis, and Vascular Biology 22(4):566-573.
Peers C, Kang P, Boyle JP, Porter KE, Pearson HA, Smith IF, Kemp PJ. **2006** Hypoxic regulation of Ca^{2+} signaling in astrocytes and endothelial cells. Novartis Foundation Symposia 272:119-127.
Perrone L, Devi TS, Hosoya KI, Terasaki T, Singh LP. **2009** Thioredoxin interacting protein (TXNIP) induces inflammation through chromatin modification in retinal capillary endothelial cells under diabetic conditions. Journal of Cellular Physiology 221(1):262-272.
Piwonska M, Wilczek E, Szewczyk A, Wilczynski GM. **2008** Differential distribution of Ca^{2+}-activated potassium channel 4 subunit in rat brain: Immunolocalization in neuronal mitochondria. Neuroscience 153(2):446-460.
Pollard PJ, Briere JJ, Alam NA, Barwell J, Barclay E, Wortham NC, Hunt T, Mitchell M, Olpin S, Moat SJ, Hargreaves IP, Heales SJ, Chung YL, Griffiths JR, Dalgleish A, McGrath JA, Gleeson MJ, Hodgson SV, Poulsom R, Rustin P, Tomlinson IP. **2005** Accumulation of Krebs cycle intermediates and over-expression of HIF1alpha in tumours which result from germline FH and SDH mutations. Human Molecular Genetics - Oxford Journals 14(15):2231-2239.
Poornima IG, Parikh P, Shannon RP. **2006** Diabetic cardiomyopathy: the search for a unifying hypothesis. Circulation Research 98(5):596-605.
Prabu SK, Anandatheerthavarada HK, Raza H, Srinivasan S, Spear F, Avadhani NG. **2006** Protein kinase A-mediated phosphotylation modulates cytochrome c oxidase function and augments hypoxia and myocardial ischemia-related injury. Journal of Biological Chemistry 28(4):2061-2070.
Privratsky JR, Wold, LE, Sowers JR, Quinn MT, Ren J. **2003** AT1 blockade prevents glucose-induced cardiac dysfunction in ventricular myocytes: Role of the AT1 receptor and NADPH oxidase. Hypertension 42:206-212.
Puddu P, Puddu GM, Galletti L, Cravero E, Muscari A. **2005** Mitochondrial dysfunction as an initiating event in atherogenesis: a public hypothesis. Cardiology 103(3):137-141.
Qian S, Huo D, Wang S, Qian Q. **2011** Inhibition of glucose-induced vascular endothelial growth factor expression by Salvia miltiorrhiza hydrophilic extract in human microvascular endothelial cells: Evidence for mitochondrial oxidative stress. Journal of Ethnopharmacology 137(2):985-991.
Quinlal CL, Orr AL, Perevoshchikova V, Treberg JR, Ackrell BA, Brand MD. **2012** Mitochondrial complex II can generate reactive oxygen species at high rates in both the forward and reverse reactions. Journal of Biological Chemistry 287(32):27255-27264.
Quinlan CL, Orr AL, Perevoshchikova IV, Treberg JR, Ackrell BA, Brand MD. 2012 Mitochondrial complex II can generate reactive oxygen species at high rates in both the forward and reverse reactions. Journal of Biological Chemistry 287(32):27255-27264.
Quintero M, Colombo SL, Godfrey A, Moncada S. **2006** Mitochondria as signaling organelles in the vascular endothelium. Proceedings of the National Academy of Sciences of the United States of America 103(14):5379-5384.
Raaz U, Toh R, Maegdefessel L, Adam M, Nakagami F, Emrich F Spin JM, Tsao PS. **2014** Hemodynamic regulation of reactive oxygen species: Implications for vascular diseases. Antioxidants and Redox Signaling 20(6):914-928.

Radi R, Cassina A, Hodara R, Quijano C, Castro L. **2002** Peroxinitrite reactions and formations in mitochondria. Free Radical Biology and Medicine 33(11):1451-1464.
Raha S and Robinson BH. 2000 Mitochondria, oxygen free radicals, disease and ageing. Trends in Biochemical Sciences 25(10):502-508.
Reaven GM, Hollenbeck C, Jeng Cy, Wu MS, Chen YD. **1988** Measurement of plasma glucose, free fatty acid, lactate and insulin for 24 h in patients with NiDDM. Diabetes 37(8):1020-1024.
Recchioni R, Marcheselli F, Moroni F, Pieri C. **2002** Apoptosis in human aortic endothelial cells induced by hyperglycemic condition involves mitochondrial depolarization and is prevented by N-acetyl-L-cysteine. Metabolism 51(11):1384-1388.
Reed JS and Ragan CI. 1987 The effect of rate limitation by cytochrome c on the redox state of the ubiquinone pool in reconstituted NADH: cytochrome c reductase. Biochemical Journal 247(3):657-662.
Ricquier D and Bouillaud F. 2000 The uncoupling protein homologues: UCP1, UCP2, UCP3 StUCP and AtUCP. Biochemical Journal 345(Pt2):161-719.
Ritchie RH and Delbridge LM. 2006 Cardiac hypertrophy, substrate utilization and metabolic remodelling: Cause or effect? Clinical and Experimental Pharmacology and Physiology 33(1-2):159-166.
Rizzuto R, De Stefani D, Raffaello A, Mammucari C. **2012** Mitochondria as sensors and regulators of calcium signalling. Nature Reviews Molecular Cell Biology 13(9):566–578.
Roberts SB, Savage J, Coward WA, Chew B, Lucas A. **1988** Energy expenditure and intake in infants born to lean and overweight mothers. New England Journal of Medicine 318(8):461-466.
Rousset S, Alves-Guerra MC, Mozo J, Miroux B, Cassard-Doulcier AM, Bouillaud F, Ricquier D. **2004** The biology of mitochondrial uncoupling proteins. Diabetes 53(1):130-135.
Rowlands DJ, Islam MN, Das SR, Huertas A, Quadri SK, Horiuchi K, Inamdar N, Emin MT, Lindert J, Ten VS, Bhattacharya S, Bhattacharya J. **2011** Activation of TNFR1 ectodomain shedding by mitochondrial Ca^{2+} determines the severity of inflammation in mouse lung microvessels. Journal of Clinical Investigation 121(5):1986-1999.
Rubinstein JL, Walker JE, Henderson R. **2003** Structure of the mitochondrial ATP synthase by electron cryomicroscopy. EMBO Journal 22(23):6182–6192.
Rumsey WL, Schlosser C, Nuutinem EM, Robiolio M, Wilson DF. **1990** Cellular energetics and the oxygen dependence of respiration in cardiac myocytes isolated from adult rat. Journal of Biological Chemistry 256(26):15392-15402.
Rutter GA. 2001 Nutrient-secretion coupling in the pancreatic islet beta-cell: recent advances. Molecular Aspects of Medicine 22(6):247-284.
Sale MM, Hsu F, Palmer ND, Gordon CJ, Keene KL, Borgernik HM, Sharma AJ, Bergman RN, Taylor KD, Saad MF, Norris JM. **2007** The uncoupling protein 1 gene, UCP1, is expressed in mammalian islet cells and associated with acute insulin response to glucose in African American families fromthe IRAS family study. BMC Endocrine Disorders 7(1).
Sanborn T, Gavin W, Berkowitz S, Perille T, Lesch M. **1979** Augmented conversion of aspartate and glutamate to succinate during anoxia in rabbit heart. American Journal of Physiology 237(5):H535-H541.
Sazanov LA and Hinchliffe P. 2006 Structure of the hydrophilic domain of respiratory complex I from Thermus thermophilus. Science 311(5766):1430-1436.
Schonenberger MJ and Kovacs WJ. 2015 Hypoxia signaling pathways: modulators of oxygen-related organelles. Frontiers in Cell and Developmental Biology 3:42.
Schrauwen P, Mensink M, Schaart G, Moonen-Kornips E, Sels JP, Blaak EE, Russell AP, Hesselink MK. **2006** Reduced skeletal muscle uncoupling protein-3 content in prediabetic subjects and type 2 diabetic patients: restoration by rosiglitazone treatment. The Journal of Clinical Endocrinology and Metabolism 91(4):1520-1525.
Schroder K, Zhang M, Benkhoff S, Mieth A, Pliquett R, Kosowski J, Kruse C, Luedike P, Michaelis UR, Weissmann N, Dimmeler S, Shah AM, Brandes RP. **2012** Nox4 is a protective reactive oxygen species generating vascular NADPH oxidase. Circulation Research 110(9):1217-1225.
Schulz E, Dopheide J, Schuhmacher S, Thomas SR, Chen K, Daiber A, Wenzel P, Münzel T, Keaney JF. **2008** Suppression of the JNK pathway by induction of a metabolic stress response prevents vascular injury and dysfunction. Circulation 118(13):1347-1357.
Schulze PC, Yoshioka J, Takahashi T, He Z, King GL, Lee RT. **2004** Hyperglycemia promotes oxidative stress through inhibition of thioredoxin function by thioredoxin-interacting protein. Journal of Biological Chemistry 279(29):30369-30374.
Schumacker PT. 2002 Hypoxia anoxia and O_2 sensing: the search continues. American Journal of Physiology - Cell Physiology 283(5):L918-L921.
Scrinivasan S, Yeh M, Danziger EC, Hatley ME, Riggan AE, Leitinger N, Berliner JA, Hedrick CC. **2003** Glucose regulates monocyte adhesion through endothelial production of interleukin-8. Circulation Research 92(4):371-377.

Selemidis S, Sobey CG, Wingler K, Schmidt HH, Drummond GR. **2008** NADPH oxidases in the vasculature: Molecular features, roles in disease and pharmacological inhibition. Pharmacology and Therapeutics 120(3):254-291.
Semenza G. 2002 Signal transduction to hypoxia-inducible factor 1. Biochemical Pharmacology 64(5-6):993-998.
Semenza GL. 2003 Targeting HIF-1 for cancer therapy. Nature Reviews Cancer 3(10):721-732.
Semenza GL. 2007 Oxygen-dependent regulation of mitochondrial respiration by hypoxia-inducible factor 1. Biochemical Journal 405(1):1-9.
Sena LA and Chandel NS. 2012 Physiological role of mitochondrial reactive oxygen species. Molecular Cell 48(2):158-167.
Shen E, Li Y, Li Y, Shan L, Zhu H, Feng QP, Arnold MO, Peng TP. **2009** Rac1 is required for cardiomyocyte apoptosis during hyperglycemia. Diabetes 58(10):2386-2395.
Shimasaki Y, Pan N, Messina LM, Li C, Chen K, Liu L, Cooper MP, Vita JA, Keaney JF. **2013** Uncoupling protein 2 impacts endothelial phenotype via p53-mediated control of mitochondrial dynamics. Circulation Research 113(7):891-901.
Siebles I and Drose S. 2013 Q-site inhibitor induced ROS production of mitochondrial complex II is attenuated by TCA cycle dicarboxylates. Biochomica and Biophisica Acta – Bioenergerics 1827(10):1156-1164.
Siemen D, Loupatatzis C, Borecky J, Gulbins E, Lang F. **1999** Ca^{2+}-activated K channel of the BK-type in the inner mitochondrial membrane of a human glioma cell line. Biochemical and Biophysical Research Communications 257(2):549-554.
Skalska J, Bednarczyk P, Piwonska M, Kulawiak B, Wilczynski G, Dolowy K, Kudin AP, Kunz WS, Szewczyk A. **2009** Calcium ions regulate K^+ uptake into brain mitochondria: The evidence for a novel potassium channel. International Journal of Molecular Sciences 10(3):1104-1120.
Skalska J, Piwonska M, Wyroba E, Surmacz L, Wieczorek R, Koszela-Piotrowska I, Zielinska J, Bednarczyk P, Dolowy K, Wilczynski GM, Szewczyk A, Kunz WS. **2008** A novel potassium channel in skeletal muscle mitochondria. Biochimica et Biophysica Acta - Bioenergetics 1777(7-8):651-659.
Skulachev VP. 1991 Fatty acid circuit as a physiological mechanism of uncoupling of oxidative phosphorylation. FEBS Letters 294(3):158-162.
Skulachev VP. 1996 Role of uncoupled and non-uncoupled oxidations in maintaince of safely low levels of oxygen and its one-electron reductants. Quarterly Reviews of Biophysics 29(2):169-202.
Skulachev VP. 1998 Uncoupling new approaches to an old problem of bioenergetics. Biochimica et Biophysica Acta 1363(2):100-124.
Sluse FE, Jarmuszkiewicz W, Navet R, Douette P, Mathy G, Sluse-Goffart CM. **2006** Mitochondrial UCPs: New insights into regulation and impact. Biochimica et Biophysica Acta - Bioenergetics 1757(5-6):480-485.
Spahr R, Krutzfeldt A, Mertens S, Siegmund B, Piper HM. **1989** Fatty acids are not an important fuel for coronary microvascular endothelial cells. Molecular and Cellular Biochemistry 88(1-2):59-64.
Spitaler MM and Graier WF. 2002 Vascular targets of redox signalling in diabetes mellitus. Diabetologia 45(4):476-494.
Srinivasan S, Hatley ME, Bolick DT, Palmer LA, Edelstein D, Brownlee M, Hedrick CC. **2004** Hyperglycaemia-induced superoxide production decreases eNOS expression via AP-1 activation in aortic endothelial cells. Diabetologia 47(10):1727-1734
Stowe DF, Aldakkak M, Camara AK, Riess ML, Heinen A, Varadarajan SG, Jiang MT. **2006** Cardiac mitochondrial preconditioning by Big Ca^{2+}-sensitive K^+ channel opening requires superoxide radical generation. American Journal of Physiology - Heart and Circulatory Physiology 290(1):H434-H440.
Sudarshan S, Sourbier C, Kong HS, Block K, Valera Romero VA, Yang Y, Galindo C, Mollapour M, Scroggins B, Goode N, Lee MJ, Gourlay CW, Trepel J, Linehan WM, Neckers L. **2009** Fumarate hydratase deficiency in renal cancer induces glycolytic addiction and hypoxia-inducible transcription factor 1alpha stabilization by glucose-dependent generation of reactive oxygen species. Molecular and Cellular Biology 29(15):4080-4090.
Sumimoto H. 2008 Structure, regulation and evolution of Nox-family NADPH oxidases that produce reactive oxygen species. FEBS Journal 275(13):3249–3277.
Sun J, Pu Y, Wang P, Chen S, Zhao Y, Liu C, Shang Q, Zhu Z, Liu D. **2013** TRPV1-mediated UCP2 upregulation ameliorates hyperglycemia-induced endothelial dysfunction. Cardiovascular Diabetology 12:1-14.
Suttorp N, Toepfer W, Roka L. **1986** Antioxidant defense mechaanism of endothelial cells: glutathione redox cycle versus catalase. American Journal of Physiology - Cell Physiology 251(5Pt1):C671-C680.
Sweet IR, Gilbert M, Maloney E, Hockenbery DM, Schwartz MW, Kim F. **2009** Endothelial inflammation induced by excess glucose is associated with cytosolic glucose 6-phosphate but not increased mitochondrial respiration. Diabetologia 52(5):921-931.

Swida-Barteczka A, Woyda-Ploszczyca A, Sluse FE, Jarmuszkiewicz W. **2009** Uncoupling protein 1 inhibition by purine nucleotides is under the control of the endogenous ubiquinone redox state. Biochemical Journal 424(2):297-306.
Szabadkai G and Duchen MR. **2008** Mitochondria: the hub of cellular Ca^{2+} signaling. Physiology 23:84-94.
Szabo I and Zoratti M. 2014 Mitochondrial channels: ion fluxes and more. Physiological Reviews 94(2):519-608.
Szabo I, Leanza L, Gulbins E, Zoratti M. **2012** Physiology of potassium channels in the inner membrane of mitochondria. Pflugers Archiv European Journal of Physiology 463(2):231-246.
Szewczyk A, Jarmuszkiewicz W, Kunz WS. **2009** Mitochondrial potassium channels. International Union of Biochemistry and Molecular Biology Life 61(2):134-143.
Taegtmeyer H, McNulty P, Young ME. **2002** Adaptation and maladaptation of the heart in diabetes I. General concepts. Circulation 105(14):1727-173.
Tait SW, Oberst A, Quarato G, Milasta S, Haller M, Wang R, et al. **2013** Widespread mitochondrial depletion via mitophagy does not compromise necroptosis. Cell Reports 5(4):878–885.
Tang X, Luo YX, Chen HZ, Liu DP. **2014** Mitochondria, endothelial cell function, and vascular diseases. Frontiers in Physiology 5:175.
Therade-Matharan S, Laemmel E, Carpentier S, Obata Y, Levade T, Duranteau J, Vicaut E. **2005** Reactive oxygen species production by mitochondria in endothelial cells exposed to reoxygenation after hypoxia and glucose depletion is mediated by ceramide. American Journal of Physiology - Regulatory, Integrative and Comparative Physiology 289(6):R1756-R1762.
Thomas SR, Witting PK, Drummond GR. **2008** Redox control of endothelial function and dysfunction: molecular mechanism and therapeutic opportunities. Antioxidants and Redox Signaling 10(10)1713-1765.
Tian XY, Wong WT, Xu A, Lu Y, Zhang Y, Wang L, Cheang WS, Wang Y, Yao X, and Huang Y. **2012** Uncoupling protein-2 protects endothelial function in diet-induced obese mice. Circulation Research 110(9):1211-1216.
Tormos VT and Chandel NS. 2010 Inter-connection between mitochondria and HIFs. Journal of Cellular and Molecular Medicine 14(4)795-804.
Trenker M, Malli R, Fertschai I, Levak-Frank S, Graier WF. **2007** Uncoupling proteins 2 and 3 are fundamental for mitochondrial Ca^{2+} uniport. Nature Cell Biology 9(4):445-452.
Trumpower BL. 1990 The protonmotive Q cycle. Energy transduction by coupling of proton translocation to electron transfer by the cytochrome bc1 complex. Journal of Biological Chemistry 265(20):11409-11412.
Tsukihara T, Aoyama H, Yamashita E, Tomizaki T, Yamaguchi H, Shinzawa-Itoh K, Nakashima R, Yaono R, **Yoshikawa** S. **1996** The whole structure of the 13-subunit oxidized cytochrome c oxidase at 2.8 A. Science 272(5265):1136-1144.
Tsukihara T, Itoh-Shinzawa K, Yoshikawa S. **1996** Structures of metal centers of bovine heart cytochrome c oxidase. Tanpakushitsu Kakusan Koso. Protein, Nucleic Acid, Enzyme Jourbal 41(9):1353-1362.
Turrens JF, Freeman BA, Levitt JG, Crapo JD. **1982** The effect of hyperoxia on superoxide production by lung submitochondrial particles. Archives of Biochemistry and Biophysics 217(2):401-410.
Turrens JF. 2003 Formaction of reactive oxygen species. Journal of Physiology 552(2):335-344.
Valle I, Alvarez-Barrientos A, Arza E, Lamas S, Monsalve M. **2005** PGC-1α regulates the mitochondrial antioxidant defense system in vascular endothelial cells. Cardiovascular Research 66(3)562-573.
Van den Bergen CW, Wagner AM, Krab K, Moore AL. **1994** The relationship between electron flux and the redox poise of the quinone pool in plant mitochondria. Interplay between quinol-oxidizing and quinone-reducing pathways. European Journal of Biochemistry 226(3):1071-1078.
Vindis C, Seguelas MH, Lanier S, Parini A, Cambon C. **2001** Dopamine induces ERK activation in renal epithelial cells through H_2O_2 produces by monoamine oxidase. Kideny International 59(1):76-86.
Walter DH, Haendeler J, Galle J, Zeiher AM, Dimmeler S. **1998** Cyclosporin A inhibits apoptosis of human endothelial cells by preventing release of cytochrome C from mitochondria. Circulation 98(12):1153-1157.
Wang W, Wang Y, Long J, Wang J, Haudek SB, Overbeek P, Chang BH, Schumacker PT, Danesh FR. **2012** Mitochondrial fission triggered by hyperglycemia is mediated by rock1 activation in podocytes and endothelial cells. Cell Metabolism 15(2):186-200.
Wang XR, Zhang MW, Chen DD, Zhang Y, Chen AF. **2011** AMP-activated protein kinase rescues the angiogenic functions of endothelial progenitor cells via manganese superoxide dismutase induction in type 1 diabetes. American Journal of Physiology – Endocrinology and etabolism 300(6):E1135-E1145.
Waypa GB and Schumacker PT. 2002 O_2 sensing in hypoxic pulmonary vasoconstriction: the mitochondrial door re-opens. Respiratory Physiology and Neurobiology 132(1):81-91.
Waypa GB and Schumacker PT. 2005 Hypoxic pulmonary vasoconstriction: redox events in oxygen sensing. Journal of Applied Physiology 98(1):404-414.
Weir EK, Lopez-Barneo J, Buckler KJ, Archer SL. **2005** Acute oxygen-sensing mechanism. New England Journal of Medicine 353(19):2042-2055.

Widlansky ME and Gutterman DD. 2011 Regulation of endothelial function by mitochondrial reactive oxygen species. Antioxidants and Redox Signaling 15(6):1517-1530.
Wieckowski MR, Giorgi C, Lebiedzinska M, Duszynski J, Pinton P. **2009** Isolation of mitochondria-associated membranes and mitochondria from animal tissues and cells. Nature Protocols 4(11):1582-1590.
Williams SB, Goldfine AB, Timimi FK, Ting HH, Roddy MA, Simonson DC, Creager MA. **1998** Acute hyperglycemia attenuates endothelium-dependent vasodilation in humans in vivo. Circulation 97(17):1695-1701.
Williamson JR, Chang K, Frangos M, Hasan KS, Ido Y, Kawamura T, Nyengaard JR, Kilo C, Tilton RG. **1993** Hyperglycemic pseudohypoxia and diacetic complications. Journal of Diabetes 42(6):801-813.
Wojtovich AP, Sherman TA, Nadtochiy SM, Urciuoli WR, Brookes PS, Nehrke K. **2011** Slo-2 is cytoprotective and contributes to mitochondrial potassium transport. PLoS ONE 6:e28287.
Won JC, Park JY, Kim YM, Koh EH, Seol S, Jeon BH, Han J, Kim JR, Park TS, Choi CS, Lee WJ, Kim MS, Lee IK, Youn JH, Lee KU. **2010** Peroxisome proliferator-activated receptor-γ coactivator 1-α overexpression prevents endothelial apoptosis by increasing ATP/ADP translocase activity. Arteriosclerosis, Thrombosis, and Vascular Biology 30(2):290-297.
Woyda-Ploszczyca A and Jarmuszkiewicz W. 2011 Ubiquinol (QH(2)) functions as a negative regulator of purine nucleotide inhibition of Acanthamoeba castellanii mitochondrial uncoupling protein. Biochimica et Biophysica Acta – Bioenergetics 1807(1):42-52.
Wulf H, Hay-Schmidt A, Poulsen AN, Klaerke DA, Olesen J, Jansen-Olesen I**. 2009** Molecular investigations of BKCa channels and the modulatory Î¸-subunits in porcine basilar and middle cerebral arteries. Journal of Molecular Histology 40(2):87-97.
Xi Q, Cheranov SY, Jaggar JH. **2005** Mitochondrial-derived oxygen species dilate cerebral arteries by activating Ca^{2+} sparks. Circulation Research 97(4):354-362.
Xie Z, Zhang J, Wu J, Viollet B, Zou MH. **2008** Upregulation of mitochondrial uncoupling protein-2 by the AMP-activated protein kinase in endothelial cells attenuates oxidative stress in diabetes. Diabetes 57(12):3222-3230.
Xu W, Liu Y, Wang S, McDonald T, Van Eyk JE, Sidor A, O'Rourke B. **2002** Cytoprotective role of Ca^{2+}-activated K+ channels in the cardiac inner mitochondrial membrane. Science 298(5595):1029-1033.
Yankovskaya V, Horsefield R, Törnroth S, Luna-Chavez C, Miyoshi H, Léger C, Byrne B, Cecchini G, Iwata S. **2003** Architecture of succinate dehydrogenase and reactive oxygen species generation. Science 299(5607):700-704.
Yoshikawa S, Muramoto K, Shinzawa-Itoh K, Aoyama H, Tsukihara T, Shimokata K, Katayama Y, Shimada H. **2006** Proton pumping mechanism of bovine heart cytochrome c oxidase. Biochimica et Biophysica Acta 1757(9-10):1110-1116.
Yu T, Robotham JL, Yoon Y. **2006** Increased production of reactive oxygen species in hyperglycemic conditions requires dynamic change of mitochondrial morphology. Proceedings of the National Academy of Sciences of the United States of America 103(8):2653-2658.
Zafari AM, Ushio-Fukai M, Minieri CA, Akers M, Lassegue B, Griendling KK. **1999** Arachidonic acid metabolites mediate angiotensin II-induced NADH/NADPH oxidase activity and hypertrophy in vascular smooth muscle cells. Antioxidants and Redox Signaling 1(2):167-179.
Zaritsky JJ, Eckman DM, Wellman GC, Nelson MT, Schwarz TL. **2000** Targeted disruption of Kir2.1 and Kir2.2 genes reveals the essential role of the inwardly rectifying K^+ current in K^+-mediated vasodilation. Circulation Research 87(2):160-166.
Zhang C, Baffy G, Perret P et al. **2001** Uncoupling protein-2 negatively regulates insulin secretion and is a major link between obesity, β cell dysfunction, and type 2 diabetes. Cell 105(6)745-755.
Zhang DX and Gutterman DD. 2007 Mitochondrial reactive oxygen species-mediated signaling in endothelial cells. American Journal of Physiology - Heart and Circulatory Physiology 292(5):H2023-H2031.
Zhang H, Bosch-Marce M, Shimoda LA, Tan YS, Baek JH, Wesley JB, Gonzalez FJ, Semenza GL. **2008** Mitochondrial autophagy is an HIF-1-dependent adaptive metabolic response to hypoxia. Journal of Biological Chemistry 283(16):10892-10903.
Zhang M, Kho AL, Anilkumar N, Chibber R, Pagano PJ, Shah AM, Cave AC. **2006** Glycated proteins stimulate reactive oxygen species production in cardiac myocytes: Involvement of Nox2 (gp91phox)-containing NADPH oxidase. Circulation 113(9):1235-1243.
Zhang R, Al-Lamki R, Bai L, Streb JW, Miano JM, Bradley J, Min W. **2004** Theirodoxin-2 inhibits mitochondria-located ASK1-mediated apoptosis in a JNK-independent manner. Circulation Research 94:1483-1491.
Zhao Y, Wang ZB, Xu JX. **2003** Effect of cytochrome c on the generation and elimination of $O_2^{-\bullet}$ and H_2O_2 in mitochondria. Journal of Biological Chemistry 278(4):2356-2360.
Zhdanov AV, Dmitriev RI, Golubeva AV, Gavrilova SA, Papkovsky DB. **2013** Chronic hypoxia leads to a glycolytic phenotype and suppressed HIF-2 signaling in PC12 cells. Biochimica et Biophysica Acta 1830(6):3553-3569.

Zhdanov AV, Dmitriev RI, Golubeva AV, Gavrilova SA, Papkovsky DB. **2013** Biochimica et Biophysica Acta Chronic hypoxia leads to a glycolytic phenotype and suppressed HIF-2 signaling in PC12 cells. 1830(6):3553-3569.
Zheng Z, Chen H, Ke G, Fan Y, Zou H, Sun X, Gu Q, Xu X, Ho PC. **2009** Protective effect of perindopril on diabetic retinopathy is associated with decreased vascular endothelial growth factor-to-pigment epithelium-derived factor ratio: involvement of a mitochondria-reactive oxygen species pathway. Diabetes 58(4):954-964.
Zheng Z, Chen H, Zhao H, Liu K, Luo D, Chen Y, Chen Y, Yang X, Gu Q, and Xu X. **2010** Inhibition of JAK2/STAT3-mediated VEGF upregulation under high glucose conditions by PEDF through a mitochondrial ROS pathway in vitro. Investigative Ophthalmology and Visual Science 51(1):64-71.
Zhou M, Diwu Z, Panchuk-Voloshina N, Haugland RP. **1997** A stable nonfluorescent derivative of resorufin for the fluorometric determination of trace hydrogen peroxide: Applications in detecting the activity of phagocyte NADPH oxidase and other oxidases. Analytical Biochemistry 253:162-168.